QUANTIFICATION OF CELL ATTACHMENT ON DIFFERENT MATERIALS AS CANDIDATE ELECTRODES FOR MEASUREMENT OF QUANTAL EXOCYTOSIS

A Thesis presented to the Faculty of the Graduate School

University of Missouri

In Partial Fulfillment

Of the Requirements for the Degree

Master of Science

by

ATANU SEN

Dr. Shubhra Gangopadhyay, Thesis Supervisor

AUGUST, 2008

The undersigned, appointed by the dean of the Graduate School, have examined the thesis entitled

QUANTIFICATION OF CELL ATTACHMENT ON DIFFERENT

MATERIALS AS CANDIDATE ELECTRODES FOR

MEASUREMENT OF QUANTAL EXOCYTOSIS

Presented by ATANU SEN,

A candidate for the degree of Master of Science

And hereby certify that in their opinion it is worthy of acceptance.

_____

Dr. Shubhra Gangopadhyay, Biological Engineering

_____

Dr. Kevin Gillis, Biological Engineering

_____

Dr. Luis Polo Parada, Medical Pharmacology and Physiology

ACKNOWLEDGEMENTS

My tryst with real science kicked off at Mizzou. Prior to this I had no hands on experience on anything close to defining an engineer. The journey has been as tough as an ordeal but its been an overwhelming learning experience throughout. The realm of science is indeed fascinating and I consider myself immensely fortunate to have made my foray into it.

My doors to science opened in the labs of one of the most well-known scientists in the field of microfabrication technology - Dr. Shubhra Gangopadhyay, as my advisor. Her laboratory is home to state-of-the-art instruments and technologies required for an independent research facility. The diversity of research performed by the members of the Nanocenter inclusive of graduate students, postdoctoral and research associates has left me spellbound. Working with her has not only made me aware of the deficiencies within me but also made me tougher and fearless as an individual. I can foresee a life where I can fight harder than I could have before I met her. Thanks Dr. G for giving me the opportunity.

At Mizzou I have been exposed to more than one lab. Apart from working at Engineering Building West, I would have to work at Dalton Cardiovascular Research Center with my co-advisor Dr. Kevin Gillis. Again, its a blessing for me to have met one of the most eminent scientists in electrophysiology. His friendly and down to earth nature enabled me to approach him with the most trivial questions a learner could have, to which he would always reply with undying gusto. It was in his laboratory that I nurtured my biological skills of cell culture. Today I feel proud to label myself as a 'biological' engineer in the true sense of the word, thanks to Dr. Gillis's laboratory.

TABLE OF CONTENTS

LIST OF FIGURES

viii

xiv

QUANTIFICATION OF CELL ATTACHMENT ON DIFFERENT MATERIALS AS CANDIDATE ELECTRODES FOR MEASUREMENT OF QUANTAL EXOCYTOSIS

Atanu Sen

Advisor: Dr. Shubhra Gangopadhyay

Co-Advisor: Dr. Kevin Gillis

ABSTRACT

A high throughput BioMEMS or lab-on-a-chip device is being developed for single cell capture for the purpose of high time resolution quantal exocytosis measurement with high probability of cell docking. This device makes use of DLC (Diamond like Carbon) deposited on a conducting ITO (Indium Tin Oxide) film to bring about a suitable electrode incorporating biocompatibility, transparency and low resistivity and electrochemical activity to enhance cell docking and detect catecholamine release. Various materials have been tested for their ability to promote cell attachment. Diamond like Carbon being an established biocompatible and cytophilic material has been compared with other metal electrodes for cell attachment using an assay developed for this study. Cells tested for attachment were either the insulin-secreting cell line INS-1 or catecholamine-secreting bovine chromaffin cells. With either cell type, I found that the rank order of cell attachment following overnight culture was DLC > ITO, Pt > Au. Teflon has also tested as a candidate insulating material to prevent cell attachment outside of this docking site. The cell attachment can be enhanced by coating of poly-d-lysine on the metal while retaining the electrochemical activity of the metal electrode.

The fraction of cells that were dead following overnight culture were similar among the tested material. In summary, my results suggest that electrodes fabricated from poly-d-lysine coated DLC insulated with Teflon will selectively promote attachment of cells to measurement electrodes.

CHAPTER 1

INTRODUCTION

With all major branches of science now trying to explore the vast unknown in life sciences and biology, a promising future is ahead. Cells are the fundamental unit of life, and studies on cell contribute to reveal the mystery of life. A plethora of cells exist in each gene pool and each cell type has a specific role in the body. For instance, osteoblasts make up the skeletal framework of mammals; red blood cells (RBCs) transport oxygen to tissue; neurons transmit nerve signals to and from the brain; chromaffin cells release adrenaline or nor-adrenaline by exocytosis to stimulate flight or fight reaction in an individual. All such cellular behavior can be comprehended at the micro and nano level with the help of a lab on a chip or a micro-total analytical system which is a miniaturized version of a whole laboratory on a hand held device. However, since variability exists between individual cells even of the same type, increased emphasis has been put on the analysis of individual cells to understand how they work.

Microchip devices provide the capability of integrating the whole process of single-cell analysis and various detection techniques into a miniaturized microchip, and afford a versatile and automated platform and are emerging as the next revolutionary tools for single-cell analysis. Microchip devices have the potential to enable complex single-cell studies to be carried out, and many biological measurements that are otherwise impractical could be realized by using a multifunctional platform. However, tremendous

1

challenges exist to achieve this potential and a vast amount of effort needs to be put in before it becomes an easy-to-use and robust tool. There is no doubt that highly integrated microdevices will find overwhelming applications in many areas of biological research. Cell functions must be investigated in a rapid and high throughput manner necessitating robust and portable point-of-care (POC) devices.

1.1. Objectives and Goals

The overall objective of the project is to develop a microchip consisting of an array of electrodes at the bottom of wells wherein cells can be captured and then elicit amperometric electrochemical signals upon release of transmitter. This will enable rapid collection of data and at a rate much higher than existing techniques as described in Section 1.3. Driven by such goals, the search ensues for suitable materials to serve as electrodes for signal measurement. These microelectrodes are required to have biocompatibility, transparency, low resistivity and electrochemical activity. The first requirement is biocompatibility such that the electrode material will not lead to cell damage. The electrode should also promote cell attachment, i.e., be "cytophilic". The most common electrodes for single-cell measurement of quantal exocytosis are fabricated from carbon fibers therefore it is logical to integrate carbon into the microchip. Since carbon fiber can not be integrated into a chip, the rationale is to have carbon as a film. Such a need can be met by employing DLC (diamond like carbon) as the electrode since it has been well established as a biomaterial. DLC also satisfies the second requirement of transparency upto a thickness well in excess of 100 nm. However, use of DLC does

not satisfy the third pre-requisite of low resistivity which is a drawback when it comes to stimulating the cell and measurement of vesicle release spikes. This issue has been solved by depositing DLC on Indium Tin Oxide (ITO) by magnetron sputtering. Such a double layered electrode has low resistivity owing to the presence of ITO at the bottom while at the same time retaining cytophilicity and transparency. The deposition conditions of DLC on ITO have been optimized to get the most suitable electrode for measurement of vesicular release.

The aim of this dissertation is to compare candidate electrode materials. In order to perform this comparison a robust protocol has also been developed to quantify cell attachment. Cell attachment has been promoted without interfering with electrochemical activity by surface modification with polylysine. Alongside these conducting electrodes, the feasibility of using Teflon as a "cytophobic" insulating material has been established. The end device is an array of such microelectrodes to which cells will be docked allowing acquisition of multiple signals at the same time. Analysis of these signals will help scientists to comprehend the molecular mechanisms of catecholamine (adrenaline, nor-adrenaline, dopamine) release and detect abnormalities in cases of pathological conditions such as with Parkinson's disease.

Numerous studies of cell attachment to a material surface have been carried out but the conclusions of these studies often disagree. This could well be because of use of different cells and different protocols by different researchers. It is important to match the experimental conditions to the goals of the project. This study has been performed using

both primary Bovine Chromaffin cells and the INS-1 cell line, because these cells are commonly used to study quantal exocytosis. I also emphasized short-term culture of cells on the various materials to match the expected conditions of the microchip experiments.

1.2. Exocytosis

Exocytosis is defined as a process of cellular secretion or excretion in which substances as neurotransmitters, enzymes, peptide hormones and antibodies contained in vesicles are discharged from the cell by fusion of the vesicular membrane with the outer cell membrane. Many cellular processes involve exocytosis, for example:

- secretion of proteins like enzymes, peptide hormones and antibodies from cells.
- turnover of plasma membrane
- release of neurotransmitter from presynaptic neurons
- placement of integral membrane proteins
- acrosome reaction during fertilization
- antigen presentation during the immune response
- recycling of plasma membrane bound receptors

Exocytosis in endocrine cells share many features with that in neurons although certain differences do exist (Augustine and Neher 1992). Nevertheless, results found with chromaffin cells are helpful in comprehending the release form neurons. Various exocytosis mechanisms have been proposed such as the "kiss and run" mechanism (MacDonald and others 2005).
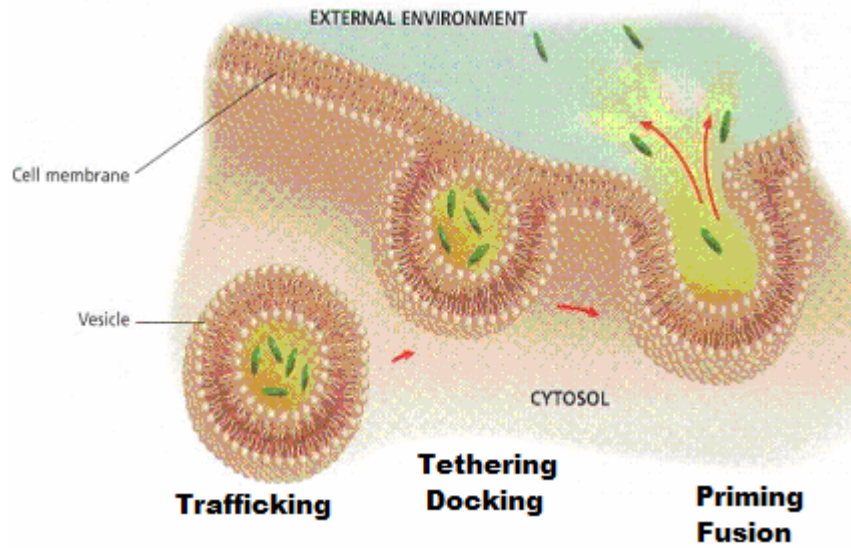
Fig. 1.1 Schematic of Exocytosis

Exocytosis can be broken down into the following (Sugita 2008):

i). Vesicle Trafficking:

Vesicles carrying neurotransmitter move through the cytosol towards the cell membrane.

ii). Vesicle Tethering:

The vesicles establish a tether on the inner side of the membrane at the site for eventual exocytosis.

iii). Vesicle Docking:

In this step, the vesicle comes in contact with the cell membrane, where it begins to chemically and physically merge with the proteins in the cell membrane.

iv). Vesicle Priming:

In those cells where chemical transmitters are being released, this step involves the chemical preparations for the last step of exocytosis.

v). Vesicle Fusion:

In this last step, the vesicle membrane fuses with the cell membrane, pushing the vesicle contents (chemical transmitters) out of the cell. This step is the primary mechanism for the increase in size of the cell's plasma membrane.

Exocytosis occurs by fusion of discrete vesicles, therefore transmitter release is "quantal" in nature. The release of the contents of an individual vesicle usually occurs over a time interval of <100 ms therefore necessitating high time resolution assays in order to resolve individual "quantal" secretion events. Resolving quantal release provides information about the number of transmitter molecules in the vesicle.

The exocytotic process can produce electrical signals. Study of such signals is of deep interest in electrophysiology in order to comprehend neuron to neuron communication or crosstalk or various aspects of cell signaling.

1.3. Carbon Fibre Amperometry

Amperometry refers to the measurement of faradaic current while the electrode potential is held at a constant value. This allows measurement as the analyte is oxidized

Fig. 1.2 A typical exocytosis measurement setup based on a patch-clamp system. From left to right is: Faraday cage shielded microscope bench with piezoelectric micromanipulator and head stage preamplifier; instrument rack of patch-clamp amplifier, AD/DA module, monitor etc.; computer control for voltage/current clamp and data acquisition. (Courtesy of Dr. Gillis's electrophysiology lab at Dalton Cardiovascular Research Center)

or reduced on the electrode surface with high time resolution although the identity and concentration of the analyte can not be detected. The most commonly used electrochemical electrode for measuring exocytosis is made of carbon fiber. In brief, amperometric measurements involve the carbon fiber electrode being held at a constant potential (e.g., >650 or 800mV for serotonin and catecholamines, respectively) exceeding the redox

potential of the substance of interest. When molecules such as epinephrine or serotonin hit the carbon surface, electrons are transferred and a current can be measured as spikes, each spike representing a single vesicle release event (Bruns 2004).
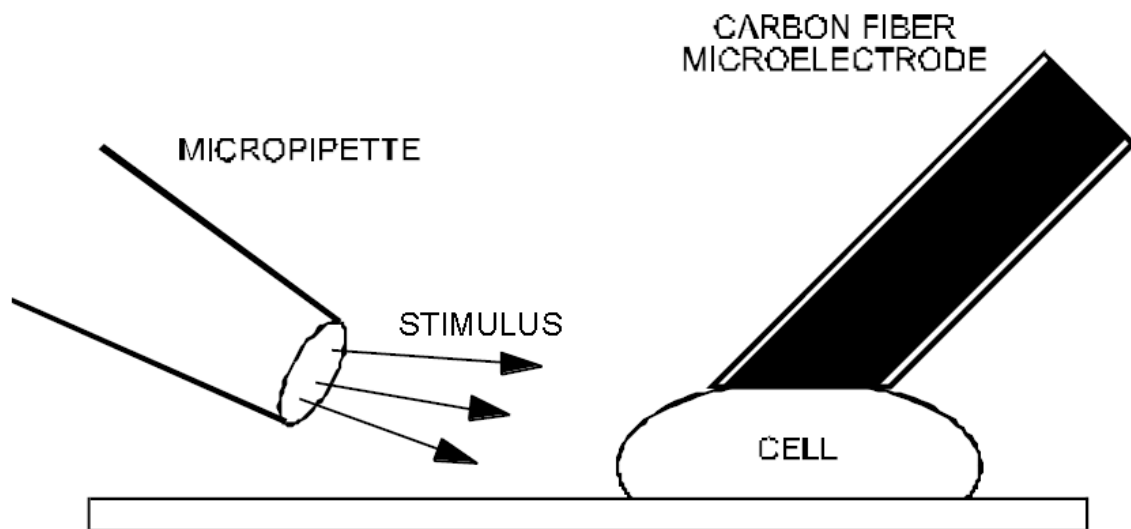
Fig. 1.3. Diagram of a general experimental setup for the electrochemical detection of exocytosis with a carbon fiber microelectrode (Hochstetler and Wightman 1998)

Carbon is the material of choice for constructing microelectrodes for biological measurements because it is electrochemically stable in biological environments. Also, it can be obtained in the form of carbon fibers with diameters in the micron range, thus meeting the requirement of small size.

Parameters from these amperometric spikes contain a lot of significant information regarding the exocytosis process (Fig. 1.4). For example, integration of these amperometric currents indicates the amount of transmitter released from a single vesicle. The time course of the spike also provides important information about vesicle fusion and release kinetics. With

amperometry, one can achieve millisecond time resolution and sensitivity of less than 1,000 molecules of released transmitters.
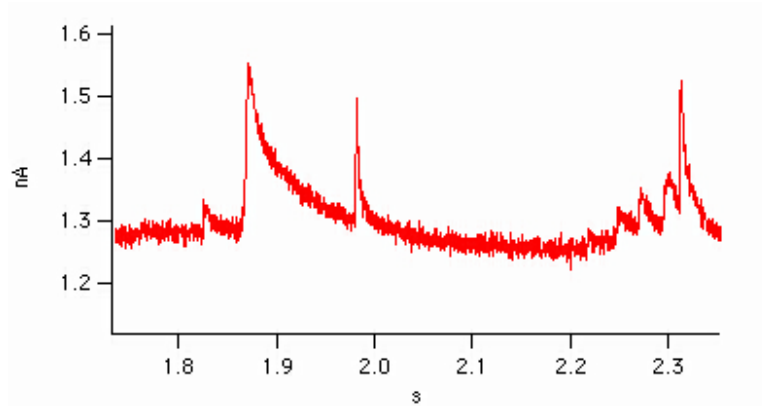
Fig. 1.4. Spikes representing current obtained by amperometry

Owing to the complexity, labor, and low efficiency of carbon-fiber measurements, there is a dire need felt for a BioMEMS device performing high throughput assay of quantal exocytosis.

1.4. BioMEMS

BioMEMS (Bio-Micro-Electrical-Mechanical systems, or "biochips") refers to the use of miniaturization in the fields of biotechnology, pharmaceuticals and medical applications. BioMEMS devices are also sometimes referred to as micro total analytical systems (µTAS) or "lab-on-a-chip" technology. BioMEMS technology promises the possibility of mass production of miniaturized, smart, and cheaper biomedical devices that could revolutionize research and clinical practice in our everyday life. Given the advent of the interdisciplinary nature of modern research, BioMEMS fuses with many

other technologies such as nanotechnology, clinical applications, surgical instruments, tissue repair, artificial organs, diagnostic tools, drug delivery systems, etc. Among the several prominent advantages of BioMEMS are the miniaturization of a lab scaled down onto a mere chip, low energy consumption, realization of an easy batch production process resulting in higher economy, requirement of minimal sample volumes, an increased heat and mass transport etc. The miniaturization renders the erstwhile bulky instruments redundant by bringing about lightweight portable versions. The advantage of smaller sample size can reduce the consumption of expensive or limited reagents or the production of (toxic) waste, thus making these devices more ecofriendly. The miniaturization can too make complex systems really small and highly integrated thus making their interface with sensors and electronics user-friendly (Gao 2006). There are some Lab on Chip applications already available in the market today such as Roche Diagnostic's Amplichip. The Amplichip identifies patient's genotype and predicts phenotype which aids in expected medication behavior and therefore prescription.

Bio-MEMS is a fast growing area of research that continues to accelerate as its developments continue to find real world applications. In fact the entire MEMS market has been growing rapidly and is expected to be valued at over 12.5 billion US dollars in the year 2010. In medical applications Bio-MEMS have been received with great interest. Bio-MEMS would allow enhancement of many surgical tools and procedures. Scalpels with strain gauges, that provide force feedback or surgical instruments that identify the type of tissue they are in contact with, enable envisioning an era of non-invasive surgery. To be truly successful these MEMS devices will need to be self

sufficient on power especially without wires (e.g. surgical applications). Furthermore, as the technology matures, becomes more complex, and gains medical regulatory approval these MEMS will slowly begin to proliferate and improve many processes and lives. During the past two decades, various techniques have been developed for single-cell analysis. Capillary electrophoresis for instance, is an excellent technique for identifying and quantifying the contents of single cells. The microfluidic devices afford a versatile platform for single-cell analysis owing to their unique characteristics.

1.4.1. BioMEMS devices to perform assays on the Single-Cell level

It is important to quantify the distribution of behavior amongst a population of individual cells to reach a more complete quantitative understanding of cellular processes. Single cell analysis of drug toxicity with physiologically relevant perfused dosages is to be investigated for comprehending cell signaling pathways and systems biology.

Microchips that perform directed capture of single cells have been developed. Improved throughput analysis of single cell behavior requires uniform conditions for individual cells with controllable fluid flow. Uniform cell arrays for static culture of adherent cells have previously been constructed using protein micropatterning or stamping techniques but beset with lack of ability to retain electrochemical activity of the measuring electrode.
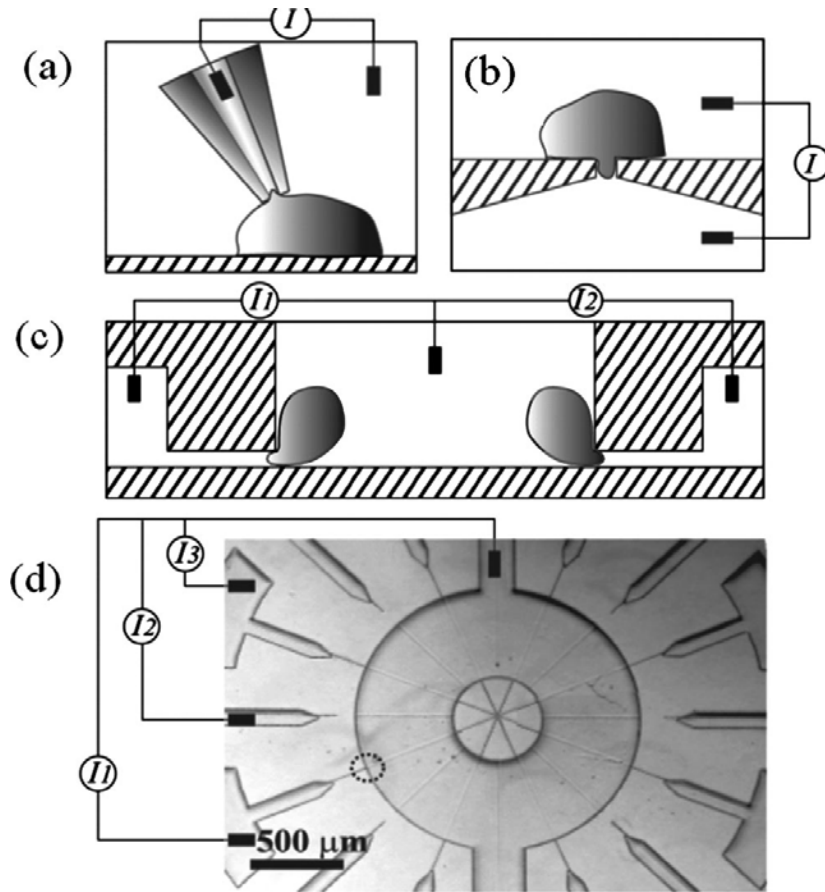
Fig. 1.5. Comparison of patch-clamp setups: (a). Traditional patch-clamp based on a glass micropipette. (b) On-chip planar patch clamp. (c) Microarray design with patch channels on the sides of a large central channel for cell delivery. A section containing two patch sides is shown. (d) Top view of the patch-clamp array device showing the center channel and 14 radial patch channels. The connectivity of the reference electrode and three of the patch electrodes is shown schematically. The small circle indicates one of the patch sites. (Seo and others 2004)

As depicted in Fig. 1.5. , considerable research has been done to develop a patch-clamp on a chip device by microfabrication techniques. The strategy employed is to apply a suction pressure (about 2Psi) to form the seal between the cell and an aperture. The design has varied from planar-chip form (Fig. 1.5.b) to lateral patch (Fig. 1.5.c).

A microfluidic based dynamic single cell capture array that allows both arrayed culture of individual adherent cells and dynamic control of fluid perfusion with uniform

environments for individual cells has been developed without any surface modification strategy (Carlo and others 2006). The device consists of arrays of physical U-shaped hydrodynamic trapping structures with geometries that are biased to trap only single cells as shown in Fig. 1.6.
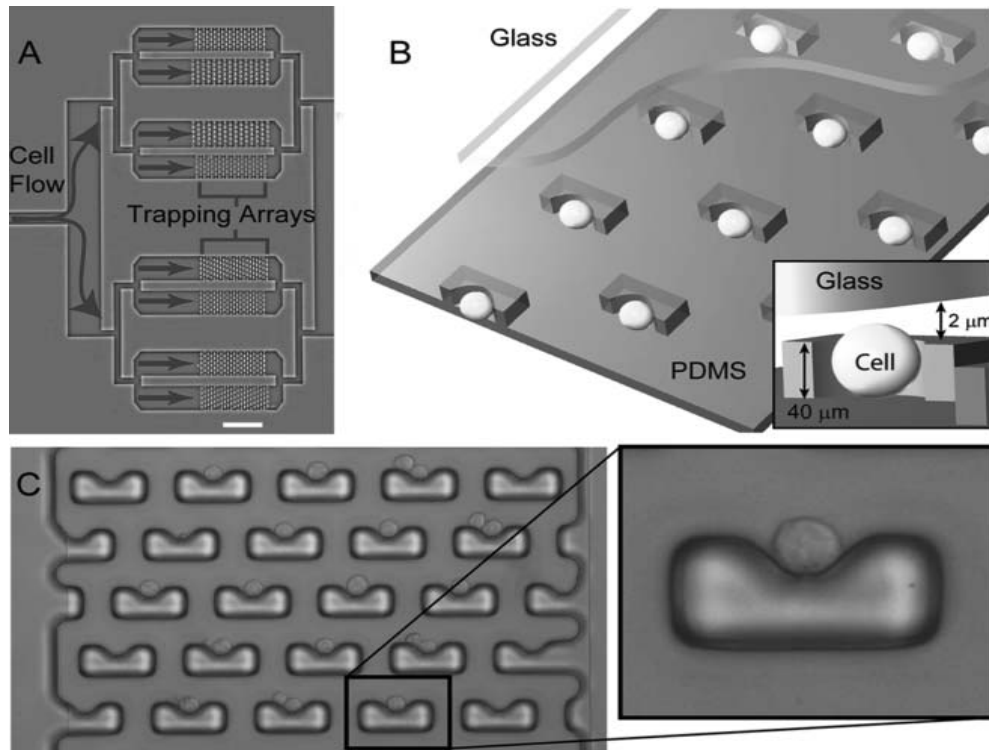
Fig. 1.6. Single cell trapping arrays (Carlo and others 2006).

The branching architecture and trapping chambers with arrays of traps are shown in Fig. 1.6.A. Cell and media flow enters from the left and enters the individual trapping chambers where it is distributed amongst the individual traps. Traps are molded in PDMS and bonded to a glass substrate. Trap size biases trapping to predominantly one or two cells.
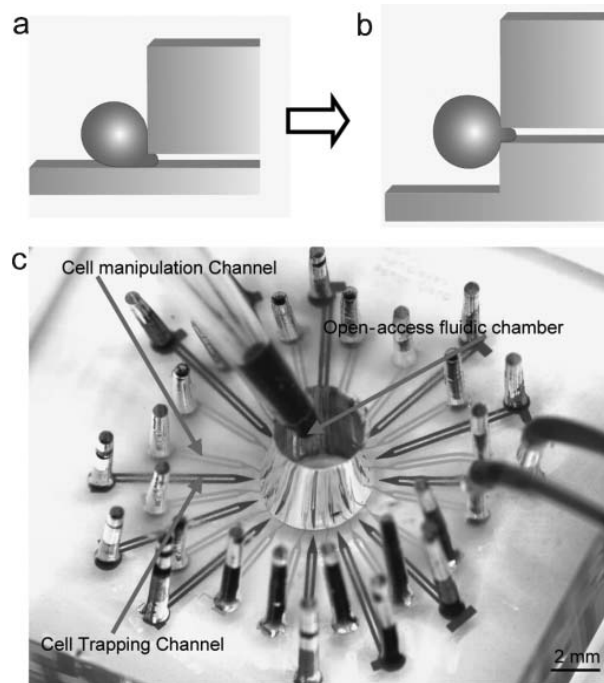
Fig. 1.7. (a) Cross-sectional illustration showing how the cell is trapped in an earlier design (Seo and others 2004) (b) Cross-sectional illustration showing an improved design of cell trapped in the device. (c) Angled view of the device. Patch channels and cell manipulation channels were filled with two different dyes. The open access chamber is shown in the image, where cells or drug samples can easily be pipetted in. (Lau and others 2006)

Lee and others (2004) have worked on single cell capture for patch clamp on a chip. They improved over their earlier design since it yielded unnatural deformations to the cells when they are being trapped at the trapping site (Fig. 1.7 (a)). The proposed method circumvents the problem by combining a regular PDMS microdevice processing method with a macroscale punching approach. The novelty in this fabrication process is that the melded PDMS channel is bonded onto a thin PDMS membrane. Afterwards a 4 mm hole- puncher is cut through the device vertically, opening up the micro-channels while creating an open-access fluidic chamber. The channel opening created with this method is raised above the flat substrate, giving a patching site comparable to the

traditional micropipette setting (Lau and others 2006). Fig. 1.7 (c) shows the device at an angled view, and demonstrates how solution can be supplied into the open chamber simply through a pipette tip. The open access chamber is also compatible with the common solution perfusion set-up developed for traditional patch-clamp. In fact, most equipment set-up described here is similar to the traditional patch-clamp set-up. The major difference is that instead of interfacing the electrode to a glass micropipette, the electrode is interfaced through PTFE (Polytetrafluoroethylene) tubing to the device. This simplifies the patch-clamp system architecture by eliminating all the micromanipulation tools and the requirement for a vibration-free environment.

A different approach uses an array of Si nozzles to replace glass pipettes (Lehnert and Gijs). The Si nozzles at the top interact with the cell membrane to form a gigaseal by application of negative pressure through the bigger opening at the bottom. The Si/SiO_2 microstructure itself is shown in Fig. 1.8 (b). A SiO_2 tube extends from a top-side pit in the chip to a larger backside hole (Fig. 1.8 (c)). The SiO_2 tubes can be realized with an inner diameter of 1 to 2 μm by means of deep reactive ion etching (DRIE). However, the biocompatibility of Si over the regular borosilicate glass pipettes is questionable.
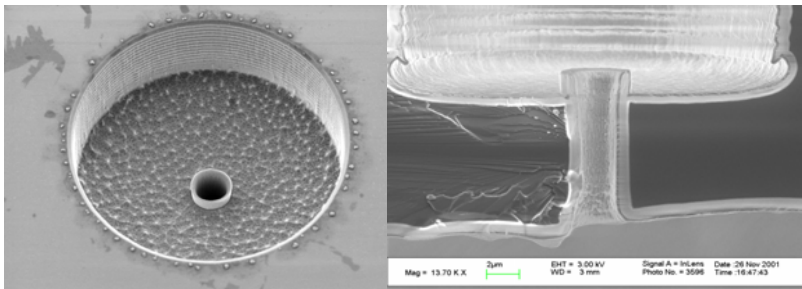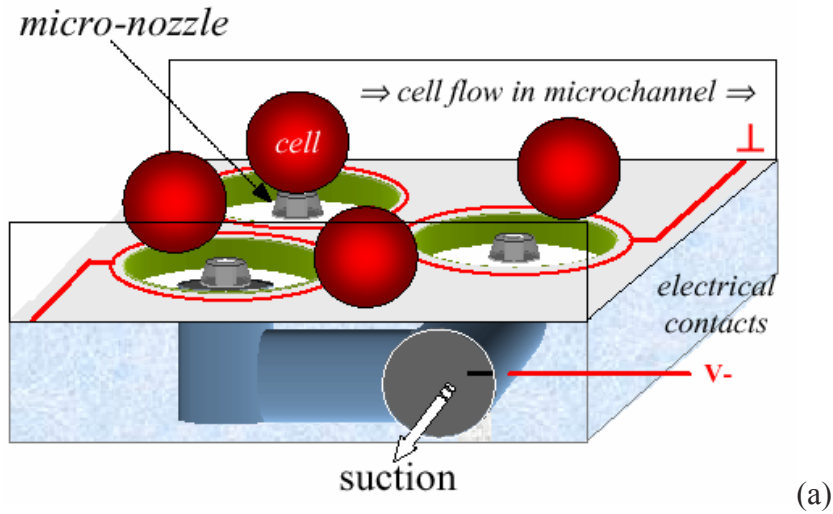
Fig. 1.8. Schematic representation of the patch-clamp microsystem with an array of Si nozzles (Lehnert and Gijs)

Lee and others (2004) have developed a newer technique of individual cell attachment over gold electrodes which employ electric field-directed adhesion and its use for the rapid capture and chemical activation of living single cells in a microchip (Toriello and others 2003). The approach is to label the cell surface with thiol functional groups using endogenous receptors to the cell adhesion peptide sequence RGD.
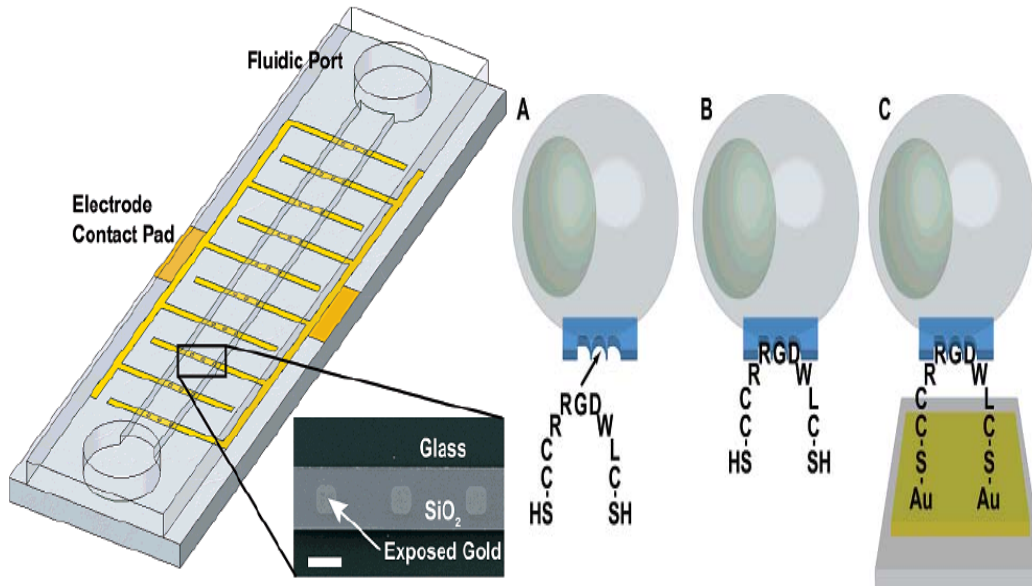
Fig. 1.9. Schematic of cell capture array on surface modified Gold (Toriello and others 2003)

The cell capture system is comprised of interdigitated gold electrodes microfabricated on a glass substrate within PDMS channels. The cell surface is labeled with thiol functional groups using endogenous RGD receptors, and adhesion to exposed gold pads on the electrodes is directed by applying a driving electric potential. Multiple cell types can thus be sequentially and selectively captured on desired electrodes. Single-cell capture efficiency is optimized by varying the duration of field application. The results demonstrate the ability to direct the adhesion of selected living single cells on electrodes in a microfluidic device and to analyze their response to chemical stimuli.

A noteworthy approach to measuring exocytosis signals from cells could be the use of aligned MWCNTs (multi-walled carbon nanotubes) as nanoelectrodes (NE) (Li 2005). CNTs are a family of materials consisting of seamless graphitic cylinders with

17

extremely high aspect ratios. By applying an electric field perpendicular to the substrate, these CNTs can be aligned perpendicularly (Fig. 1.10).

(a)   (b)
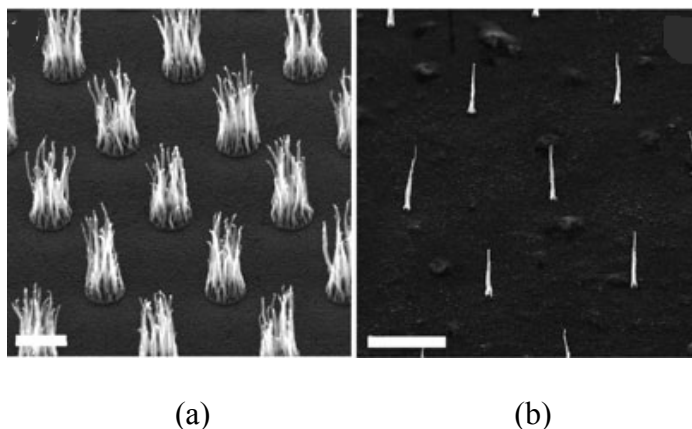
Fig. 1.10. SEM images of array of MWNTs at UV-lithography and e-beam patterned Ni spots respectively [Scale bars (a) 2µm (b) 5µm] (Li 2005)

The structure of these MWCNTs resembles a series of bamboo-like closed graphitic shells along the tube axis, which is due to the fact that the graphitic layers are not perfectly parallel to the tube axis. These behave as nanorod electrodes with a large active surface area. Although the closed graphitic shells bring about a high electrical resistance but are advantageous from the measurement perspective because of their ability to prevent electrolytes from seeping into the hollow channel at the core thereby reducing the background noise. Each nanotube is isolated from others by surrounding dielectric SiO_2 matrix. Electrochemical analysis performed with analytes 1mM $K_4Fe(CN)_6$ and 1M KCl have rendered these nanoelectrodes as highly conductive and sensitive. Various surface modifications have been done to selectively functionalize the tips of the MWCNTs and prevent non-specific adsorption to the surrounding SiO_2.

1.5. Biomaterials

The interface between biological systems and engineered materials is a key element in biomedical engineering. Any substance (other than a drug) or combination of substances synthetic or of natural origin, which can be used for any period of time, as a whole or as a part of a system which treats, augments, or replaces any tissue, organ, or function of the body can be defined as a biomaterial.
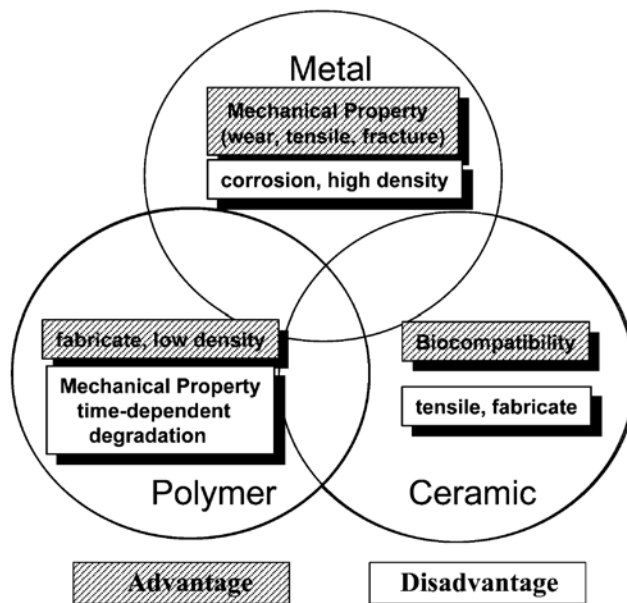
Fig. 1.11. Intrinsic properties of materials (Lee and others 2002)

1.5.1 DLC as a Biomaterial

Diamond like Carbon (DLC) has been widely studied as a potential biomaterial. The principal factors that make it a commendable biomaterial are high hardness, high

density, low friction coefficient, chemical inertness, high thermal conductivity, visual transparency, and biocompatibility.

Because of its favorable properties as a biomaterial, DLC has found applications in rotary blood pumps, artificial hearts, mechanical heart valves, and coronary artery stents apart from being the best proven tribological material for metal hip and knee joints [Fig. 1.12].

Fig. 1.12. DLC-coated femoral head (left) knee implant (right) (Huang and others 2004)

Though it is tagged ''diamond-like'', DLC is not alike crystalline diamond for it is black, not as hard, and is virtually amorphous (Dearnaley and Arps 2005). Its microstructure allows the incorporation of other species, and DLC comprises a family of such materials, the properties of which can be tailored far more readily than those of diamond. Hydrogen is frequently present in amounts up to 40 atomic %, occupying regions of low electron density in the matrix. Its presence strongly influences the mechanical and tribological behavior of DLC coatings. Other additives often introduced include nitrogen, silicon, sulfur, tungsten, titanium, or silver.

As is well known, carbon–carbon interatomic bonds can be of two types: the near-planar trigonal or sp^2 form found in graphite, or the tetragonal sp^3 variety that occurs in diamond. It is the three-dimensional character of sp^3 bonding, together with the strength of the short C–C covalent bond that gives diamond its great strength. DLC is intermediate in that it contains both types of bonding and clearly it is harder and more brittle if the $sp^3 : sp^2$ ratio is high.

Many methods have been developed for the deposition of DLC coatings, from a variety of carbonaceous precursor materials (Dearnaley and Arps 2005). They include direct ion beam deposition, pulsed laser ablation, filtered cathodic arc deposition, ion beam conversion of condensed precursor, magnetron sputtering, RF plasma-activated chemical vapor deposition and plasma source ion implantation and deposition. In this work magnetron sputtering was used for depositing DLC. A drawback of undoped DLC films prepared by sputtering is that they are not highly conductive because of the presence of diamond-like sp^3 hybridized state. One approach to increase conductivity of DLC has been to nitrogen dope in-situ during the deposition process. The increase in the conductivity with nitrogen is believed to be due to the process of sp^2-bonded carbon clustering (Gupta and others 2002) and/or introduction of midgap states within the gap which help to downshift the Fermi level or open the conduction band. Likewise, post-annealing can also further increase the conductivity attributed to the clustering phenomenon mentioned above, but this treatment leads to poor adhesion of the film to a glass substrate. A second approach was to deposit DLC:N on top of a highly conductive layer such as chromium or indium tin oxide (ITO), which offers the additional advantage

of being transparent. Transparent electrodes are desirable because they allow visualization of cells sitting on top of electrodes using conventional inverted microscopes.

Prior research shows that DLC can well be used to coat implants without triggering any inflammatory reactions invivo. Invitro experiments have yielded no activation of platelets on DLC and has been deemed highly haemocompatible (Nurdin and others 2003). These platelets have not morphologically spread out their pseudopodia as observed on other materials. The morphological behavior of osteoblasts cells on DLC coatings in vitro has also been studied by Du et al (Du 1998). They found that after a period of 2 weeks, the cells attached, spread, and proliferated on the DLC-coated surfaces without apparent impairment of cell physiology. The effect of DLC coating on cellular metabolism was studied by measuring the production of three osteoblast-specific marker proteins: alkaline phosphatase, osteocalcin and type 1 collagen. The presence of DLC films had no adverse effect on these measured parameters. In vivo studies of DLC coated cobalt-chromium cylinders implanted in intra-muscular locations in rats and transcortical sites in sheep for a period of 90 days were well tolerated confirming no signs of toxicity (Allen and others 2001a). Linder et al. (Linder and others 2002) reported on the biocompatibility of DLC coating with respect to adhesion and activation of primary human monocytes and macrophages in vitro and concluded that DLC coatings did not enhance therefore would not be expected to enhance inflammatory responses in vivo (Linder and others 2002). For application in heart valve prostheses, DLC-coated titanium surfaces were reported to reduce protein adsorption and platelet attachment suggesting

good in vivo hemocompatibility properties (Jones and others 2000). These coatings have been found to decrease thrombogenicity in coronary stent implants by reducing the release of metal ions in the blood (De Scheerder and others 2000; Gutensohn and others 2000).

The response of glial cells and fibroblasts on DLC has been quantified (Singh and others 2003). They have demonstrated that these cells spread and attach comfortably as expected. Similar studies with platelets, macrophages and neutral granulocytes has also been done (Li 2002) to demonstrate that high energy ion bombardment to DLC leads to more sp^3 bonds making it more hydrophobic and decreasing cell attachment as compared to low energy bombarded DLC.

Studies have also been done with Platinum or Titanium doped DLC to enhance conductivity of DLC to incorporate electrical conductivity and biocompatibility at the same time. Various types of cells have been observed for their response to DLC attachment in the past and this work has been carried out on primary bovine chromaffin cells as well as INS-1 cell lines to add to the ever growing list. A detailed review of DLC as a biomaterial as tested on various cell types as osteoblasts, macrophages, fibroblasts, glial cells, platelets, monocytes, endothelial cells can be found in the bibliography. (Alanazi and others 2000; Allen and others 2001b; Chai and others 2008; Chen and others 2002; Cui and Li; Du 1998; Jones and others 1999; Jones and others 2000; Kelly and others 2008; Li 2002; Linder and others 2002; Nurdin and others 2003; Okpalugo and others; Okpalugo and others 2004a; Okpalugo and others 2004b; Singh and others 2003; Yang and others 2003; Yokota and others 2006)

CHAPTER 2

CELL ATTACHMENT-
Literature Review

Cell adhesion is a widely researched field in biological sciences. It deals with the study of cell interaction with each other, with tissue, with extra-cellular matrix (ECM) or with material surfaces. Most eukaryotic cells must adhere to other cells or to the ECM to function properly in vivo. This tendency is followed suit invitro when they are subjected to interaction with biomaterials. Such interactions and adhesion dynamics are required to be understood in a variety of biomedical applications. Depending on the application, promoting or inhibiting cell adhesion to biomaterials may be required. Tissue engineering applications are influenced by adhesion because adhesive events are involved in differentiation, migration, and ingrowth within natural or synthetic polymeric scaffolds. In the scope of this work, the point of interest is cellular attachment to material surface to explore cell attachment response.

2.1. Protein Adsorption on Surfaces

Proteins are made up of a linear chain of amino acids which have a highly ordered structure composed of hydrogen bond stabilized α-helices and β-sheets. These intramolecular hydrogen bonds reduce the rotational mobility of bonds in the polypeptide chain and hence the entropy of conformation (Lord 2006). Structural rearrangements affect protein surface interactions and hence cell attachment. An important finding in this context of cell attachment has been that proteins in aqueous medium adsorb as

monolayers on surfaces quickly (Horbett 1996). The rapid adsorption of proteins from serum effectively translates the structure and composition of the foreign surface into a biological language decipherable by the cells and thereby respond, contributing to the ultimate outcomes in both implantation and tissue culture situations. The thickness of this adsorbed protein monolayer is approximately in the range of (1-10nm) (Castner and Ratner 2002). Upon adsorption proteins may undergo conformational changes due to their low structural stability revealing previously hidden binding sites or disruption of binding sites. The inherent tendency of the proteins is to unfold and allow further bonding with the substrate (Horbett 1994).
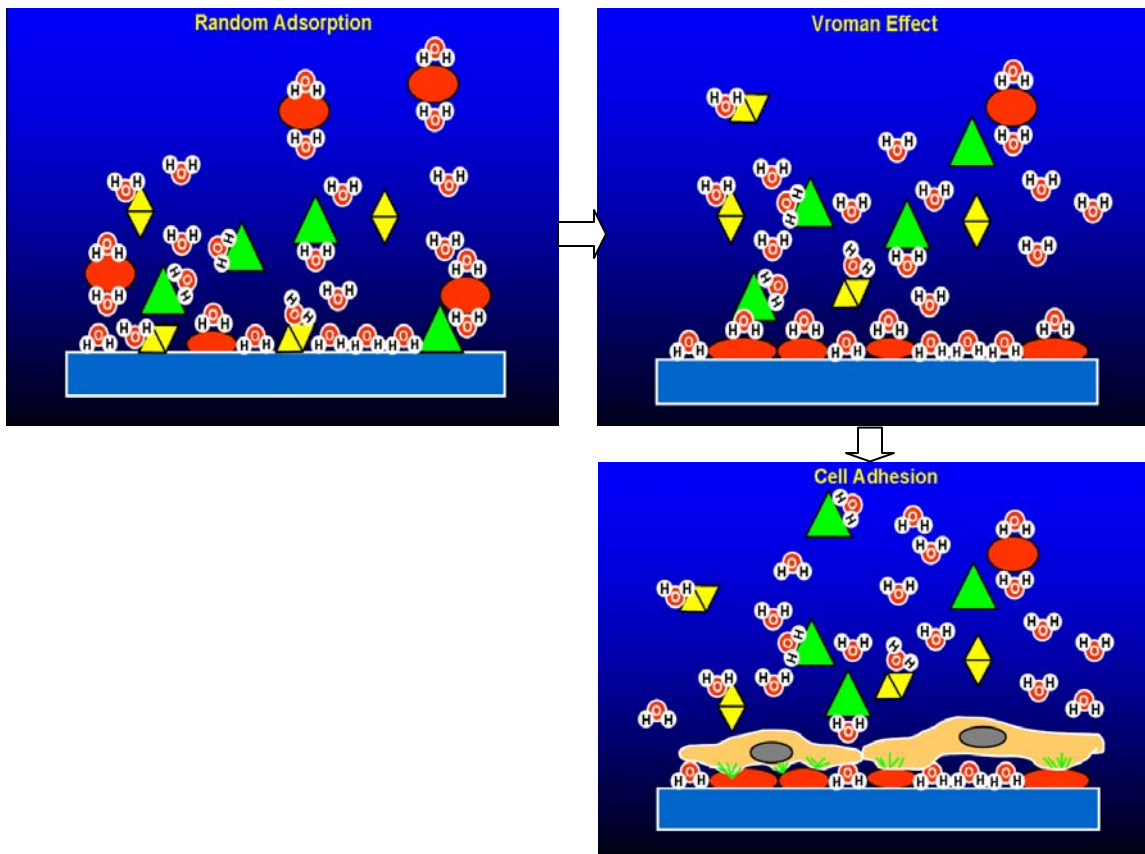
Fig. 2.1. Sequence of protein adsorption events leading to cell attachment

(Produced from online lectures with permission from Dr. Manfred Maitz)

25

In case of multi-protein mixture present in the medium, which is mostly the case, a competitive process occurs between the different proteins for adsorption to the surface (shown in Fig. 2.1). This phenomenon is called Vroman effect (Holmberg and others 2008; Vroman and others 1982; Vroman 1987). The first important factor that influences the adsorption of proteins from the multi-protein medium is that the mass transfer rate of a given solute molecule to a surface is directly related to its solution concentration and inversely related to its molecular weight (Latour 2004).

Formation of such a protein layer can thus be envisioned as a 'cushion' for the cells and formation of such a cushion could be a function of surface roughness, surface energy and charge. Cells spread out their membrane into pseudopodia on a surface if they have a continuous protein monolayer adsorbed onto it. Moreover, the protein monolayer should also have receptor binding sites exposed to the cells; else cell binding will not take place. Once the cells attach and begin to settle comfortably, they synthesize their own matrix molecules to maintain adhesive interactions with matrix proteins in an attempt to ensconce to their newly found environment.

2.2. Cell Membrane Structure and Biochemistry

Cells are limited by an outer cell membrane which is made up of phospholipid bilayer with various proteins embedded into it as shown in Fig. 2.2. The various proteins in the cell membrane are transport proteins, channel proteins, carrier proteins, gated channels, receptor proteins and recognition proteins. The receptor proteins are of special interest in this context to establish a relation to cell attachment.
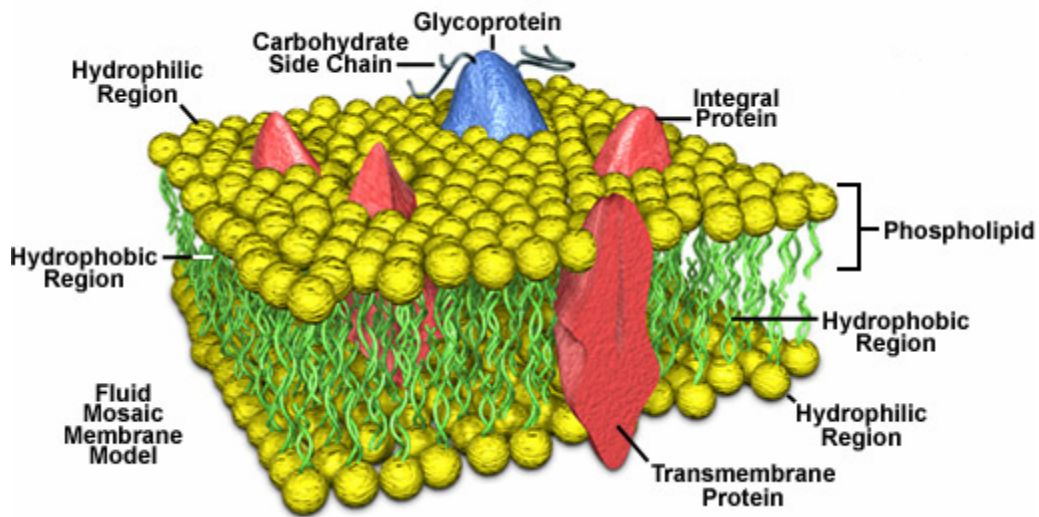
Fig. 2.2. Structure of Cell membrane

Adhesion of cells occurs to the protein 'cushion' monolayer (as described in Section 2.1) based on non-covalent receptor-ligand interactions resulting in the receptors undergoing a number of functional changes followed by subsequent initiation of signaling events. While binding takes place on the extracellular region, a chain of intracellular cytoskeletal machinery is triggered to enable the cell to undergo spreading onto the substrate.

There exist 5 classes of adhesion molecules namely cadherin, immunoglobulins (Ig) superfamily, integrins, selectins and mucins. Adhesion among these molecules is of two types- homotypic and heterotypic. Homotypic refers to adhesion between two similar adhesion molecules as cadherins adhering to cadherins while heterotypic is between an adhesion molecule and extracellular matrix proteins as integrins binding with ECM proteins fibronectin, collagen or laminin. Cadherins are mainly involved in cell to cell

adhesion being specific to given tissues. The Ig superfamily molecules are involved in both homotypic and heterotypic forms of adhesion. Selectins are adhesion proteins that bind to mucins- adhesive molecules with adhesive region as carbohydrate. Selectins play a major role in initial attachment of leukocytes to the endothelium. Heterotypic adhesion is the subject of interest in this dissertation because an attempt is being made to correlate cell attachment quantification studies to different electrodes wherein serum protein adsorption is involved. These proteins create the ECM environment for the cells to interact with, therefore the more viable the protein adsorption, the better the cell attachment to the electrode material.

Integrins are made up of two chains, α and β. The twenty different arrangements between the various α and β chains result in the binding of integrins to a wide variety of ligands, regulated by calcium binding.

2.3. Cell Attachment

When cells in suspension medium are dropped over a substrate, the membrane receptors bind non-covalently to the protein ligands adhered to the material surface. When cells attach, the ligands and receptors diffuse in the plasma membrane and react in the small region of contact. The sequence of events taking place at such region of contacts is depicted in Fig. 2.3.
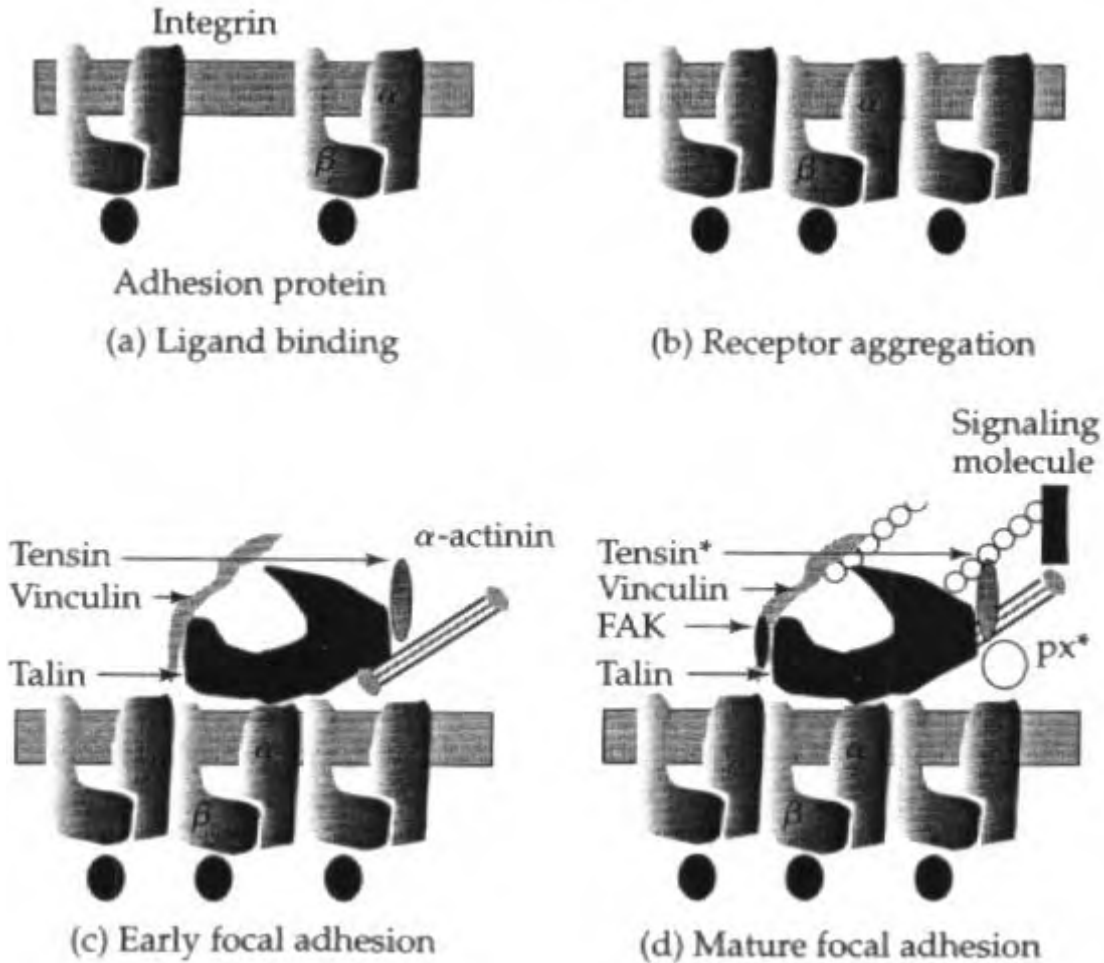
Fig. 2.3. Sequence of events at region of cell attachment (Truskey and others 2004)

Following ligand binding, the receptors aggregate by decrease of inter-receptor distance. Biesalski et al have proposed a universal length scale of 58–73nm, i.e. distance of individual integrins, as optimum for integrin clustering and activation (Biesalski and others 2006). The clustered integrin receptors then bind α-actinin, tensin, talin, and vinculin to their cytoplasmic portions. Subsequently, Focal adhesion kinase (FAK) binding and tyrosine phosphorylation stimulate the interaction of cytoskeleton and signaling molecules with focal contact proteins. The actin filaments synthesized by the

intracellular machinery bring about changes in shape of the cell becoming more oblong and spread out with pseudopodia formation (Fig. 2.4).
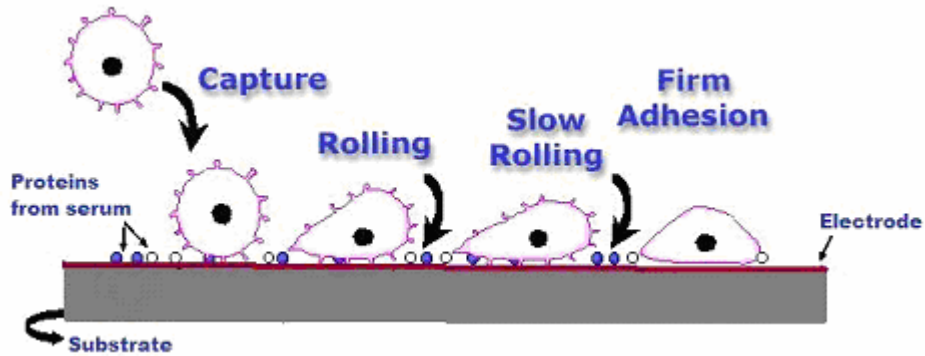
Fig. 2.4. Cell adhesion cascade

(Image Courtesy: http://bric.postech.ac.kr/webzine/plan/foreign_iv/images/kcib-8-1.gif&imgrefurl)

Fig. 2.4 is inspired from leukocyte rolling and attachment to endothelium (Chang and others 2000; Lawrence and others 1997; Lawrence and Springer 1991). The same mechanism of attachment can be visualized for any other cell interacting with a surface. The whole process consists of 4 phases: cell capture, rolling, slow rolling and firm adhesion. First, the cell gradually approaches the surface which has been covered with proteins, the mere cell contact termed as capture. Secondly, surface interaction involves the search of a suitable site for ligand-receptor binding, which once attained tethers the cell at the site. Once a tether is formed, the cell rolls further although not detaching from the tether and culminates in firm adhesion by spreading of the tether into pseudopodia.

2.4. Fibronectin and RGD

Fibronectin (FN) is one of the major ECM proteins playing an active role in hemostasis, cell migration, proliferation, phagocytosis, thrombosis, embryogenesis in vivo. It is a glycoprotein that promotes attachment of cells to the surface of the substrate or biomaterial (Sousa and others 2005). Fibronectin does not undergo displacement by other serum proteins and is known to displace other bound proteins from the substrate surface thereby bringing about Vroman effect phenomena as described in Section 2.1. Each Fibronectin monomer is composed of three different types of protein modules F1, F2 and F3 (as shown in Fig. 2.5.) which have been found in several other proteins also (Potts and Campbell 1996).
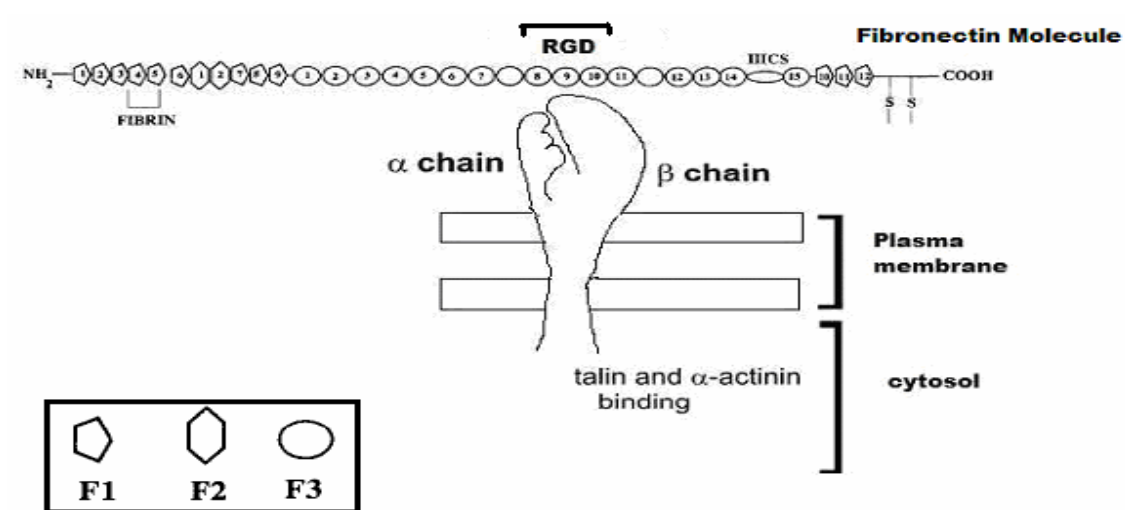
Fig. 2.5. Schematic representing binding affinity of Fibronectin ligand with $\alpha_5 \, \beta_1$ receptor (Potts and Campbell 1996; Siebers and others 2005)

Integrins have affinity for specific binding sites within the ECM protein and do not bind nonspecifically. The most common binding site is the tripeptide amino acid

sequence RGD and nearly half of the over 20 known integrins recognize this sequence in their adhesion to protein ligands. Although the primary integrin dependent cell binding site has been detected on [10]F3, it is supplemented for the cell binding activity by 'synergistic sites' [8]F3 and [9]F3, without which, the cell adhesive activity is decreased (Obara and others 1988; Potts and Campbell 1996). RGD sequence has also been found on various other proteins as vitronectin (VN), fibrinogen, von Willebrand factor, entactin, thrombospondin, and collagen (Yamada 1991) each of which can bind to one or more integrins (Hautanen and others 1989). $\alpha_5\beta_1$ is one such integrin receptor found widely to have high affinity to RGD sequence on FN (Fig. 2.7) while $\alpha_V\beta_3$ is a similar integrin for VN (Ruoslahti 1996a).
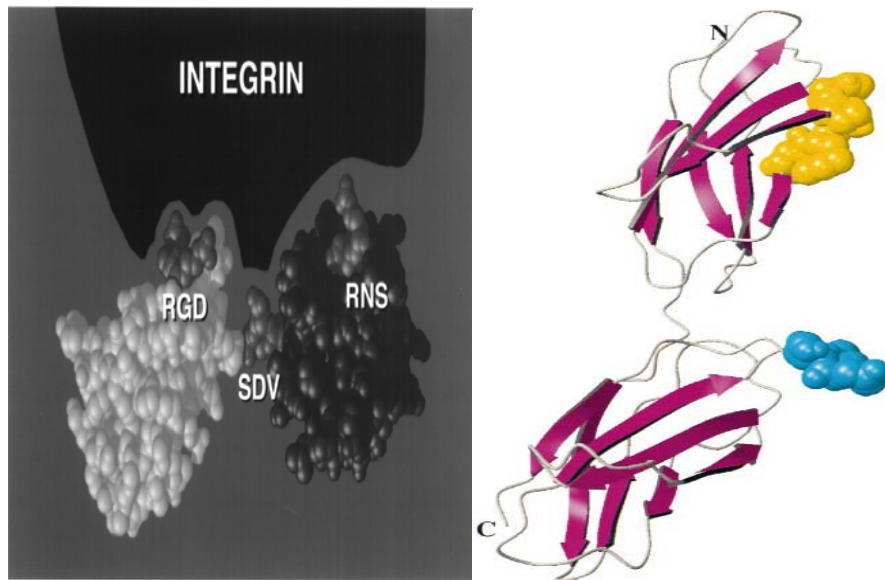
Fig. 2.6. A model for the recognition of the fibronectin RGD site and auxiliary sites by an Integrin NMR studies have shown that the RGD region and the relative orientation of these two domains are not very well defined. The two sites that have been shown by mutagenesis to interact with integrin binding sites are shown; the PHSRN sequence (in yellow) on the ninth F3 module and the RGD sequence (in cyan) on the tenth F3 module (Campbell and Downing 1998; Ruoslahti 1996b)
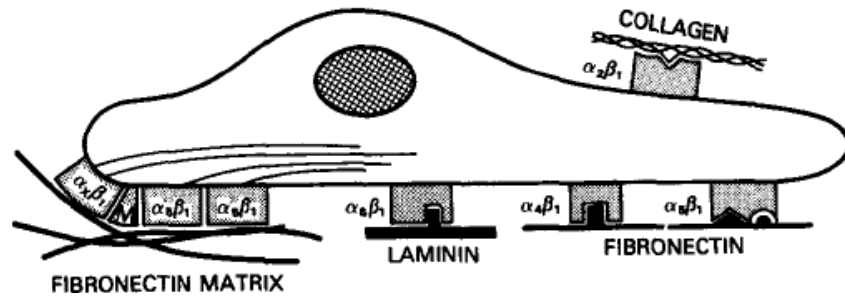
Fig. 2.7. Different receptors are present on the cell membrane to bind to different ligands/proteins (Yamada 1991)

Fibronectin has been widely found to be a cell adhesion promoting factor. Exhaustive research on different types of cells as platelets or osteoblasts has repeatedly proven that cells have an affinity to Fibronectin and its inherent RGD sequence. Coating a substrate with FN or with RGD peptides enhance cell adhesion. Cells need freedom and levity to spread and be motile in order to adhere, which is possible only when the RGD motifs are accessible or exposed to receptors for binding (Siebers and others 2005). Although, integrin receptors do not bind non-specifically, many of them have also exhibited "promiscuous" behaviour in their affinity to ligand binding sites (Horbett 1994). Integrin receptors $\alpha_5\beta_1$ and $\alpha_{5v}\beta_3$ competitively bind to RGD-sites of fibronectin.
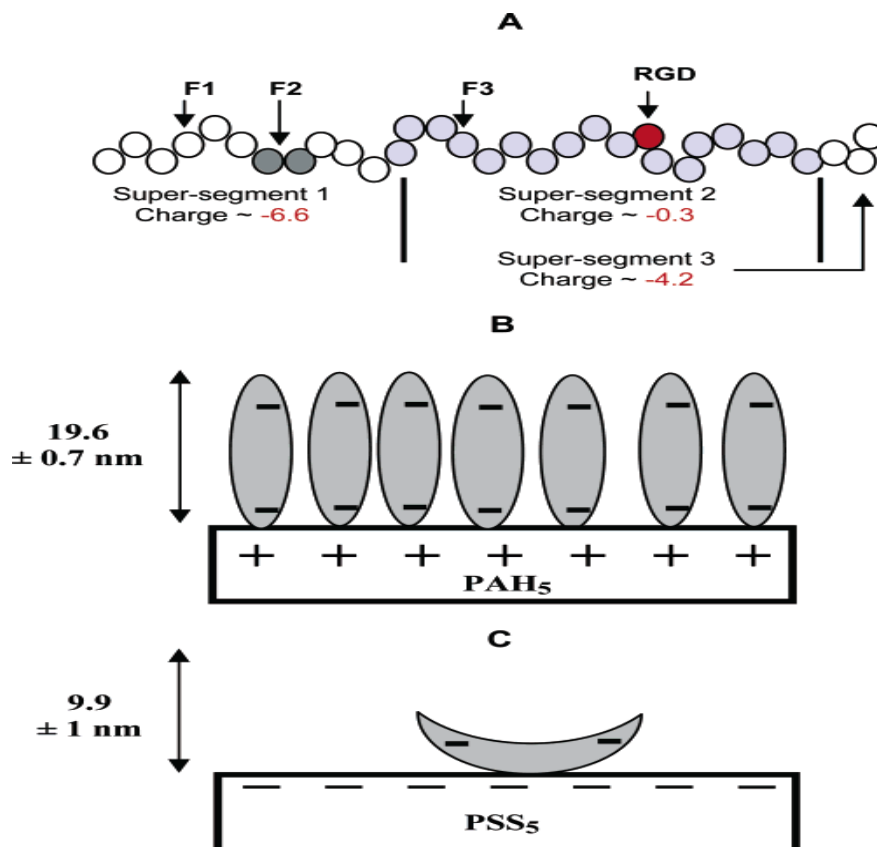
Fig. 2.8. Schematic of the modular FN molecule with charge distribution based on constituent amino acids at pH 7.4 (Ngankam and others 2004)

As shown in Fig. 2.8A it can be surmised that the modular FN is made up of three adjacent supersegments carrying approximate charges of -6.6, -0.3, and -4.2 on the basis of the known charges of the constituent amino acids at the buffer pH. It can be seen that the end segments carry strong negative charges whilst the middle segment is close to being neutral. Thus, if FN were to adhere to a positively charged surface it would adsorb in a nearly linear or vertical conformation (Fig. 2.8B) while in a V-like conformation on a negatively charged surface (Fig. 2.8C). In context to our application, it can be contemplated that modifying the surface with polylysine results in a positively charged

surface as shown in Fig. 2.8 B thereby promoting protein adsorption from the serum in a configuration that presumably promotes cell attachment.

2.5. Factors Affecting Protein Adsorption

Having understood the mechanism of cell attachment and also the biomolecular machinery driving it, the intriguing question now arises as to what could be the parameters influencing the protein adsorption on the electrode surface. This again is a heavily researched topic, although this process remains incompletely understood. While surface energy as a factor of hydrophilicity or hydrophobicity has been put forward as an obvious rationale, it has not been conclusive. Effects of surface roughness and topography have been studied, as have the effects of charge and surface chemistry (Michael and others 2003).

Fig. 2.9. Cartoon depicting protein adsorption

Protein adsorption is a dynamic process involving noncovalent interactions, including receptor-ligand binding, hydrophobic interactions, electrostatic forces, hydrogen bonding, and Van der Waals forces. Apart from the parameters already

mentioned, protein characteristics including primary structure, size, and structural stability have been identified as key factors influencing the adsorption process. Adsorption-induced changes in protein structure and activity are not dominated by surface hydrophobicity alone.

2.5.1. Effect of Surface Topography

A number of studies have demonstrated that cells could "sense" surface topography at the micrometer scale (Cai and others 2006). Cai et al. also reported that the surface roughness had little effect on protein adsorption and cell proliferation on titanium materials with roughness values in the range of 2–21 nm.

Fig. 2.10. Probable cell pseudopodia behavior on rough surfaces (Miura and Fujimoto 2006)

Protein molecules are estimated to be of sizes around 10 nm. Although nano-scale will be too small and is unlikely to affect protein adsorption (Cai and others 2006), micro-scale roughness may influence the way proteins form the monolayer on the surface. As shown in Fig. 2.10, it can be contemplated that the pseudopodia invaginates into the surface grooves which is possible if the serum proteins have formed a sheath inside the grooves. It is also hypothesized that a rough surface, creates a wavy protein

layer to form which will have higher surface area exposed for receptor binding, thereby increasing cell attachment.

2.5.2. Effect of Surface Chemistry and Charge

It is intuitive to believe that electrostatic forces play a role in protein adsorption. Since fibronectin has a negative charge, it might be hypothesized that a positively charged surface will enhance cell adhesion. However, surface charges present are shielded by hydrating water, modulated by pH and counterbalanced by small ions (Wilson and others 2005). In addition, the presence of ions such as Na^+, K^+, Ca^{2+} and Cl^- result in the formation of an electrical double layer at charged surfaces. It has been found that a slight positive potential applied to ITO (Indium Tin Oxide) results in higher attachment of rat marrow stromal cells as compared to control glass substrate (Qiu and others 1998). However, the cells do not spread out on positively charged ITO as should have been the aftermath of sound attachment although they do so on the control substrate. It appears that the cells have been forced to bind electrostatically without triggering the usual intracellular cytoskeletal machinery and therefore does not culminate in pseudopodia formation and spreading. Perhaps binding has not occurred at the integrin-RGD level.

Various surface modifications have been tried and it has been found that nitrided or aminated surface are cytophilic. It has been found that Integrin $\alpha_5\beta_1$ shows a strong affinity to −OH and −NH2 surfaces, whereas $\alpha_5\beta_1$ and $\alpha_5v\beta_3$ bind also to −COOH but show poor binding capacities on −CH3 surfaces (Jäger 2007).

37

It has been observed that attachment of some cell types can be enhanced with polylysine adsorption to the surface (Mazia 1975; Sorribas and others 2001). Two different forms of polylysine are the dextro (d) and laevo (l) forms depending upon their chair conformations.
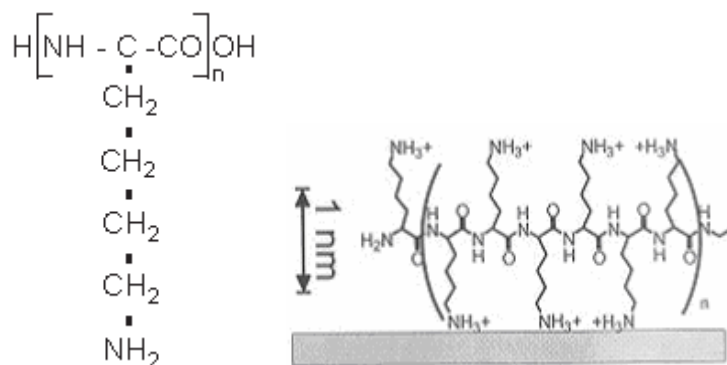
Fig. 2.11. Polylysine (Sorribas and others 2001; van den Beucken and others 2006)

I have observed more cell attachment to poly-d-lysine as compared to poly-l-lysine. This observation is only empirical and not statistically significant and there is no known difference in adsorption conformation of the two isomers on a substrate.

2.5.3. Effect of Surface Energy

Very hydrophilic surfaces (i.e., hydrogels or agarose) are not supportive of cell attachment and growth, and maximal cell adhesion has been reported on surfaces of

intermediate wettability. Surfaces defined as hydrophobic have contact angles exceeding 65º.

Xu and Siedlecki (2007) have found that there is a sharp transitional increase in protein adhesion on substrates with contact angle in the range 60º- 65º. Proteins adhere to moderately hydrophobic surfaces more than hydrophilic ones (Klebe and others 1981). Generally hydrophobic surfaces are considered to be more conducive to protein adsorption compared to hydrophilic surfaces owing to the strong hydrophobic interactions on the former, in contrast to the repulsive solvation forces arising from strongly bound water at the hydrophilic surface (Xu and Siedlecki 2007). Hydrophobic effects in an aqueous environment occur upon spontaneous dehydration by either protein or surface or both entities and aggregation of the non-polar components. Such interactions arise due to the tendency of water to exclude non-polar groups which results in a large increase in entropy of the water molecules released and hence a reduction in the Gibb's energy of the system. If both a protein and the contacting surface is hydrophobic, the entropic gain due to dehydration acts as a driving force for protein adsorption. However, this does not occur in case of superhydrophobic surfaces as Teflon thereby this rationale is subject to speculation. Conversely, if the protein and interface are hydrophilic, hydration of the surface is energetically favorable and removal of water from the surface via adsorption of the protein is not favored ($\Delta G > 0$) (Lord 2006).

Surface wettability is therefore not the only predictive parameter for cell attachment phenomenon to a substrate. The whole process is complex with other factors of protein size and structure interplay and Vroman effect. Observations regarding the

effects of surface wettability on protein adhesion have not always been consistent. Comparison between studies investigating the role of chemical functionalities in cell attachment and growth is complicated by the use of different cell lines, varying proteins in culture medium and different cell interaction protocols. Therefore, it is necessary to study cell adhesion under condition specific to this microchip application.

CHAPTER 3

MATERIALS AND METHODS

3.1. Cell Culture

3.1.1. Preparation of Bovine Adrenal Chromaffin Cells

Chromaffin cell preparation was modified from previously published protocols (Ashery and others 1999) and has been described in details in a recent paper by Yang et al (Yang and others 2007). Fresh bovine adrenal glands were collected from a local abattoir (Jennings Premium Meat, New Franklin, MO) within 30-40 minutes of death of the animal. The glands were cleared of surrounding fat and immersed in a Ca^{2+} - free and Mg^{2+}-free buffer solution (Buffer 1 solution, pH= 7.2, mOSM = 310) and placed in an ice bath while being transported back to the laboratory. Residual fat was trimmed off from the glands using sterile scissors in a sterile laminar flow hood. Blood inside each gland was rinsed out by injecting Buffer 1 solution into the adrenal vein opening by means of a 30 ml sterile syringe followed by gentle massaging of the gland to allow the solution to flow out. This step was repeated several times until the rinsed solution was free of blood. Collagenase P dissolved into Buffer 1 solution at a concentration of 1 mg/ml was injected into each gland through the opening of the adrenal vein in the gland. The glands were placed into a sterile beaker covered with aluminum foil and put in a 37°C shaking water bath for 8 min. This step was repeated once again to ensure good digestion. This collagenase digestion step allows separation of the inner medulla from the outer cortical

tissue. On a sterile petri dish, the gland was cut open using autoclaved scissors along the circumference of the cortex, to reveal the white gel-like medullary mass, which was peeled off and immersed into Buffer 1 solution in another Petri dish. The medulla was then thoroughly minced into small pieces using scissors. The medulla-containing Buffer 1 solution was filtered through a nylon mesh (70 μm opening). After filtration, the solution was centrifuged at 140g or 1000 rpm for 10 min at room temperature. The supernatant was aspirated and the pellet resuspended in 20 ml Buffer 1 solution. In another sterilized tube, Percoll gradient solution was mixed with a 10-fold concentration Buffer 1 solution in a ratio of 9:1 to make a solution with optimum physiological tonicity and pH of 7.2. The Percoll solution was mixed with the cell suspension in a 1:1 ratio and then centrifuged at 15,000 rpm for 30 min at 18°C. Following centrifugation, the Percoll gradient yielded 4 layers: dead cells in the top layer, norepinephrine and epinephrine secreting chromaffin cells in the middle two layers, and red blood cells in the bottom layer. The middle two layers were gently pipetted out and transferred separately to 50 ml tubes. For cell attachment experiments, only the epinephrine secreting cells were used since they were farther from the dead cell layer. Buffer 1 solution was added to fill the tube and the cell suspension was centrifuged at 1000 rpm for 10 minutes at room temperature. The supernatant was aspirated and the cell pellet was resuspended in Buffer 1 solution. Chromaffin cell culture media (containing 89% DMEM with high glucose, 10% FBS and 1% Penicillin; Invitrogen) was added in a 1:3 ratio into the cell suspension to help cells to adapt to normal Ca^{2+}-containing media. The suspension was centrifuged again at 1000 rpm for another 10 minutes at room temperature and the supernatant was removed. The cell pellet was resuspended in chromaffin cell culture media. Cell density

was calculated and cell solution was then diluted to a density of 10^6/ml (as described in Section 3.2) and preserved in a tube in an ice bath until further experiments were performed on the same day of culture.

3.1.2. INS-1 Cell Line Culture

The INS-1 cell line was established from cells isolated from an x-ray-induced rat transplantable insulinoma. These cells were a kind gift from C. Wollheim, University of Geneva, Switzerland, were maintained and prepared as described in (Asfari 1992; Yang and Gillis 2004). In short, these cells were maintained in culture media consisting of RPMI 1640 medium supplemented with 50µM 2-mercaptoethanol (Acros Organics), 2mM L-glutamine, 10 mM HEPES (from Life Technology, GIBCOBRL), 100 units/ml Penicillin, 100 g/ml streptomycin, 1 mM Sodium Pyruvate and 10% FBS (Fetal Bovine Serum). The cells were cultured in 25 cm^2 tissue culture flasks (manufactured by SARSTEDT) and incubated at 37ºC in 5% CO_2 -95% air. The medium was replaced every other day which is thrice a week and cells were subcultured once per week when they reached a 90-95% confluence level. INS-1 cells required for cell attachment studies were procured during subculture. During subculture, the medium was aspirated and 1 ml of Trypsin/EDTA (0.05% Trypsin with EDTA 4Na, 1X; purchased from Cell Core, MU) for digestion. After cells had detached, serum-containing medium was added to inactivate the trypsin. More cells are detached by triturating several times. The cell suspension was then centrifuged at 2000 rpm for 7 minutes followed by aspiration of medium and resuspension of pellet into fresh medium. The cell density was diluted to 10^6 cells/ml (as

described in Section 3.2) and preserved in a tube in ice till cell attachment experiments are performed on the same day.

3.2. Hemacytometer and Trypan Blue Assay

A hemacytometer (also spelled hemocytometer) is a device used for counting cells. It is an etched glass chamber with raised sides that hold a quartz coverslip exactly 0.1 mm above the chamber floor constituting the Neubauer ruled surface. An H-shaped moat forms two counting areas, or plateaus. A "V" groove acts as the loading side of each plateau facilitating cell suspension spreading by capillary action and reducing the possibility of overflow into the moat (Fig. 3.1). Volume of fluid is limited over a square mm at 0.1 mm^3 and over each of 400 squares (within the central square mm) to 0.00025 mm^3. Contact of the flat, polished cover glass surface with cover glass supports produces an exact volume of fluid over the counting area.
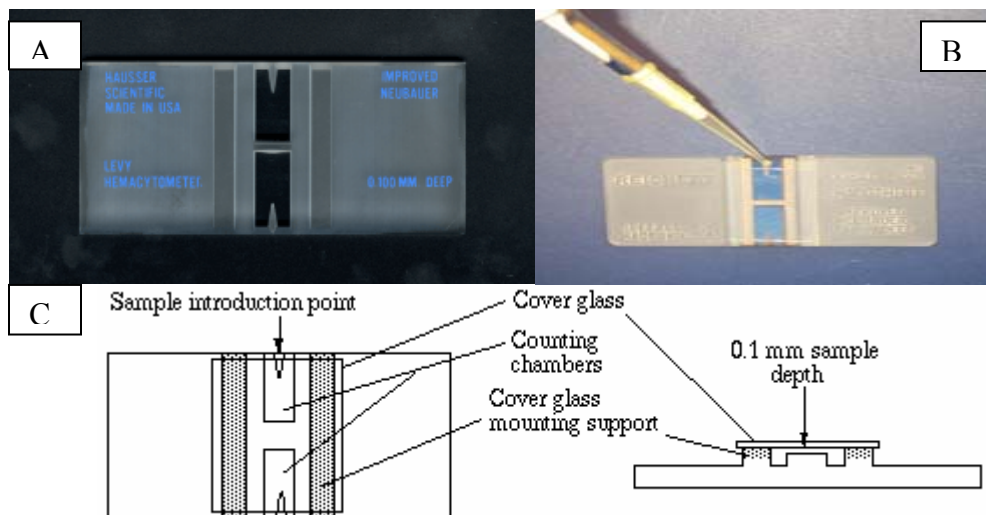
Fig. 3.1.(A).Hemocytometer (manufactured by Hausser Scientific) (B). Cell suspension loaded at V-groove (C). H-moat separates two counting chambers,glass cover-slip is 0.1mm above the ruled surface

The hemocytometer (manufactured by Hausser Scientific) has an important role to play in this work, being involved in determining cell density and aiding dilution to a fixed cell density over different sets of cell attachment experiments. 10µl of cell suspension is introduced into the V-groove of each counting plateau (Fig. 3.1.B). The counting area as seen under optical microscope is shown in Fig. 3.2.
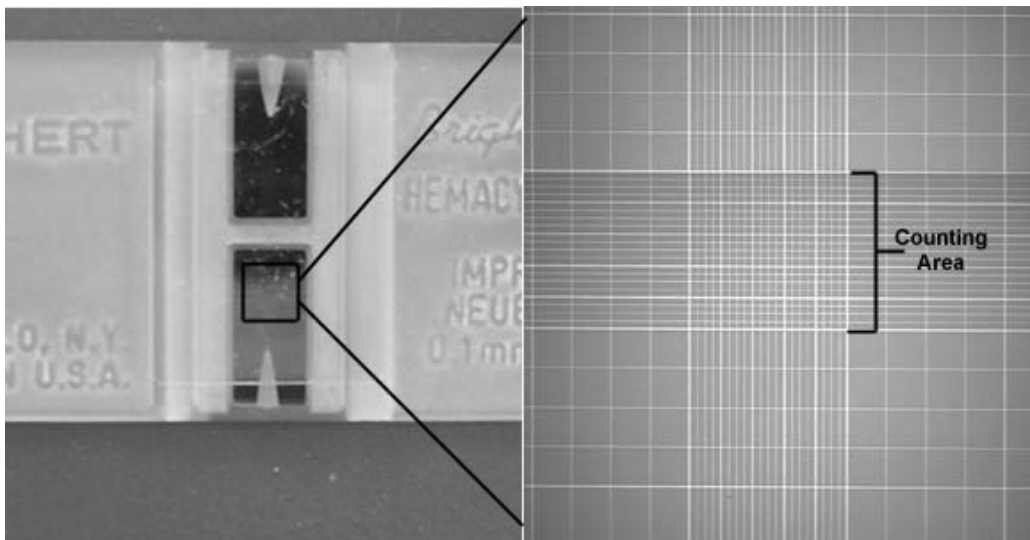
Fig. 3.2. Counting area on the hemacytometer

Two methods of counting protocols can be followed as represented in Fig. 3.3 (A,B).

Method A:

Cell are counted in the four regions marked 'W' and cell concentration is calculated as follows:

Cell concentration per milliliter = Total cell count in 4 squares x 2500 x dilution factor

MethodB:

Cell are counted in the large central square in the regions marked 'R' and cell concentration is calculated as follows:

Cell concentration per milliliter = Total cell count in 5 squares x 50,000 x dilution factor
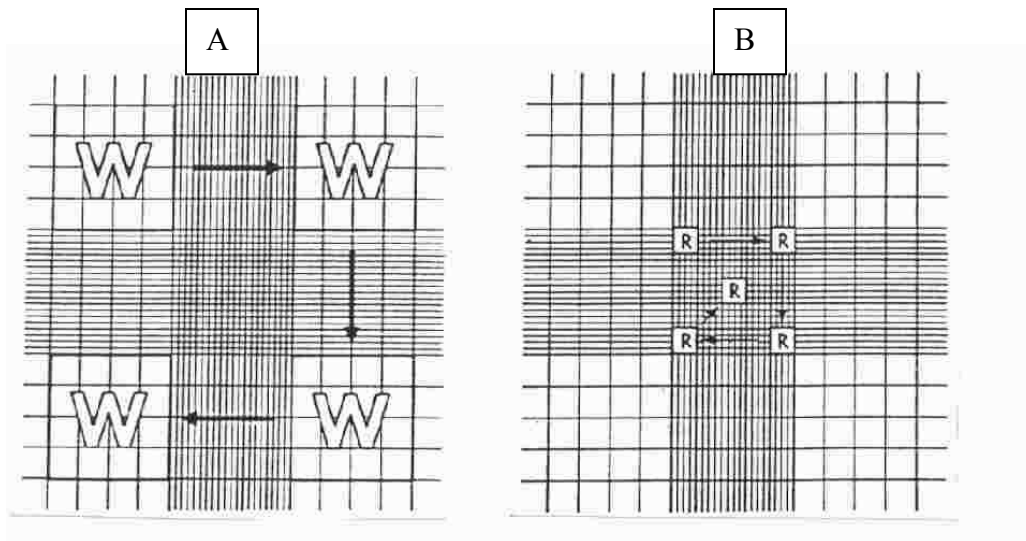
Fig. 3.3. Method A (left) and Method B (right) to count cells on the hemocytometer

Cell suspensions have been mixed with equal volume of Trypan Blue [0.4% (w/v) Trypan blue in PBS, purchased from Sigma] which stains the dead cell nuclei and enables excluding them while counting only viable cells and thereby increasing the accuracy of cell attachment data. The Trypan Blue works in staining by entering through the membrane of dead or ruptured cells. This method of cell counting is called Dye Exclusion method. 30µl of cell suspension was mixed in 1:1 ratio with Trypan Blue and kept at room temperature for 5 minutes followed by placing 10µl on each counting chamber of hemacytometer and visualized under upright microscope (Olympus

BX51W1) at 10X magnification. A camera (Axiocam MRc, Carl Zeiss) was used to take images of the four 1mm^2 regions (marked 'W' in Fig. 3.3.A) on both the counting plateaus. An average of both counts was concluded to be the cell count and appropriate amount of cell medium added to attain cell suspension density of 10^6 cells/ml.

3.3. Preparation of Substrates

Glass slides (1"x3"; Fisher Scientific) were used as substrates for all electrode depositions. The slides were cleaned by soaking in 3:1 mixture of Sulphuric acid and Hydrogen Peroxide, called Piranha Solution, for 10 minutes at room temperature followed by rinsing in 18.2 MΩ water and then blown dry with nitrogen. The slides were then taped onto a silicon wafer for deposition by magnetron sputtering.

3.3.1. Deposition of Different Materials by Magnetron Sputtering

The metal to be deposited as an electrode is fixed as target and depending upon the material, RF or DC power sources applied. The deposition chamber pressure is reduced to 10^{-4} Torr before the power source is switched on. Argon gas is let into the chamber and this leads to the formation of plasma. The plasma ionizes the target and directs them to the target.

For deposition of DLC on ITO, the conditions used for initial deposition of base layer ITO were RF power supply of 180W, Argon flow rate of 20 sccm at a substrate temperature of 50ºC under chamber pressure of 4mTorr. These conditions were

maintained for 20 minutes yielding an ITO layer of approximate thickness 100 nm. The DLC deposition involved switching over to a DC power supply of 400W, Argon flow rate of 15 sccm, Nitrogen flow rate of 5 sccm under the same conditions of temperature and pressure without having to break the vacuum. These conditions were maintained for 15 minutes and resulted in a DLC coating approximately 25 nm thick. The nitrogen flow is aimed at promoting cell attachment in accordance with popular belief and also to increase conductivity of DLC.

DLC doped with Titanium has been deposited to circumvent ITO deposition. For such films, the two targets were co-sputtered with DC power supply of 400W for DLC target and RF power supply of 42W to Titanium target at Argon flow rate of 20 sccm under chamber pressure of 4mTorr and substrate at room temperature.

Platinum was deposited by supplying RF power of 90W to the platinum target, Argon flow rate of 20 sccm under chamber pressure of 4 mTorr and ambient temperature. Gold deposition requires an adhesion layer of Titanium. This base layer was deposited by supplying RF power of 100 W to Titanium target, Argon flow rate of 30 sccm under chamber pressure of 4 mTorr and ambient temperature. The gold deposition is done without breaking the vacuum at the same chamber pressure, substrate temperature and Argon flow rate by switching RF power supply of 100 W to gold target.

3.3.2. Preparation of Teflon Substrates

Teflon substrates were prepared by spin coating 5% FSM 660 (manufactured by 3M) as an adhesion layer at 3500 rpm for 30 seconds on glass slides followed by baking at 100 ºC for 10 min. Two percent Teflon (DuPont) in FC-75 (manufactured by 3M) solution was then spun on it at 3000 rpm for 30 s followed by baking in 3 steps beginning at 115ºC for 15 min, 230ºC for 15 min and 300ºC for 1hr.

3.4. Contact Angle Measurements

The sessile drop method was used for contact angle analysis using deionized water. The sample was mounted on an X-Y stage illuminated by a lamp. A droplet of deionised water (5 μl, measured using a pipette) was formed on the end of the pipette tip and lowered onto the surface of the sample, and the pipette withdrawn when the drop detached. Images were recorded by a high speed Fire Wire Digital Video camera 'Sony DFW SX-900'. The images were captured using 'National Instruments Acquisition Software' and then analyzed using ImageJ software. Three different areas were measured for each sample. All measurements were performed at ambient temperature.

3.5. Tape Test

A good electrode deposition means that it adheres to the glass substrate strong enough to withstand external peel-off forces. This is examined by the 'tape-test' wherein tape is adhered onto a sample and peeled off with optimum force. A feeble film will peel

off and will not be able to pass the tape-test. Such test was performed on all electrodes deposited. All good samples were stored in a humidity controlled desicator cabinet until cell attachment experiments.

3.6. Preparation of Gaskets

Gaskets were made of PDMS (Polydimethyl siloxane) by using Sylgard Elastomer Kit (manufactured by Dow Corning Corp., Midland USA). Sylgard elastomer curing agent was mixed with elastomer base in a ratio of 1:3 and the mixture stirred to ensure good mixing on a petri plate. The mixture was degassed in vacuum to remove bubbles. The degassed mixture was then oven baked at 60ºC for 45 minutes. The PDMS is now ready to be cut into gaskets or wells for use in cell attachment experiments. This is done by using a hollow punch tool kit (manufactured by Mayhew Tools). Using a pair of hollow punches of radii 5 and 12 mm, the PDMS mold is punched to yield several gaskets of radii 5 mm (Fig. 3.4).

Fig. 3.4. PDMS gasket or well

3.7. Cell-attachment assay

All substrates were taken out of the desicator and split into 4 pieces of (1"x.75") using a diamond cutter. Every piece will eventually serve as a sample for cell attachment with or without surface modifications of polylysine. Each sample was rinsed meticulously in steps of acetone, 90% ethanol and 18.2 MΩ Millipore water and blown dry. These steps ensured cleansing of any oxide layers that may have developed over time and also decontamination. All cleaned samples and all PDMS gaskets are uv-sterilised for 1 hour. Decontamination is a very crucial step in these experiments (or in any biological experiment for that matter) since it may adversely affect healthy cell attachment. Various surface modifications have been analyzed which have been described in Section 3.9. Two gaskets are adhered to each sample by means of high vacuum grease (manufactured by Dow Corning). This is to ensure two sets of measurements per sample by prevention of total loss of data from the sample in case of inadvertent leaky gaskets. Uniform distribution of the glue onto the gasket is a must to prevent any leak of cell suspension from the gasket. This is ensured by applying the grease using cotton swabs (Q-tips, manufactured by Sherwood Medical, St. Louis). Using a pipette, the diluted cell suspension (which has been stored in ice) is triturated enough to ensure uniform distribution of cells throughout. Fifty microliter of cell suspension is then pipetted into each well (Fig. 3.5). All samples are placed for incubation overnight at 37º C in a humidified environment of 5% CO_2 – 95% air.
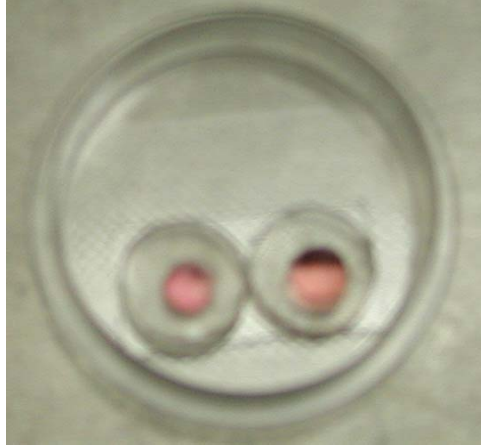
Fig. 3.5. Two wells filled with cell suspension on each sample

The samples were taken out of the incubator after 18-20 hours. The medium was aspirated off with pipette and rinsing with fresh warm medium twice to remove any unattached or loosely bound cells. Attached cells were subjected to Trypan Blue assay by adding a mixture of 3:2 chromaffin medium with Trypan Blue in each well and allowed to stand for 5 minutes at ambient temperature. After staining, fresh medium was added to each well again and the samples were returned to the incubator until image acquisition. Imaging was performed on an inverted microscope (Olympus IX71, Hitschfel Instruments Inc.) with a digital camera (AmScope) fitted to an eyepiece at 20X magnification. Images of dimensions 440μm x 330μm were captured by ScopePhoto software. Each well would yield 9-11 images along an equatorial line captured frame by frame.

3.8. Data Analysis

The total number of cells that adhered to each sample were manually counted using Adobe Photoshop CS3 count tool from each of the images that were captured. I found that manual counting was substantially more accurate than using ImageJ software. The sample data are presented as the average count of each image and the error bars represent the standard error of the mean (SE) between images. Sample results were analyzed using student's two sample t-test and they were considered statistically significant when they had a probability value less than 0.05 (* for $p < 0.05$ and ** for $p<0.01$) . Statistical analysis was performed using OriginPro 8.0 (OriginLab Corporation, MA).

3.9. Surface Modifications

DLC repeatedly proved to have superior cell attachment properties in preliminary experiments, therefore some surface modifications of DLC were tested. The most effective of these was polylysine which has been known to promote cell attachment to glass (Mazia 1975).

3.9.1. Polylysine

Both isomers of polylysine were used in experiments, and were purchased from Sigma. For the preliminary experiments, commercially available 0.1% poly-l-lysine

solution (Sigma) was used. Later on 5 mg poly-l-lysine (Sigma) dissolved in 25 ml double distilled water (0.02%) was compared with the same concentration of poly-d-lysine hydrobromide (Sigma) to compare cell attachment for the two. Substrates were immersed in polylysine for 20-30 minutes before being washed with double-distilled water on a rocking shaker (Reliable Scientific, Midwest Scientific, MO) set at 100 rocks/min for 5 minutes. Further washing was done on a 3D-rotator (Lab-Line) set at 60 rpm for 2 minutes. The substrates were left to dry in the laminar flow hood.

3.9.2. Plasma Treatment

In some experiments, the substrates were treated with mild plasma of 10.5 W for 1 minute in a plasma cleaner/sterilizer (PDC-32G, Harrick) before adding the cells.

3.9.3. Cell-Tak

BD Cell-Tak (BD Bioscience, San Jose, CA, USA) is a specially-formulated protein solution designed to be used as a coating on a substrate to immobilize cells (Hwang and others 2007a; Hwang and others 2007b). It is a formulation of the poly-phenolic proteins extracted from the marine mussel, _Mytilus edulis_. This family of related proteins is the key component of the glue secreted by the mussel to anchor itself to solid structures in its natural environment. The proteins are composed of tandemly repeated decapeptide units of similar amino acid sequence. Cell Tak is stored as stock solution in 5% acetic acid at 2-8ºC in the refrigerator and diluted in water for cell attachment

experiments. The diluted solution was placed on the substrate for approximately 30 minutes in the laminar flow hood. The solution was aspirated and the substrate washed in double-distilled water and allowed to dry.

3.9.4. Matrigel

BD-Matrigel Membrane Matrix (BD Biosciences, San Jose, CA) is a solubilized basement membrane preparation extracted from the Engelbreth-Holm-Swarm (EHS) mouse sarcoma, a tumor rich in extracellular matrix proteins. Its major component is laminin, followed by collagen IV, heparan sulfate proteoglycans, entactin and nidogen. It also contains TGF-beta, fibroblast growth factor, tissue plasminogen activator, and other growth factors which occur naturally in the EHS tumor. BD Matrigel Matrix is effective for the attachment and differentiation of both normal and transformed anchorage dependent epithelioid and other cell types (Joshi 1991; Nicosia and Ottinetti 1990). The matrigel stock solution (1:100 by volume in DMEM, Sigma) was stored in the refrigerator until use. The solution was placed onto the substrate and allowed to stand for 20 minutes followed by rinsing in sterile water and allowing to dry in the laminar flow.

3.9.5. Thermanox

Thermanox is a trademark name for a particular type of polymer in the polyolefin family. Thermanox coverslips (Thermo Fisher Scientific, Rochester, USA) contain high cell adhesive resin coated on one side. These were tested for chromaffin cell attachment also.
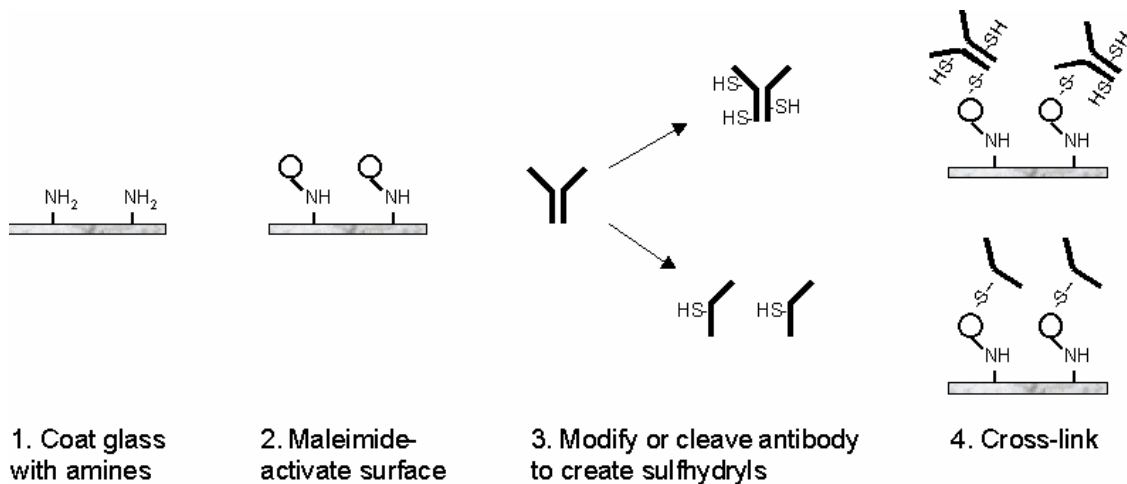
3.9.6. Maleimide

Maleimide surfaces are obtained by aminosilanizing a surface (derivatizing surface with primary amines $-NH_2$) and subsequently reacting them with heterobifunctional crosslinker Sulfo-SMCC. A maleimide activated surface can be employed to bind with the sulhydryl groups of proteins as cysteines on the cell membrane. The sulfhydryl groups can be reduced to enhance reactivity and binding of cells to these surface Maleimide groups.

The substrates were cleansed in the manner described in Section 3.7 and dried in the laminar flow. A two percent solution of aminosilane reagent 3-Aminopropyltriethoxysilane in dry (water-free) acetone was prepared. The substrate was immersed in the solution for 30 seconds. The surface was then rinsed in dry acetone and allowed to dry in the hood. A 10mM Coupling Buffer was prepared by diluting 10X Dulbecco's Phosphate Buffer Serum (Sigma, MO) to 1X in deionised water and adding EDTA. The pH of the Coupling buffer was adjusted to 7.2 by adding NaOH. Two milligrams Sulfo-SMCC [Sulfosuccinimidyl-4-(N-maleimidomethyl) cyclohexane-1-carboxylate] (Pierce) was added to 1 ml of the Coupling Buffer. The silylated surface was then covered with this silylated solution (to be used immediately to avoid hydrolysis) for 1 hour at room temperature followed by rinsing in Coupling Buffer.

Three types of cell attachment experiments were performed after maleimide activated the surface. The first was simply placing the diluted cell suspension (10^6

cells/ml) into wells placed on maleimide coated surfaces. The second was done by reducing the sulfhydryl groups on the cell membrane. For this, cells were incubated in 1 mM tris-(2-carboxyethyl) phosphine hydrochloride (Pierce), a reducing agent, for 10 min to reduce surface sulfhydryl groups, aiding in more efficient maleimide binding (Fulop and others 2005).

3.9.6.1 Antibody Attachment

| 1. Coat glass with amines | 2. Maleimide-activate surface | 3. Modify or cleave antibody to create sulfhydryls | 4. Cross-link |

Fig. 3.6. Basic steps involved in attaching an antibody onto a glass surface

Antibody NCAM-13 Alexa 488-G (BD Biosciences) was dissolved in PBS (Sigma) in ratio 1: 50 by volume. 3mg SATA (Pierce) was dissolved in 1 ml of DMSO to result in a 13mM stock solution. 25µl of this SATA solution was added to the antibody solution and kept for 30 minutes at room temperature. The modified antibody was then purified from excess SATA and other reaction by-products using a Microcon Filter and equilibrated with Coupling buffer (Ph 7.2). 348 mg of Hydroxylamine•HCl was dissolved in 9 ml Coupling buffer and the pH was adjusted to 7.2 with NaOH. Finally, the volume

was adjusted to 10ml with additional Coupling buffer to result in .5M Hydroxylamine•HCl. A 100μl Hydroxylamine solution was added to each 1 ml of SATA-modified antibody solution and allowed to stand at room temperature for 2 hours. The antibody is purified from the Hydroxylamine using a Microcon filter equilibrated with Coupling buffer. The Maleimide-activated surface was covered with the antibody solution and allowed to stand at room temperature for 2-4 hours. The solution was aspirated and the surface rinsed with Coupling buffer to ensure that only covalently attached antibody molecules remained. The surface was allowed to dry and gasket was glued onto it to pour the cell suspension for cell attachment study.

3.10. Scanning Electron Microscopy (SEM)

SEM imaging of bovine chromaffin cells was performed in DLC and ITO to scrutinize the morphology of cell spreading on these substrates. The samples were left in the incubator overnight. Primary fixation (fixation of the proteins) was done in 2% glutaraldehyde/2% paraformaldehyde in 0.1 M cacodylate buffered solution for 1 hour on a rocker at room temperature. The samples were rinsed in cacodylate buffer thrice by placing on the rocker for periods of 15 minutes each time before changing the buffer for the next rinse. Secondary fixation (fixation of the lipids) was done in 2% Osmium Tetroxide in cacodylate buffer for 1 hour on the rocker at room temperature. The samples are washed thrice for 15 minutes on the rocker with ultrapure distilled water. Dehydration of the samples in a graded acetone series was performed by placing in 25%, 50%,70% for 30 minutes each, and 95% acetone solution for 1 hour. The rationale behind graded

dehydration is to prevent osmotic shock to biological samples. The samples are then critical point dried in liquid CO_2 in Tousimis Auto-Samdri 815 automatic critical point dryer followed by mounting on suitable SEM stubs with double sided adhesive tape. The samples are grounded by applying silver paint onto the sample edges to ensure good conductivity during imaging. The samples were sputter coated with platinum, and examined using a Hitachi S4700 Field Emission SEM.

CHAPTER 4

RESULTS OF EARLY APPROACH

A vast amount of quantification experiments have been performed on different substrates. INS-1 cells were used initially enable rapid preliminary characterization of available materials. INS-1 cells are readily available whenever needed and they spread conspicuously following attachment. These cells tend to spread out and divide on a "cytophilic" substrate and clump together without spreading on "cytophobic" surfaces. The protocol to quantify cell attachment has evolved to a robust approach which yields a high reproducibility. The experiments have been repeated numerous times and conclusions can clearly be drawn.

4.1. Earlier Approaches

4.1.1. Cell-Attachment Experiments with INS-1 Cell Line

In early experiments, I simply placed approximately 500µl of undiluted cell suspension (cell density approximately 3.5×10^6 cells/ml) on substrates and counted cells in regions where they attached. Floating or unbound cells were detached by rinsing on the rocker. The count for attached cells was plotted versus time for Diamond like Carbon (DLC), Indium Tin Oxide (ITO), Aluminum, Gold, Hafnium Oxide (HfO_2), Silicon Fluorocarbon (SiCF) and Silicon Oxyfluorocarbon (SiCOF).
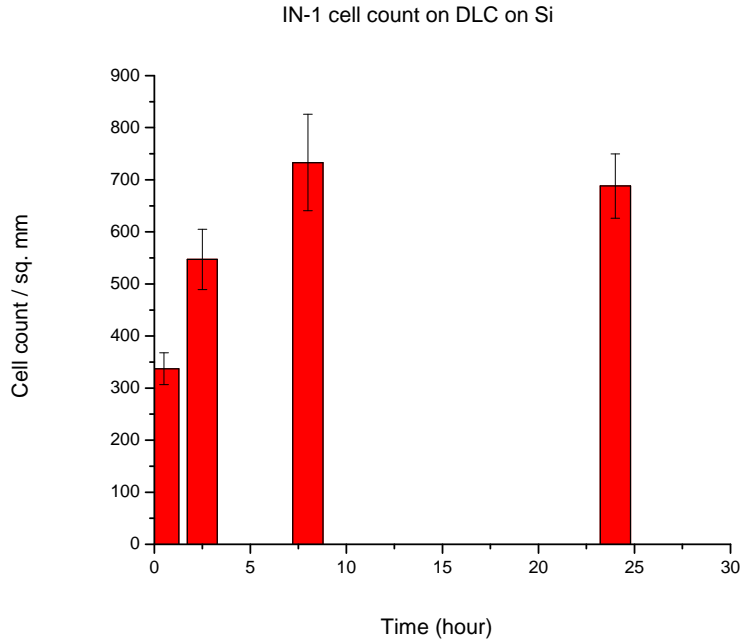
Fig. 4.1.(a). INS-1 cell attachment histogram on DLC with time
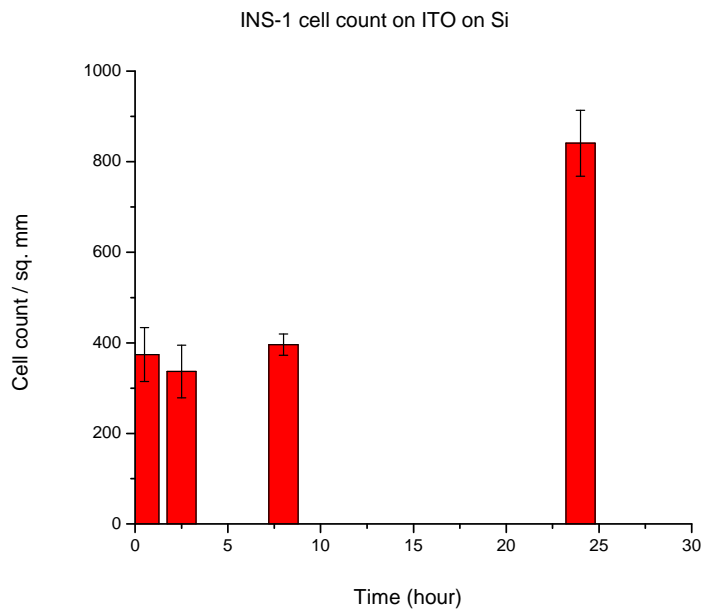
Fig. 4.1.(b). INS-1 cell attachment histogram on ITO with time

61
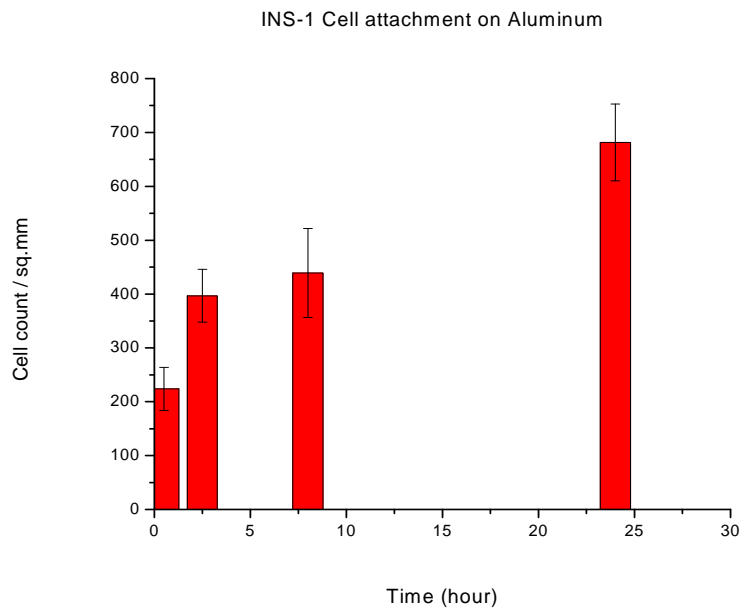
Fig. 4.1.(c). INS-1 cell attachment histogram on Aluminum with time
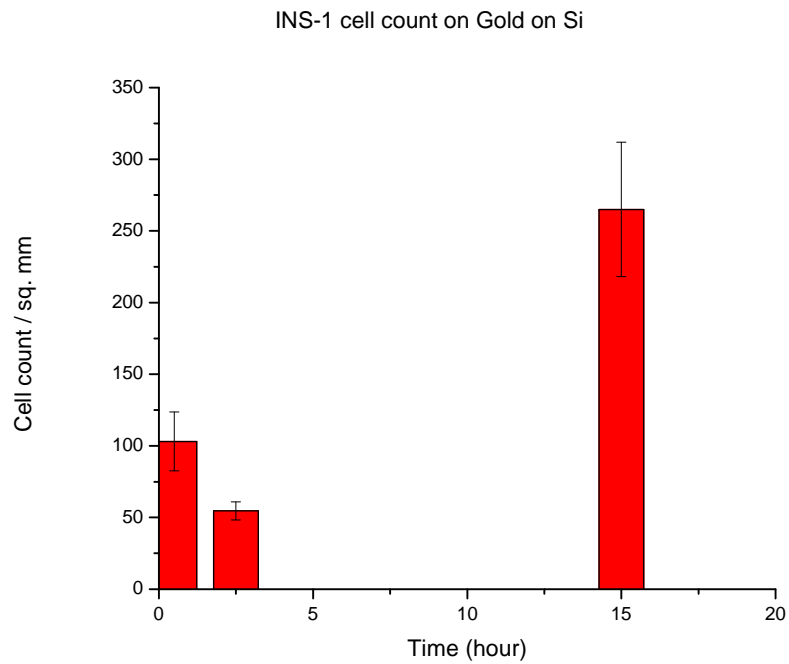
Fig. 4.1.(d). INS-1 cell attachment histogram on Gold with time
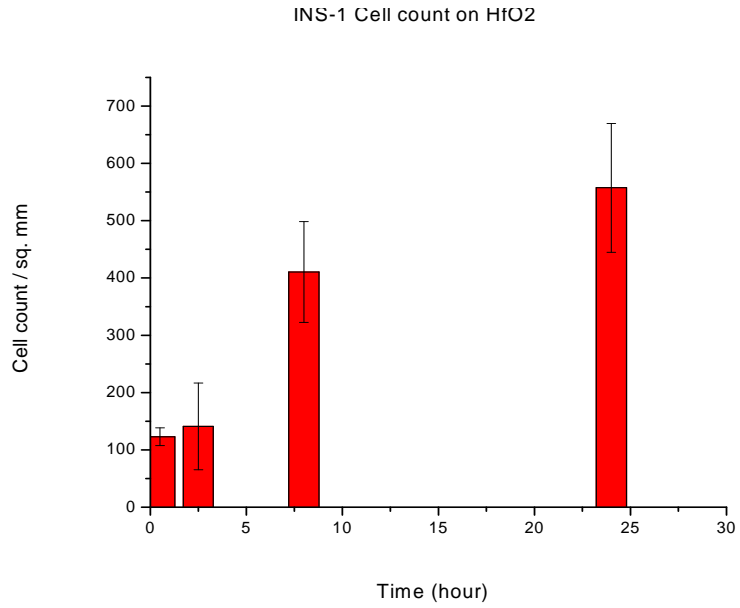
Fig. 4.1.(e). INS-1 cell attachment histogram on HfO$_2$ with time
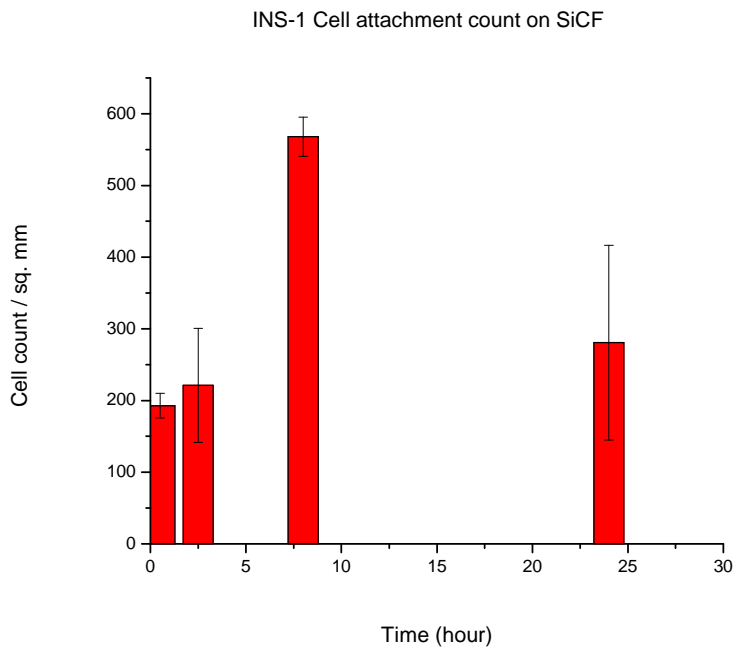
Fig. 4.1.(f). INS-1 cell attachment histogram on SiCF with time

INS-1 cell count on SiCOF on Si
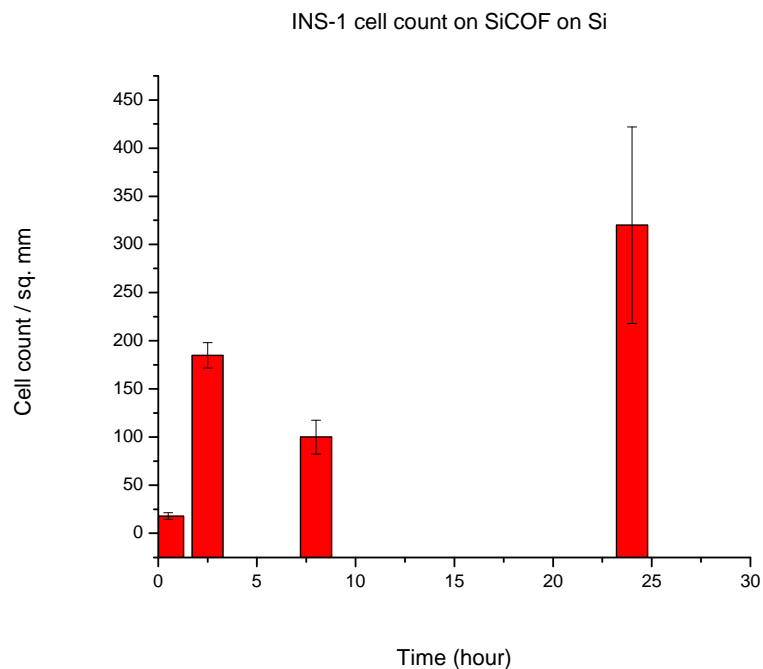
Fig. 4.1.(g). INS-1 cell attachment histogram on SiCOF with time

INS-1 cells divide in culture; therefore I chose incubation time of 2 hours in order to give time for cell attachment without substantial cell division.

INS-1 cell attachment count on different material electrodes
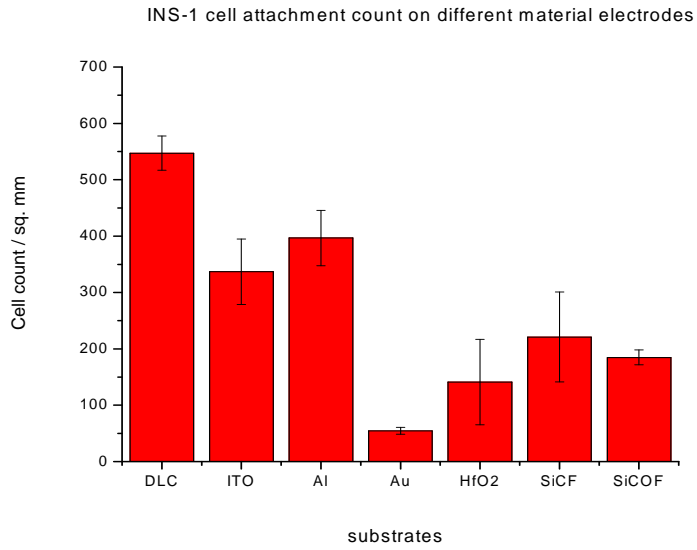
(A)

Fig. 4.2.(A). Comparison of INS-1 cell attachment on different materials after 150 minutes
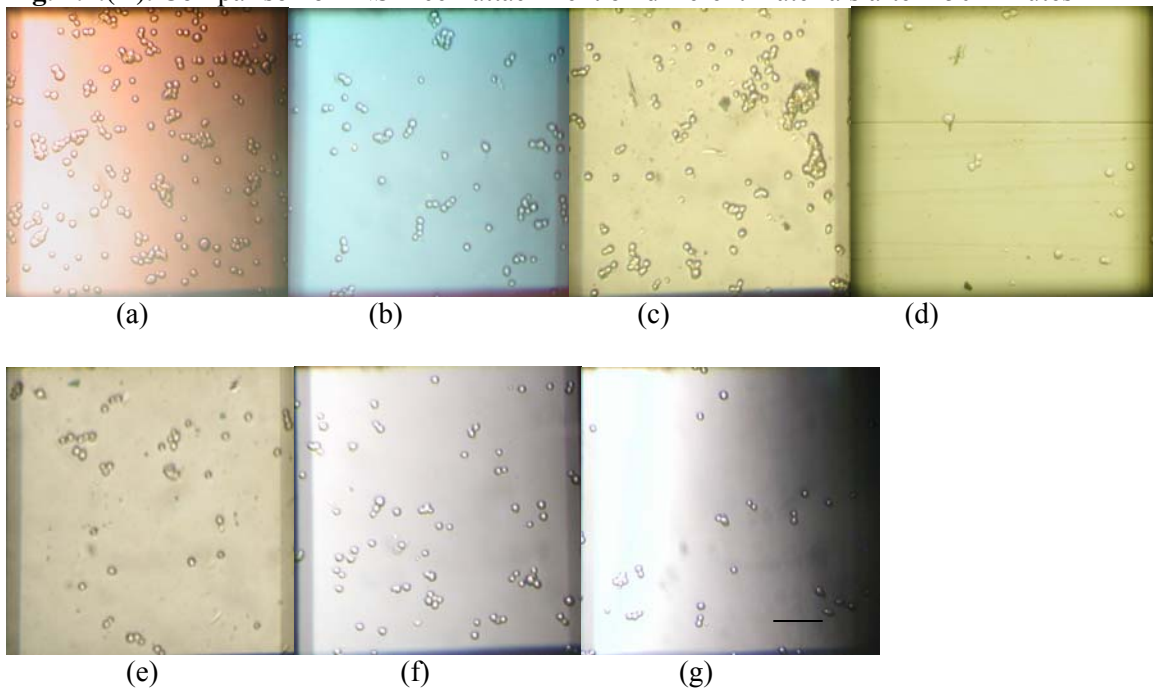
(B)

Fig. 4.2 (B). Optical micrographs of INS-1 cell attachment after 150 minutes to (a) DLC (b) ITO (c) Aluminum (d) Gold (e) HfO_2 (f) SiCF (g) SiCOF [Scale Bar represents 50μm]

4.1.2. Cell Attachment Experiments with Bovine Chromaffin Cells on DLC and Different Metals

Similar to the motivation and protocol described in Section 4.1.1, the experiments were repeated with bovine chromaffin cells on DLC and metals as Titanium (Ti), Platinum (Pt), Gold (Au) and the cell attachment studied over time.

Comparison of cell attachment on DLC and different metals after 1 hour
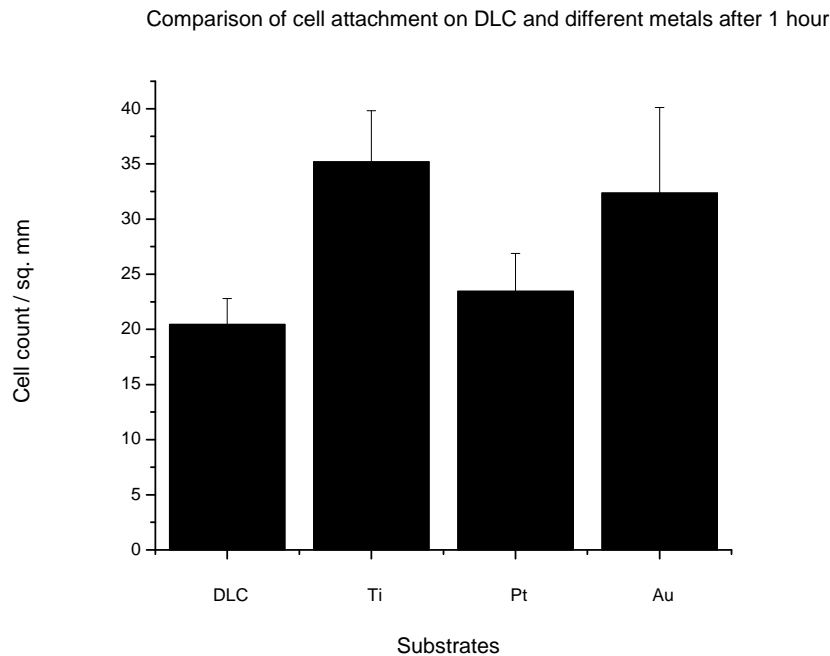
(A)
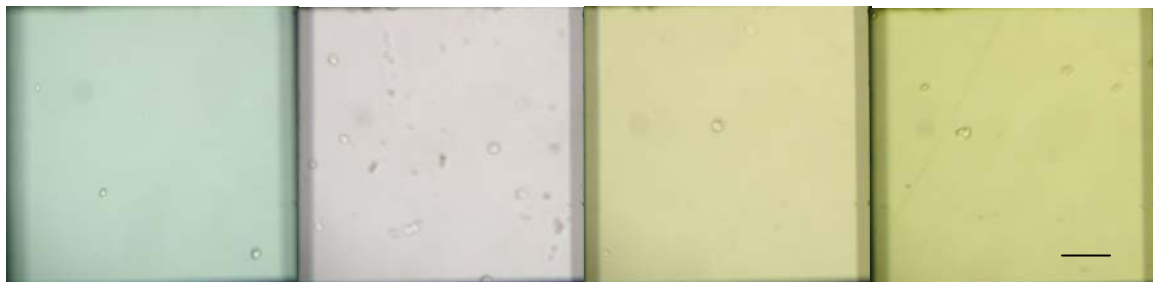
(a) (b) (c) (d)

Fig. 4.3.(A). Comparison of bovine chromaffin cell attachment on different materials after 1 hour. **(B).** Optical micrographs of bovine chromaffin cell attachment after 1 hour to (a) DLC (b) Titanium (c) Platinum (d) Gold   [Scale Bar represents 50µm]

Comparison of chromaffin cell count on different metals after 2 hours

(A)

(a)   (b)   (c)   (d)
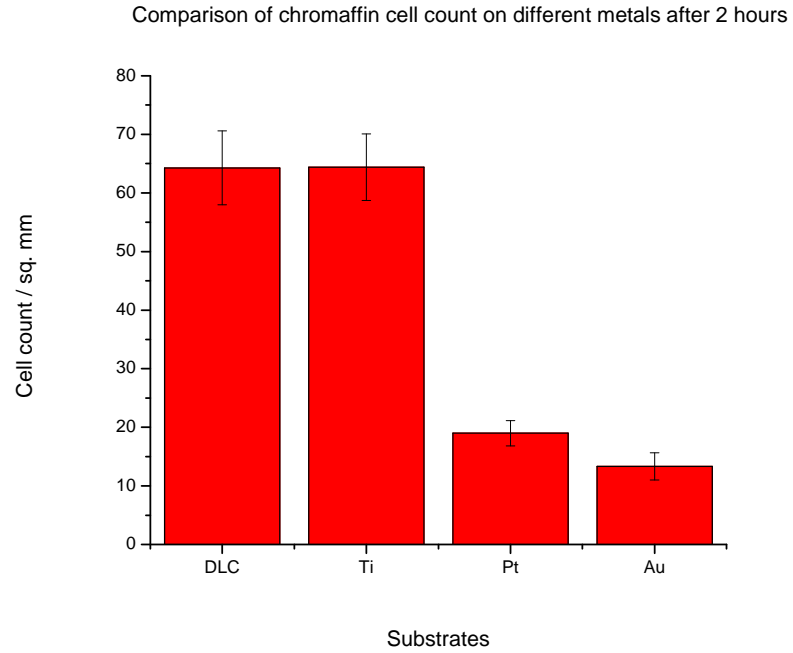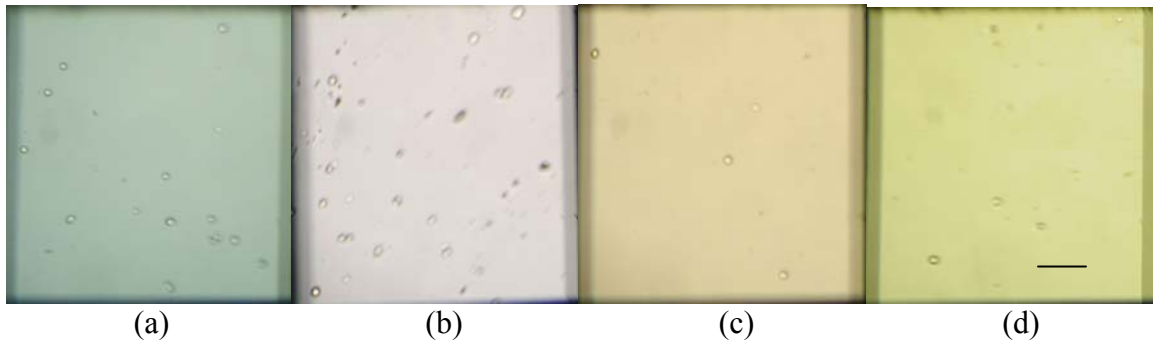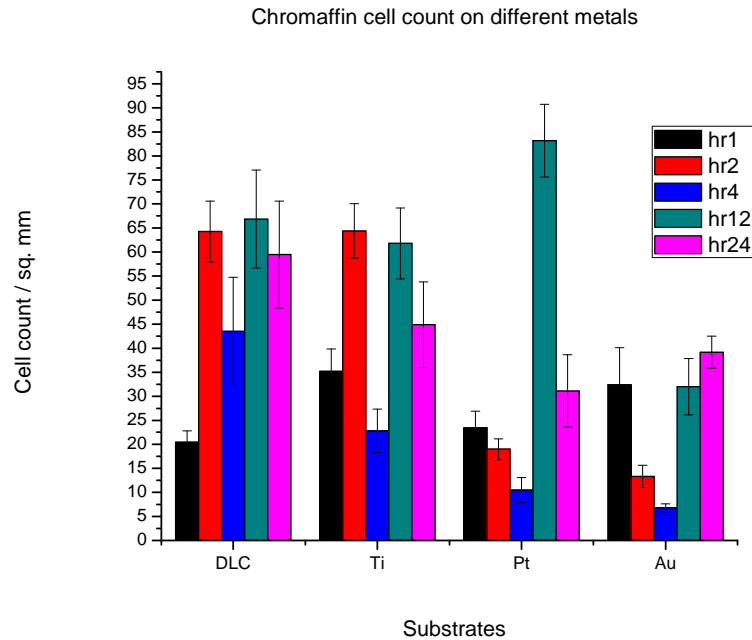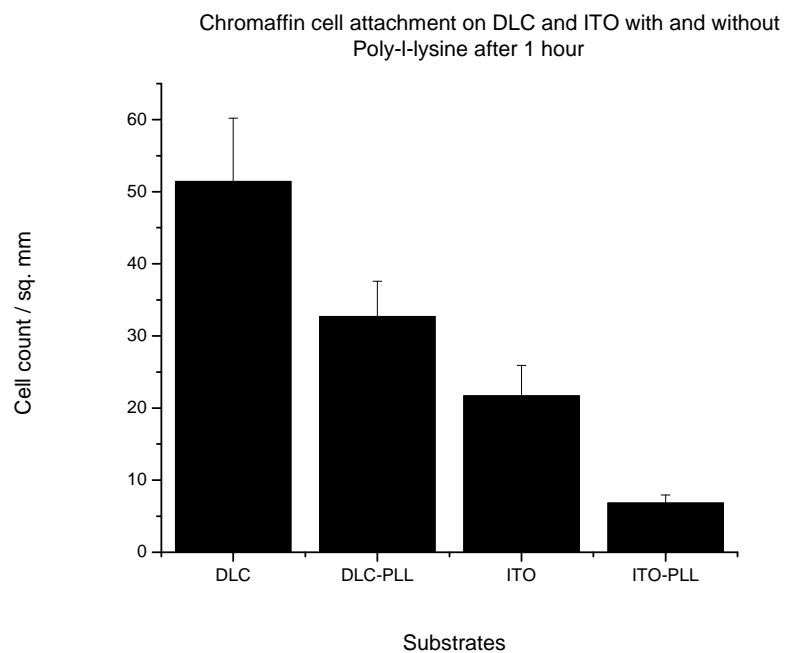
(B)

Fig. 4.4.(A). Comparison of bovine chromaffin cell attachment on different materials after 2 hours **(B).** Optical micrographs of bovine chromaffin cell attachment after 2 hours to (a) DLC (b) Titanium (c) Platinum (d) Gold [Scale Bar represents 50µm]

Comparison of chromaffin cell count on different metals after 4 hours

(A)

(a)   (b)   (c)   (d)
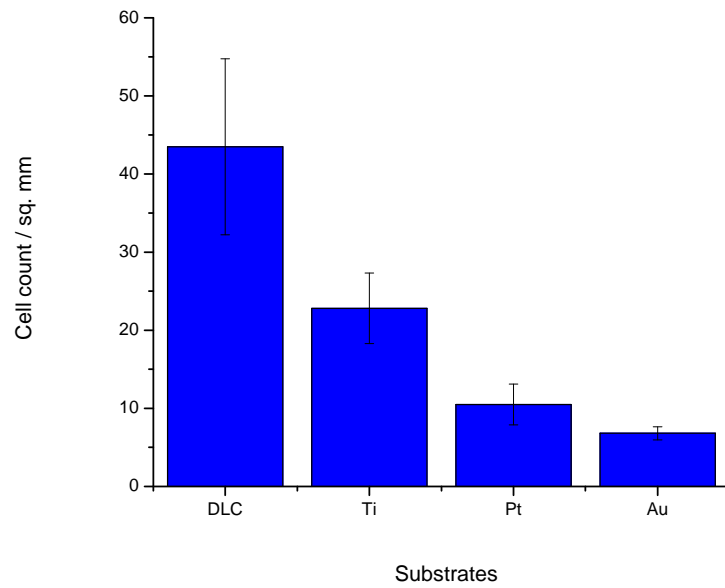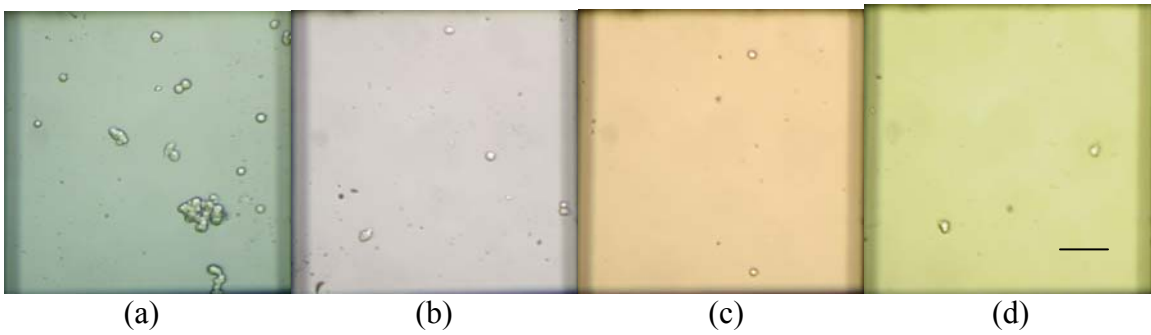
(B)

Fig. 4.5.(A). Comparison of bovine chromaffin cell attachment on different materials after 4 hours **(B).** Optical micrographs of bovine chromaffin cell attachment after 4 hours to (a) DLC (b) Titanium (c) Platinum (d) Gold [Scale Bar represents 50µm]

(A)

(a)   (b)   (c)   (d)
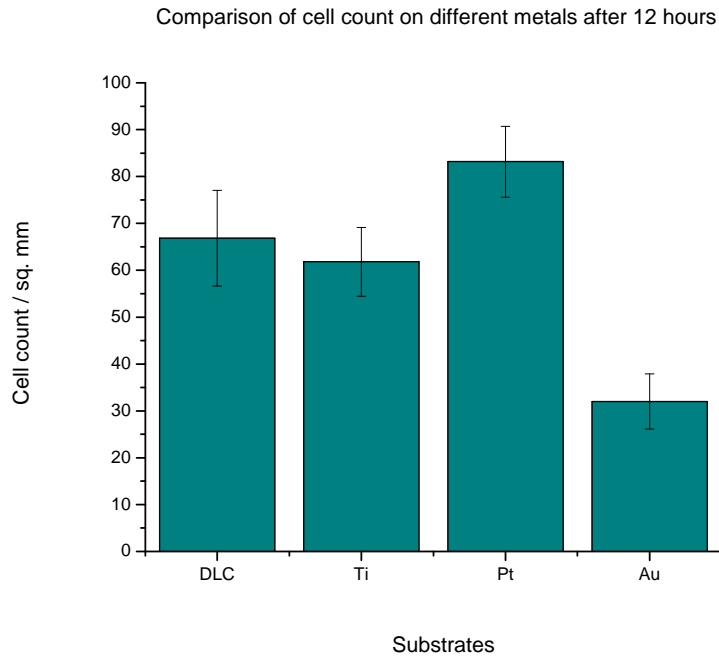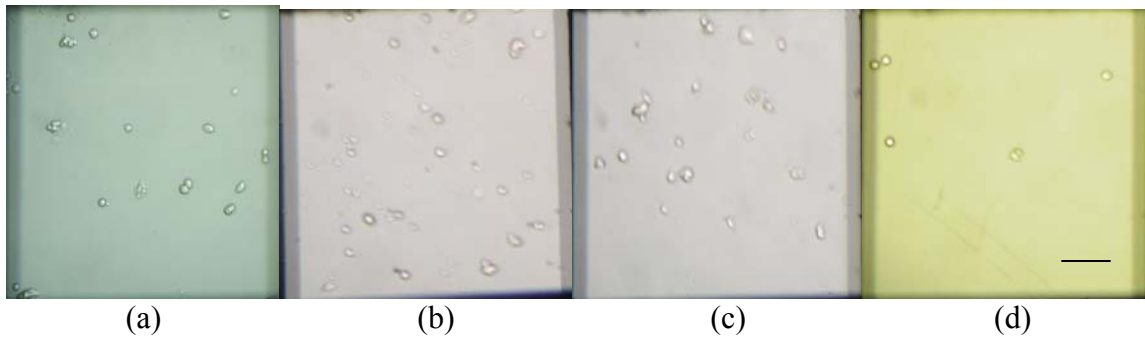
(B)

Fig. 4.6.(A). Comparison of bovine chromaffin cell attachment on different materials after 12 hours **(B).** Optical micrographs of bovine chromaffin cell attachment after 12 hours to (a) DLC (b) Titanium (c) Platinum (d) Gold [Scale Bar represents 50μm]

Comparison of cell count on different metals after 24 hours

(A)

(a)　　　　　(b)　　　　　(c)　　　　　(d)
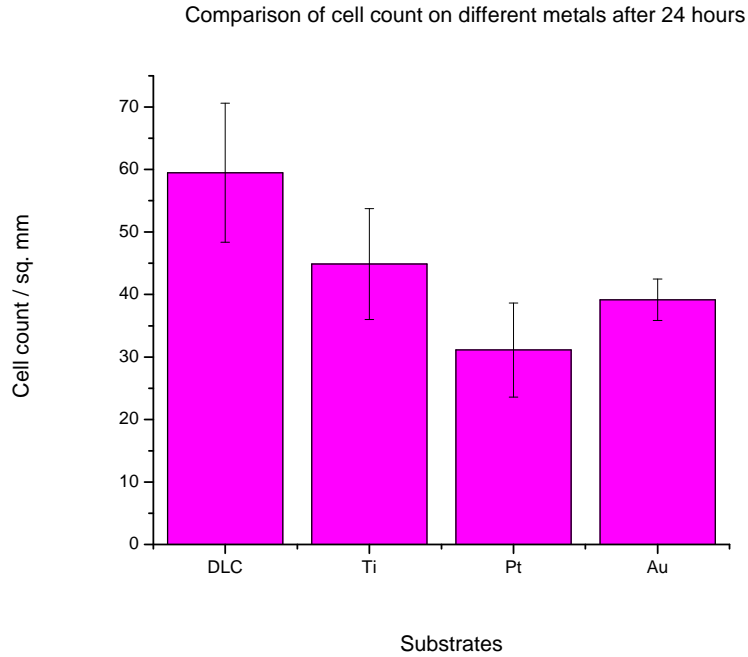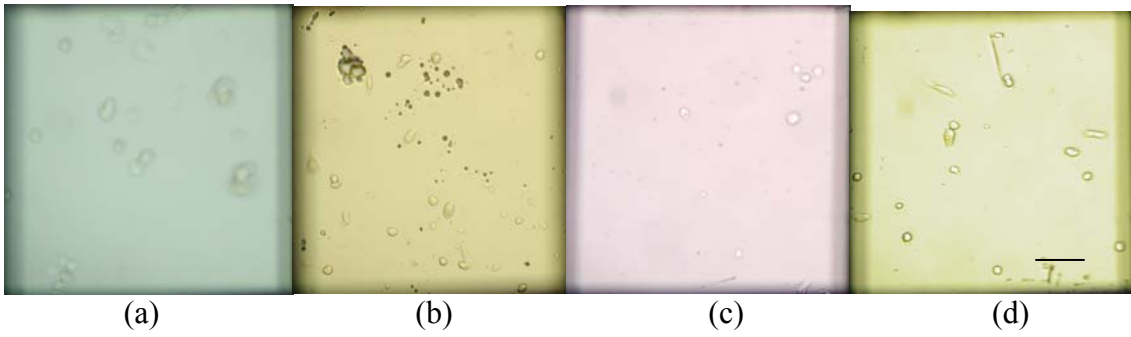
(B)

Fig. 4.7.(A). Comparison of bovine chromaffin cell attachment on different materials after 24 hours **(B).** Optical micrographs of bovine chromaffin cell attachment after 24 hours to (a) DLC (b) Titanium (c) Platinum (d) Gold [Scale Bar represents 50µm]

Chromaffin cell count on different metals

Fig. 4.8. Summary of bovine chromaffin cell attachment comparison of different substrates with time

4.1.3. Bovine Chromaffin Cell Attachment with and without Poly-lysine

As described earlier in Section 2.5.2, polylysine was used to enhance cell attachment. In this experiment, commercially available 0.1% poly-l-lysine (Sigma) was used. DLC and ITO were compared with and without polylysine surface modification over time.

Chromaffin cell attachment on DLC and ITO with and without
Poly-l-lysine after 1 hour

(A)

(a)   (b)   (c)   (d)
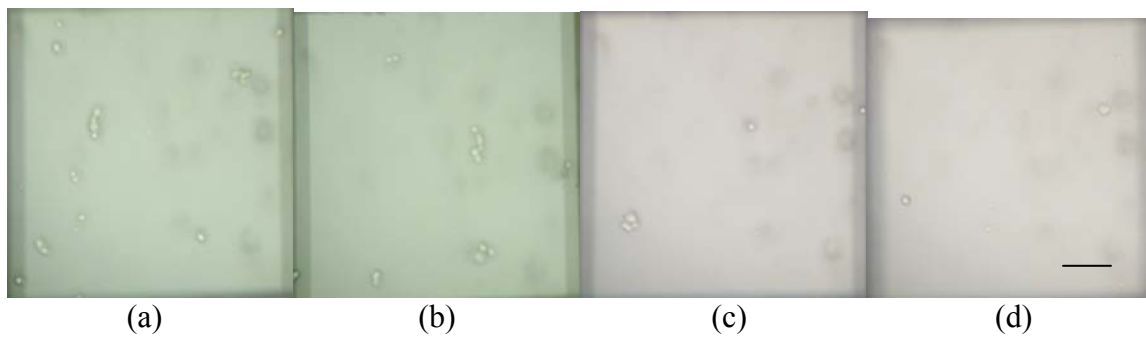
(B)

Fig. 4.9.(A). Comparison of bovine chromaffin cell attachment on DLC and ITO with and without polylysine (PLL) modification after 1 hour **(B).** Optical micrographs of bovine chromaffin cell attachment after 1 hour to (a) DLC (b) PLL coated DLC (c) ITO (d) PLL coated ITO [Scale Bar represents 50µm]
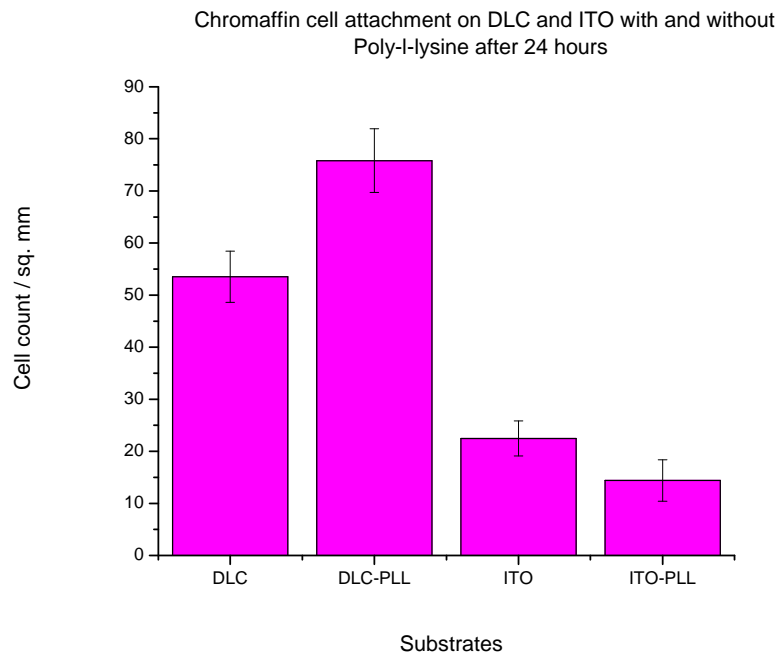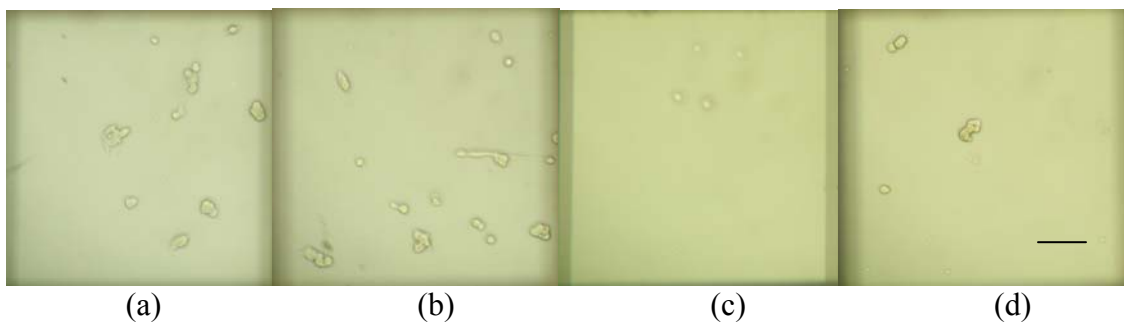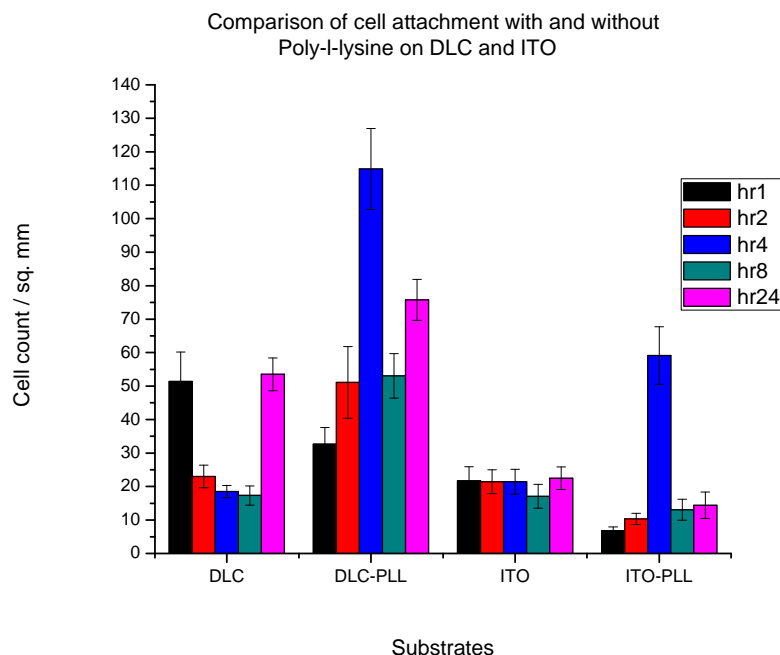
**(A)**

(a)   (b)   (c)   (d)
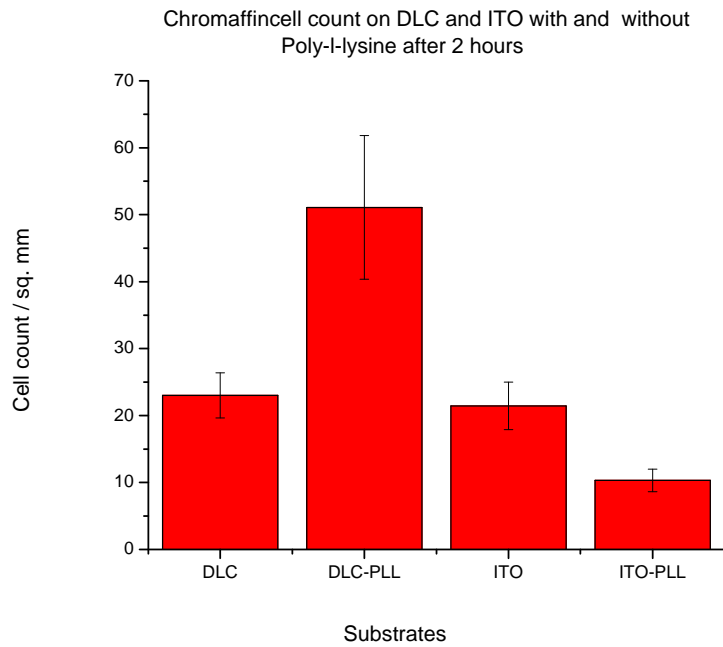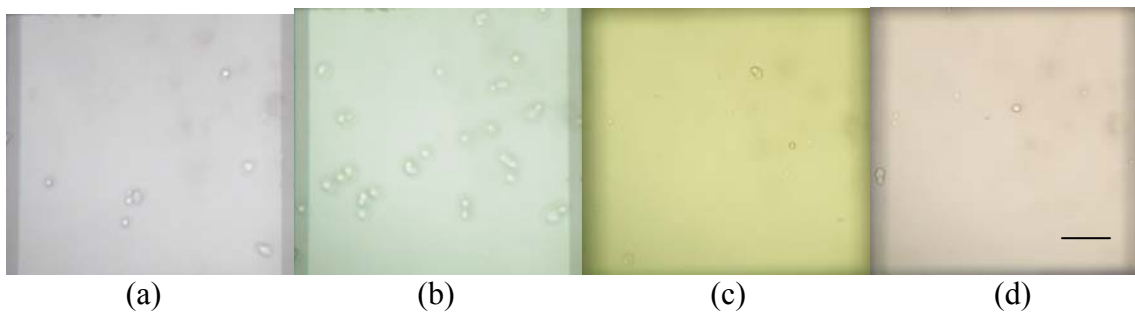
(B)

Fig. 4.10.(A). Comparison of bovine chromaffin cell attachment on DLC and ITO with and without polylysine (PLL) modification after 2 hours **(B).** Optical micrographs of bovine chromaffin cell attachment after 2 hours to (a) DLC (b) PLL coated DLC (c) ITO (d) PLL coated ITO [Scale Bar represents 50μm]

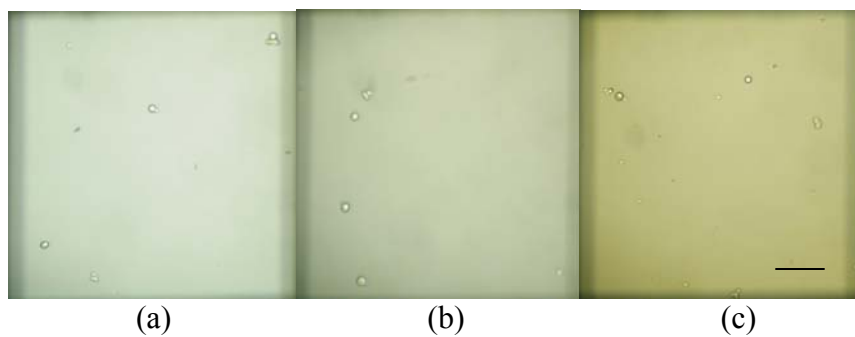Chromaffinc ell attachment on DLC and ITO with and without Poly-l-lysine after 4 hours

(A)

(a)   (b)   (c)   (d)
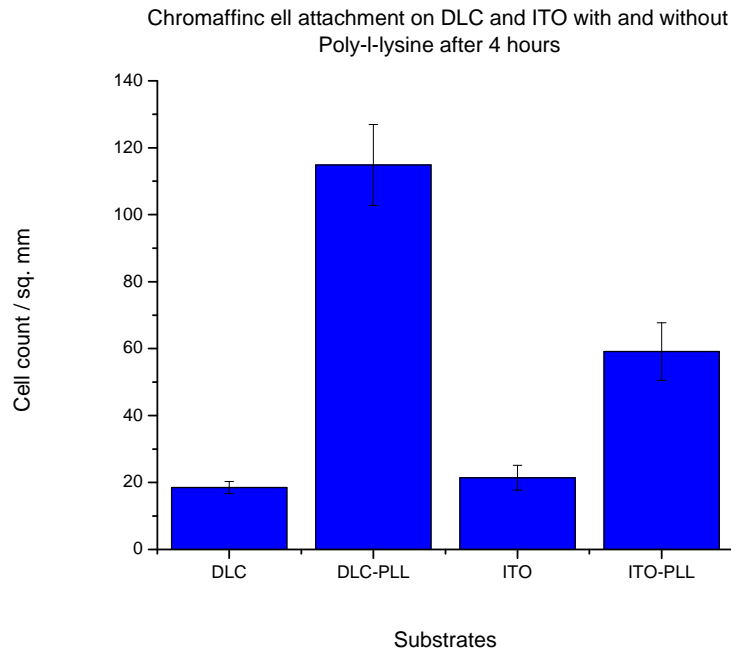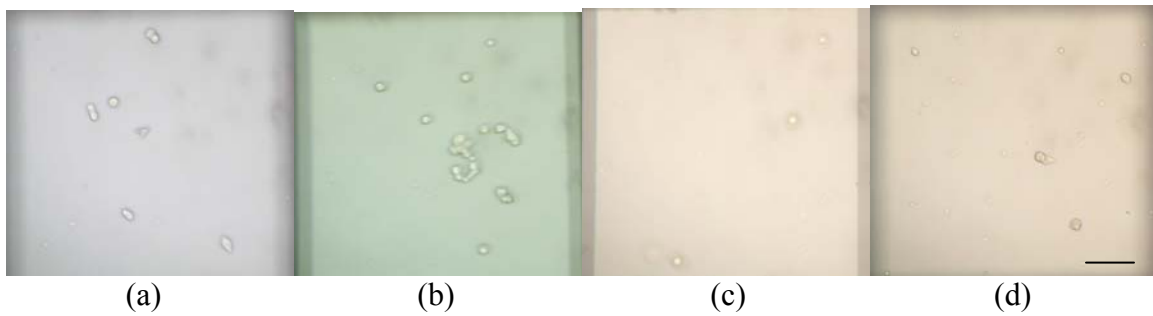
(B)

Fig. 4.11.(A). Comparison of bovine chromaffin cell attachment on DLC and ITO with and without polylysine (PLL) modification after 4 hours **(B).** Optical micrographs of bovine chromaffin cell attachment after 4 hours to (a) DLC (b) PLL coated DLC (c) ITO (d) PLL coated ITO [Scale Bar represents 50µm]

Chromaffin cell attachment on DLC and ITO with and without Poly-l-lysine after 12 hours

(A)

(a)   (b)   (c)   (d)
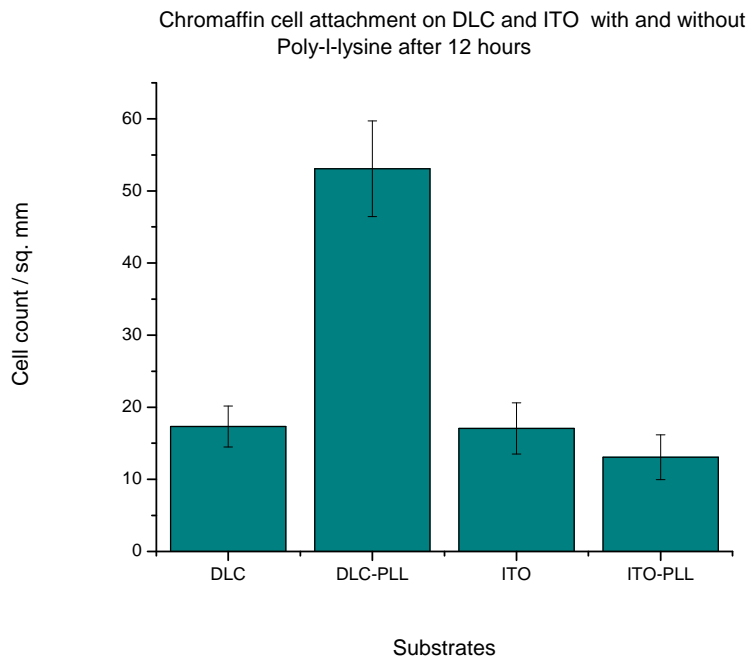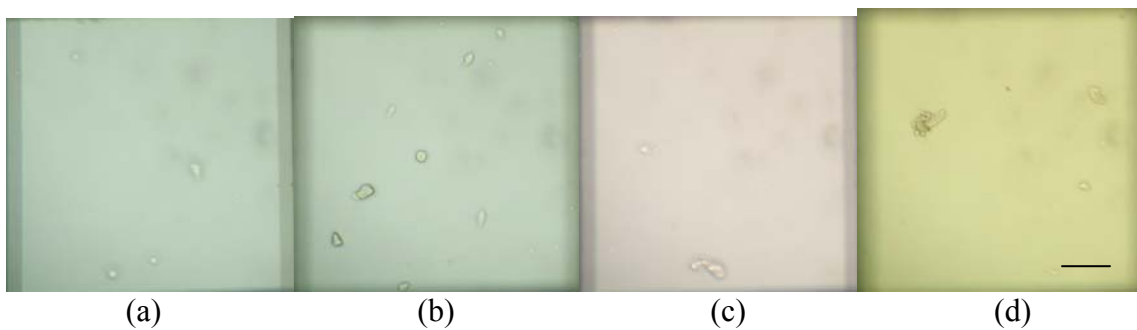
(B)

Fig. 4.12.(A). Comparison of bovine chromaffin cell attachment on DLC and ITO with and without polylysine (PLL) modification after 8 hours **(B).** Optical micrographs of bovine chromaffin cell attachment after 8 hours to (a) DLC (b) PLL coated DLC (c) ITO (d) PLL coated ITO [Scale Bar represents 50µm]

(A)

(a)   (b)   (c)   (d)

(B)

Fig. 4.13.(A). Comparison of bovine chromaffin cell attachment on DLC and ITO with and without polylysine (PLL) modification after 24 hours **(B).** Optical micrographs of bovine chromaffin cell attachment after 24 hours to (a) DLC (b) PLL coated DLC (c) ITO (d) PLL coated ITO [Scale Bar represents 50µm]

Fig. 4.14. Summary of bovine chromaffin cell attachment comparison of DLC and ITO with and without polylysine with time

4.1.4. Bovine Chromaffin Cell Attachment on with and without Plasma Treated DLC and ITO

In this set of experiments, DLC was oxygen plasma treated for 30 seconds at 10.5 W. The rationale was to develop hydroperoxide ($-COO^-$) groups on the surface of DLC to promote cell attachment. As will be seen in the data herein, the plasma treatment actually inhibited cell attachment. The oxygen plasma treated substrates were allowed to stand for about 5 minutes to allow the $-COO^-$ groups to form $-COOH$.

Chromaffin cell attachment on DLC with and without plasma treatment
in comparison wtih ITO after 1 hour

(A)

(a)   (b)   (c)
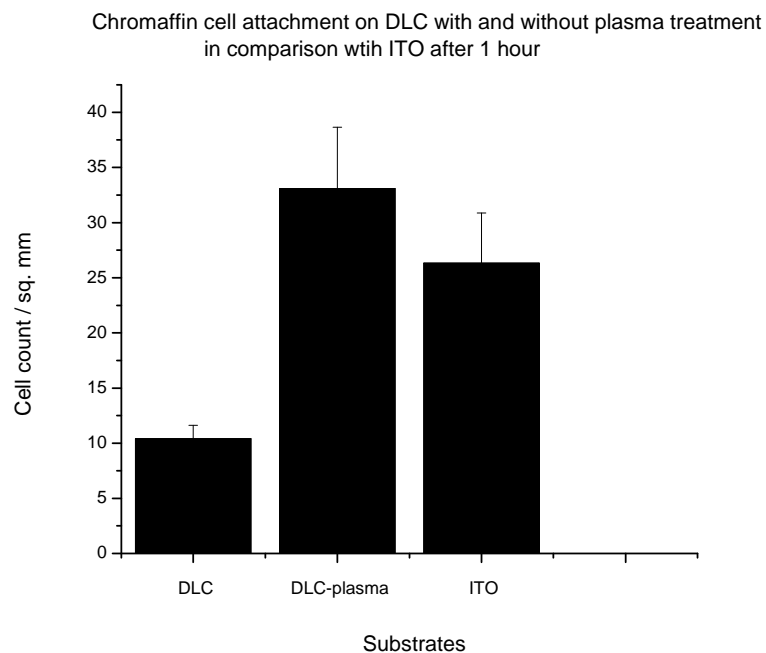
(B)

Fig. 4.15.(A). Comparison of bovine chromaffin cell attachment on as is and plasma treated DLC and ITO after 1 hour **(B).** Optical micrographs of bovine chromaffin cell attachment after 1 hour to (a) DLC (b) Oxygen plasma treated DLC (c) ITO [Scale Bar represents 50µm]
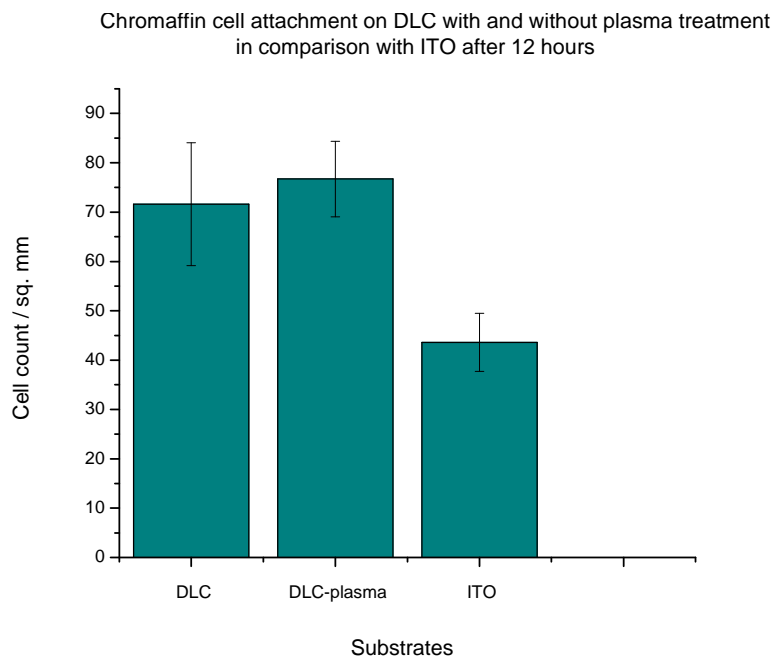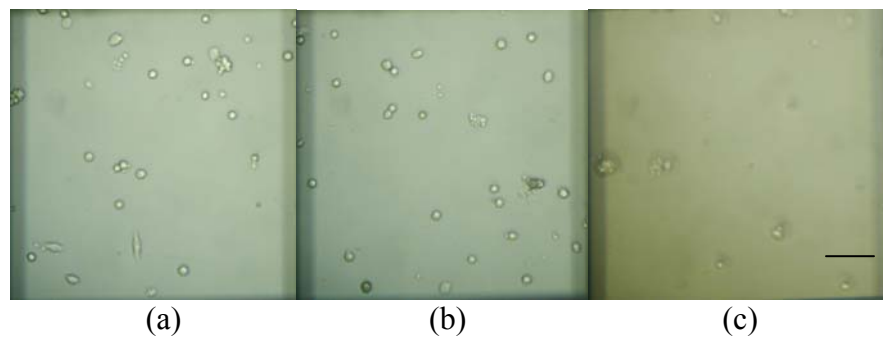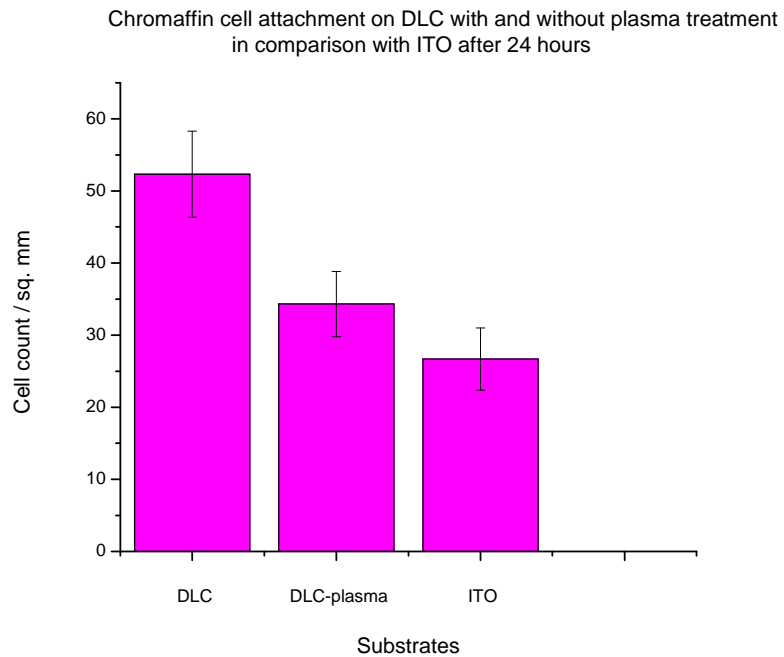
(A)

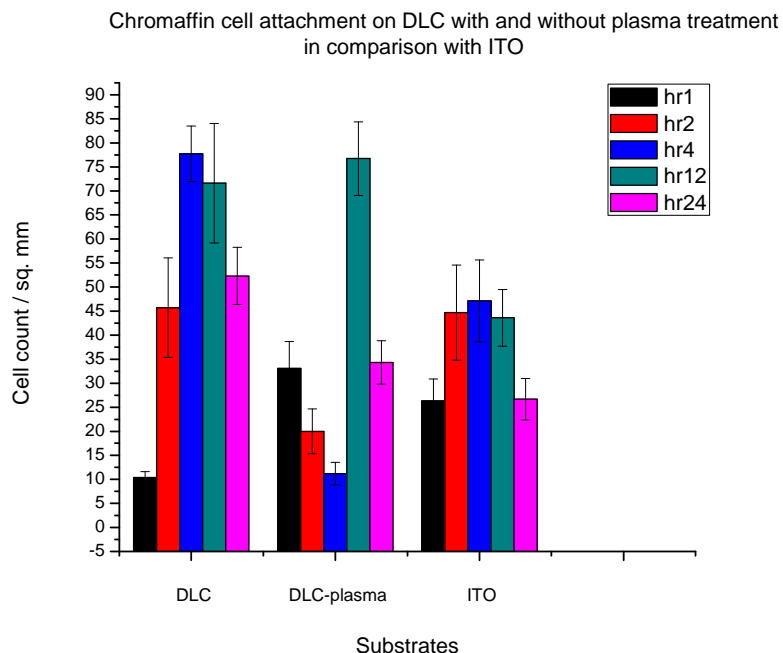(a)   (b)   (c)
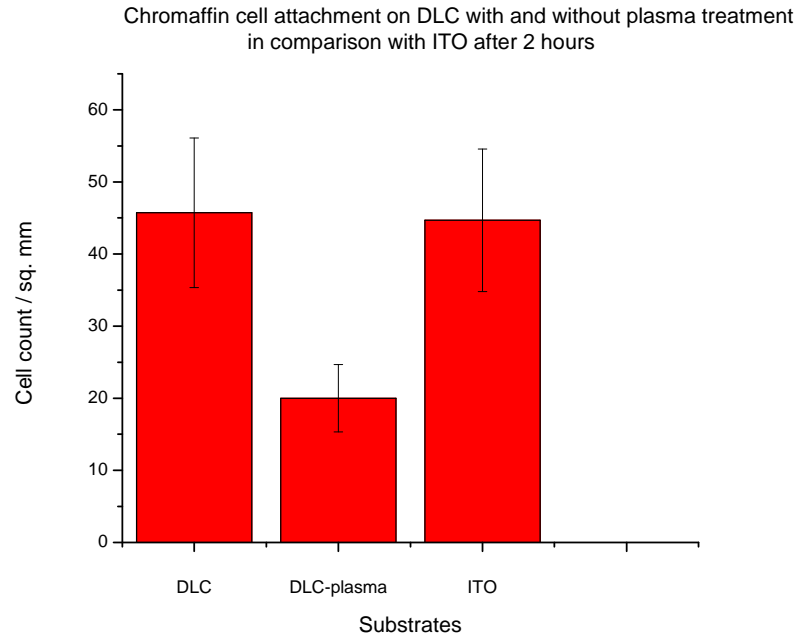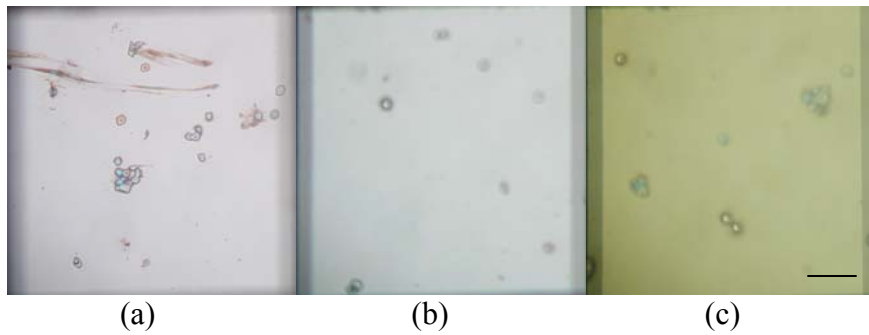
(B)

Fig. 4.16.(A). Comparison of bovine chromaffin cell attachment on as is and plasma treated DLC and ITO after 2 hours **(B).** Optical micrographs of bovine chromaffin cell attachment after 2 hours to (a) DLC (b) Oxygen plasma treated DLC (c) ITO [Scale Bar represents 50µm]

(A)

(a)   (b)   (c)
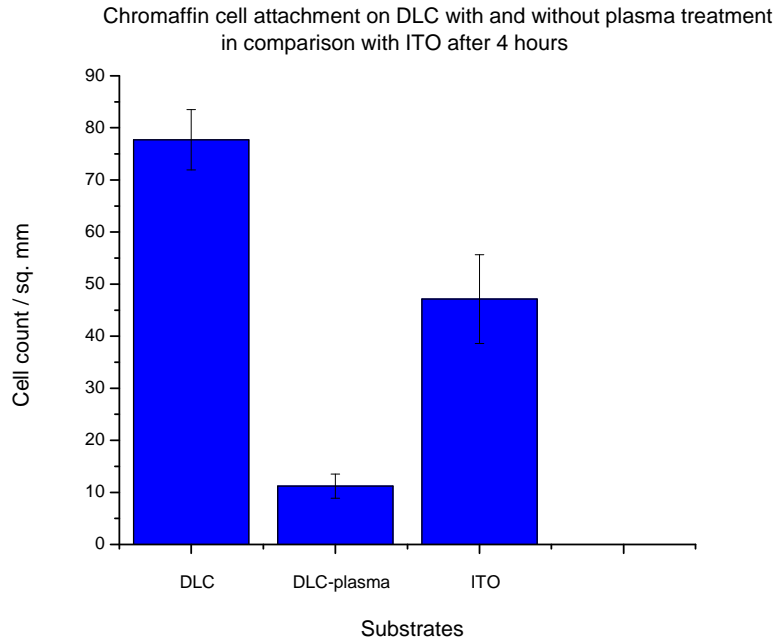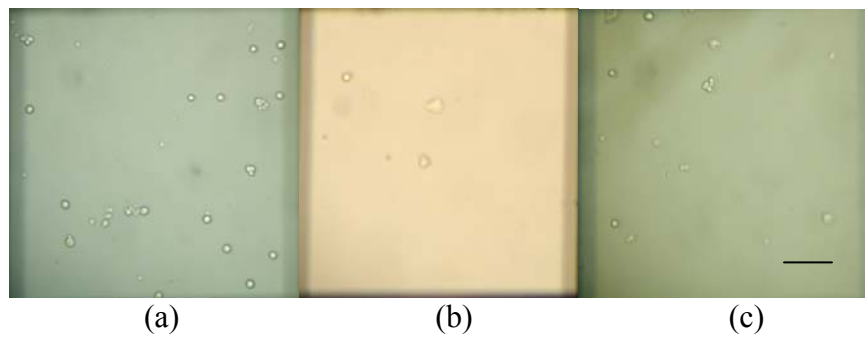
(B)

Fig. 4.17.(A). Comparison of bovine chromaffin cell attachment on as is and plasma treated DLC and ITO after 4 hours **(B).** Optical micrographs of bovine chromaffin cell attachment after 4 hours to (a) DLC (b) Oxygen plasma treated DLC (c) ITO [Scale Bar represents 50µm]

Chromaffin cell attachment on DLC with and without plasma treatment in comparison with ITO after 12 hours

(A)

(a)　　　　　　　(b)　　　　　　　(c)

(B)

Fig. 4.18. (A). Comparison of bovine chromaffin cell attachment on as is and plasma treated DLC and ITO after 12 hours **(B).** Optical micrographs of bovine chromaffin cell attachment after 12 hours to (a) DLC (b) Oxygen plasma treated DLC (c) ITO   [Scale Bar represents 50μm]

Chromaffin cell attachment on DLC with and without plasma treatment
in comparison with ITO after 24 hours

(A)

(a)　　　　　　　　　(b)　　　　　　　　　(c)

(B)

Fig. 4.19. (A). Comparison of bovine chromaffin cell attachment on as is and plasma treated DLC and ITO after 24 hours **(B).** Optical micrographs of bovine chromaffin cell attachment after 24 hours to (a) DLC (b) Oxygen plasma treated DLC (c) ITO   [Scale Bar represents 50μm]

Fig. 4.20. Summary of bovine chromaffin cell attachment comparison of as is and plasma treated DLC and ITO with time

4.2. Conclusions from early experiments

A fair degree of variability between different sets of experiments is observed due to flawed approach. Bias is introduced by only selecting regions with wells for measurement. Nevertheless, the trends are apparent. More cells attach to DLC than ITO and polylysine promotes attachment as compared to untreated samples. For INS-1 cells, incubation time of 2 hours is optimum and for bovine chromaffin cells measurements should be performed at least several hours after plating. Plasma treatment hurts cell attachment and is therefore not recommended.

Chapter 5

Results from Systematic Cell Attachment Quantification

I improved the quantification of cell attachment by systematic counting of all cells in a sample region limited by PDMS gaskets and imaging only along the equatorial line of the well after incubating for 18-20 hours. The Trypan blue assay of cell viability and the use of the same cell concentration in all wells increased the reproducibility the data generated.

5.1 Experiment I: Bovine Chromaffin Cell Attachment Assay on Different Surface Modifications of DLC

As had been described in Section 3.9, various surface modifications have been tried for cell attachment assays to enhance attachment on DLC which appears to be the best cell docking material so far.

Cell count on as is DLC substrate

(a)

Cell count on DLC coated with Celltak
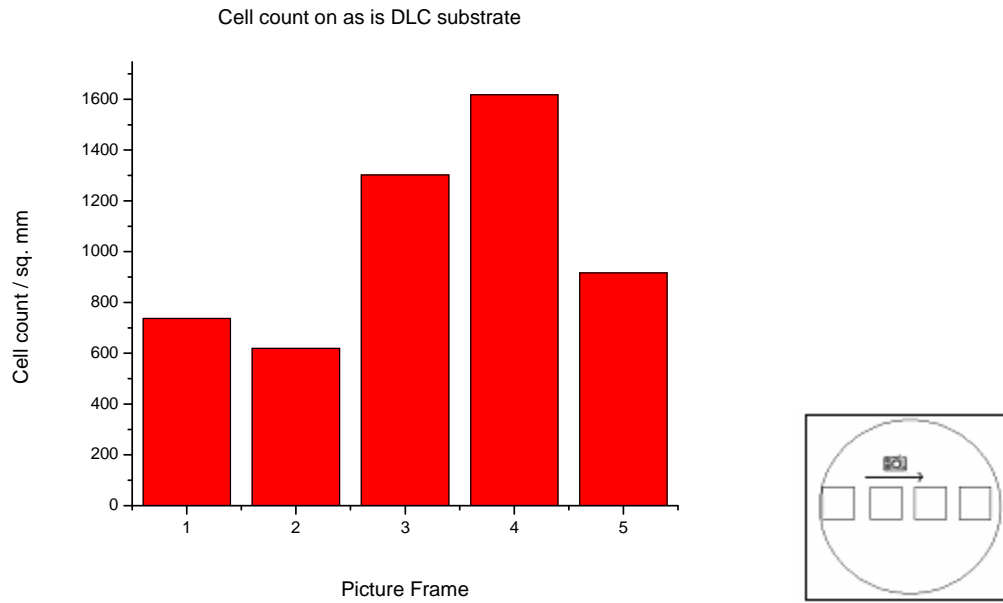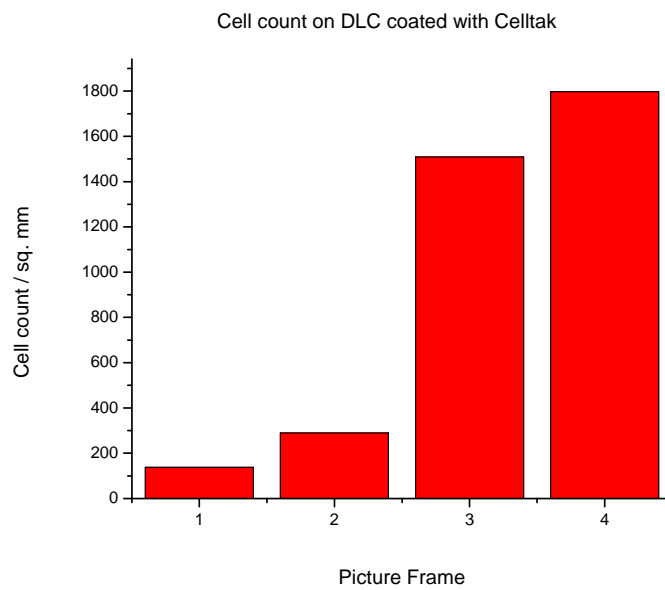
(b)

Fig. 5.1. Histograms of bovine chromaffin cell attachment on (a). As is DLC (b). CellTak coated DLC (Top Inset shows legend describing manner of imaging)

Cell count on Maleimide treated DLC
(cells not sulfhydryl reduced)

(c)

Cell count on Maleimide coated DLC
(cells sulfhydryl reduced)
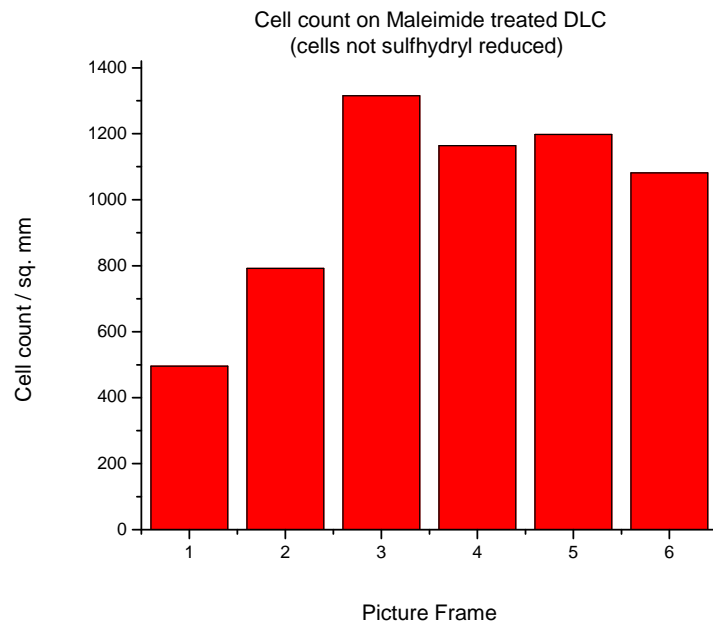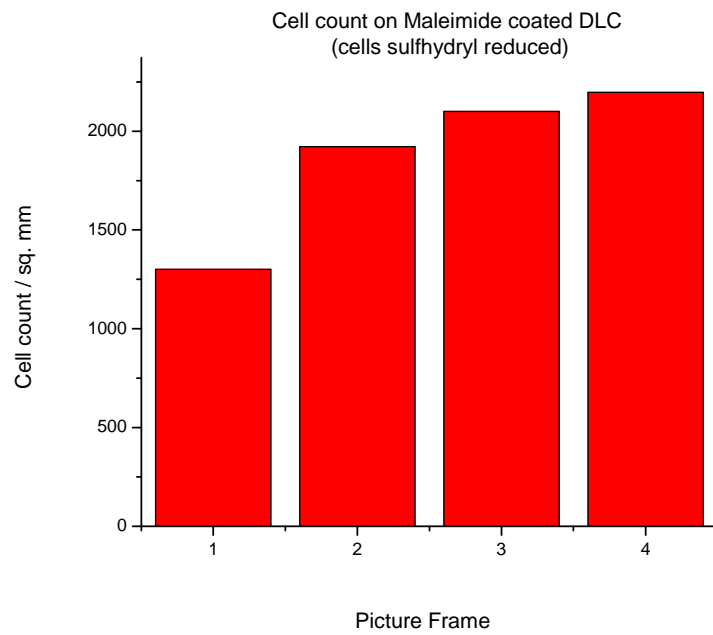
(d)

Fig. 5.1. Histograms of bovine chromaffin cell attachment to Maleimide activated DLC (c). Normal cells (d). Surface sulfhydryl group reduced cells

86

Cell count on Poly-l-lysine Coated DLC

(e)

Cell count on Poly-d-lysine coated DLC
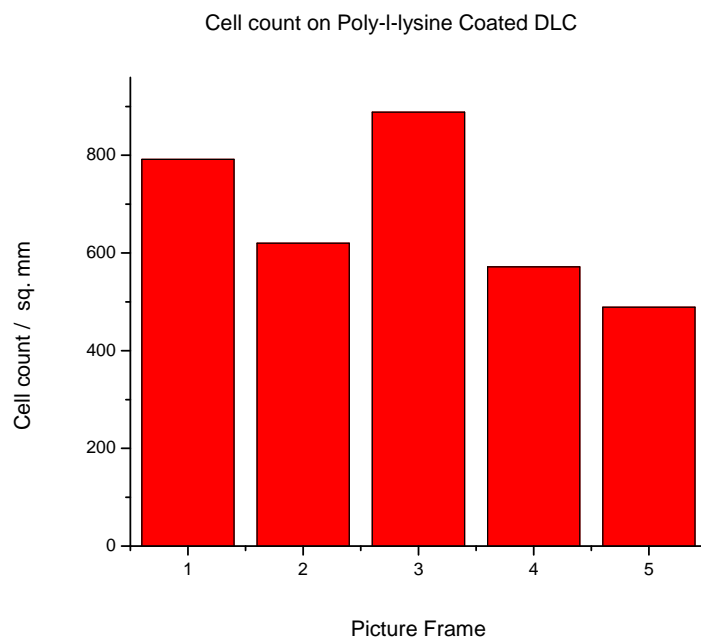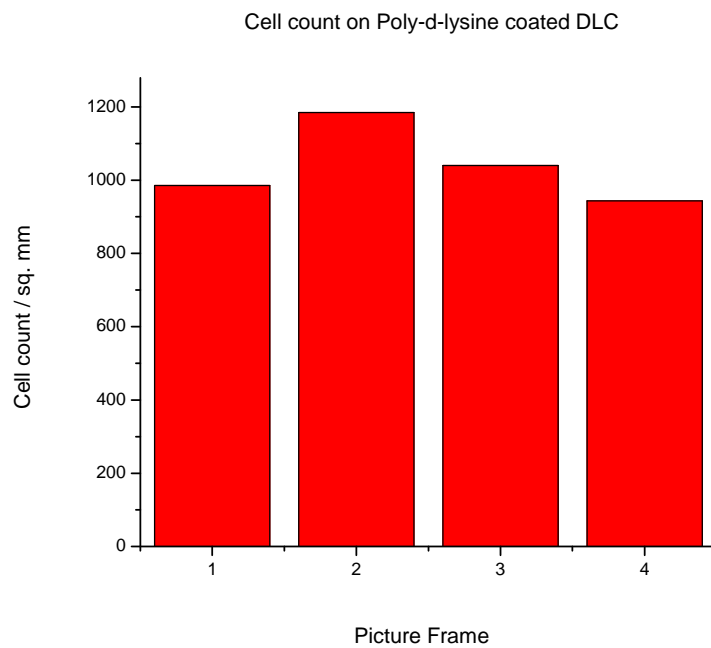
(f)

Fig. 5.1. Histograms of bovine chromaffin cell attachment to polylysine coated DLC (e). Poly-l-lysine (f). Poly-d-lysine

Cell count on Matrigel coated DLC

(g)

Cell count on Antibody-Maleimide coated DLC
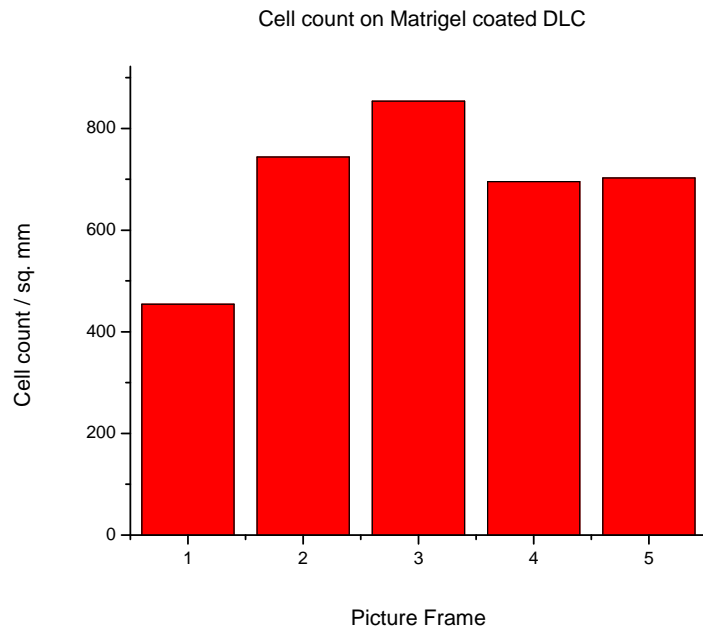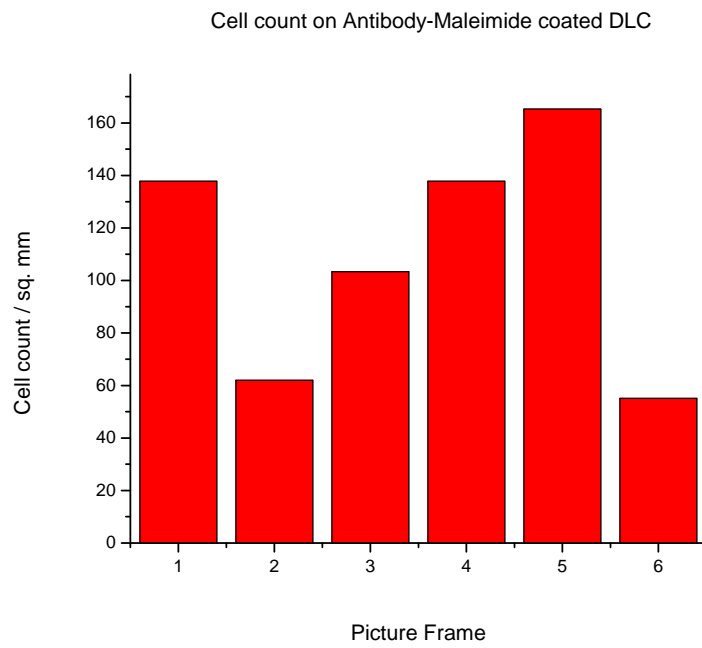
(h)

Fig. 5.1. Histograms of bovine chromaffin cell attachment to (g) Matrigel coated DLC
(h) Antibody-Maleimide activated surface

Cell count on different surface modified DLC

(A)
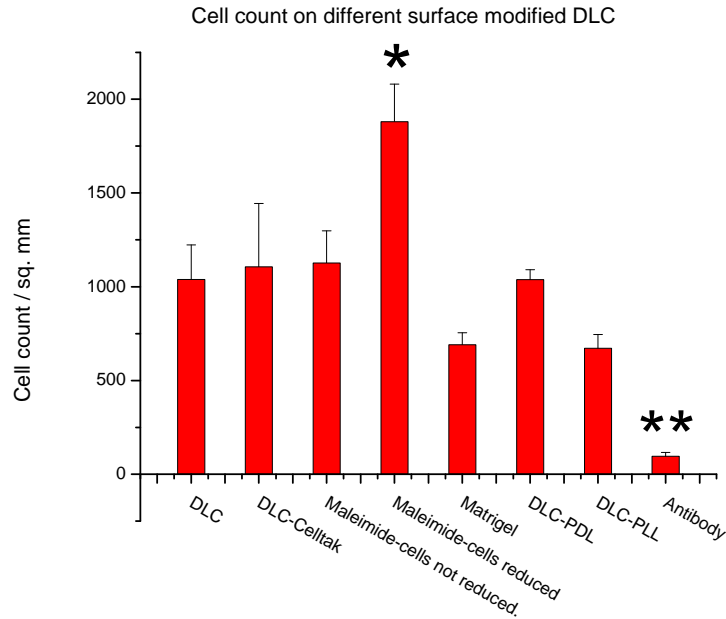
*At p<0.05, the mean cell count on DLC is significantly different from that of DLC-Maleimide-reduced cells and ** At p<0.01 DLC binds higher cells than Antibody modified DLC

(a)　　　　　(b)　　　　　(c)

(d)　　　　　(e)　　　　　(f)
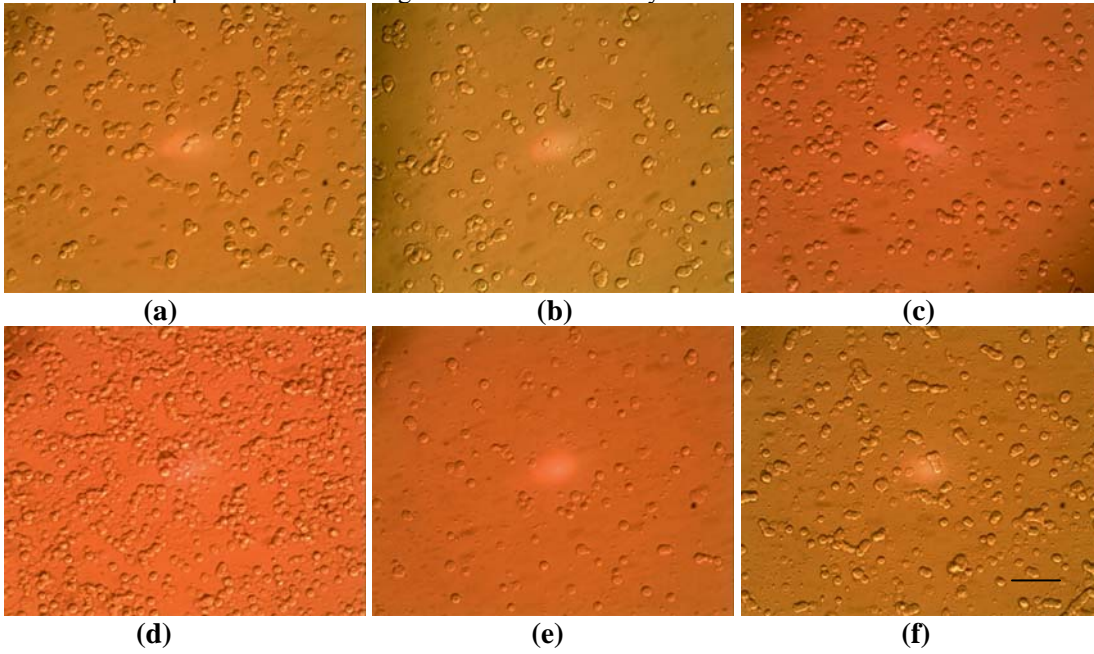
(B)

Fig. 5.2. (A). Summary of comparison of bovine chromaffin cell attachment to different surface modifications of DLC. The adhesion data are presented as the mean ± SE from 39 images compiled from 8 wells completed on one independent experiment. **(B).** Optical micrographs of bovine chromaffin cell attachment on different modifications of DLC (a) As is (b) CellTak coated (c) Maleimide activated, cells not reduced (d) Maleimide activated, cells reduced for sulfhydryl groups (e) Matrigel coated (f) Poly-d-lysine coated [Scale Bar represents 50µm]

(B)
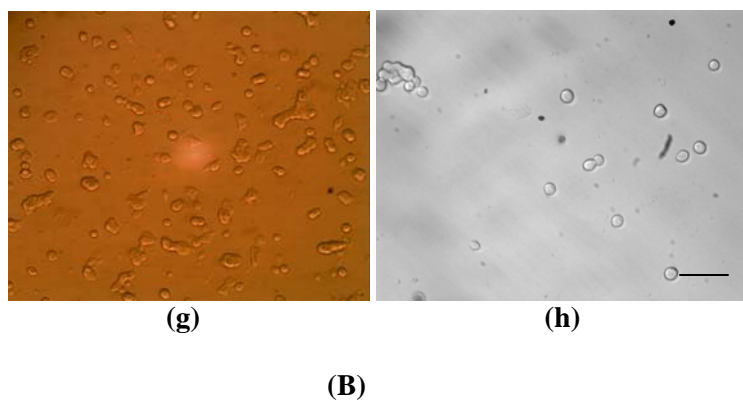
Fig. 5.2. (contd.) **(B).** Optical micrographs of bovine chromaffin cell attachment on different modifications of DLC (g) Poly-l-lysine coated (h) Maleimide activated and Antibody bound [Scale Bar represents 50μm]

As can be seen from Fig. 5.2, the highest cell adhesion has been observed on maleimide activated DLC with cells sulfhydryl reduced. Notable among other surface modifications was antibody binding which lead to reduced cell attachment as compared to the DLC control substrate ($p < 0.01$).

5.2. Experiment II: Bovine Chromaffin Cell Attachment Assays on Various Surface Modifications of DLC

Having quantified various surface modifications of DLC, it was concluded that although maleimide activation was conducive to cell attachment, it would only increase the labour involved in the microchip device fabrication, and there are speculations to the surface property of Teflon being disturbed with too many chemical processing steps. Exposing cells to reducing agents might also disrupt their function. In order to keep the process flow simple, some readily coatable material is the most suitable option. This includes polylysine, matrigel or oxygen plasma treatment of the DLC surface.

Cell count on as is DLC

(a)

Cell count on Plasma treated DLC
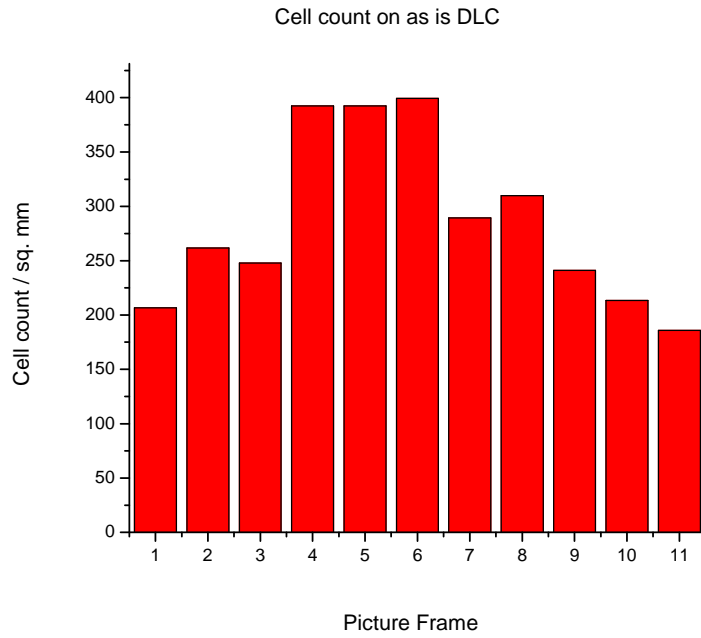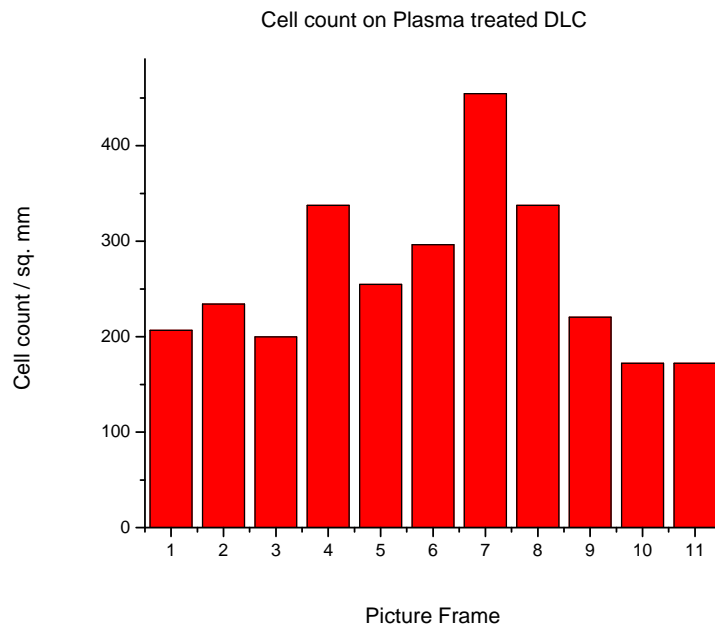
(b)

Fig. 5.3. Histograms of bovine chromaffin cell attachment on DLC (a) As is [control] (b) Oxygen plasma treated

Cell count on Matrigel coated DLC
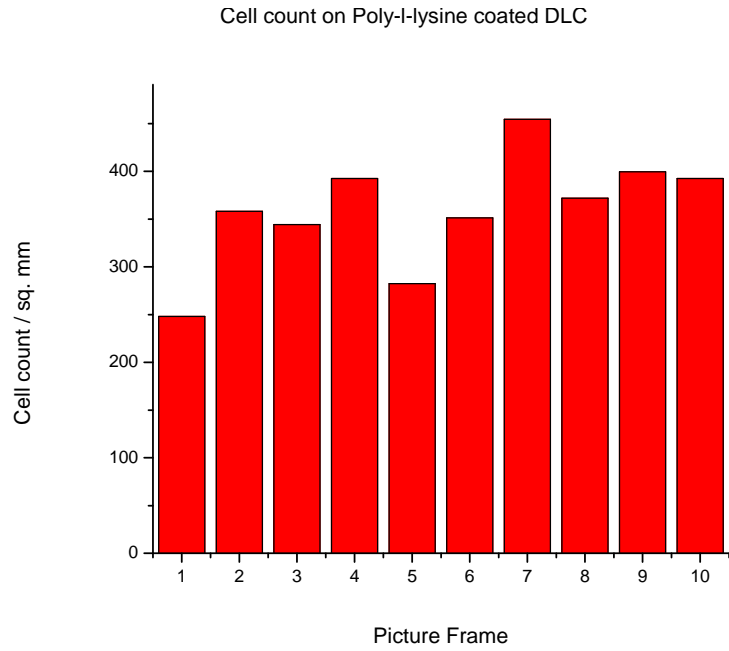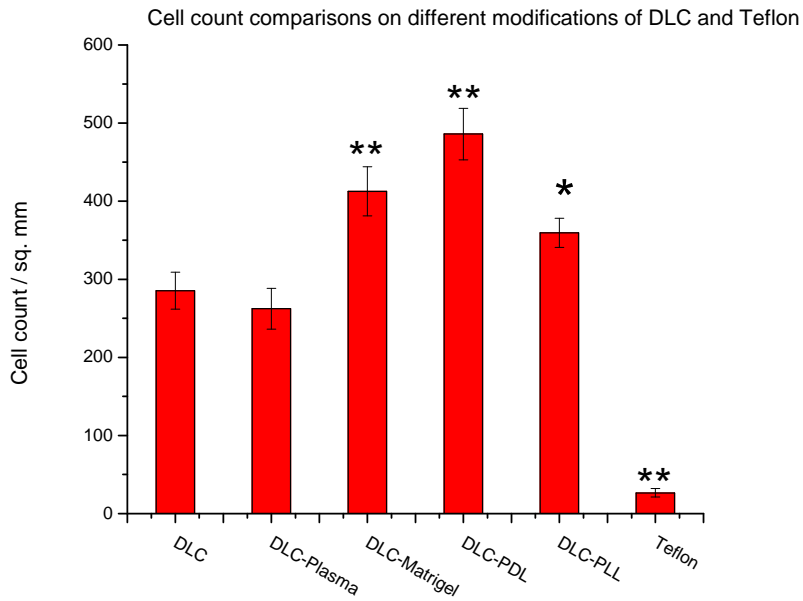
(c)
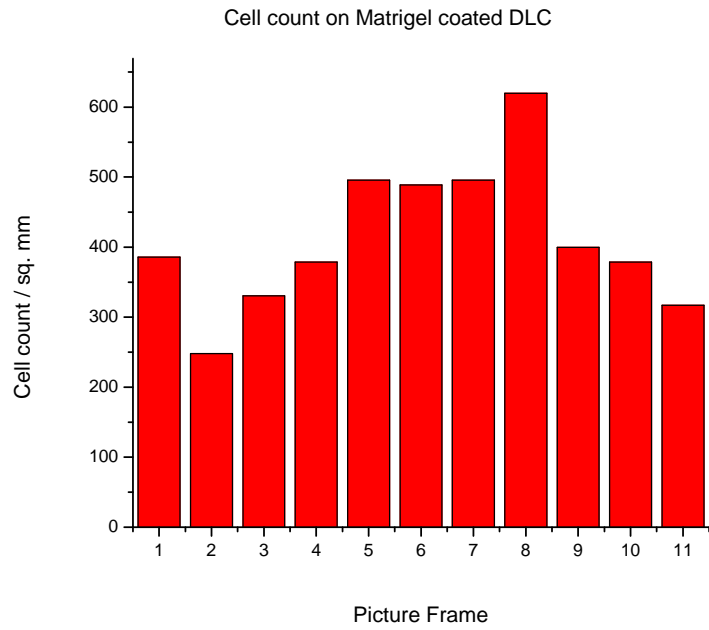
Cell count on Poly-d-lysine coated DLC
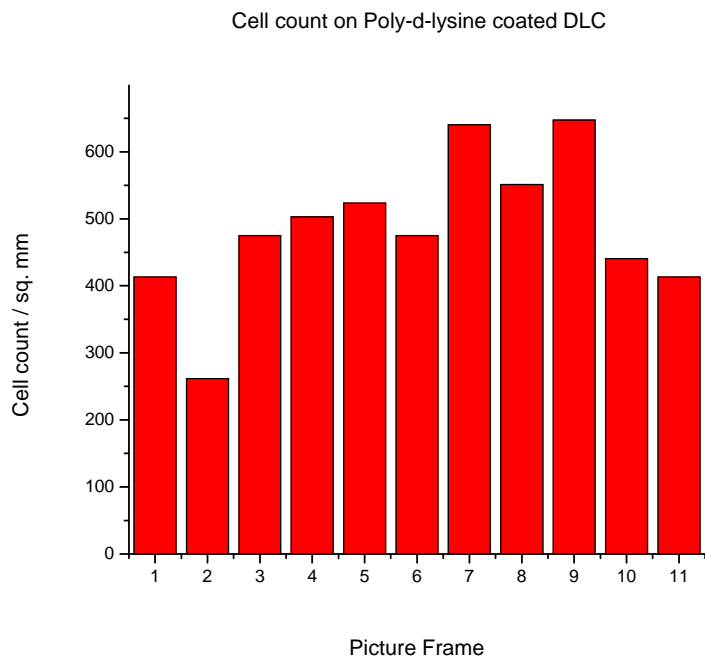
(d)

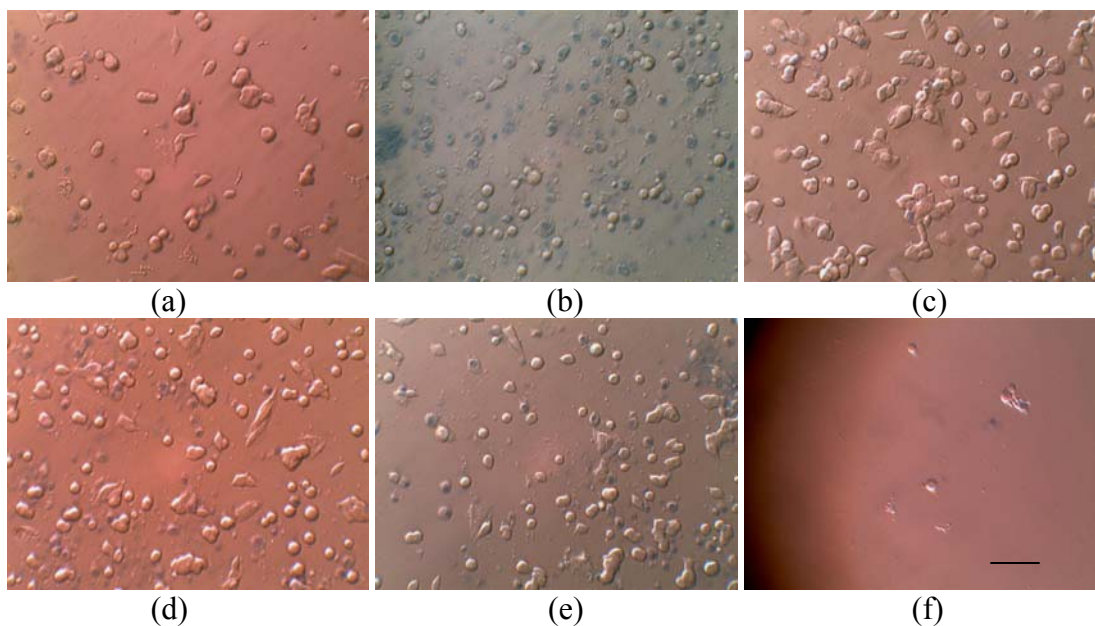**Fig. 5.3.** Histograms of bovine chromaffin cell attachment on DLC (c) Matrigel coated (d) Poly-d-lysine coated

(e)

Fig. 5.3. (e) Histogram of bovine chromaffin cell attachment on Poly-l-lysine coated DLC

Fig. 5.4. (A) Summary of bovine chromaffin cell attachment to different substrates

*At $p<0.05$, the mean live cell count is different from that of DLC and ** At $p<0.01$, the mean live cell count is different from that of DLC

Fig. 5.4. (B) Summary of bovine chromaffin cell attachment to different substrates (a) DLC as is (b) Oxygen plasma treated DLC (c) Matrigel coated DLC (d) Poly-d-lysine coated DLC (e) Poly-l-lysine coated DLC (f) Teflon [Scale Bar represents 50µm]

5.3. Experiment III: Bovine Chromaffin Cell Attachment Assay on DLC Doped and Undoped and Other Metals

Since DLC and Ti are both well characterized biomaterials, the idea was to integrate both of them into one material. DLC can be doped with Ti by co-sputtering the two. This can help replacing ITO as a deposition below DLC and bringing about a more suitable means to increase the conductivity of DLC retaining feature of transparency at the same time. This set of experiments compares 4 different substrates, namely DLC, Titanium (Ti), ITO and DLC co-sputtered with Ti.

Cell count on Ti

(a)

Cell count on DLC on ITO
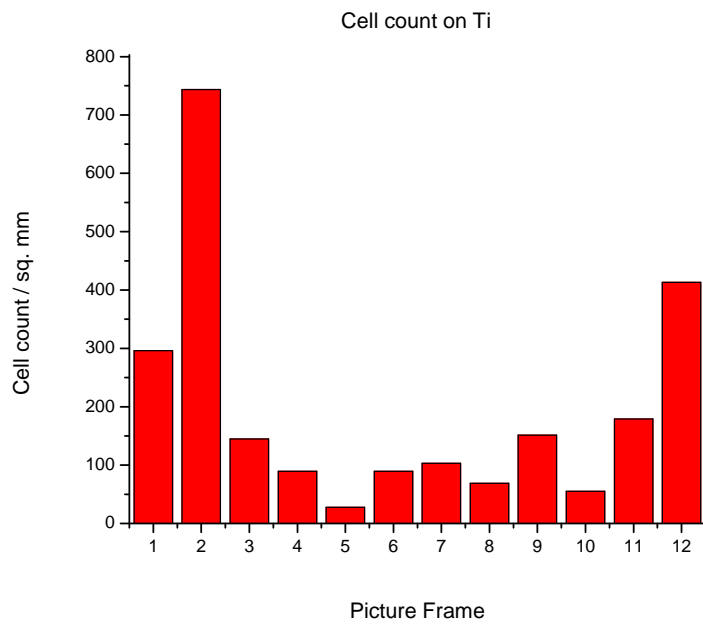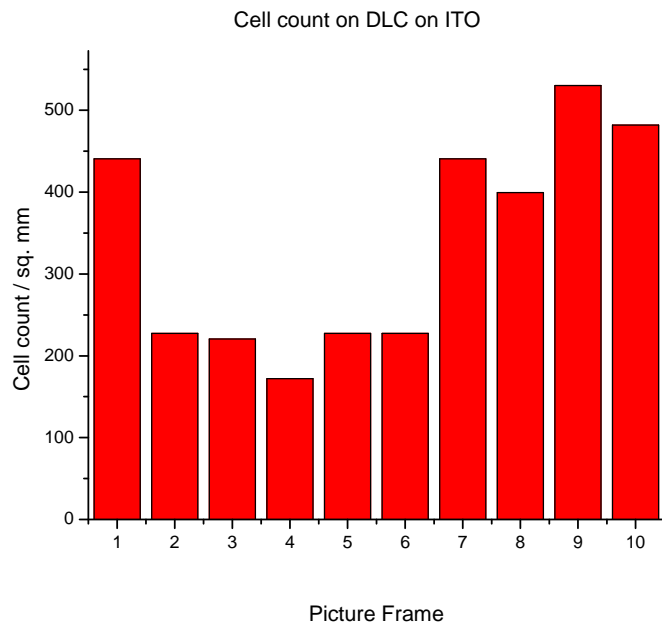
(b)

Fig. 5.5. Histograms of bovine chromaffin cell attachment on (a) Titanium (b) DLC deposited on ITO
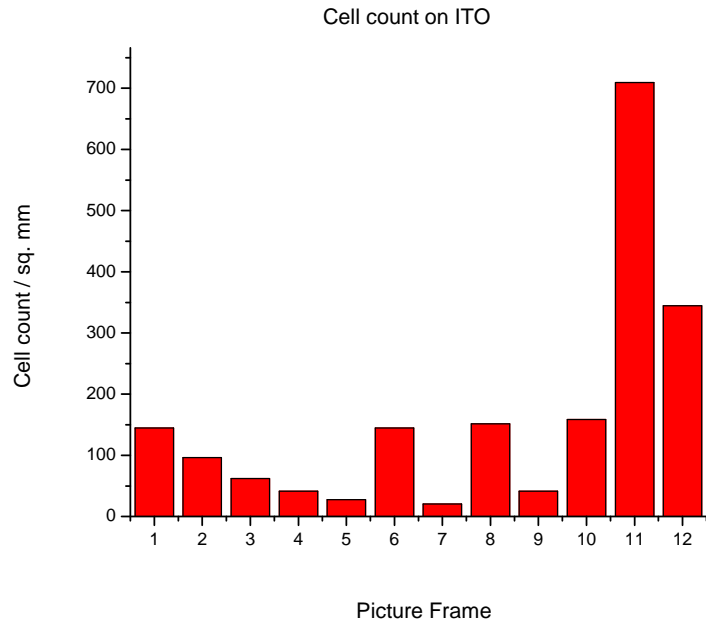
(c)
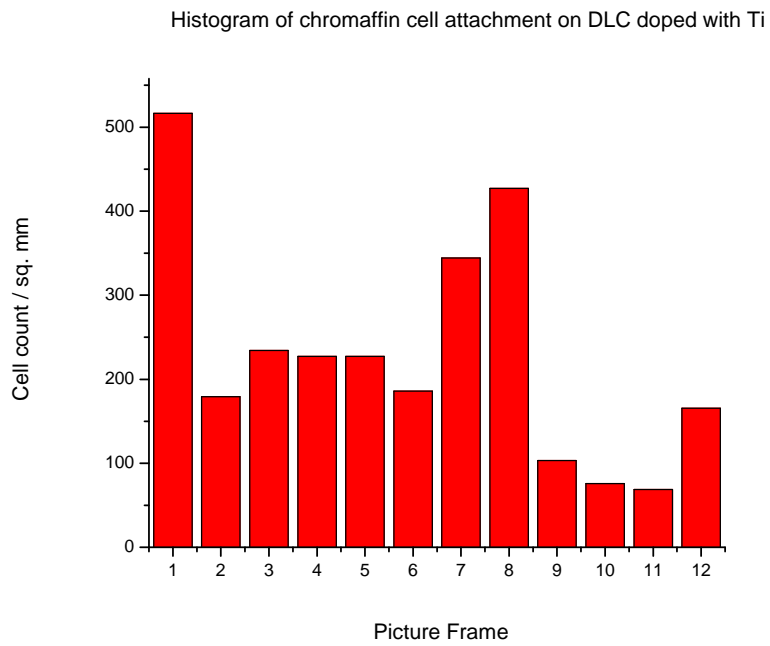
(d)

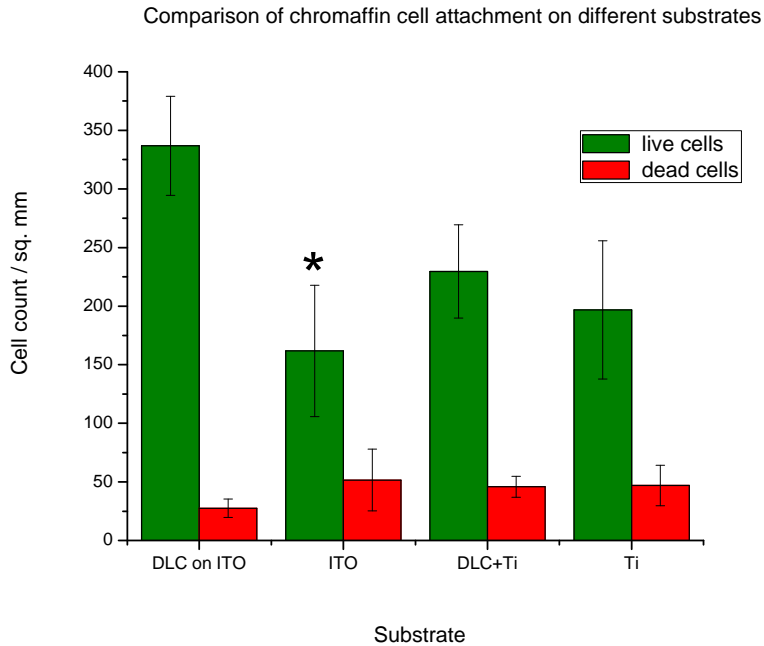**Fig. 5.5.** Histograms of bovine chromaffin cell attachment on (c) ITO (d) DLC co-sputtered with Ti

Comparison of chromaffin cell attachment on different substrates

(A)

*At p<0.05, the mean cell count is different compared to DLC on ITO

(a)   (b)   (c)

(d)
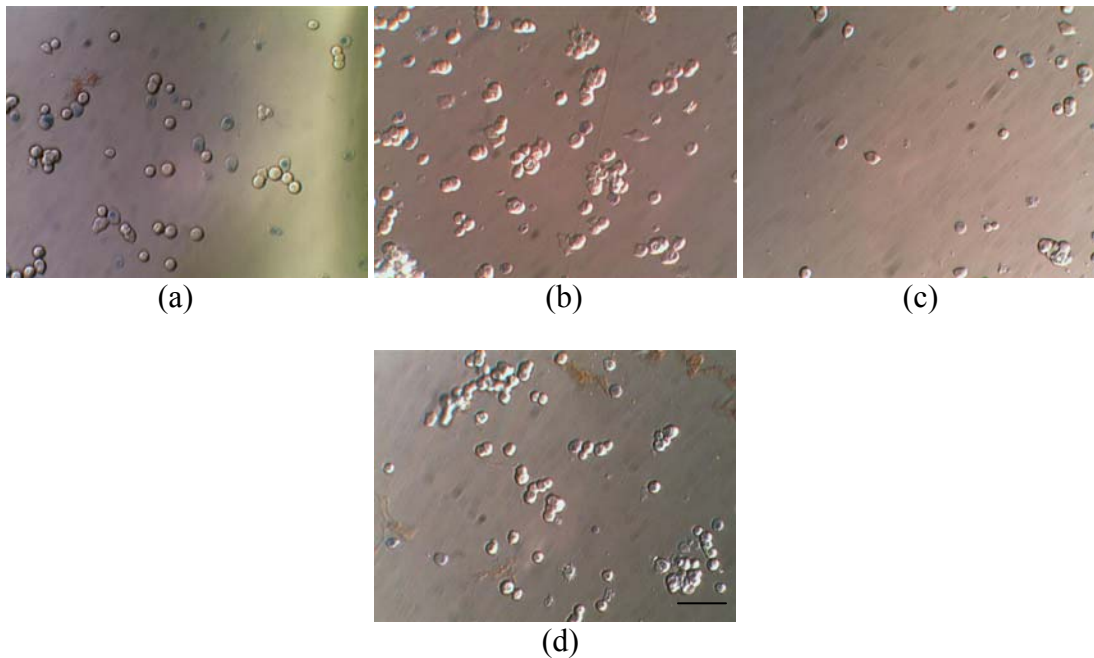
(B)

Fig. 5.6. (A) Summary of bovine chromaffin cell attachment to different substrates **(B)** Optical micrographs of bovine chromaffin cell attachment to (a) Ti (b) DLC on ITO (c) ITO (d) DLC co-sputtered wit Ti [Scale Bar represents 50μm]

5.4. Experiment IV: Bovine Chromaffin Cell Attachment Assay on As is and Various Surface Modified DLC and Other Metals

This set of experiments was performed on DLC as is, oxygen plasma treated and

hydrated DLC, polylysine coated DLC, ITO and Titanium.
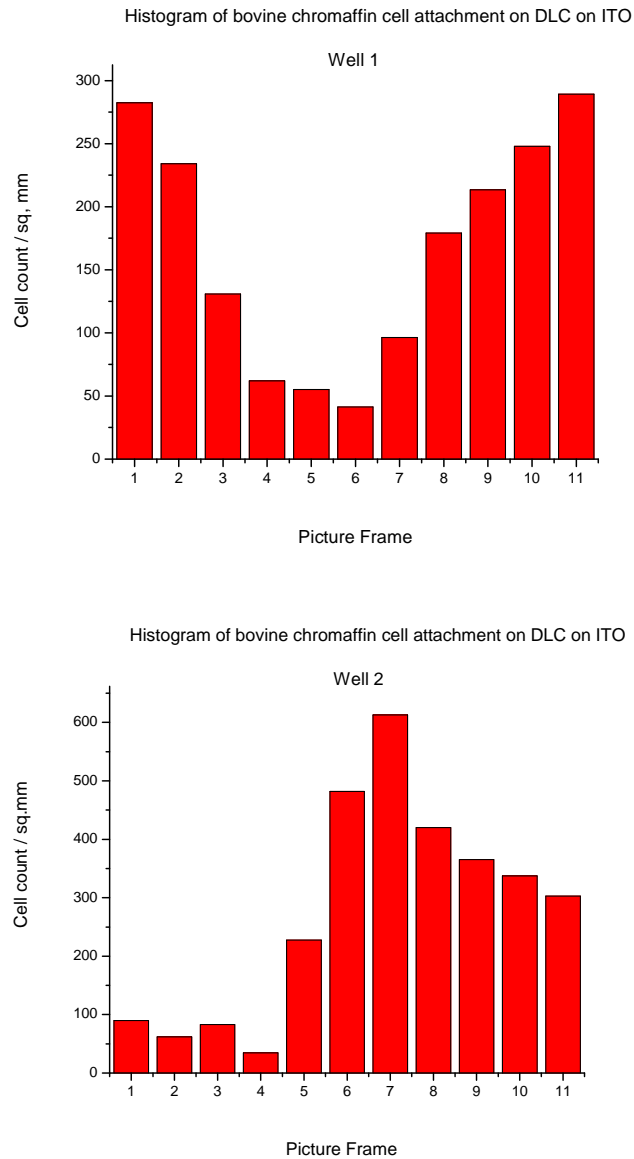
(a)

Fig. 5.7. Histograms of bovine chromaffin cell attachment on (a) DLC on ITO

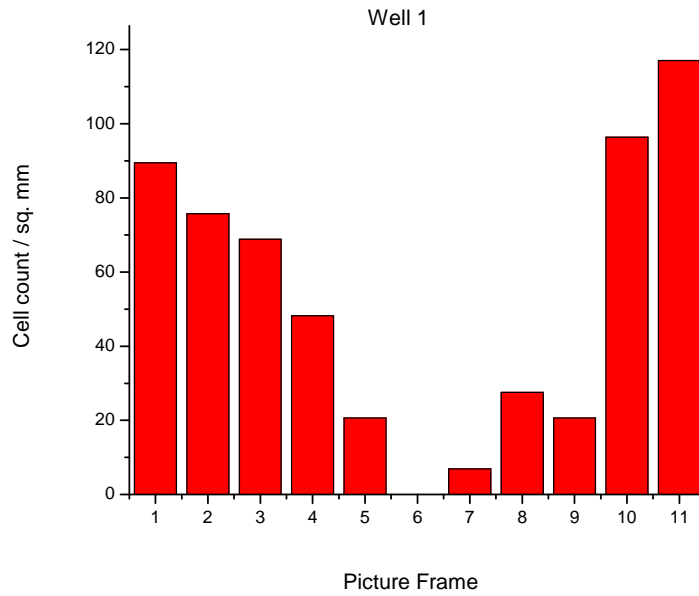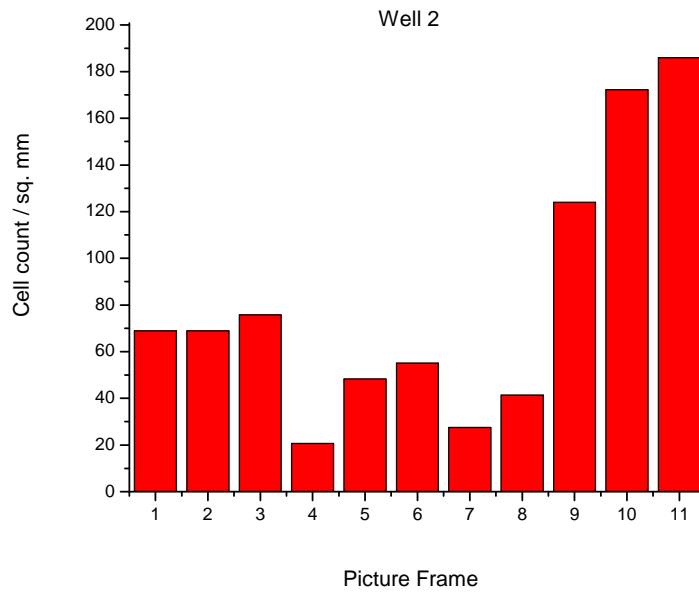Histogram of bovine chromaffin cell attachment DLC coated with Poly-d-lysine
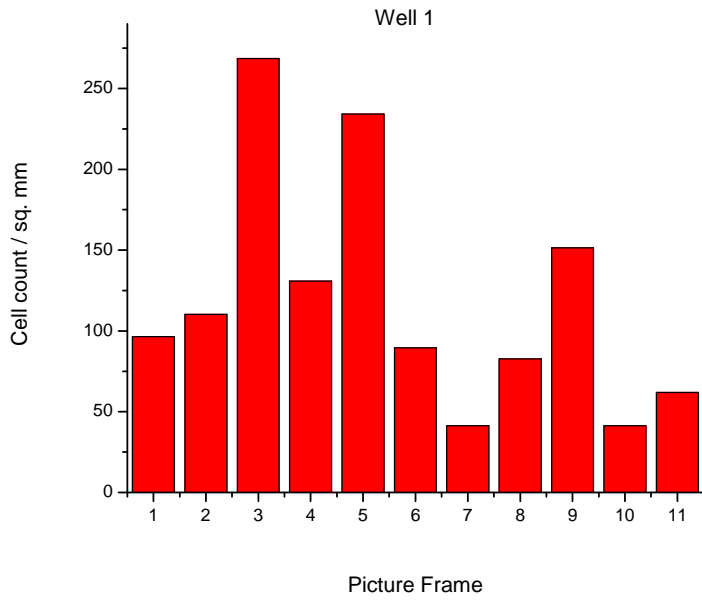
Histogram of bovine chromaffin cell attachment on DLC coated with Poly-d-lysine
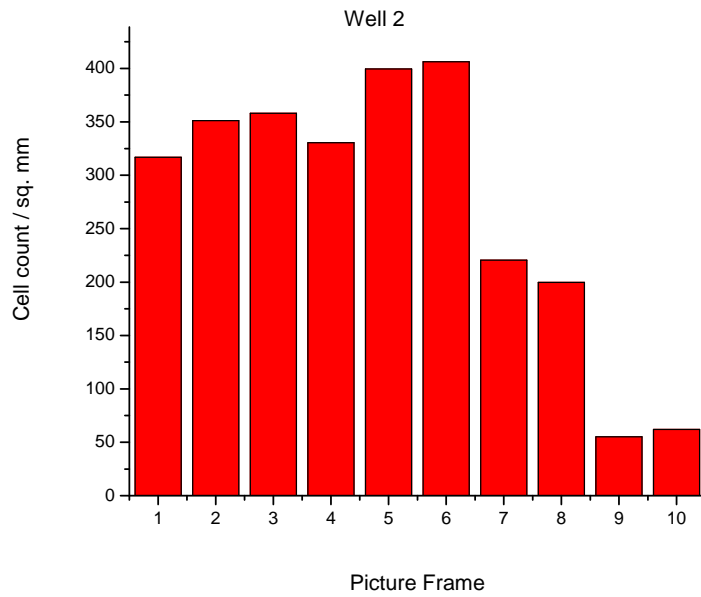
(b)

Fig. 5.7. Histograms of bovine chromaffin cell attachment on (b) DLC coated with Poly-d-lysine

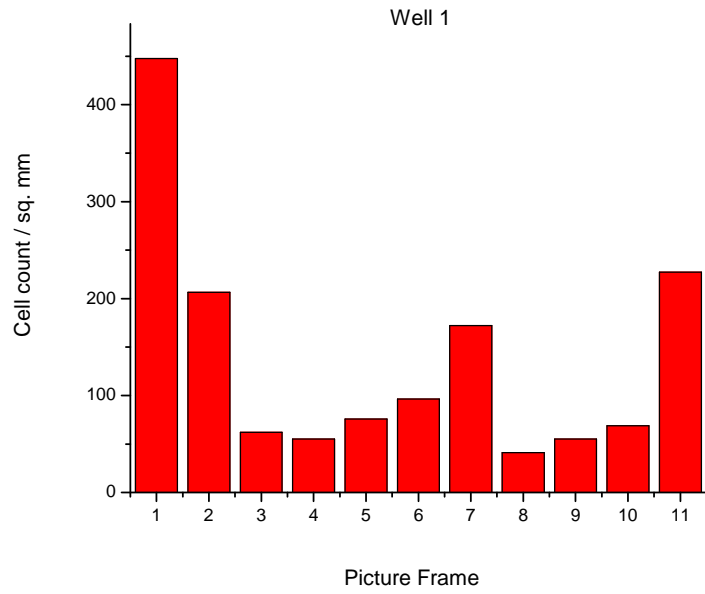Histogram of bovine chromaffin cell attachment on oxygen plasma treated DLC

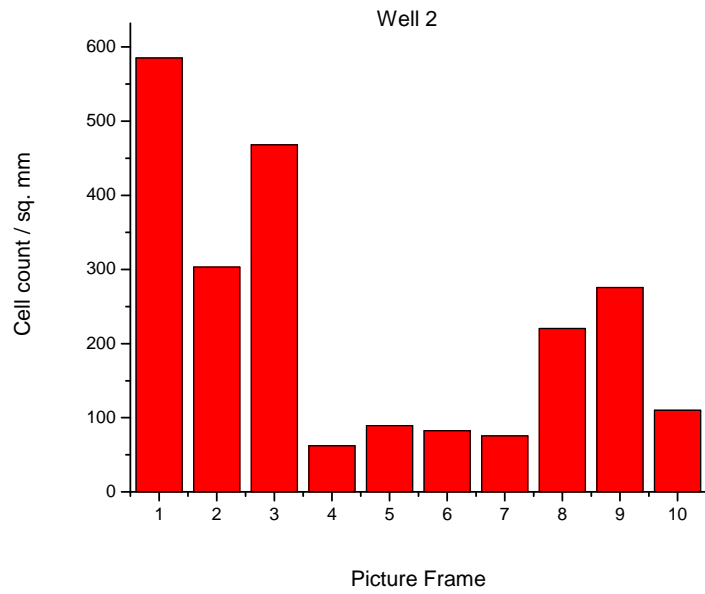Histogram of bovine chromaffin cell attachment on oxygen plasma treated DLC

(c)

Fig. 5.7. Histograms of bovine chromaffin cell attachment on (c) Oxygen plasma treated and hydrated DLC

Histogram of bovine chromaffin cell attachment on DLC coated with Poly-l-lysine
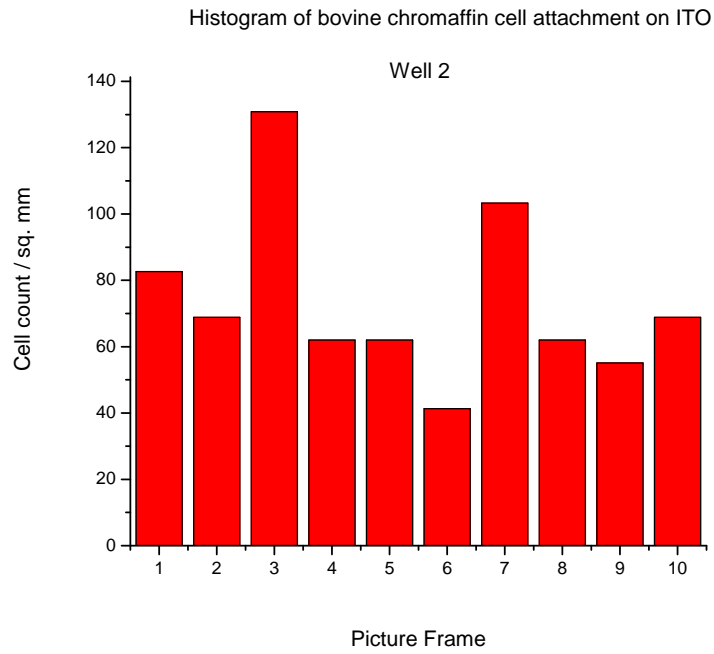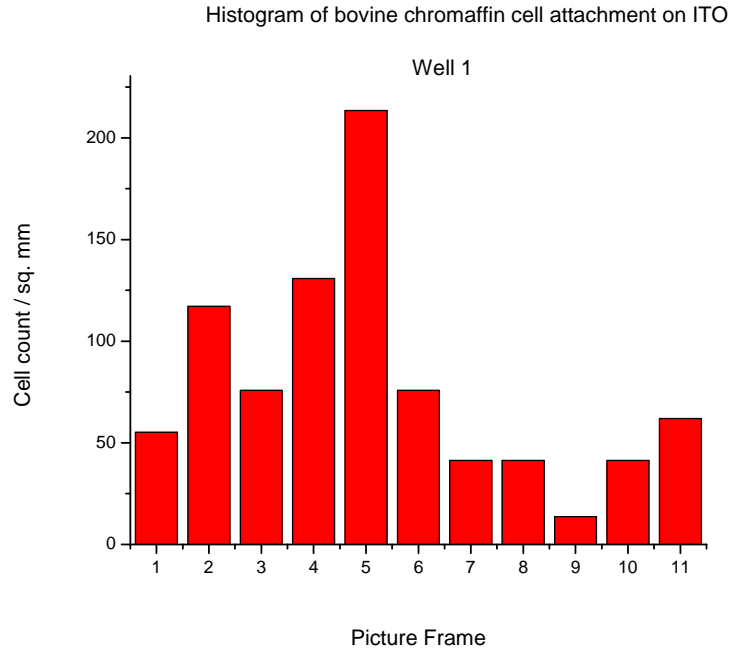
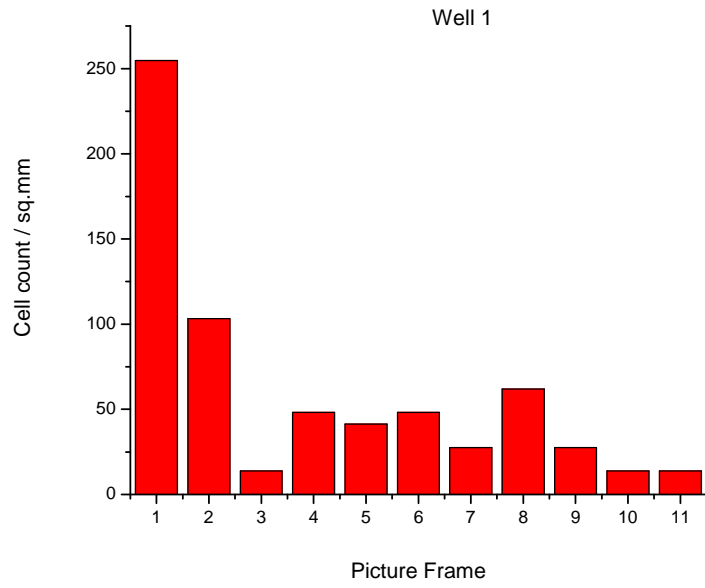

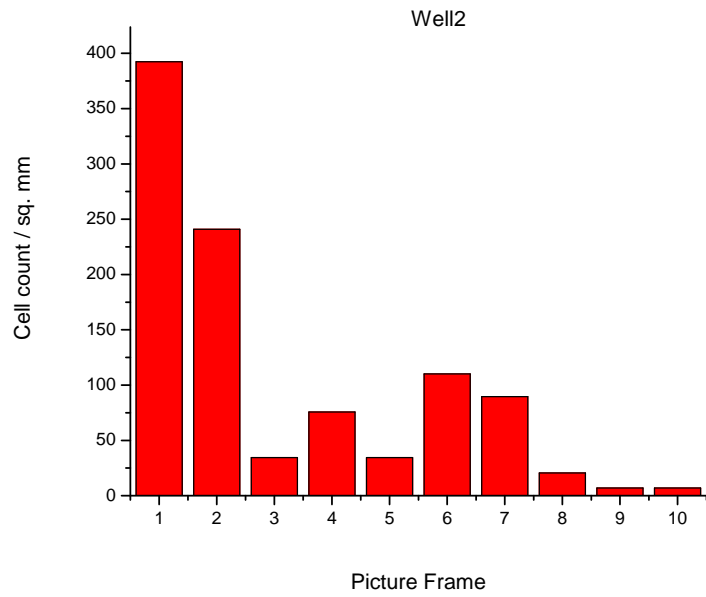Fig. 5.7. Histograms of bovine chromaffin cell attachment on (d) DLC coated with Poly-l-lysine

Fig. 5.7. Histograms of chromaffin cell attachment on (e) ITO

Histogram of bovine chromaffin cell attachment on Titanium

Well 1

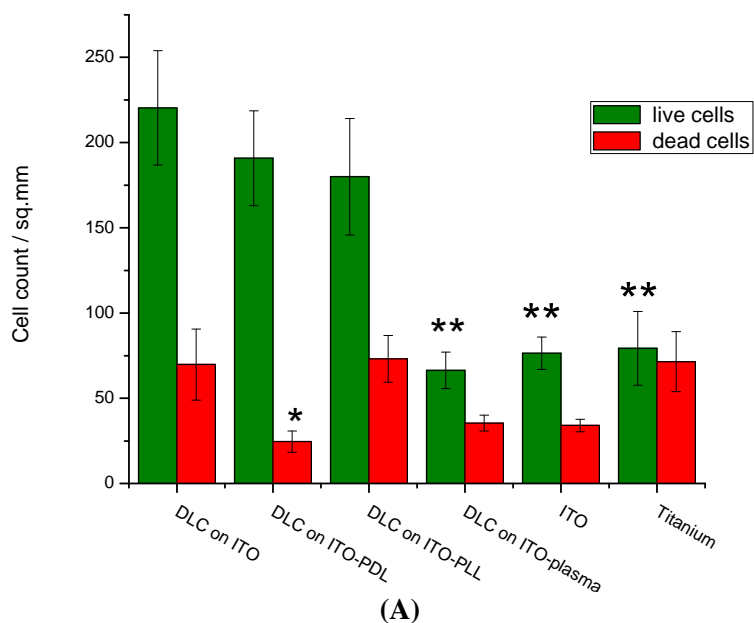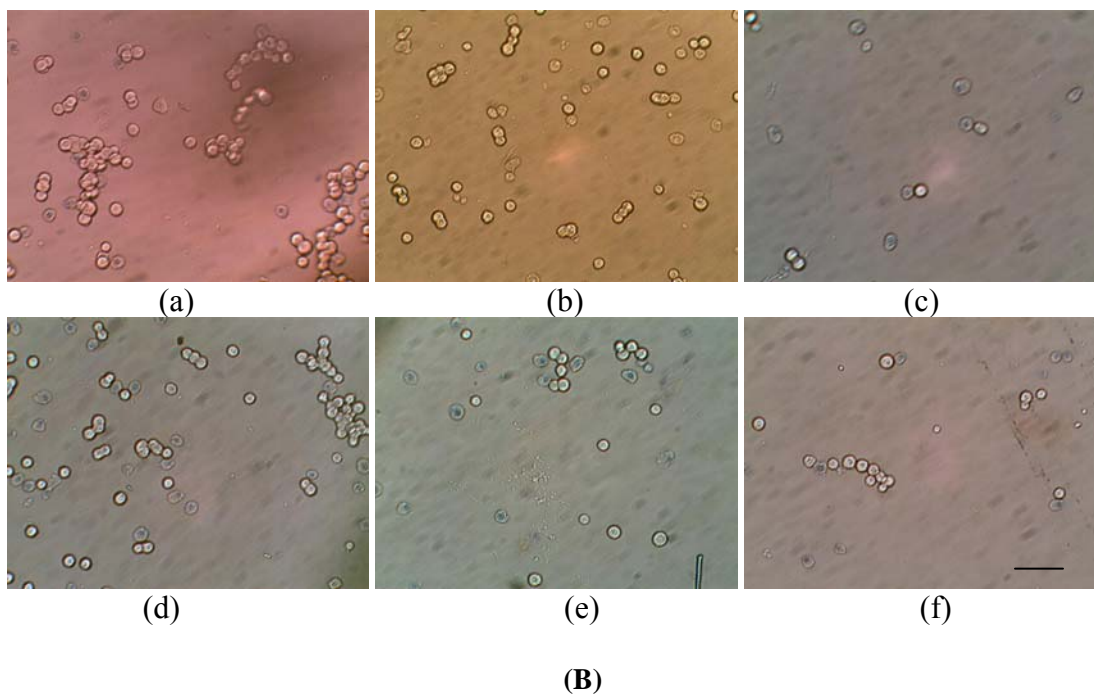Histogram of bovine chromaffin cell attachment on Titanium

Well2

(f)

Fig. 5.7. Histograms of bovine chromaffin cell attachment on (f) Titanium

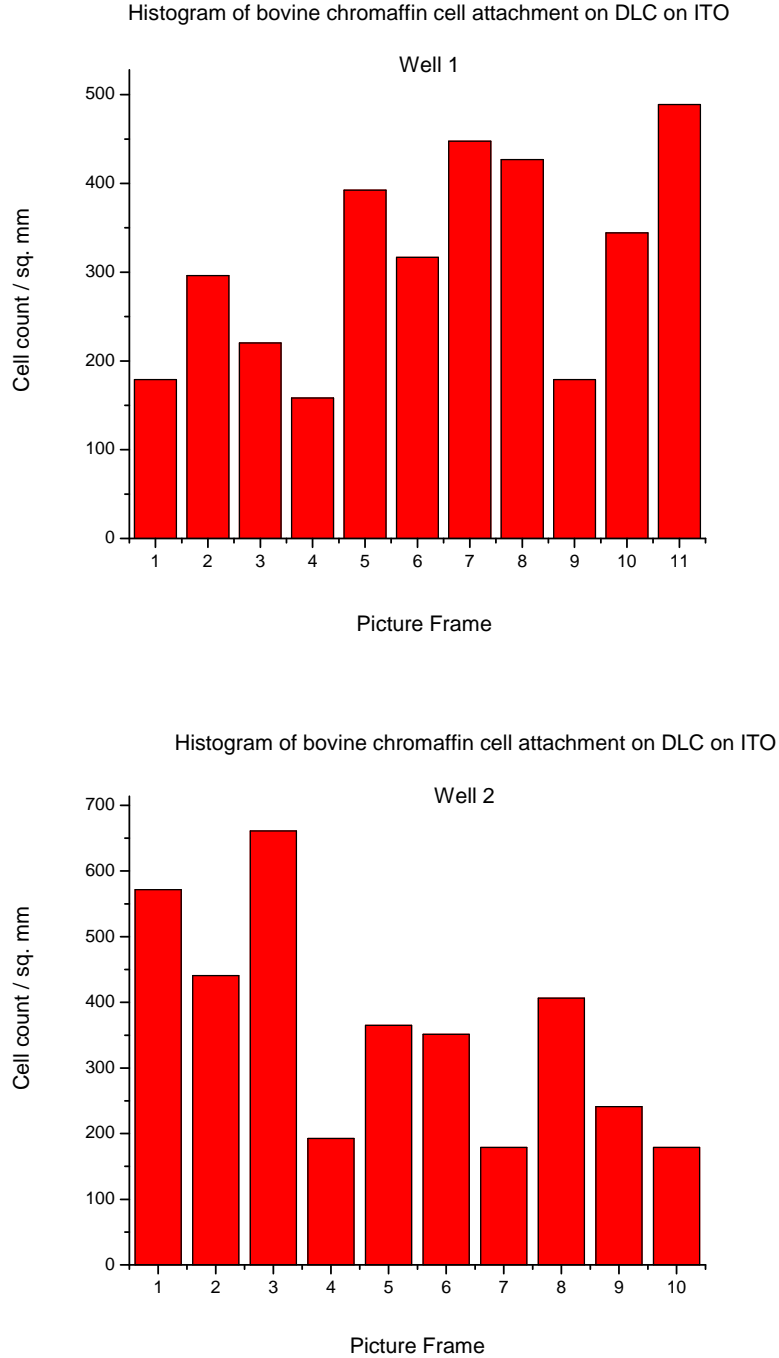Comparison of chromaffin cell attachment on different substrates

(A)

*At p<0.05, mean cell count is different from that of DLC on ITO and ** At p<0.01, mean cell count is different from that of DLC on ITO

(a)   (b)   (c)

(d)   (e)   (f)

(B)

Fig. 5.8. (A) Summary of bovine chromaffin cell attachment to different substrates **(B)** Optical micrographs of bovine chromaffin cell attachment to (a) DLC on ITO (b) PDL coated DLC (c) Oxygen plasma treated and hydrated DLC (d) PLL coated DLC on ITO (e) ITO (f) Titanium [Scale Bar represents 50μm]

5.5. Experiment V: Bovine Chromaffin Cell Attachment on Doped and Undoped DLC with Other Metals
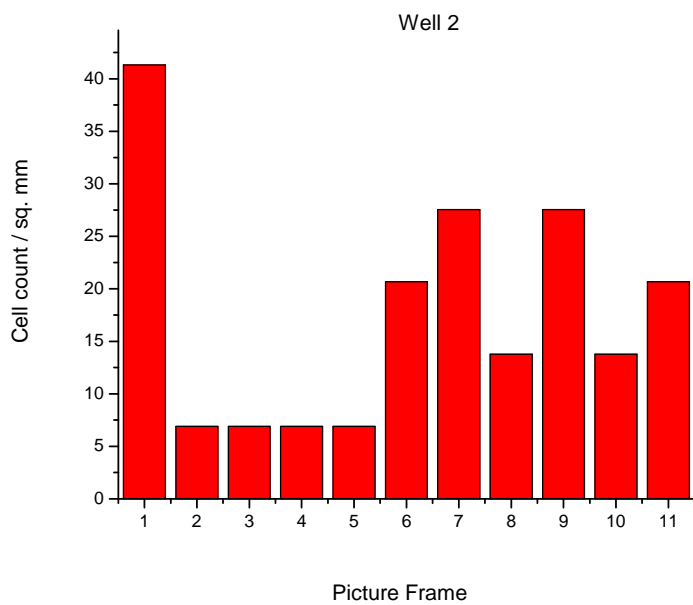

Fig. 5.9. Histograms of bovine chromaffin cell attachment on (a) DLC deposited on ITO

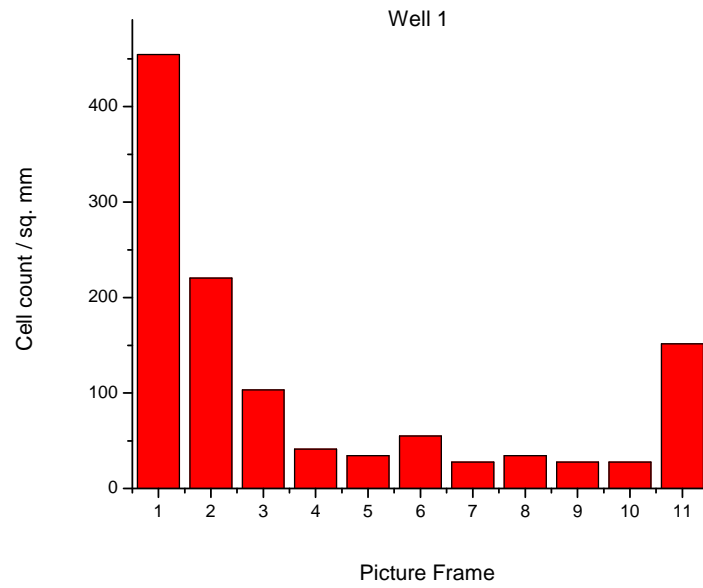Histogram of bovine chromaffin cell attachment on DLC doped with Titanium
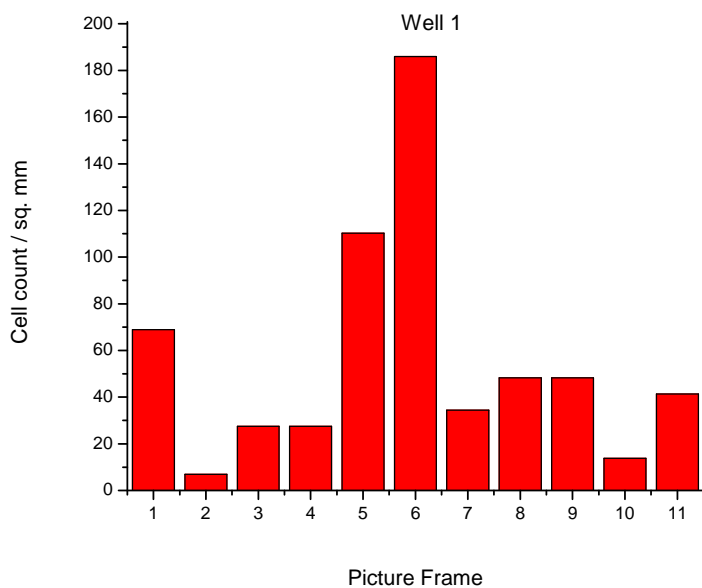
Well 1

Histogram of bovine chromaffin cell attachment on DLC doped with Ti

Well 2
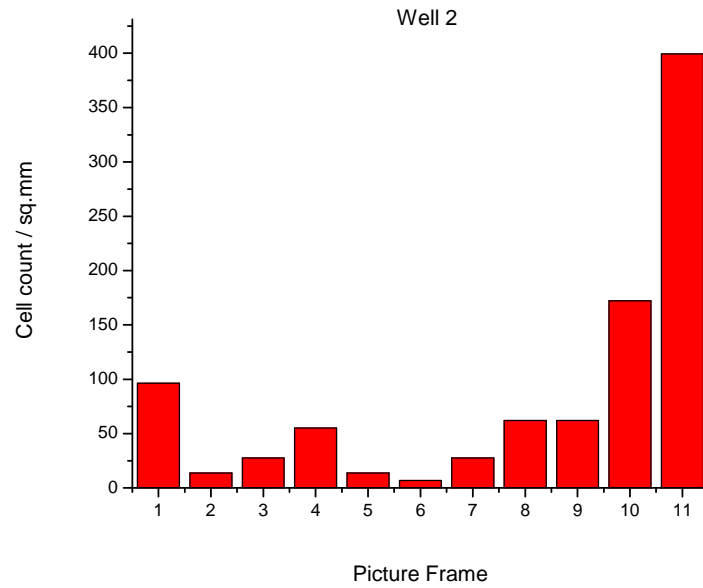

Fig. 5.9. Histograms of bovine chromaffin cell attachment on (b) DLC co-sputtered with Titanium

Histogram of bovine chromaffin cell attachment on oxygen plasma treated DLC

Well 1

Histogram of bovine chromaffin cell attachment on oxygen plasma treated DLC

Well 2

Fig. 5.9. Histograms of bovine chromaffin cell attachment on (c) Plasma treated and hydrated DLC on ITO substrate

Histogram of bovine chromaffin cell attachment on ITO

Well 1

Picture Frame

Histogram of bovine chromaffin cell attachment on ITO

Well 2

Picture Frame
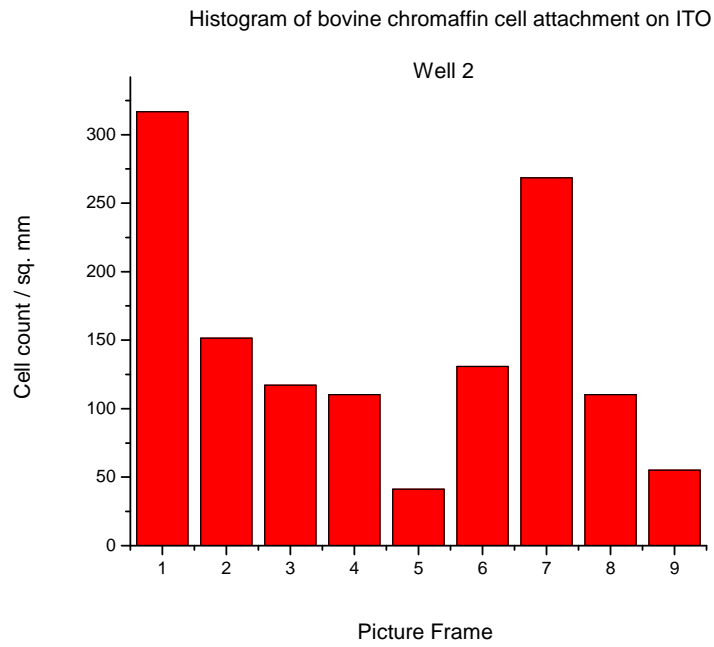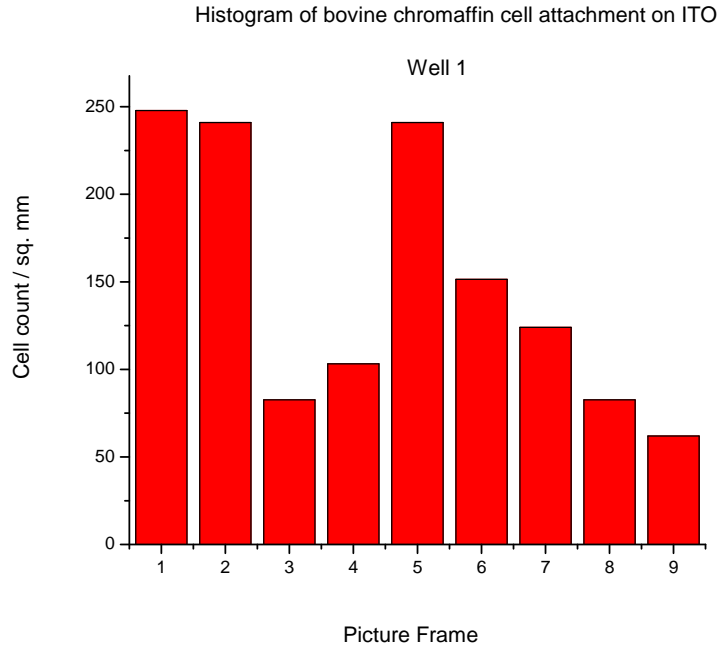
Fig. 5.9. Histograms of bovine chromaffin cell attachment on (d) ITO

Histogram of bovine chromaffin cell attachment on ITO coated with poly-d-lysine
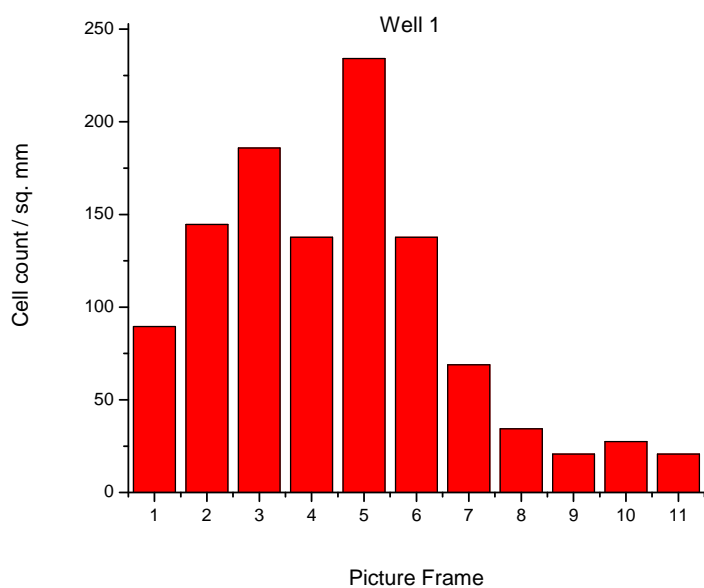
Well 1

Cell count / sq. mm

Picture Frame

Histogram of bovine chromaffin cell attachment on ITO coated with Poly-d-lysine

Well 2

Cell count / sq. mm

Picture Frame

Fig. 5.9. Histograms of bovine chromaffin cell attachment on (e) Poly-d-lysine coated DLC deposited on ITO substrate

Histogram of bovine chromaffin cell attachment on ITO coated with Poly-l-lysine

Well 1

Cell count / sq. mm

Picture Frame

Histogram of bovine chromaffin cell attachment on ITO coated with Poly-l-lysine

Well 2

Cell count / sq. mm

Picture Frame

Fig. 5.9. Histograms of bovine chromaffin cell attachment on (f) Poly-l-lysine coated DLC deposited on ITO substrate

Histogram of bovine chromaffin cell attachment on Platinum

Well 1

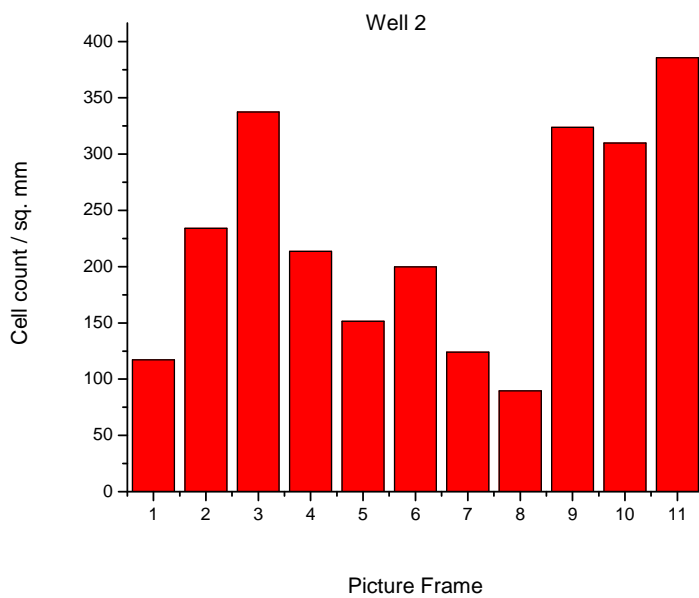Histogram of bovine chromaffin cell attachment on Platinum

Well 2

Fig. 5.9. Histograms of bovine chromaffin cell attachment on (g) Platinum substrate

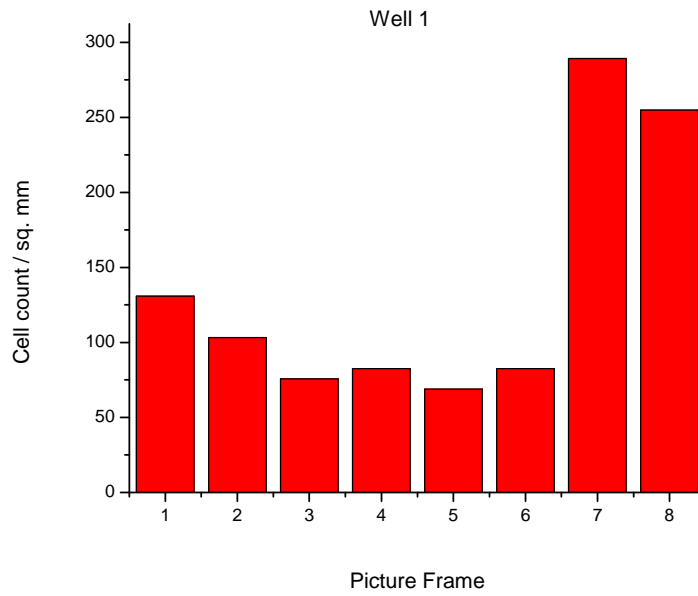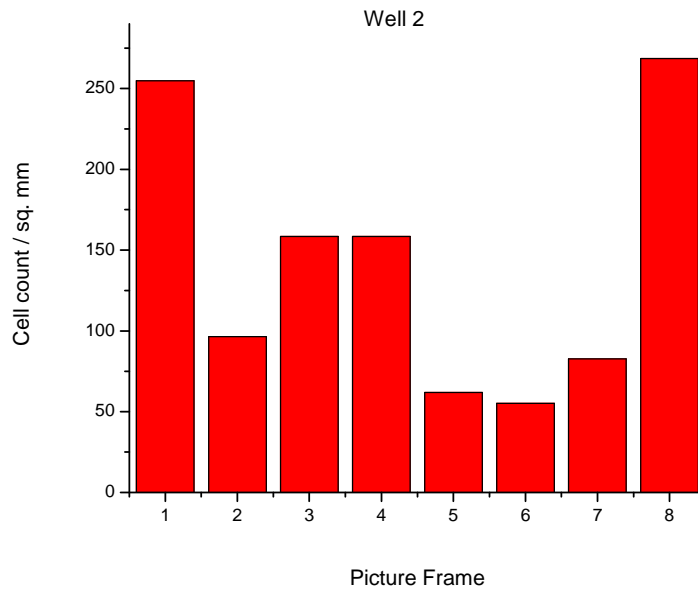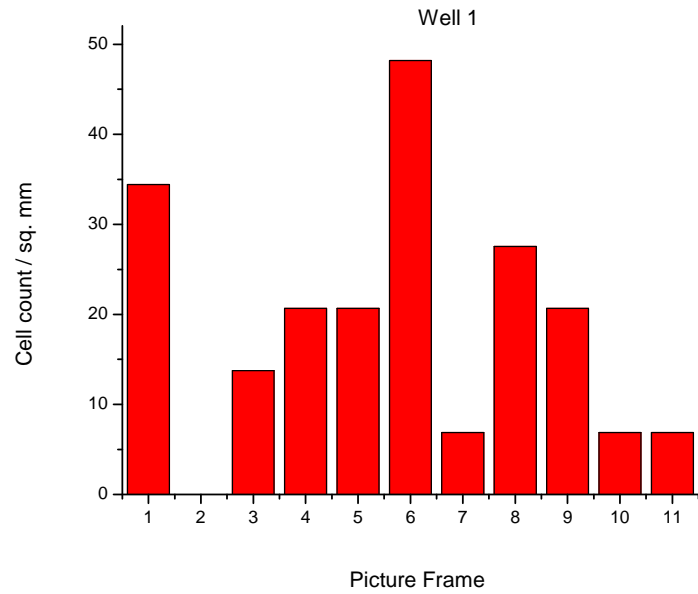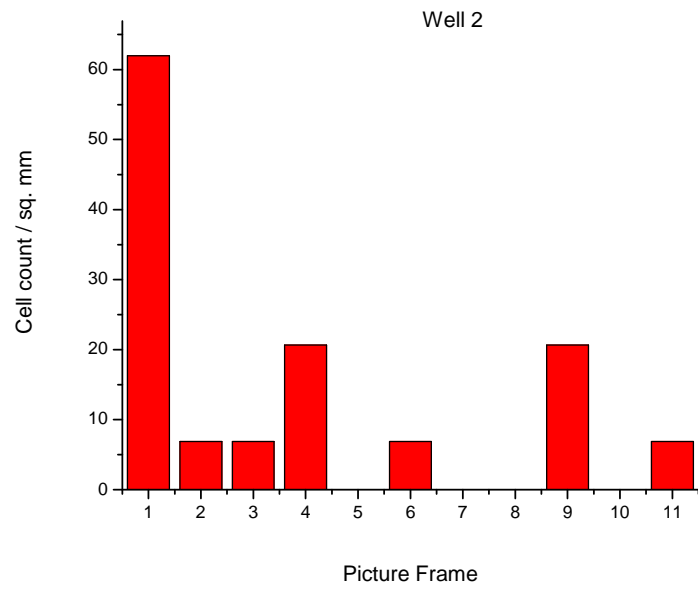Histogram of bovine chromaffin cell attachment on Titanium

Well 1

Histogram of bovine chromaffin cell attachment on Titanium

Well 2

Fig. 5.9. Histograms of bovine chromaffin cell attachment on (h) Titanium

Comparison of bovine chromaffin cell attachment on different substrates

(A)

*At p<0.05, mean cell count is different from that on DLC on ITO and ** At p<0.01, mean cell   count is different from that on DLC on ITO

(B)

Fig. 5.10. (A) Summary of bovine chromaffin cell attachment to different substrates **(B)** Optical micrographs of bovine chromaffin cell attachment to (a) DLC on ITO (b) Oxygen plasma treated and hydrated DLC (c) ITO (d) PDL coated ITO (e) PLL coated ITO (f) Platinum [Scale Bar represents 50μm]

<div style="text-align:center">(g)   (h)</div>

Fig. 5.10. (contd.) (B) Optical micrographs of bovine chromaffin cell attachment to (g) Titanium (h) DLC co-sputtered with Titanium [Scale Bar represents 50µm]

5.6. Experiment VI: Bovine Chromaffin cell attachment assay on DLC, ITO and Teflon

This set of experiments has been performed to compare DLC on ITO, ITO and Teflon with and without poly-d-lysine. Since it gave a higher average cell attachment although not statistically significant, poly-d-lysine is being chosen over its 'l' form from hereupon.
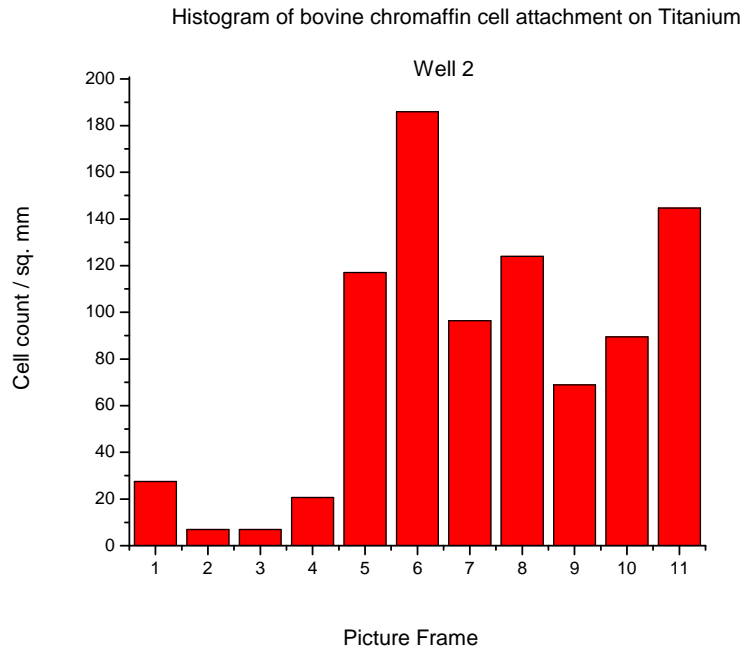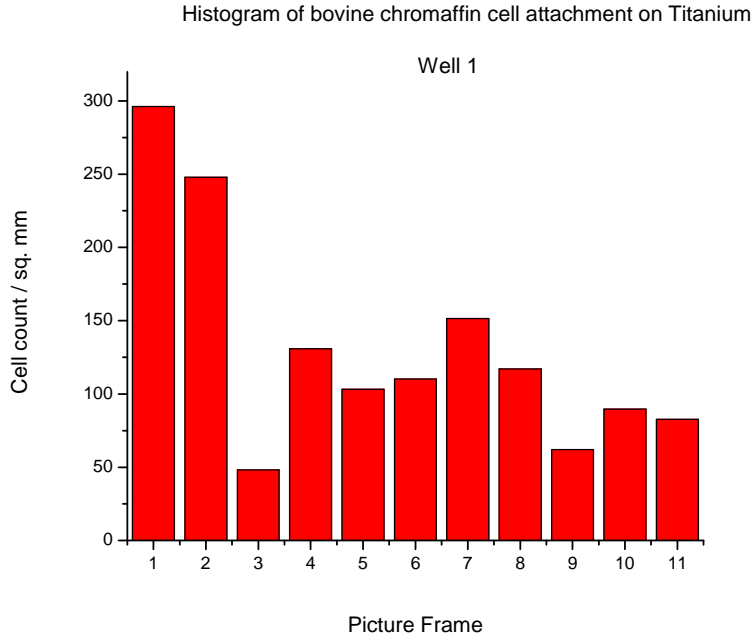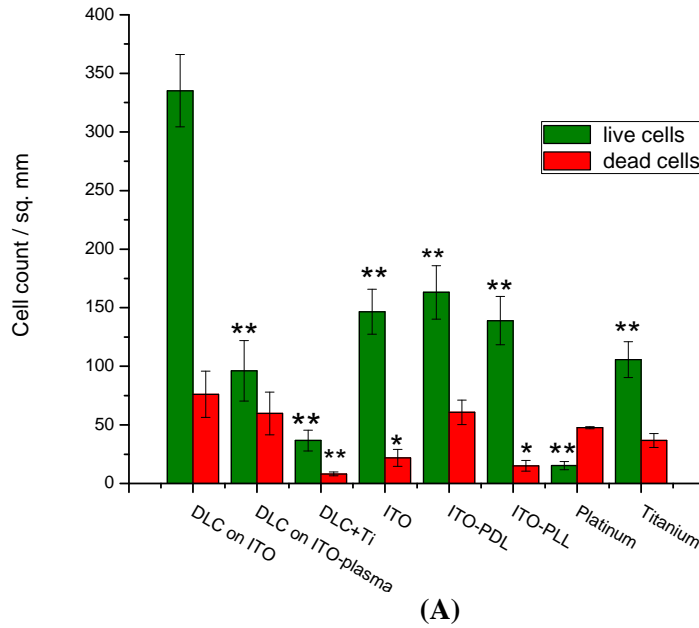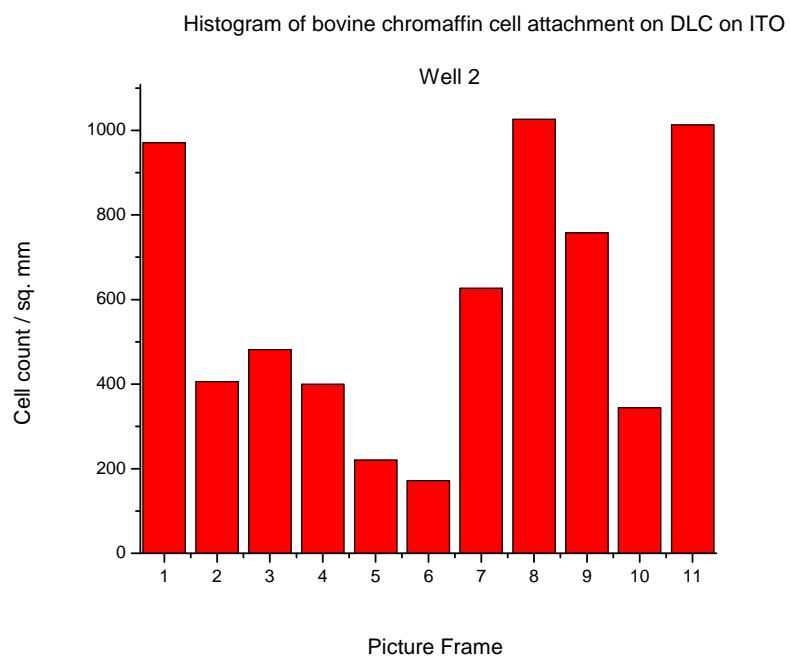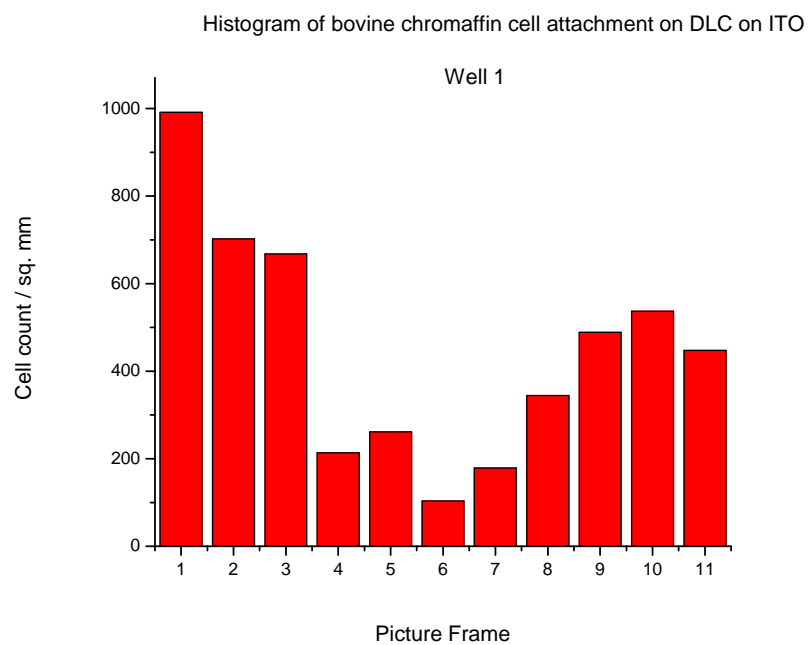
Histogram of bovine chromaffin cell attachment on DLC on ITO

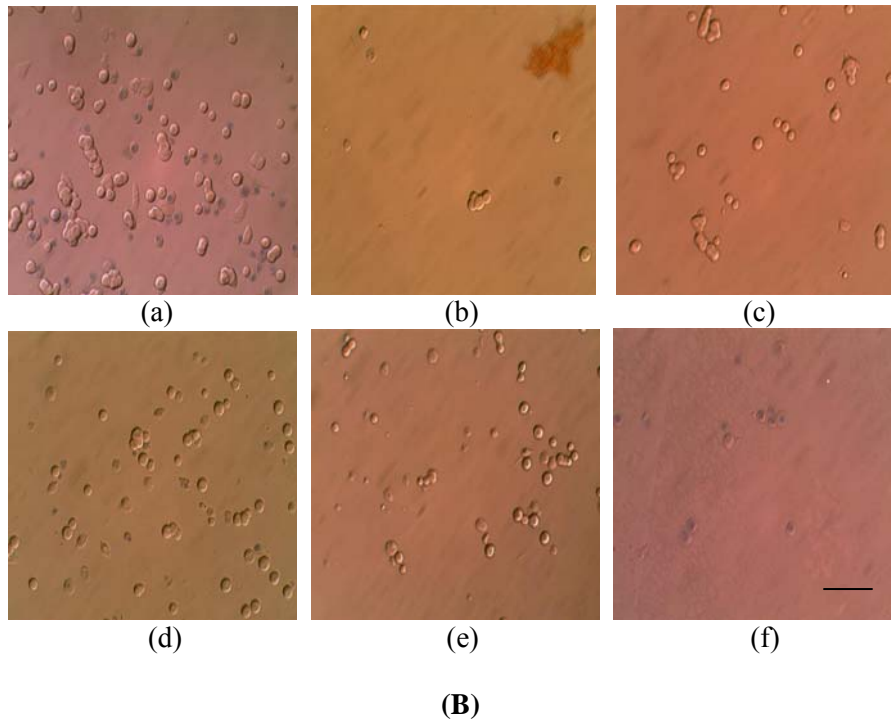**Fig. 5.11.** Histograms of bovine chromaffin cell attachment on (a) DLC on ITO

Histogram of bovine chromaffin cell attachment on ITO

Well 1

Histogram of bovine chromaffin cell attachment on ITO

Well 2

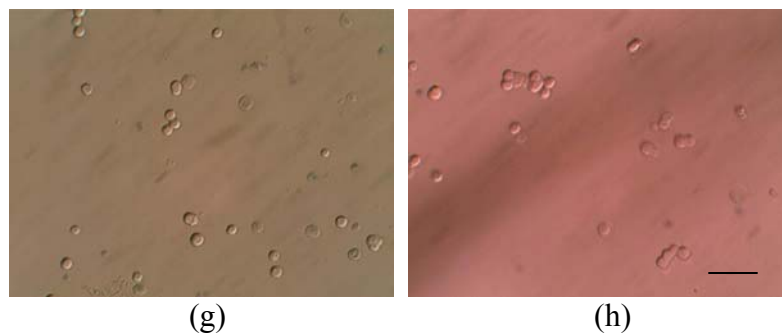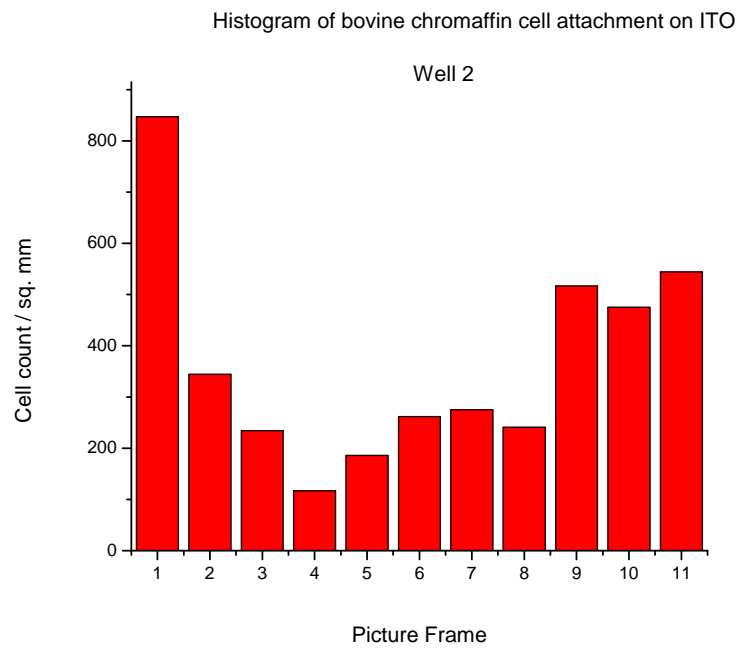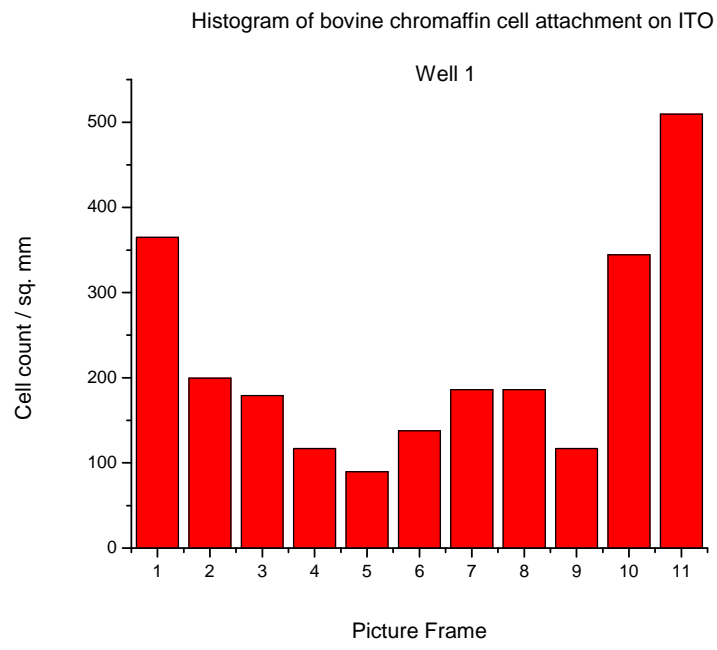**Fig. 5.11.** Histogram of bovine chromaffin cell attachment on (b) ITO

Histogram of bovine chromaffin cell attachment on ITO coated with Poly-d-lysine
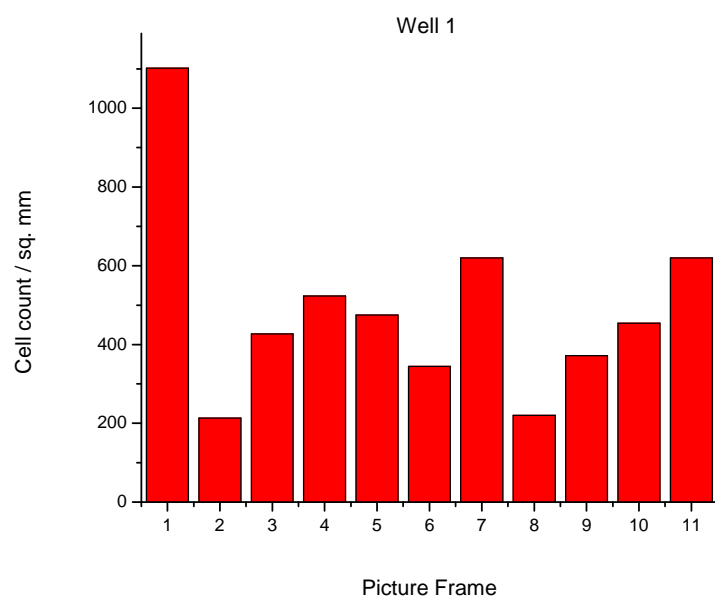
Well 1

Histogram of bovine chromaffin cell attachment on ITO coated with Poly-d-lysine

Well 2

Fig. 5.11. Histogram of bovine chromaffin cell attachment on (c) Poly-d-lysine coated ITO
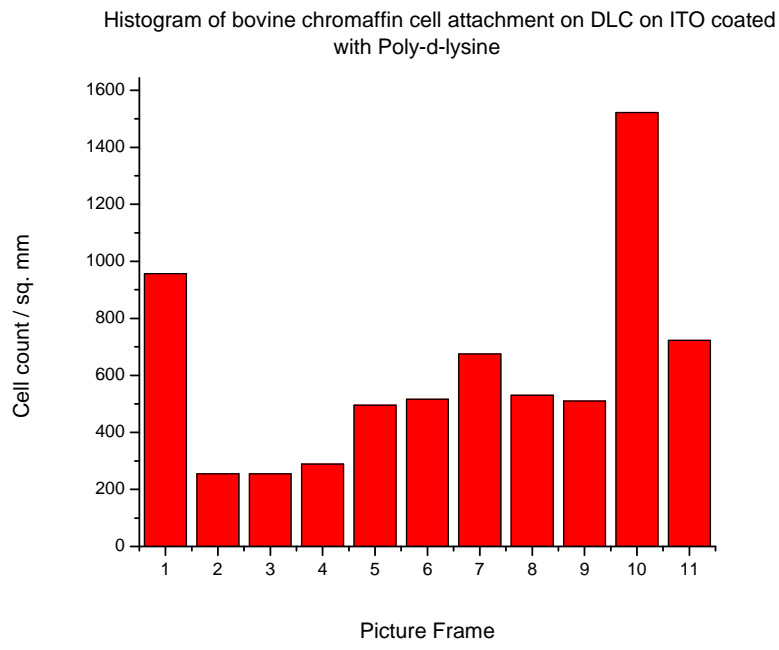
117

Histogram of bovine chromaffin cell attachment on DLC on ITO coated with Poly-d-lysine

Fig. 5.11. Histogram of bovine chromaffin cell attachment on (d) Poly-d-lysine coated DLC deposited on ITO

Histogram of bovine chromaffin cell attachment on Teflon
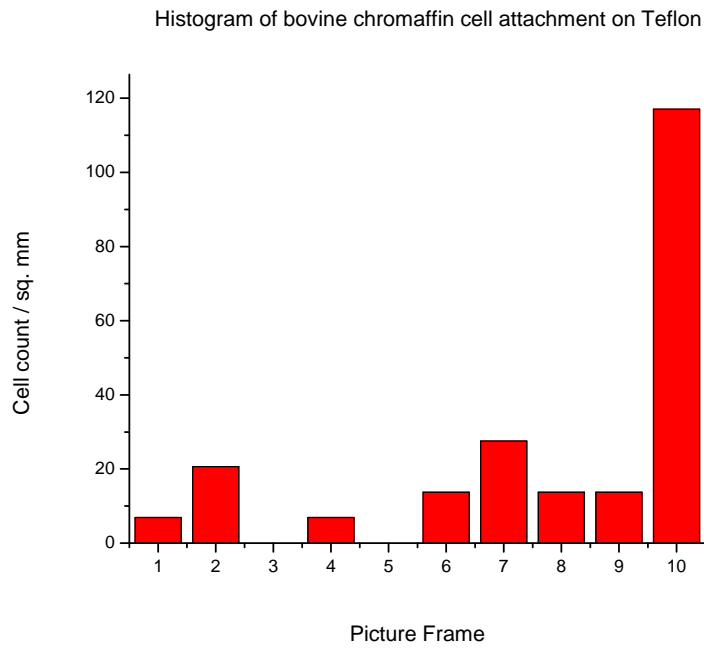
Fig. 5.11. Histogram of bovine chromaffin cell attachment on (e) Teflon

Histogram of bovine chromaffin cell attachment on Teflon coated with Poly-d-lysine

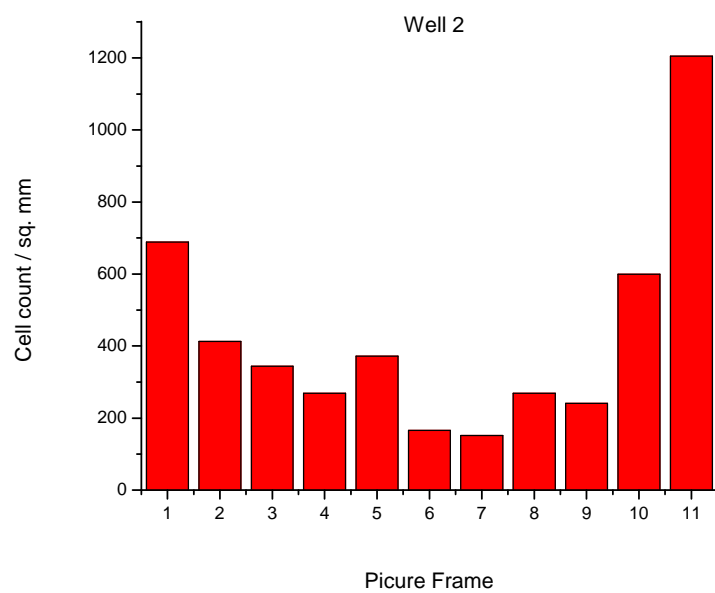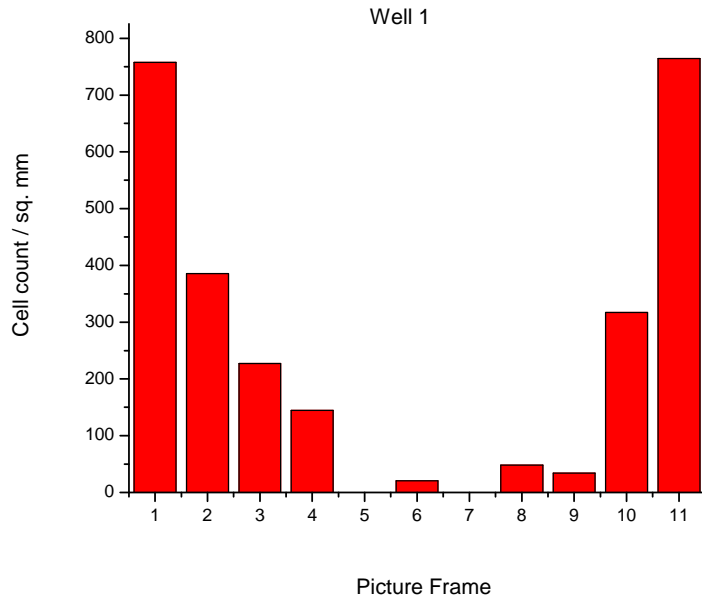Histogram of bovine chromaffin cell attachment on Teflon coated with Poly-d-lysine

Fig. 5.11. Histogram of bovine chromaffin cell attachment on (f) Teflon coated with Poly-d-lysine

(A)
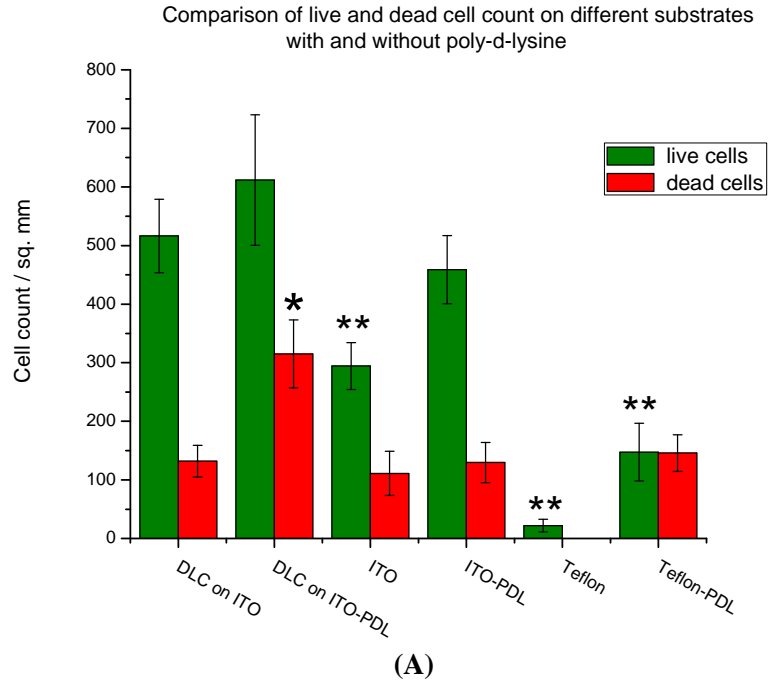
*At p<0.05, the mean cell count is different from that on DLC on ITO and ** At p<0.01, the mean cell count is different from that of DLC on ITO
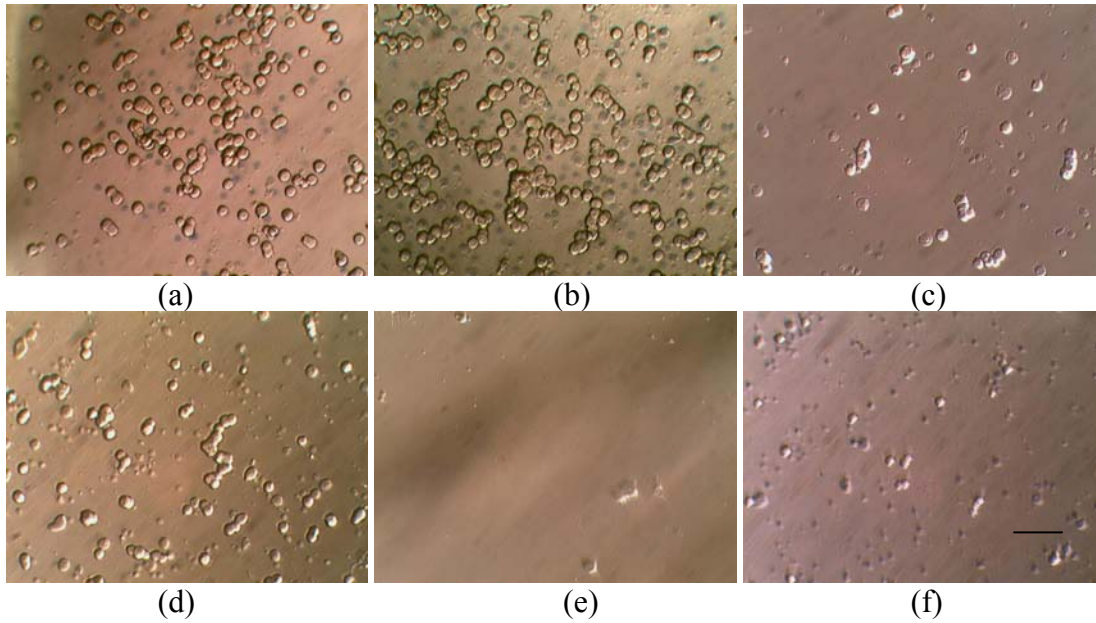
(B)

Fig. 5.12. (A) Summary of bovine chromaffin cell attachment on different substrates **(B)** Optical micrographs of bovine chromaffin cells attached to (a) DLC as is (b) Poly-d-lysine coated DLC (c) ITO (d) Poly-d-lysine coated ITO (e) Teflon (f) Poly-d-lysine coated Teflon [Scale Bar represents 50μm]

5.7. Experiment VII: INS-1 Cell Attachment Assay on Different Candidate Electrodes and Teflon

With increasing support being garnered for DLC as a bovine chromaffin cell attachment surface, it was intriguing to know whether the trend would be similar with other cells. INS-1 cells lines available in the laboratory and experiments performed using them on the substrates DLC on ITO, ITO, Platinum, Gold and Teflon with and without poly-d-lysine coating; platinum, Gold and ITO being the candidate metal electrodes in competition with DLC deposited on ITO while Teflon being tested for its cytophobicity and interaction with poly-d-lysine.
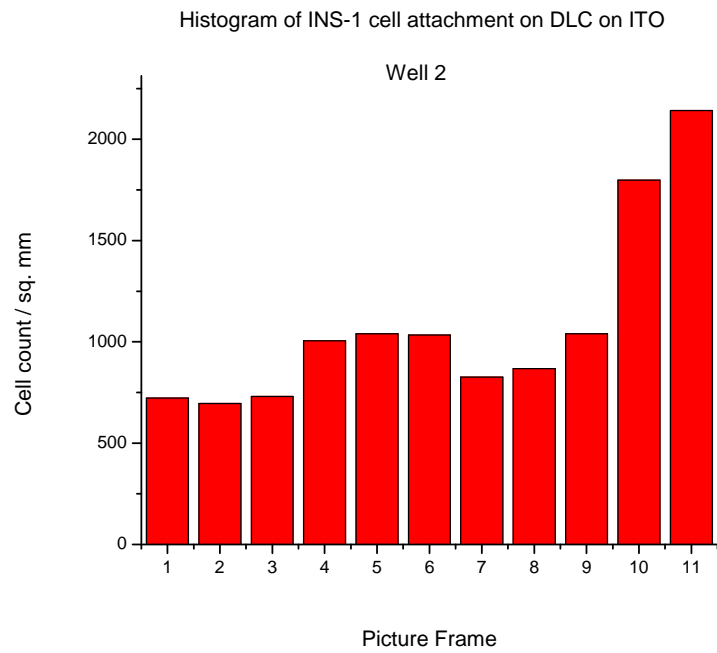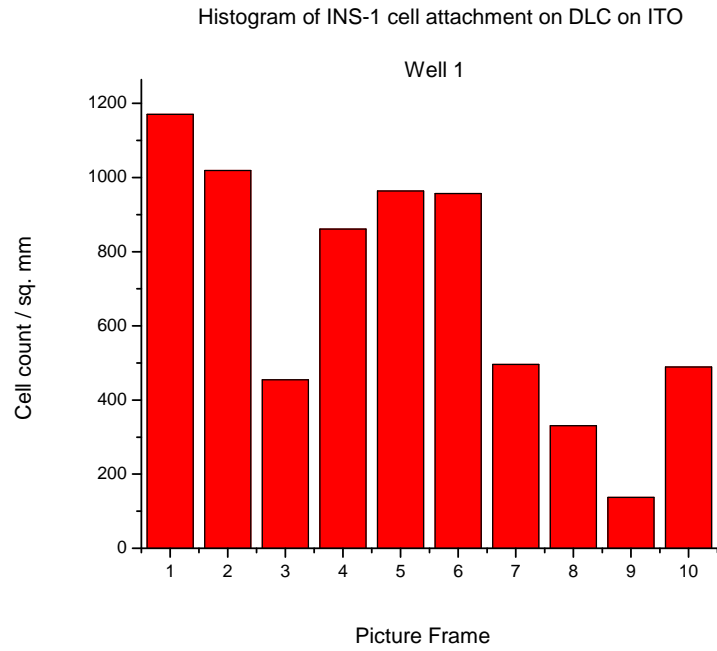
Histogram of INS-1 cell attachment on DLC on ITO

Well 1

Histogram of INS-1 cell attachment on DLC on ITO

Well 2

Fig. 5.13. Histogram of INS-1 cell attachment on (a) DLC deposited on ITO substrate

Histogram of INS-1 cell attachment on Poly-d-lysine coated DLC on ITO

Fig. 5.13. Histogram of INS-1 cell attachment on (b) Poly-d-lysine coated DLC deposited on ITO substrate
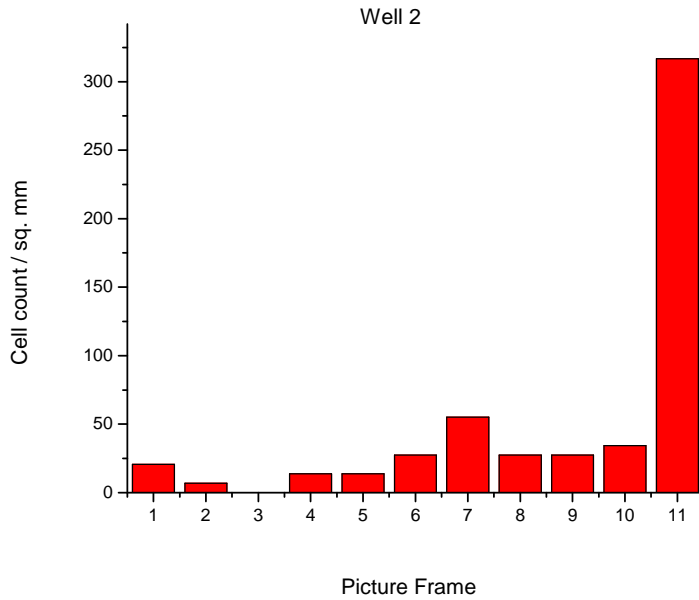
Histogram of INS-1 cell attachment on ITO

Well 1

Histogram of INS-1 cell attachment on ITO

Well 2

Fig. 5.13. Histogram of INS-1 cell attachment on (c) ITO substrate

Histogram of INS-1 cell attachment on ITO coated with Poly-d-lysine

Histogram of INS-1 cell attachment on ITO coated with Poly-d-lysine
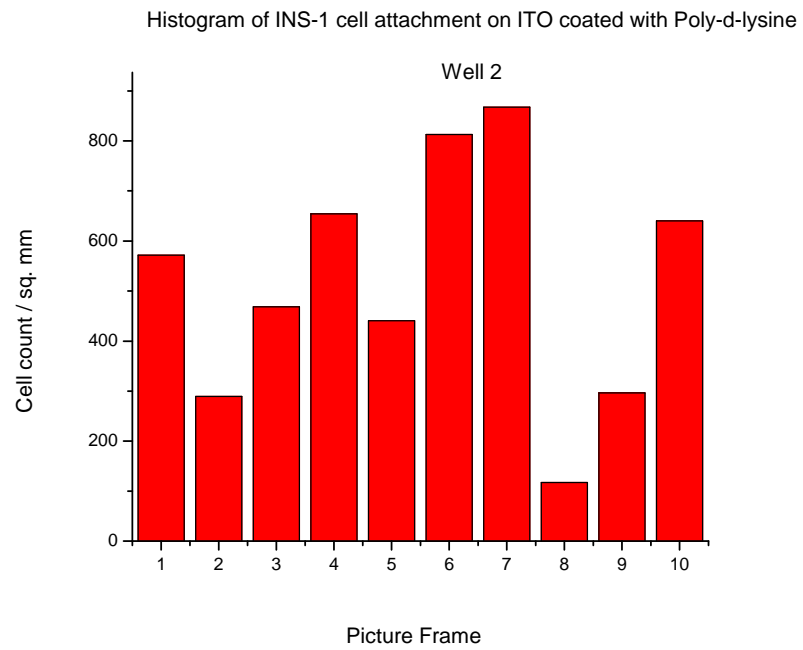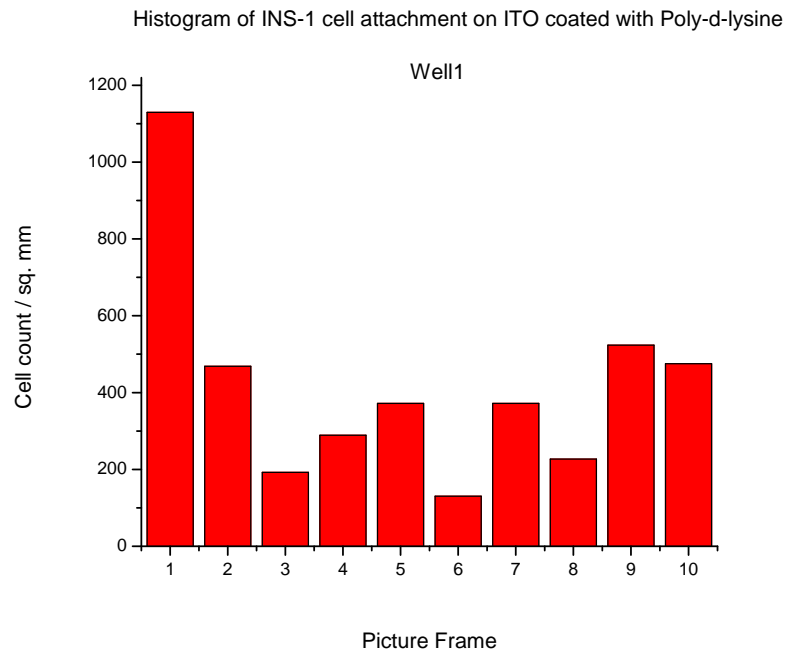
Fig. 5.13. Histogram of INS-1 cell attachment on (d) Poly-d-lysine coated ITO substrate

Histogram of INS-1 cell attachment on Platinum

Well 1

Histogram of INS-1 cell attachment on Platinum

Well 2
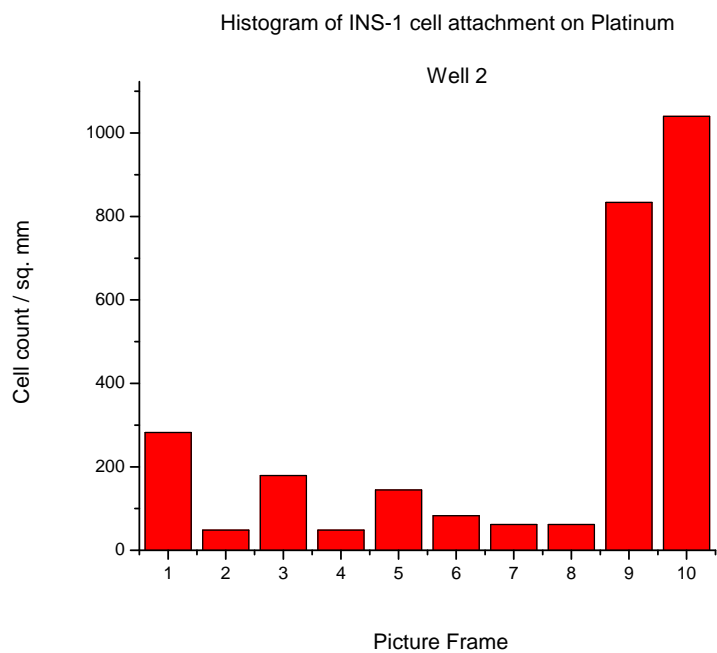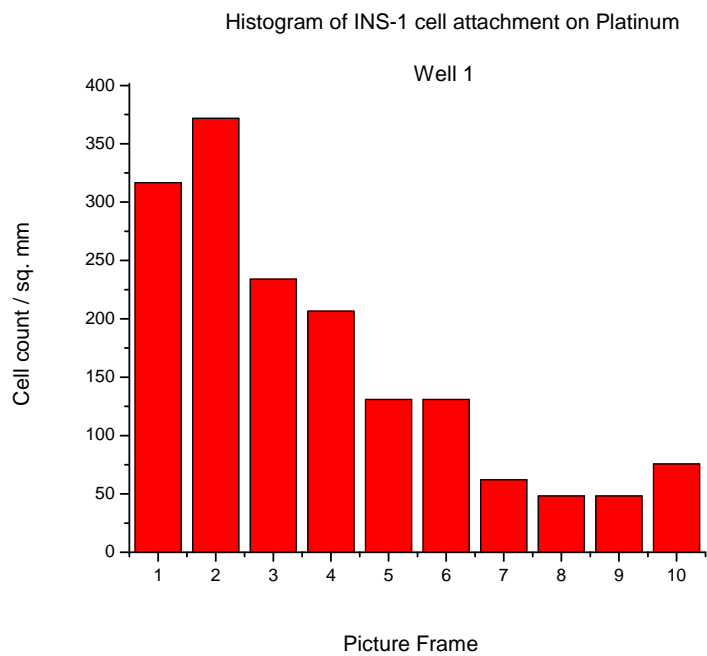
Fig. 5.13. Histogram of INS-1 cell attachment on (e) Platinum substrate

126

Histogram of INS-1 cell attachment on Platinum coated with Poly-d-lysine

Well 1

Histogram of INS-1 cell attachment on Platinum coated with poly-d-lysine

Well 2
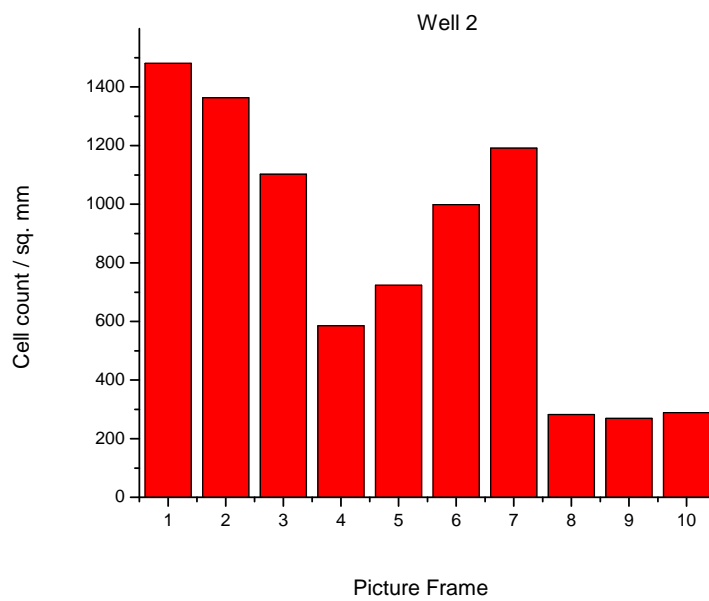
Fig. 5.13. Histogram of INS-1 cell attachment on (f) Poly-d-lysine coated Platinum substrate

Histogram of INS-1 cell attachment on Gold substrate

Well 1

Histogram of INS-1 Cell attachment on Gold substrate

Well 2
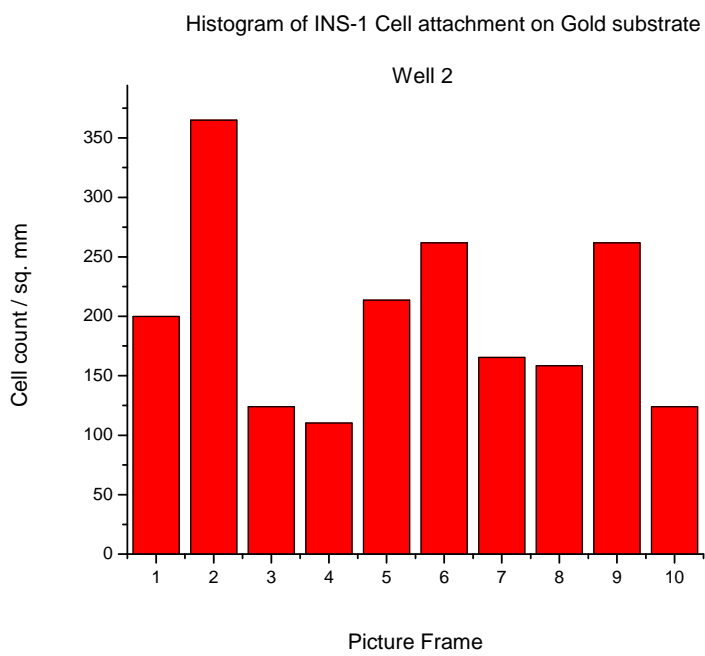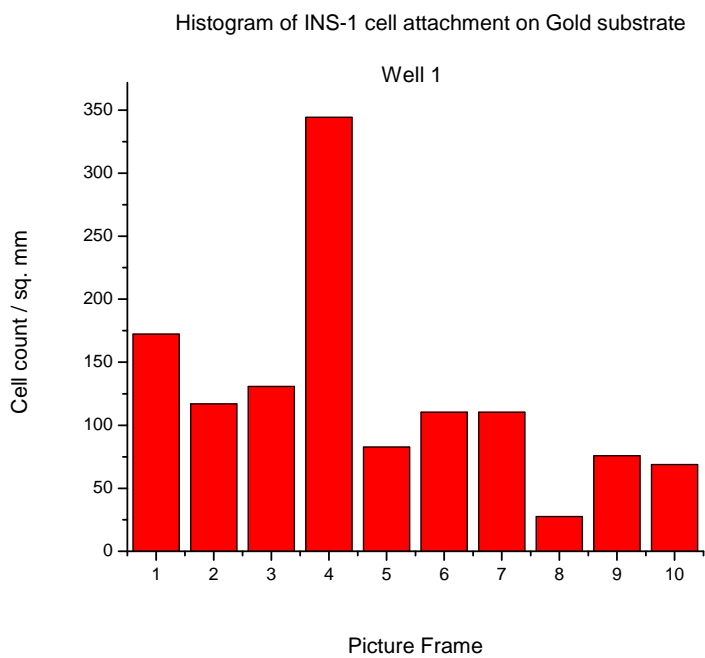
Fig. 5.13. Histogram of INS-1 cell attachment on (g) Gold substrate

Histogram of INS-1 cell attachment on Gold coated with poly-d-lysine

Well 1

Histogram of INS-1 cell attachment on Gold coated with Poly-d-lysine

Well 2
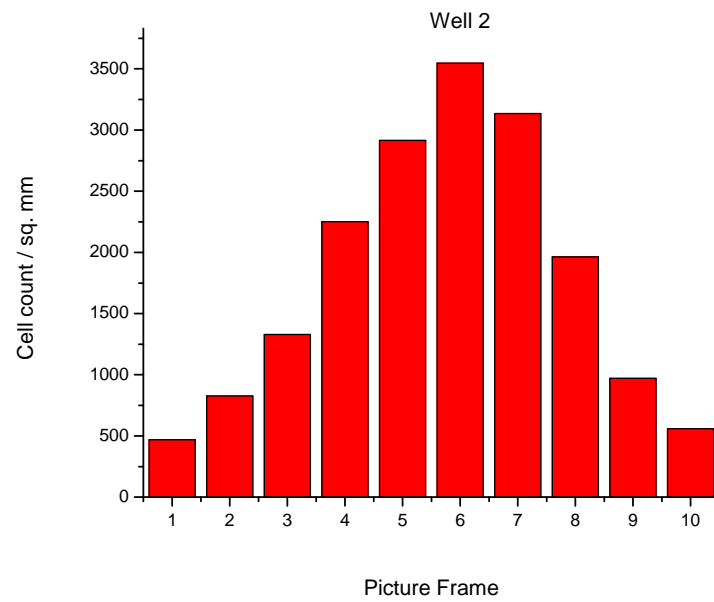
Fig. 5.13. Histogram of INS-1 cell attachment on (h) Poly-d-lysine coated Gold substrate

(A)
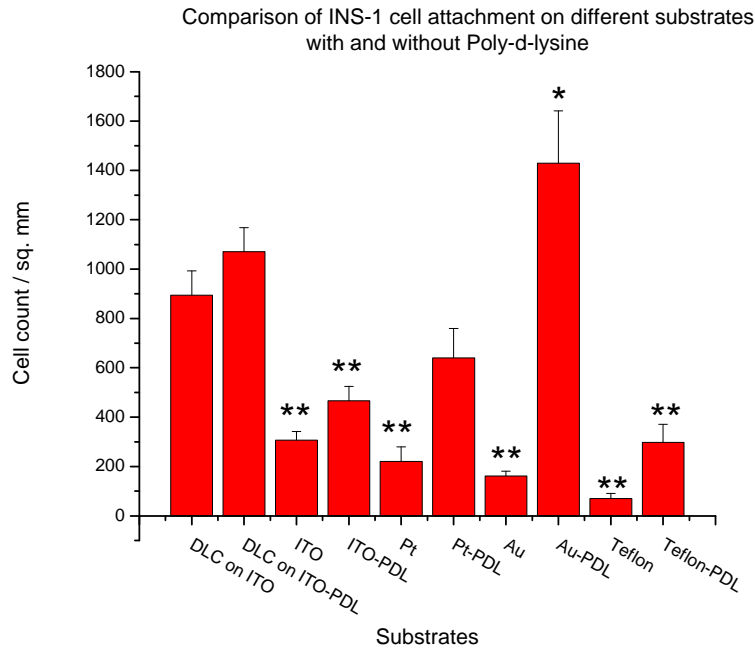
*At p<0.05, mean cell count is different from that on DLC on ITO and **p<0.01, mean cell count is different from that on DLC on ITO
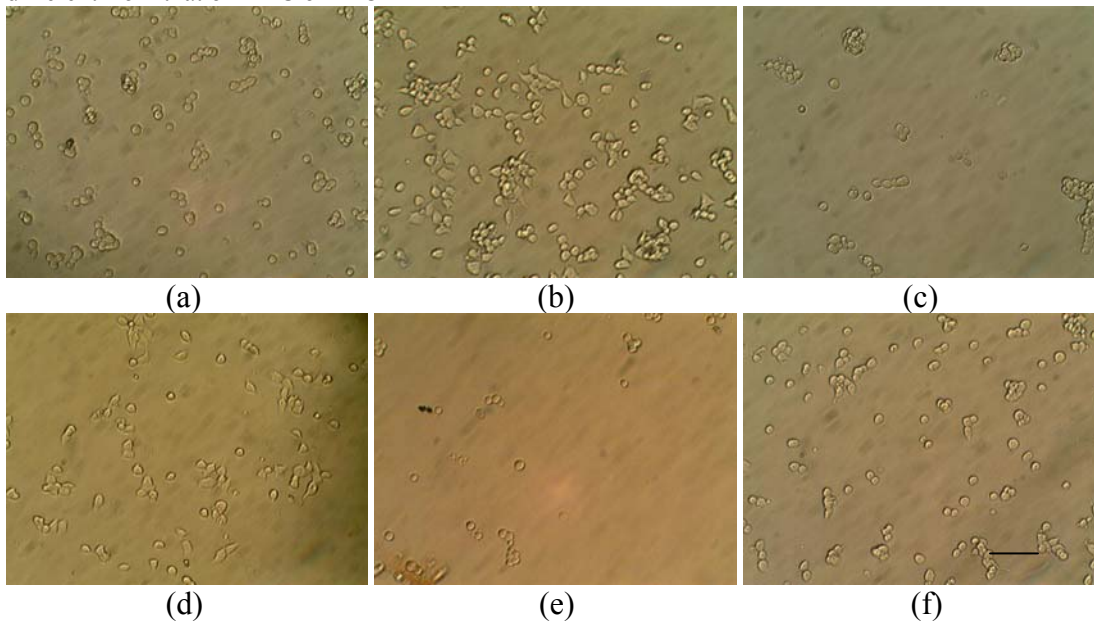
(B)

Fig. 5.14. (A). Summary of INS-1 cell attachment on different substrates with and without poly-d-lysine **(B).** Optical micrographs INS-1 cells attached to (a) DLC as is (b) Poly-d-lysine coated DLC (c) ITO (d) Poly-d-lysine coated ITO (e) Platinum (f) Poly-d-lysine coated Platinum (g) Gold (h) Poly-d-lysine coated Gold [Scale Bar represents 50µm]

(g) (h) (i)

(j)
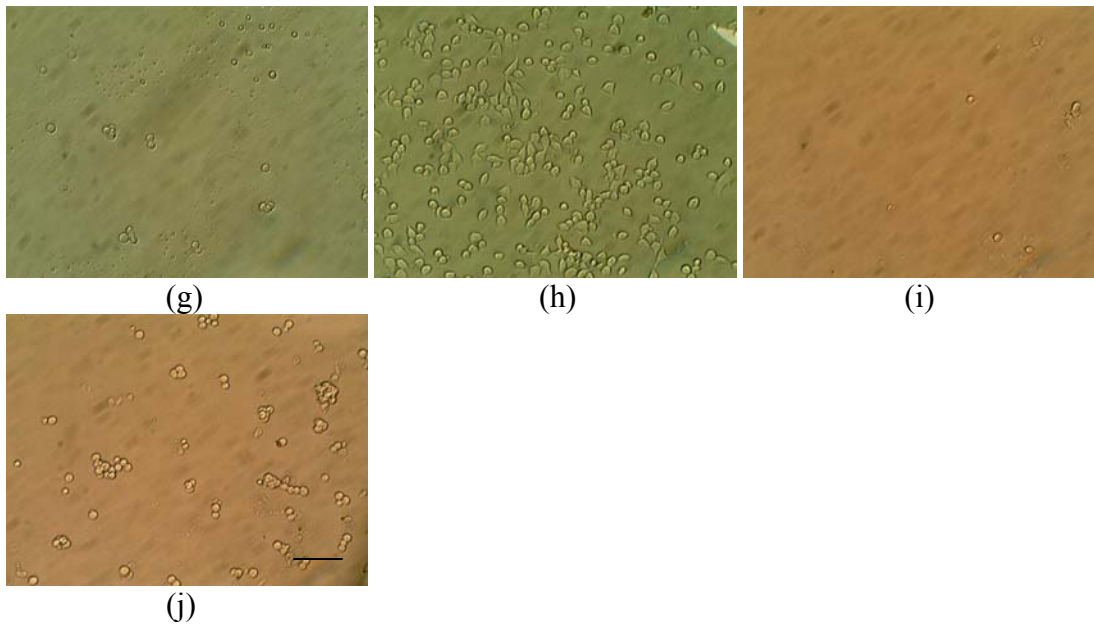
Fig. 5.14. (contd.) (B). Optical micrographs of INS-1 cells attached to (g) Gold (h) Poly-d-lysine coated Gold (i) Teflon (j) Poly-d-lysine coated Teflon
[Scale Bar represents 50µm]

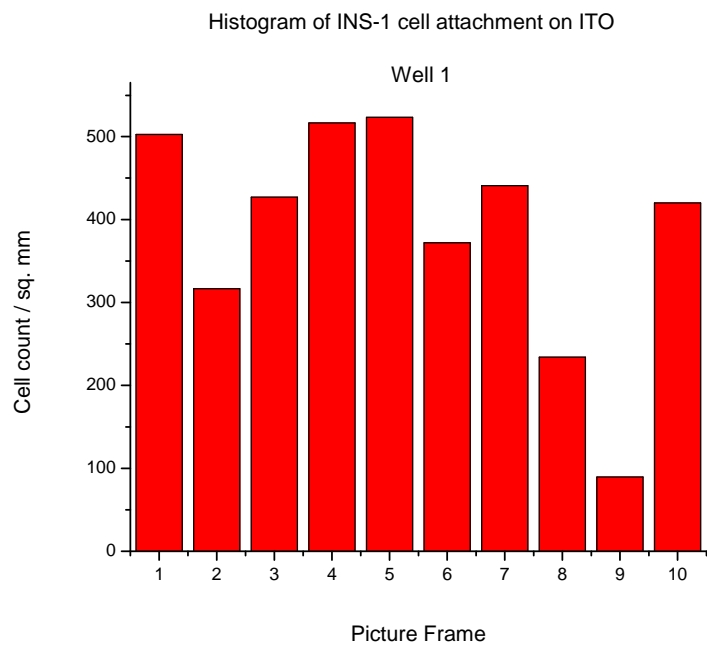## 5.8. Experiment VIII : Bovine Chromaffin Cell Attachment Assay on Different Candidate Electrodes and Teflon

Just as in Section 5.7, the same materials have been set to test on bovine chromaffin cells to collect more data and higher statistically relevant data for making an assertive statement.

Histogram of bovine chromaffin cell attachment on DLC on ITO

Well 1

Histogram of bovine chromaffin cell attachment on DLC on ITO

Well 2
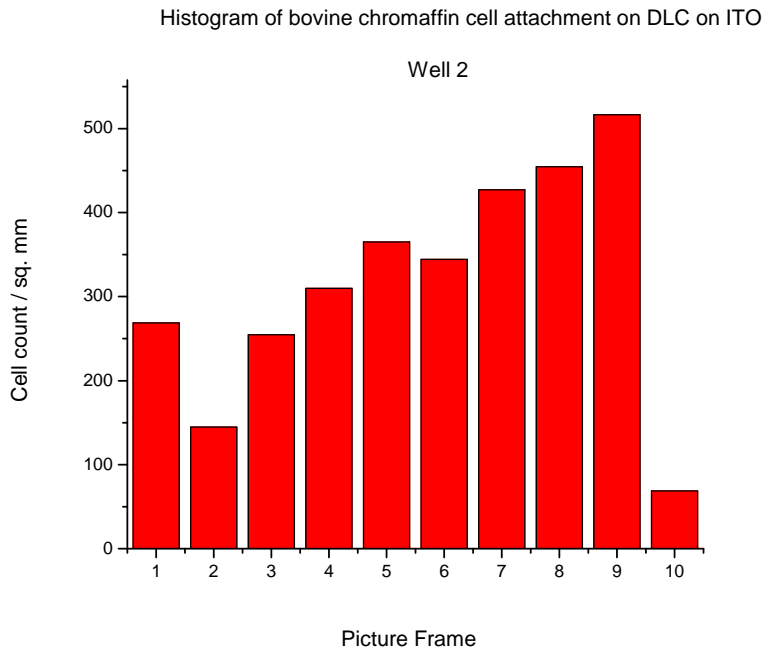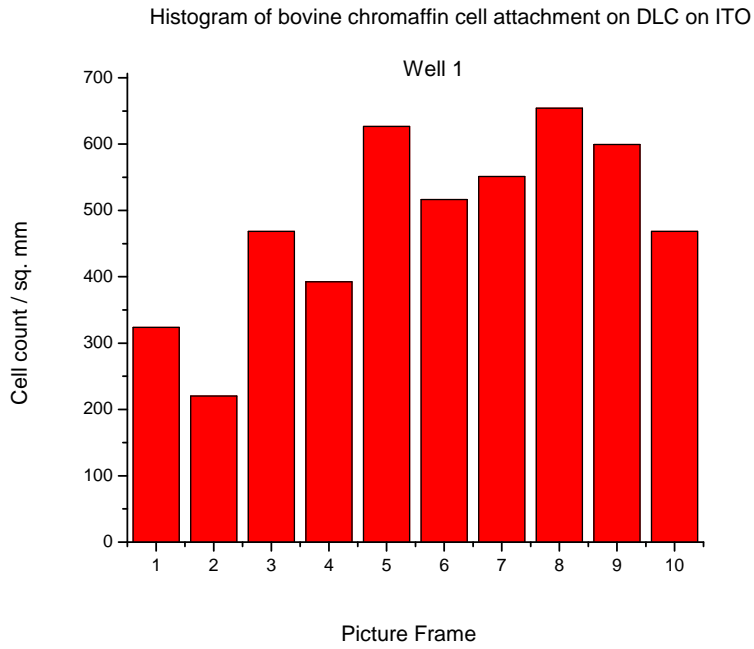
Fig. 5.15. Histograms of bovine chromaffin cell attachment on (a) DLC deposited on ITO
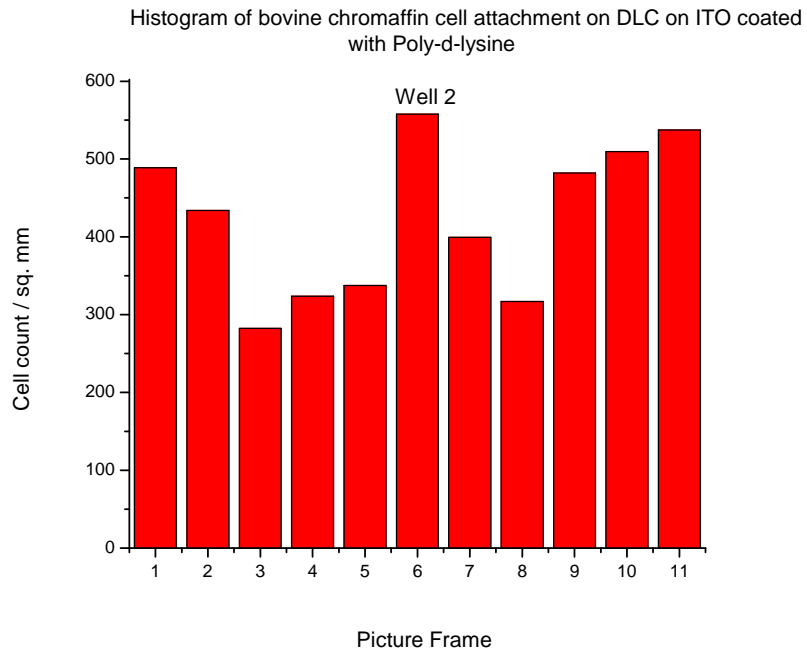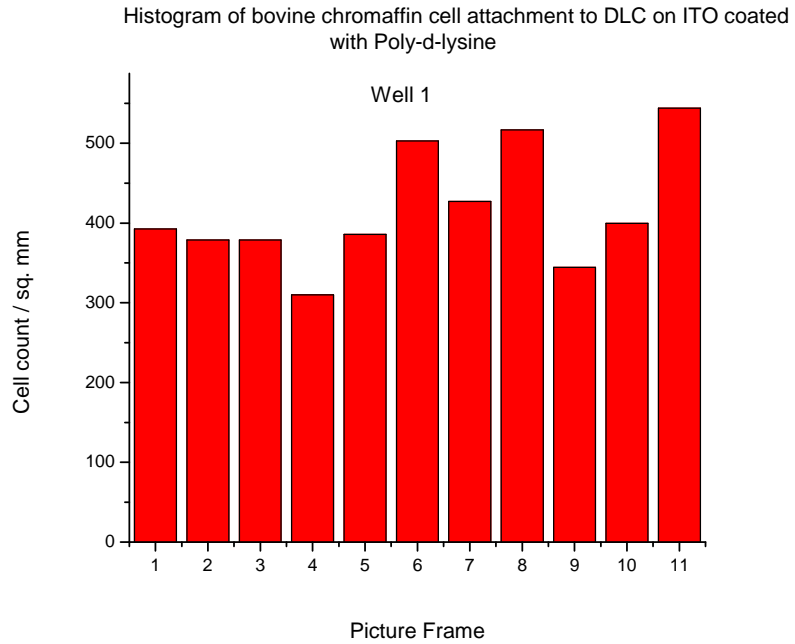
Fig. 5.15. Histograms of bovine chromaffin cell attachment on (b) DLC deposited on ITO coated with Poly-d-lysine
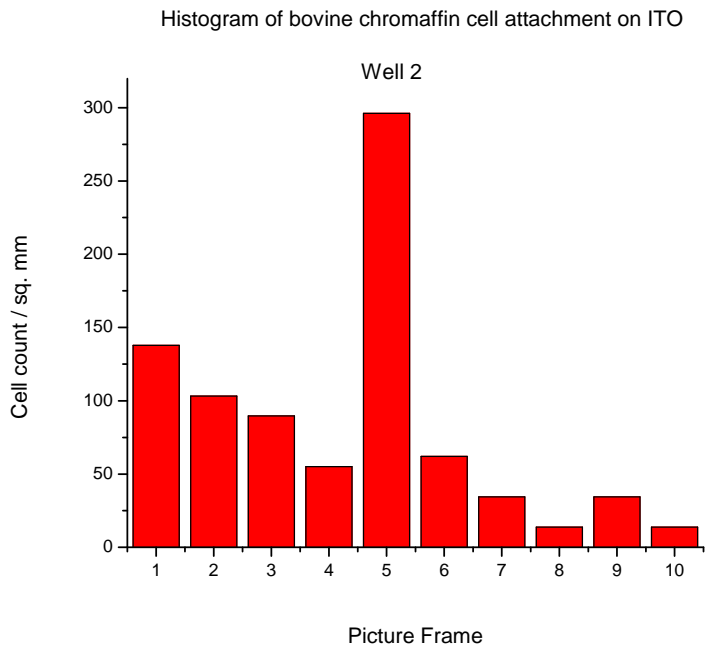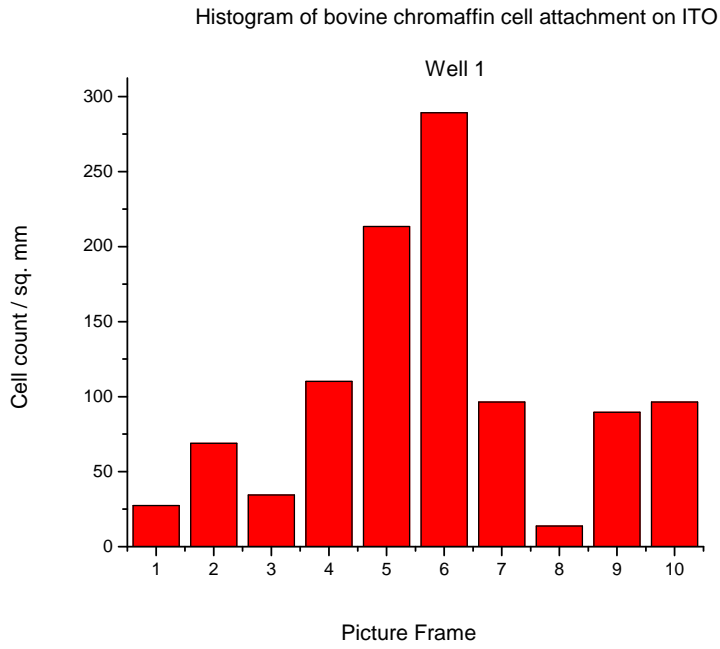
Histogram of bovine chromaffin cell attachment on ITO

Well 1

Histogram of bovine chromaffin cell attachment on ITO

Well 2

Fig. 5.15. Histograms of bovine chromaffin cell attachment on (c) ITO

Histogram of bovine chromaffin cell attachment on ITO coated with Poly-d-lysine
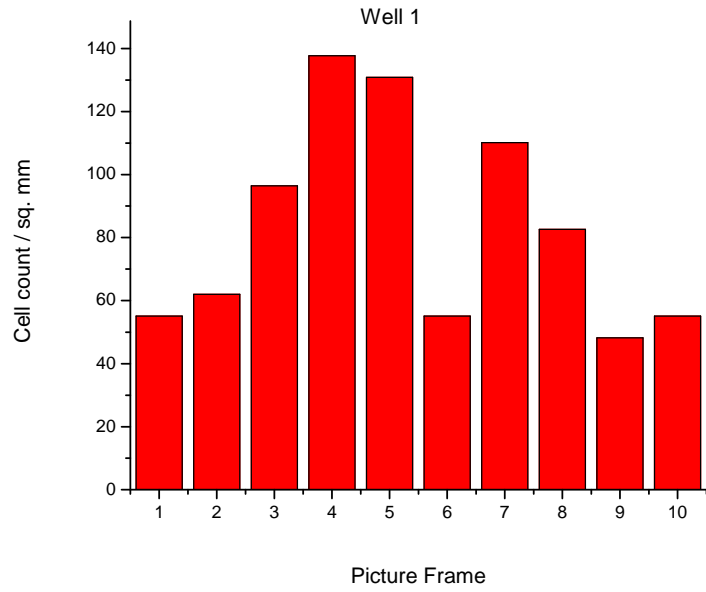
Fig. 5.15. Histograms of bovine chromaffin cell attachment on (d) ITO coated with poly-d-lysine
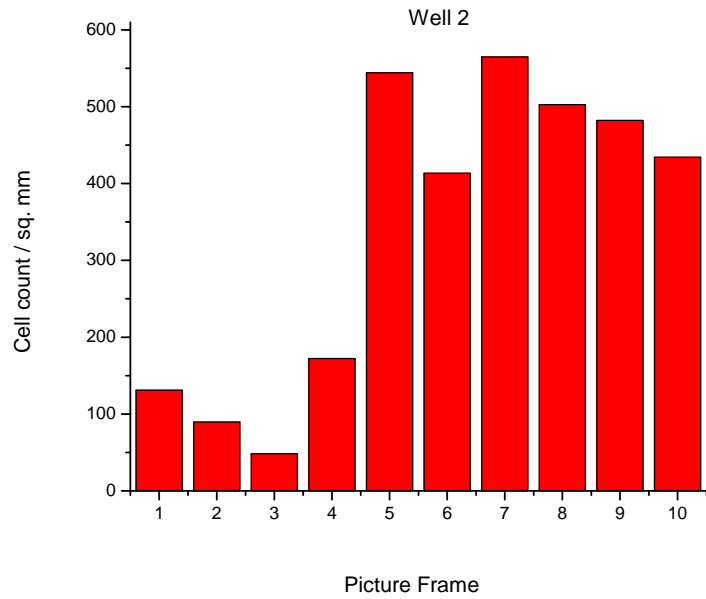
Histogram of bovine chromaffin cell attachment on Platinum
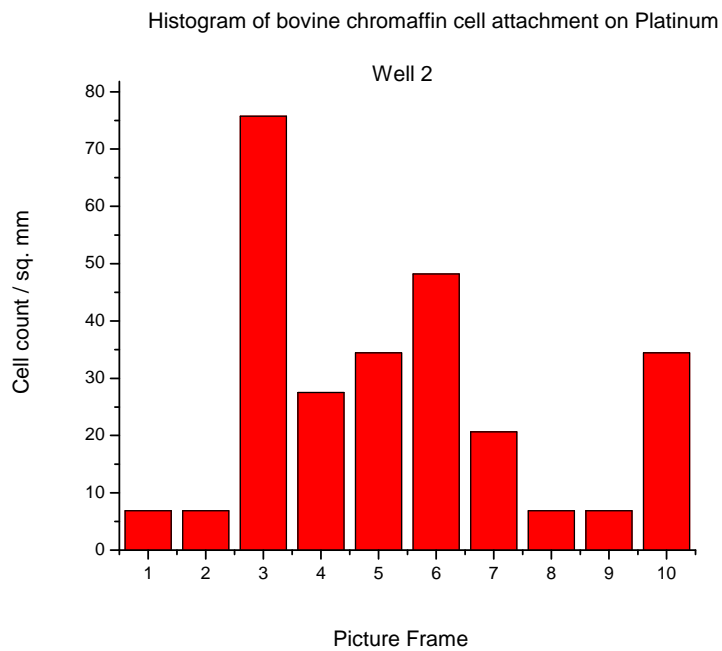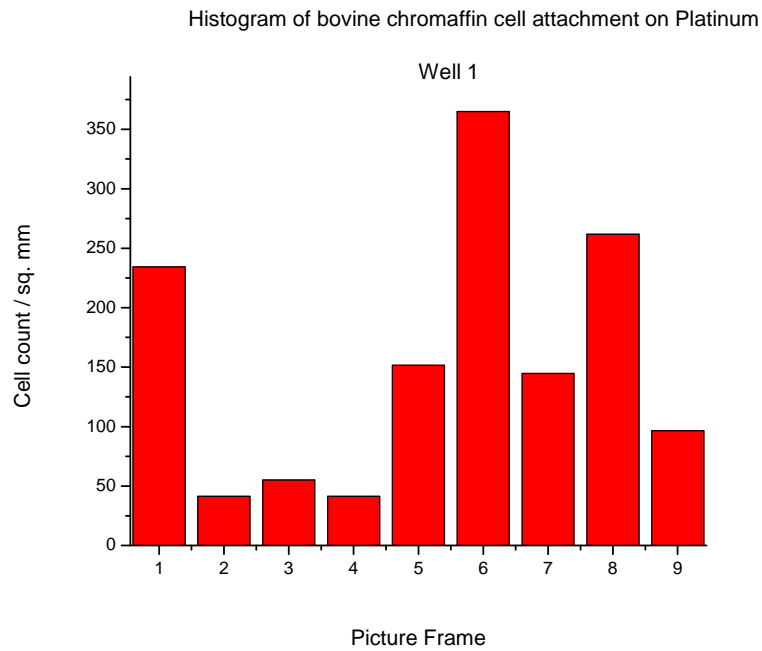
Histogram of bovine chromaffin cell attachment on Platinum

Fig. 5.15. Histograms of bovine chromaffin cell attachment on (e) Platinum

136

Histogram of bovine chromaffin cell attachment on Platinum coated with Poly-d-lysine — Well 1

Histogram of bovine chromaffin cell attachment on Platinum coated with Poly-d-lysine — Well 2

Fig. 5.15. Histograms of bovine chromaffin cell attachment on (f) Platinum coated with poly-d-lysine

Fig. 5.15. Histograms of bovine chromaffin cell attachment on (g) Gold

138

Histogram of bovine chromaffin cell attachment on Gold coated with Poly-d-lysine

Well 1

Histogram of bovine chromaffin cell attachment on Gold coated with Poly-d-lysine

Well 2
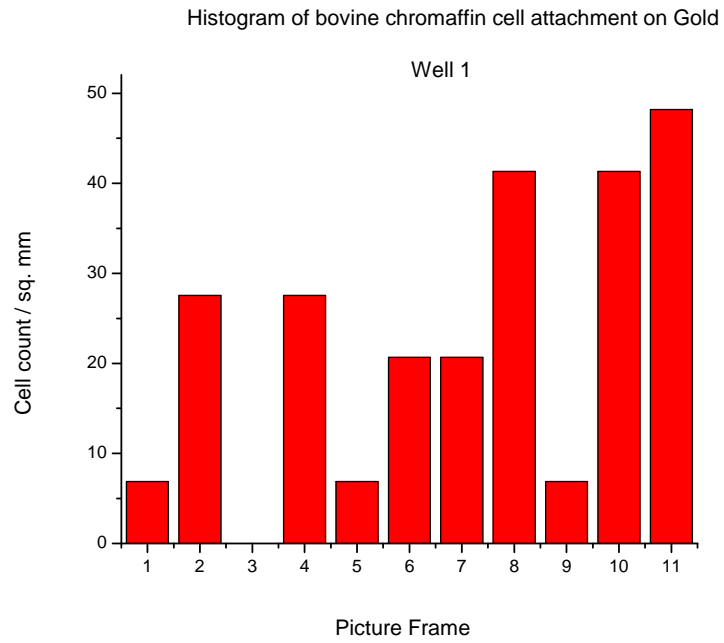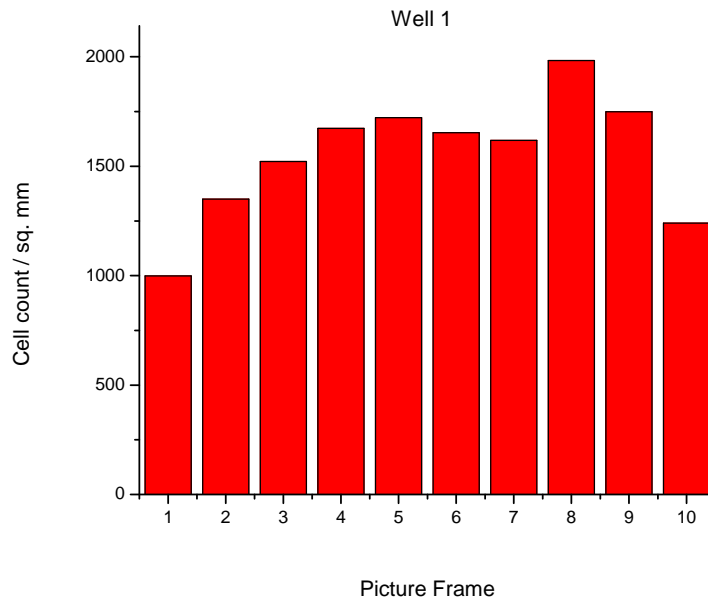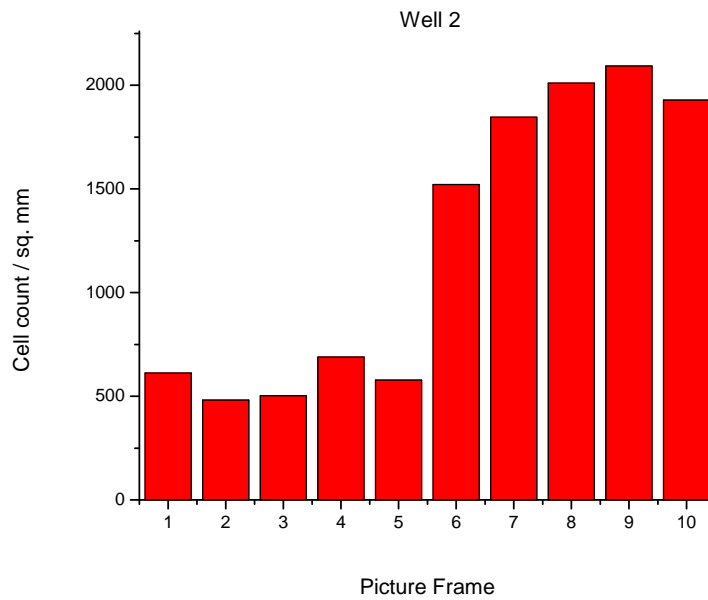
Fig. 5.15. Histograms of bovine chromaffin cell attachment on (h) Platinum coated with poly-d-lysine

139

Histogram of bovine chromaffin cell attachment on Teflon

Fig. 5.15. Histograms of bovine chromaffin cell attachment on (i) Teflon

Histogram of bovine chromaffin cell attachment on Teflon coated with Poly-d-lysine

Fig. 5.15. Histograms of bovine chromaffin cell attachment on (j) Teflon coated with Poly-d-lysine

(A)

*At p<0.05, the cell count is significantly different from that on DLC on ITO and ** At p<0.01, the cell count is significantly different from that on DLC on ITO

(B)

Fig. 5.16. (A). Summary of bovine chromaffin cell attachment on different substrates with and without poly-d-lysine **(B).** Optical micrographs of bovine chromaffin cells attached to (a) DLC as is (b) Poly-d-lysine coated DLC (c) ITO (d) Poly-d-lysine coated ITO (e) Platinum (f) Poly-d-lysine coated Platinum [Scale Bar represents 50μm]

141

(g) (h) (i)

(j)

Fig. 5.16. (B). (contd.) Optical micrographs of bovine chromaffin cells attached to (g) Gold (h) Poly-d-lysine coated Gold (i) Teflon (j) Poly-d-lysine coated Teflon [Scale Bar represents 50μm]

## 5.9. Experiment IX: INS-1 cell attachment assay on different candidate electrodes and Teflon

This set of experiments is an exact repeat of Experiment VII described in Section 5.7.
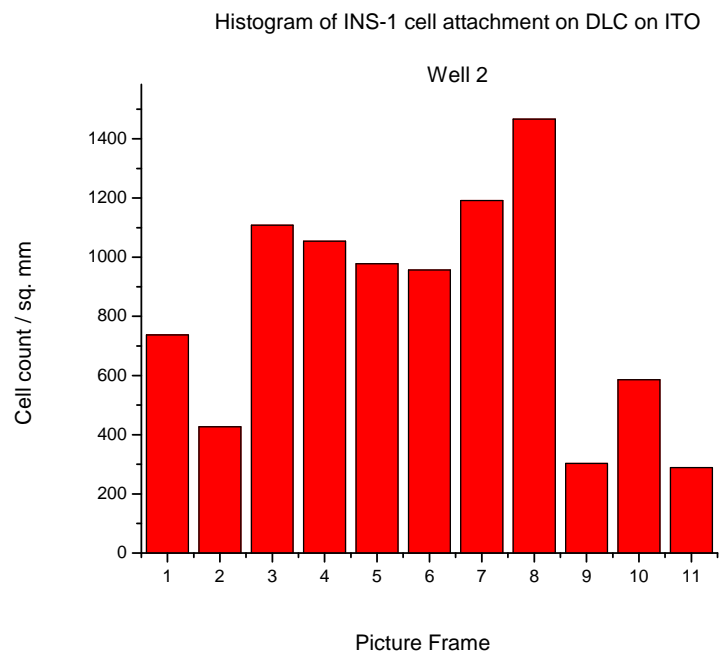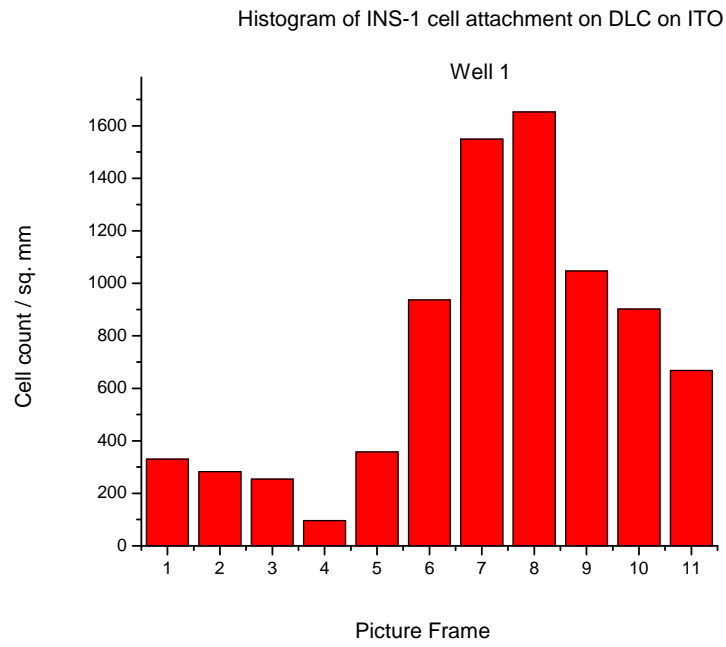
Fig. 5.17. Histograms of INS-1 cell attachment on (a) DLC deposited on ITO

Histogram of INS-1 cell attachment to DLC on ITO coated with Poly-d-lysine
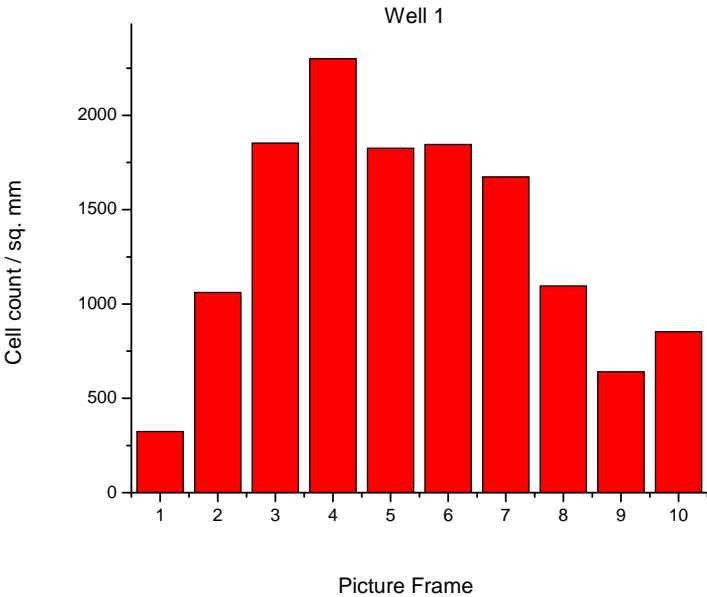
Histogram of INS-1 cell attachment on DLC on ITO coated with Poly-d-lysine
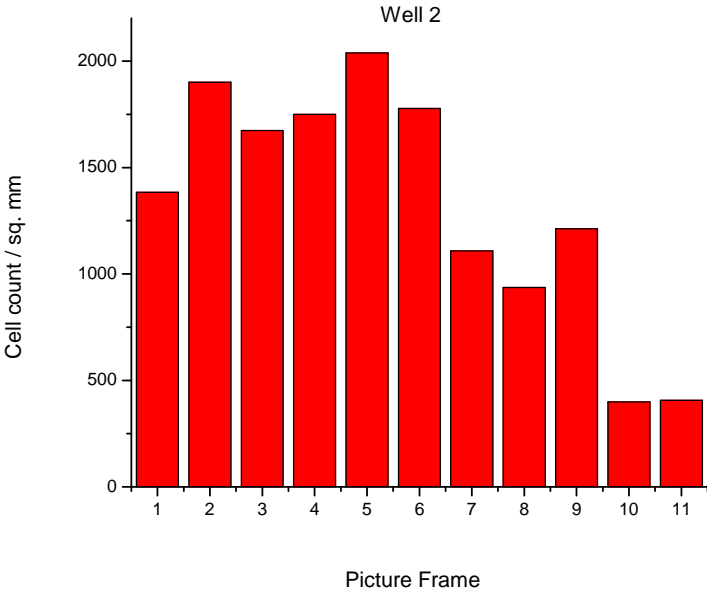
Fig. 5.17. Histograms of INS-1 cell attachment on (b) Poly-d-lysine coated DLC deposited on ITO

Fig. 5.17. Histograms of INS-1 cell attachment on (c) ITO
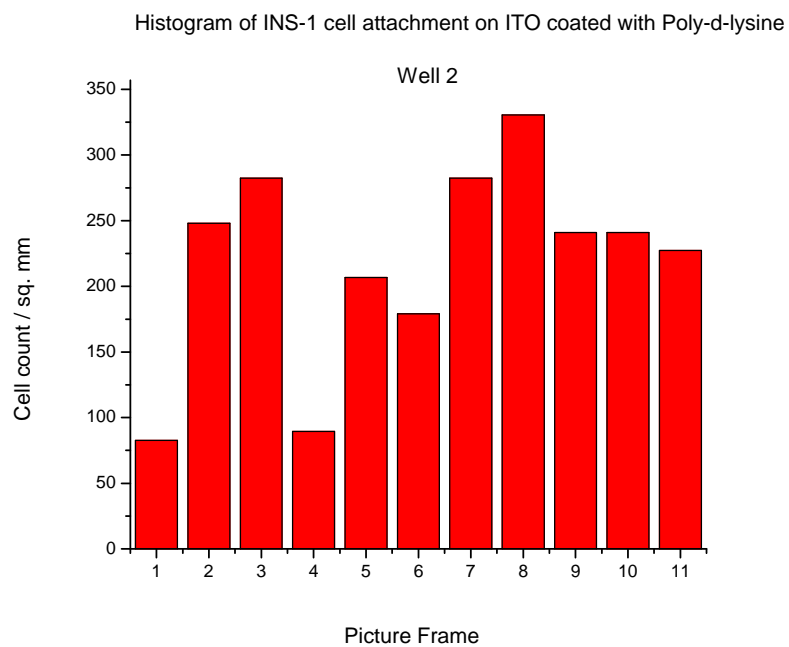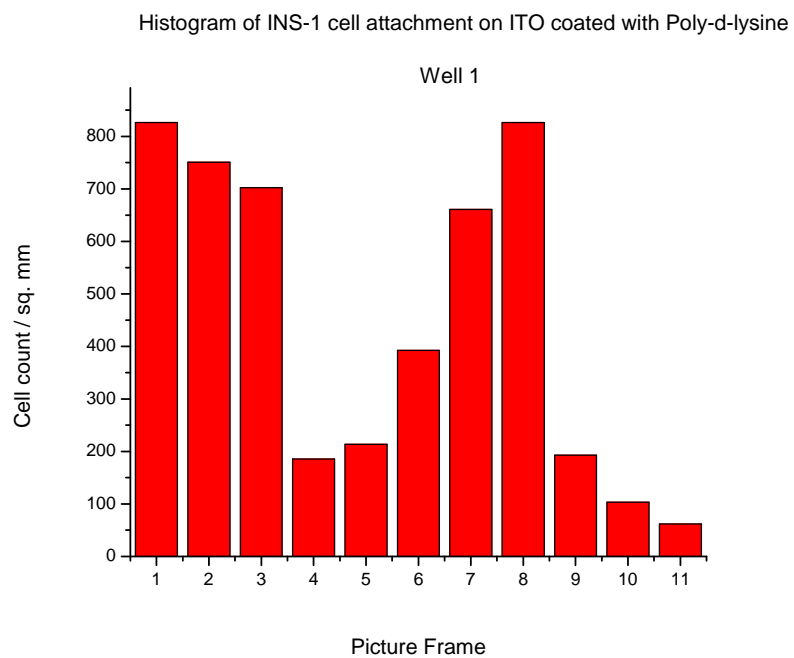
Histogram of INS-1 cell attachment on ITO coated with Poly-d-lysine

Well 1

Histogram of INS-1 cell attachment on ITO coated with Poly-d-lysine

Well 2

Fig. 5.17. Histograms of INS-1 cell attachment on (d) ITO coated with Poly-d-lysine

146

Fig. 5.17. Histograms of INS-1 cell attachment on (e) Platinum

Histogram of INS-1 cell attachment on Platinum coated with Poly-d-lysine

Fig. 5.17. Histograms of INS-1 cell attachment on (f) Platinum coated with Poly-d-lysine

Fig. 5.17. Histograms of INS-1 cell attachment on (g) Gold

Histogram of INS-1 cell attachment on Gold coated with Poly-d-lysine

Well 1

Histogram of INS-1 cell attachment on Gold coated with Poly-d-lysine

Well 2
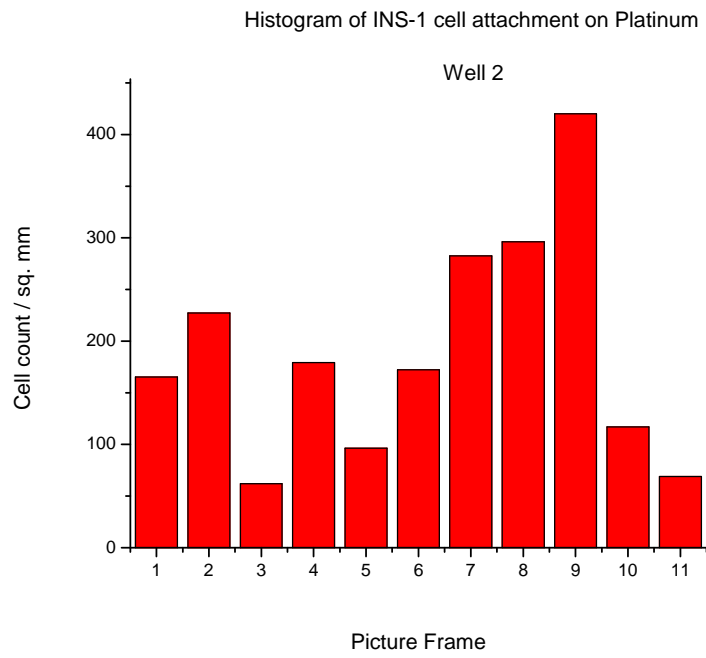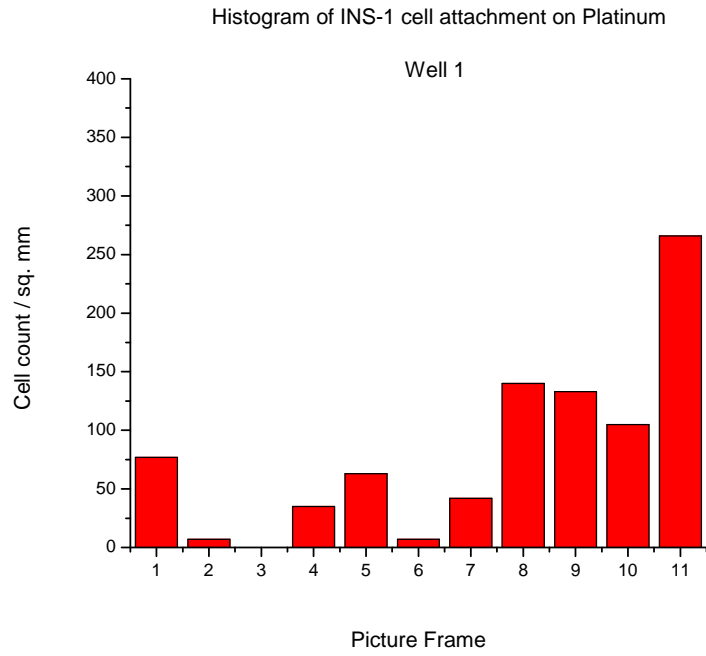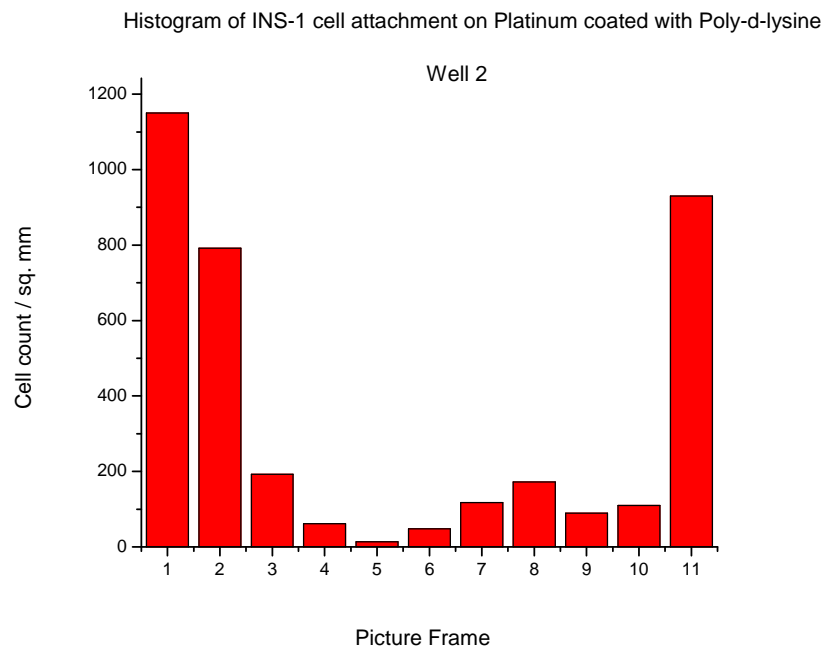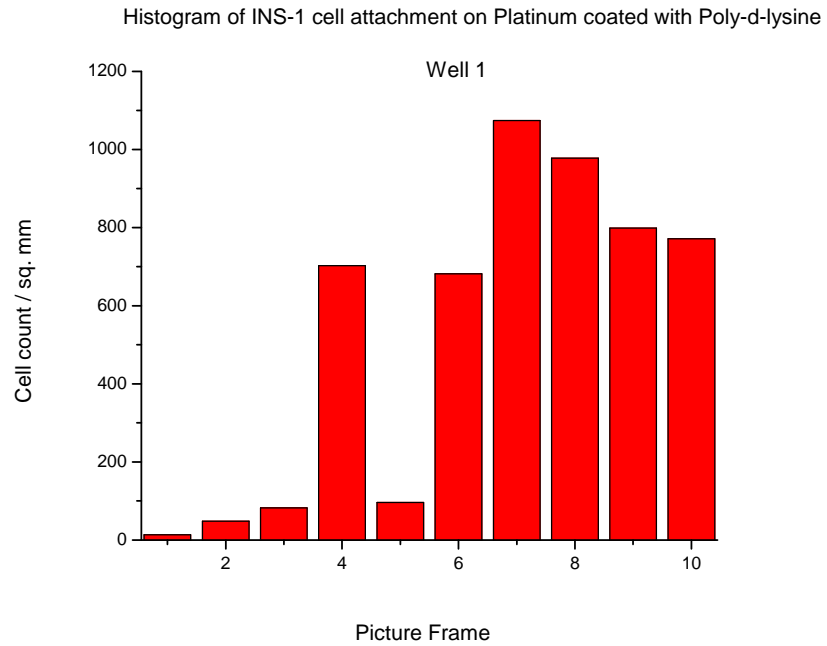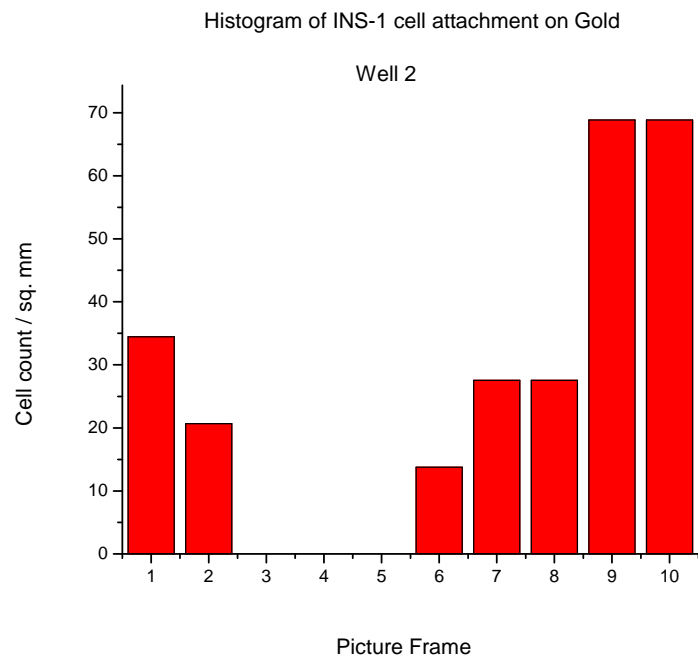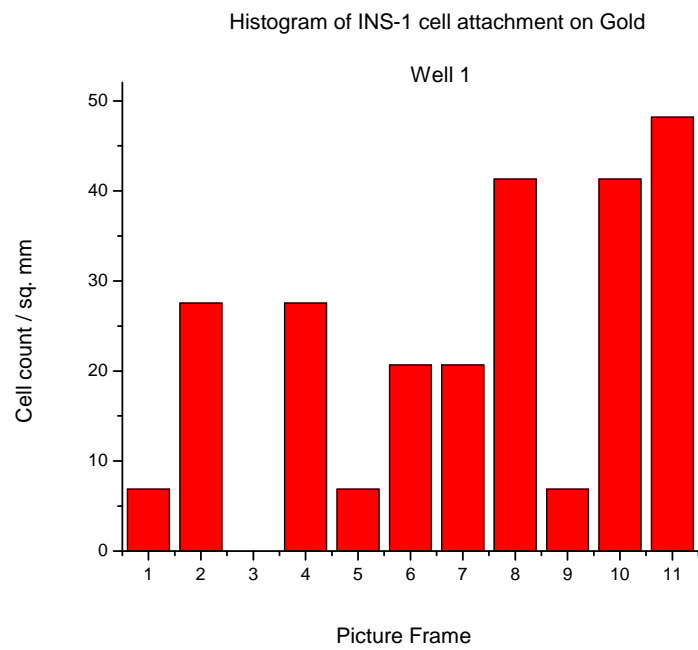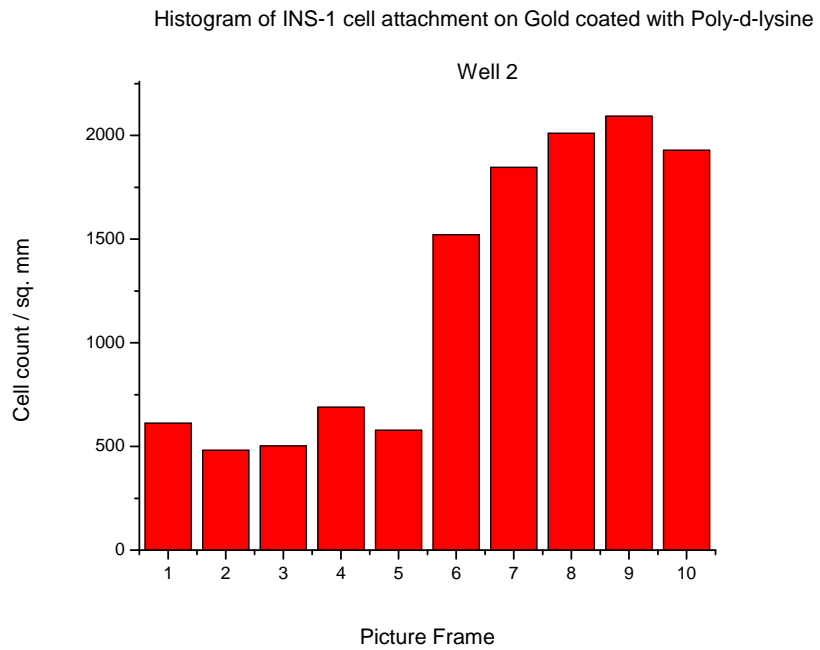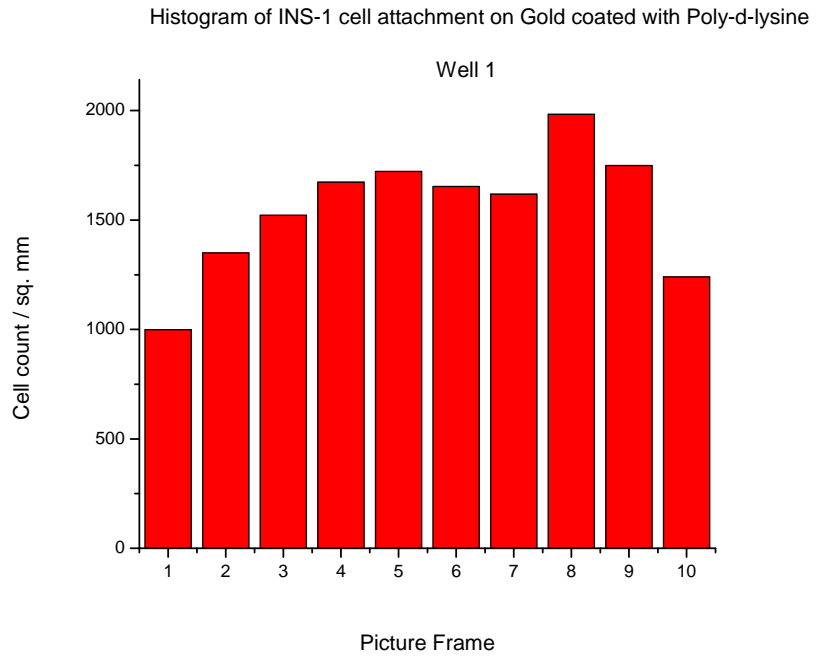
Fig. 5.17. Histograms of INS-1 cell attachment on (h) Gold coated with Poly-d-lysine
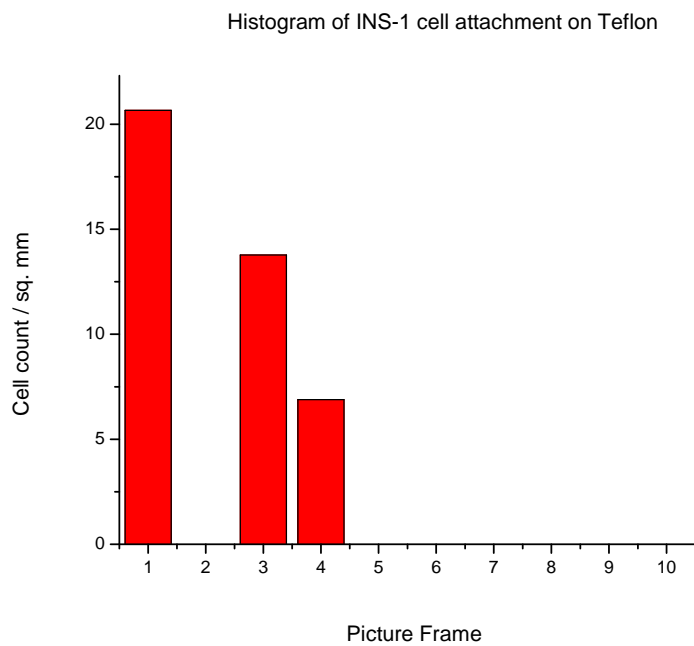
Histogram of INS-1 cell attachment on Teflon

Fig. 5.17. Histogram of INS-1 cell attachment on (i) Teflon

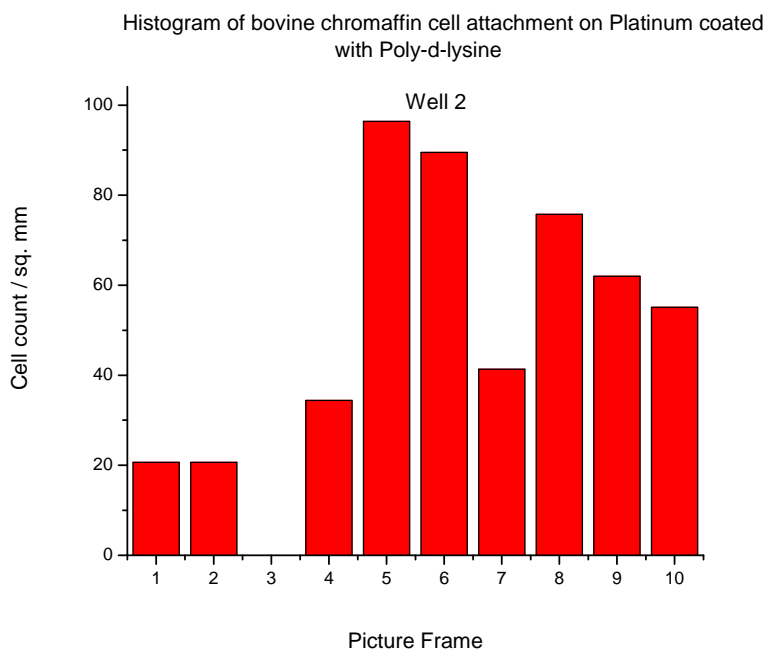Histogram of INS-1 cell attachment on Teflon coated with Poly-d-lysine
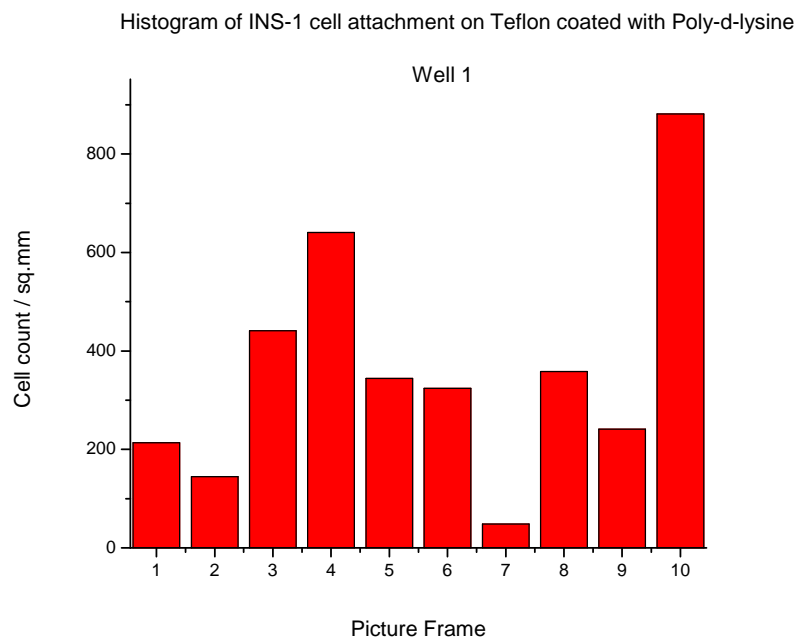
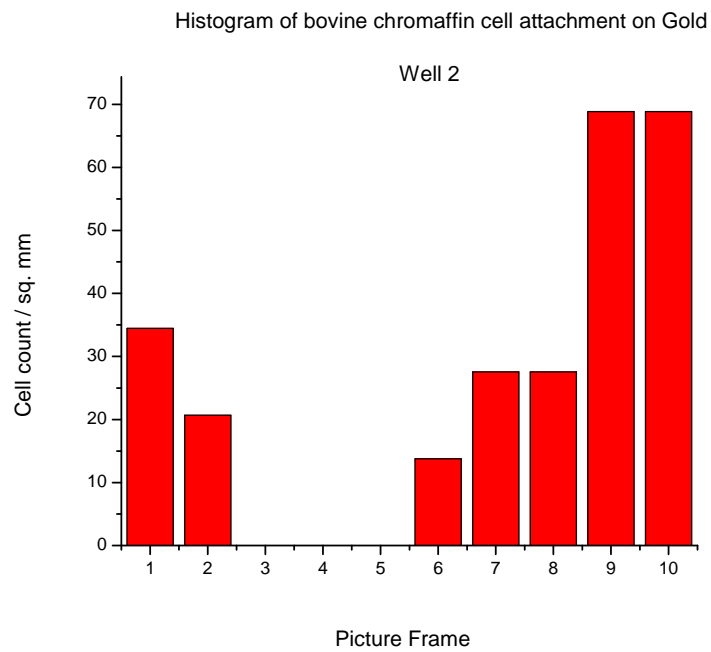**Fig. 5.17.** Histogram of INS-1 cell attachment on (j) Teflon coated with Poly-d-lysine
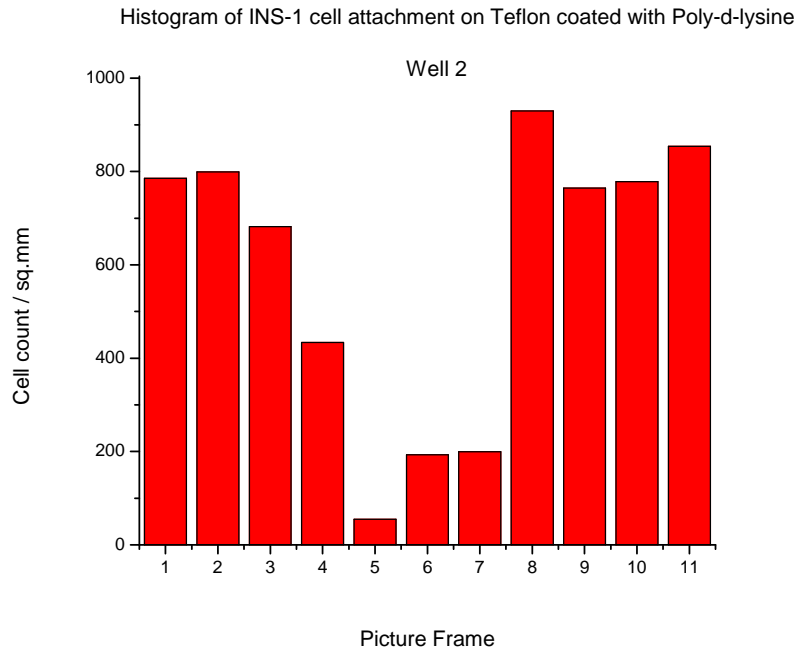
Fig. 5.17. (contd.) Histogram of INS-1 cell attachment on (j) Teflon coated with Poly-d-lysine
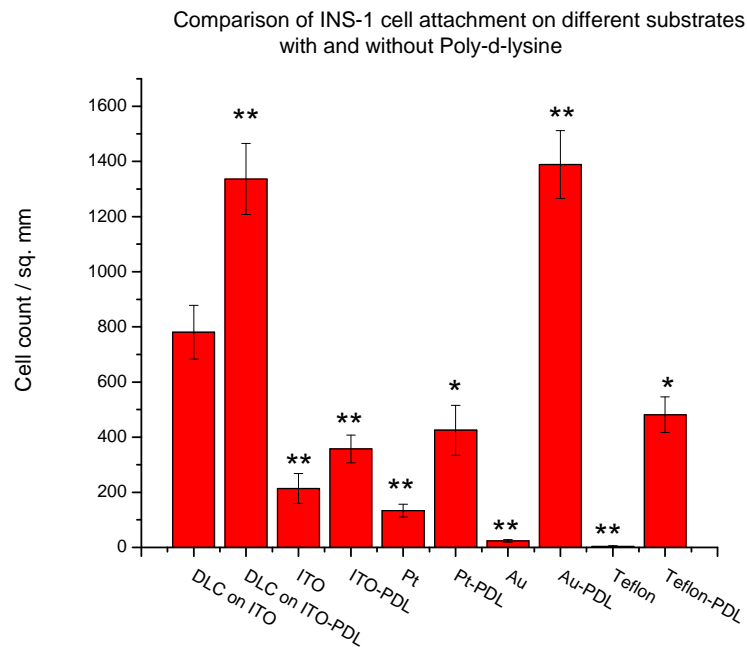
Fig. 5.18 (A). Summary of INS-1 cell attachment on different substrates with and without poly-d-lysine.

*At $p<0.05$, the cell count is significantly different from that on DLC on ITO and ** At $p<0.01$, the cell count is significantly different from that on DLC on ITO
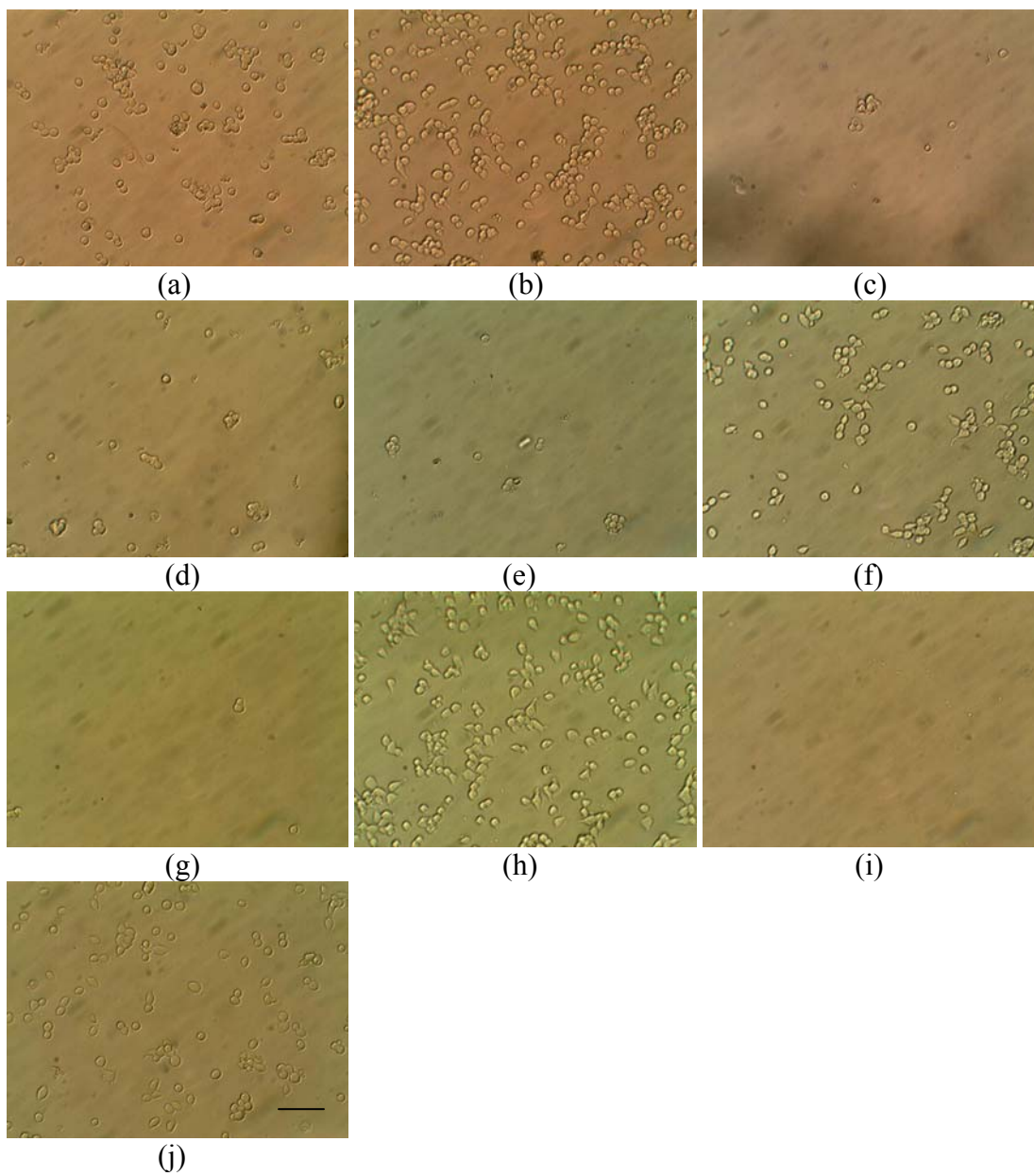
Fig. 5.18. (contd.) (B). Optical micrographs of INS-1 cells attached to (a) DLC as is (b) Poly-d-lysine coated DLC (c) ITO (d) Poly-d-lysine coated ITO (e) Platinum (f) Poly-d-lysine coated Platinum (g) Gold (h) Poly-d-lysine coated Gold (i) Teflon (j) Poly-d-lysine coated Teflon [Scale Bar represents 50µm]

5.10. Experiment X: Bovine Chromaffin Cells

This experiment set is a repeat of Experiment VIII described in 5.8.

Histogram of bovine chromaffin cell attachment on DLC

Well 1

Histogram of bovine chromaffin cell attachment on DLC

Well 2

Fig. 5.19. Histograms of bovine chromaffin cell attachment on (a) DLC deposited on ITO

Fig. 5.19. Histograms of bovine chromaffin cell attachment on (b) Poly-d-lysine coated DLC deposited on ITO

Fig. 5.19. Histograms of bovine chromaffin cell attachment on (c) ITO

156

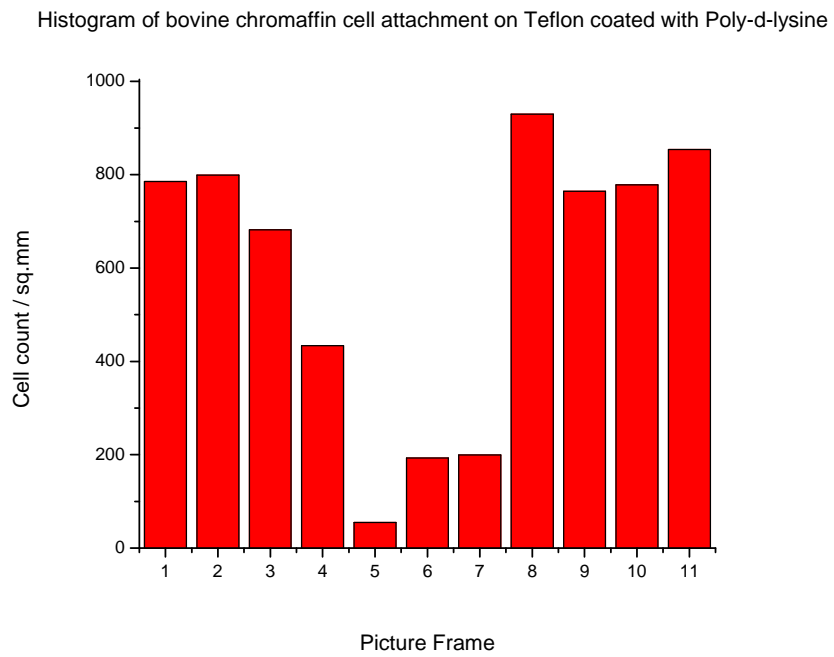Histogram of bovine chromaffin cell attachment on Poly-d-lysine coated ITO

Well 1

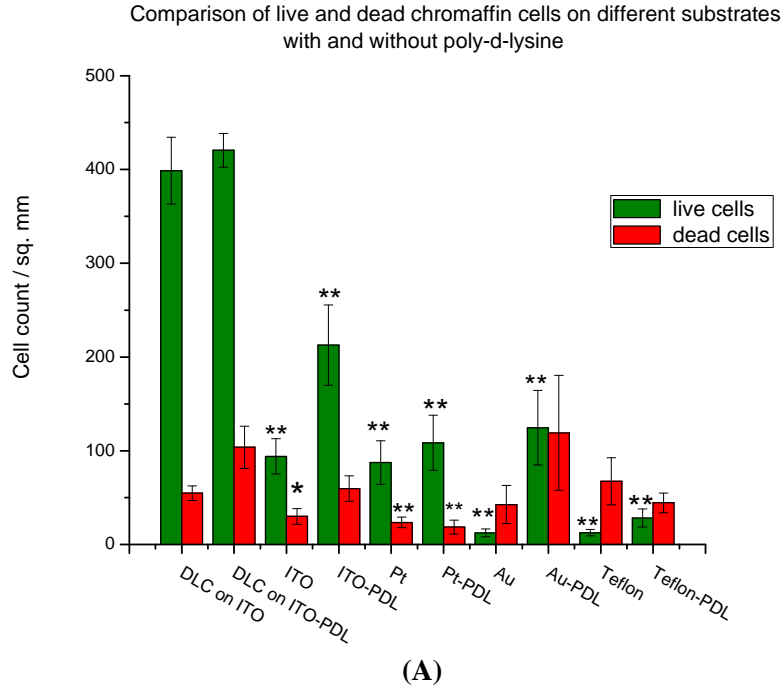Histogram of bovine chromaffin cell attachment on Poly-d-lysine coated ITO

Well 2

Fig. 5.19. Histograms of bovine chromaffin cell attachment on (d) ITO coated with Poly-d-lysine

Histogram of bovine chromaffin cell attachment on Platinum

Well 1

Histogram of bovine chromaffin cell attachment on Platinum

Well 2
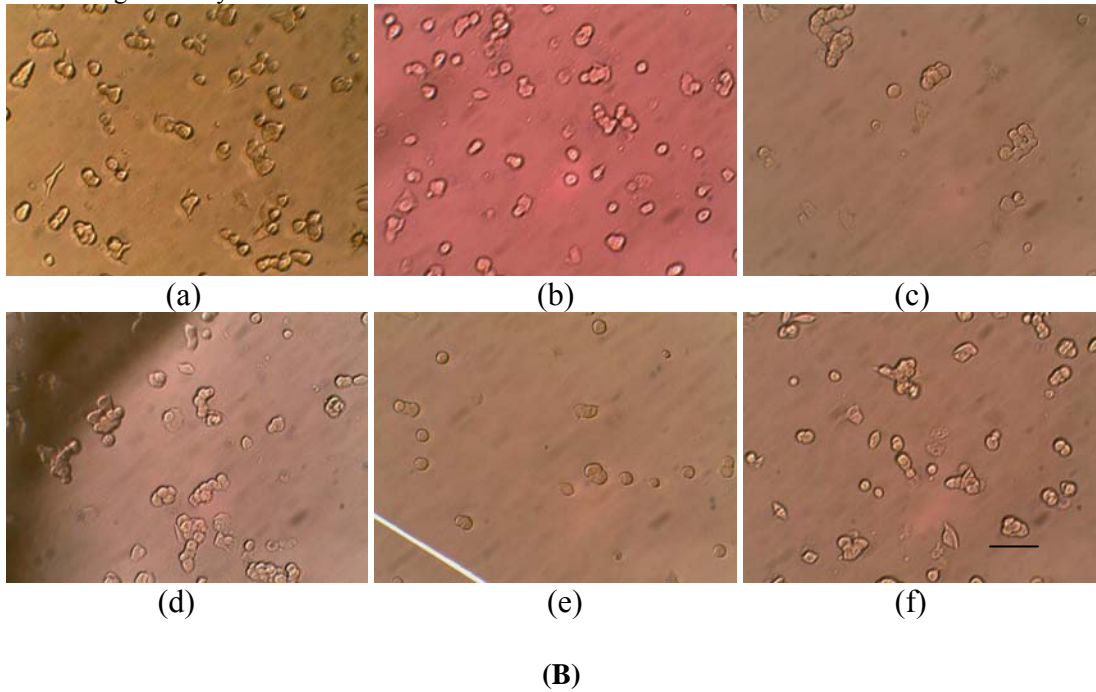
Fig. 5.19. Histograms of bovine chromaffin cell attachment on (e) Platinum

Histogram of bovine chromaffin cell attachment on Platinum coated
with Poly-d-lysine

Well 1

Histogram of bovine chromaffin cell attachment on Platinum coated
with Poly-d-lysine

Well 2

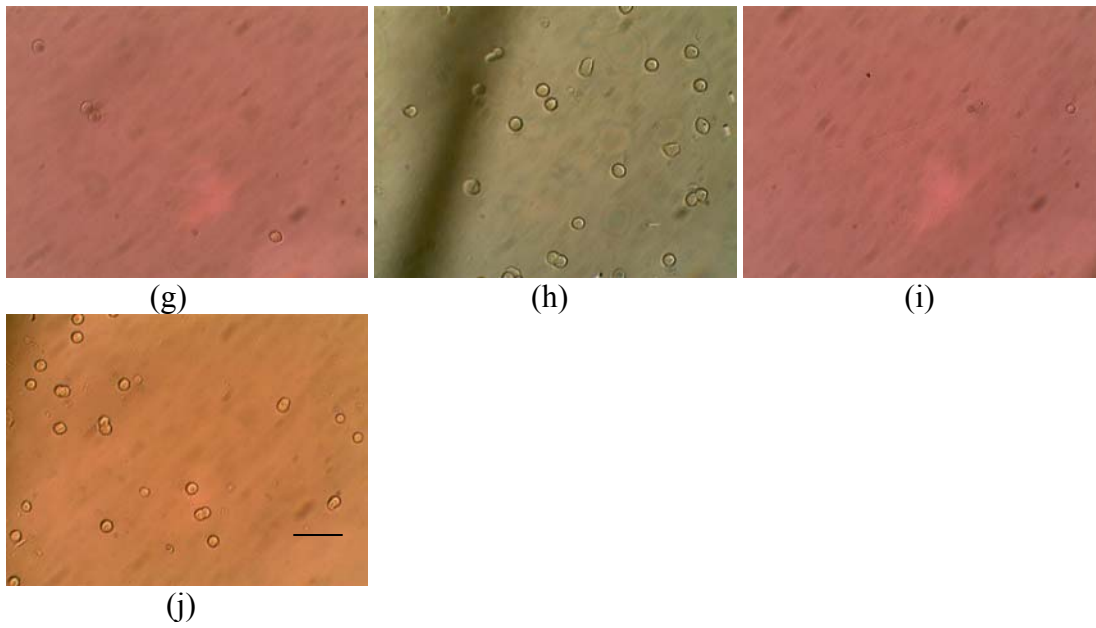**Fig. 5.19.** Histograms of bovine chromaffin cell attachment on (f) Platinum coated with Poly-d-lysine

Histogram of bovine chromaffin cell attachment on gold

Well 1

Histogram of bovine chromaffin cell attachment on Gold

Well 2

Fig. 5.19. Histograms of bovine chromaffin cell attachment on (g) Gold

Histogram of bovine chromaffin cell attachment to Poly-d-lysine coated Gold

Histogram of bovine chromaffin cell attachment to Poly-d-lysine coated gold
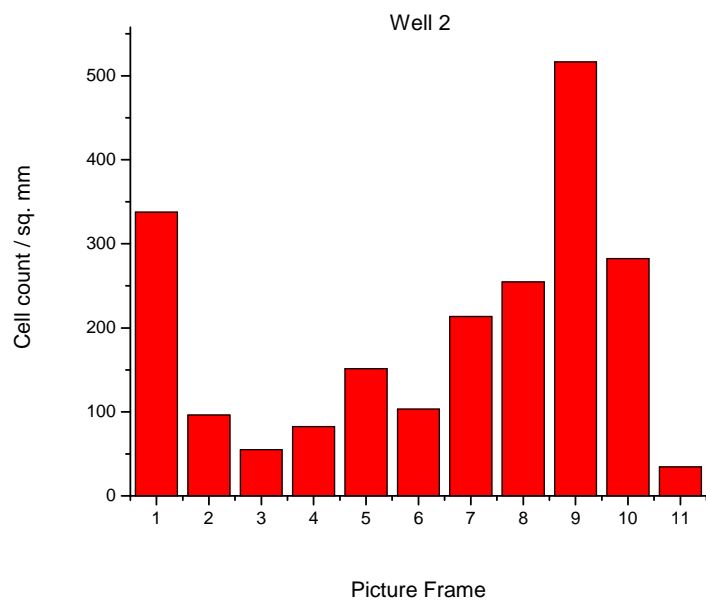
Fig. 5.19. Histograms of bovine chromaffin cell attachment on (h) Gold coated with Poly-d-lysine
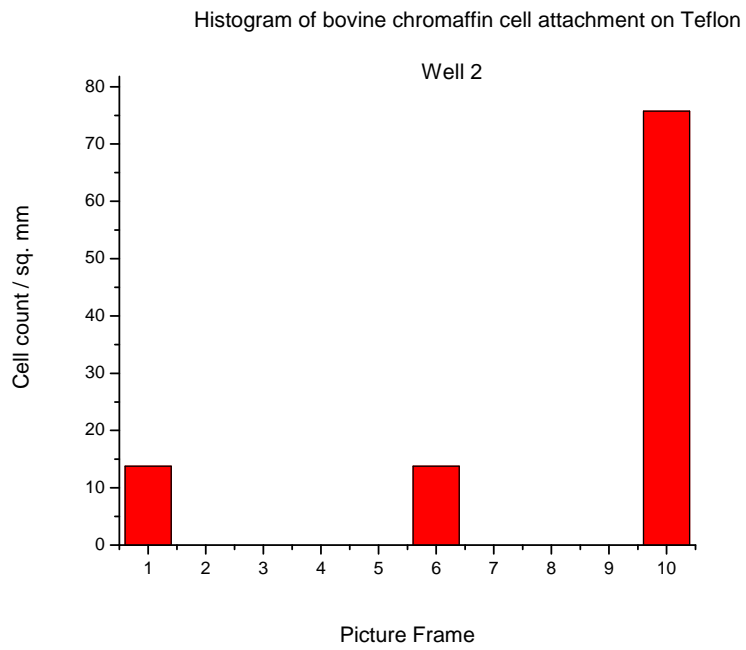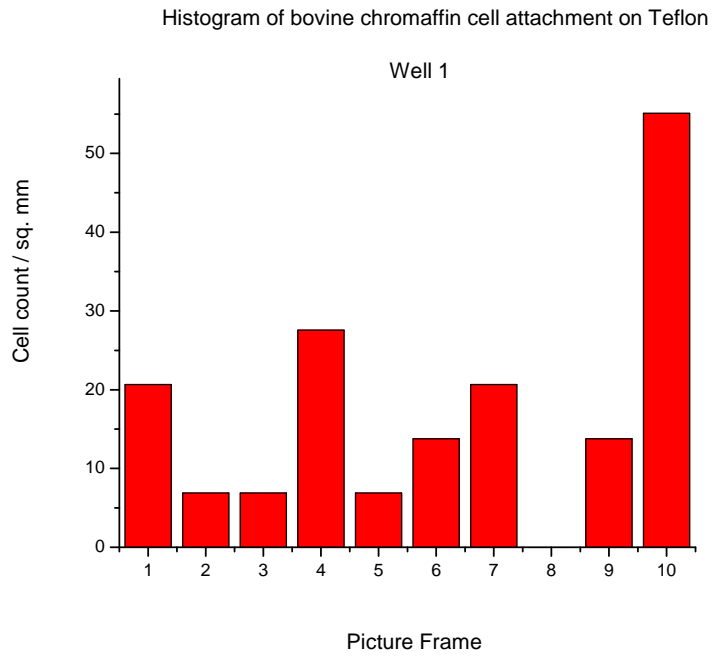
Fig. 5.19. Histograms of bovine chromaffin cell attachment on (i) Teflon
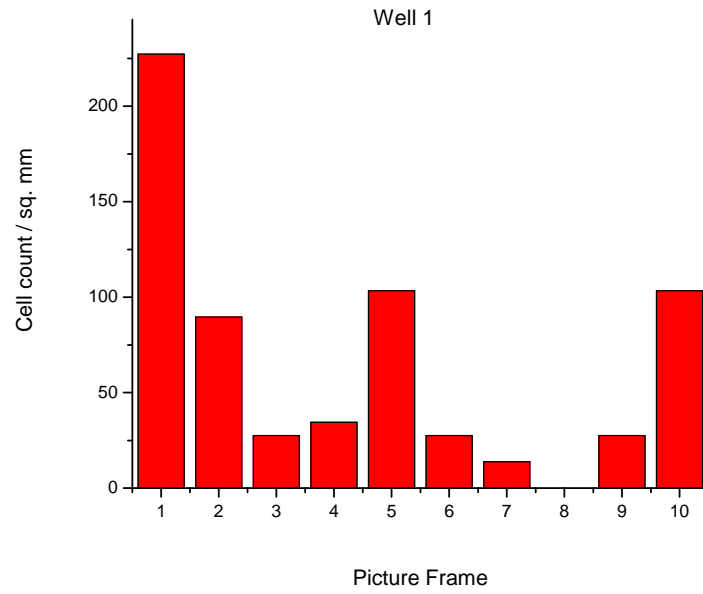
Histogram of bovine chromaffin cell attachment on Poly-d-lysine coated Teflon
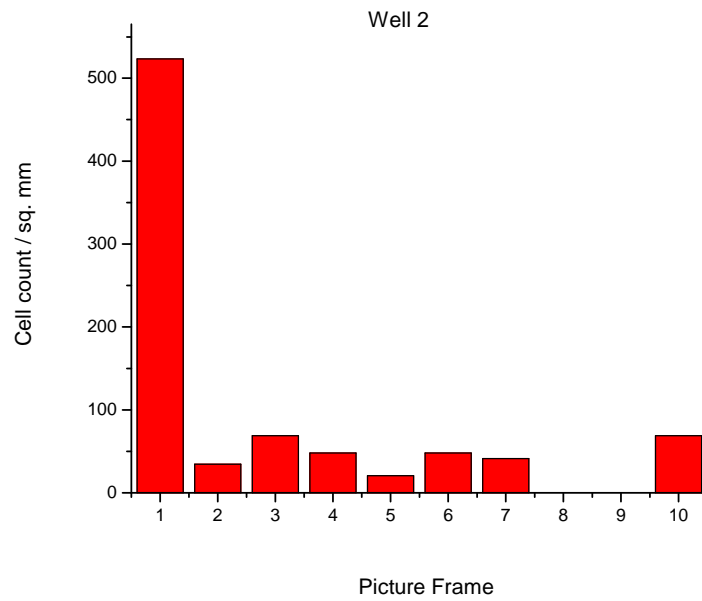
Fig. 5.19. Histograms of bovine chromaffin cell attachment on (i) Teflon coated with Poly-d-lysine

(A)
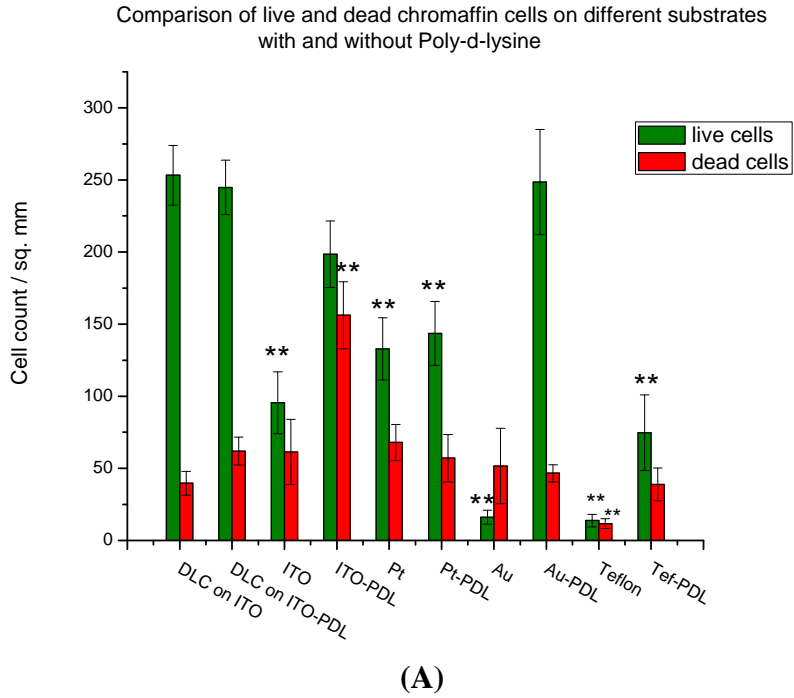
** At p<0.01, mean cell count is significantly different from (DLC on ITO)

| (a) | (b) | (c) |

| (d) | (e) | (f) |

(B)
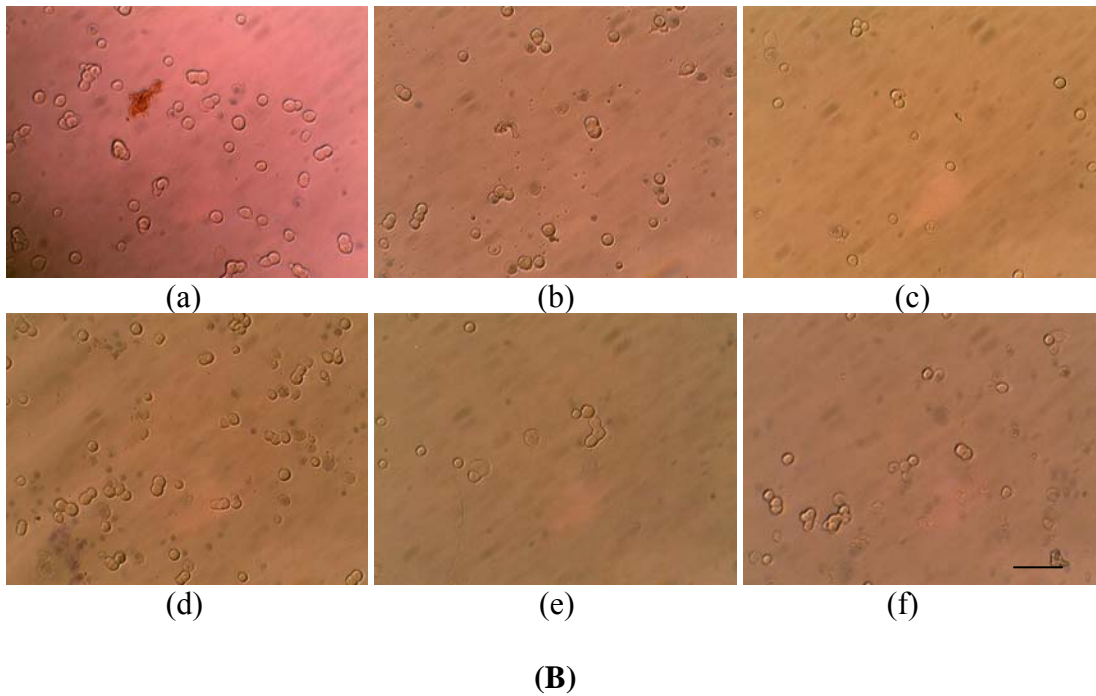
Fig. 5.20. (A). Summary of bovine chromaffin cell attachment on different substrates with and without poly-d-lysine **(B).** Optical micrographs of bovine chromaffin cells attached to (a) DLC as is (b) Poly-d-lysine coated DLC (c) ITO (d) Poly-d-lysine coated ITO (e) Platinum (f) Poly-d-lysine coated Platinum [Scale Bar represents 50 μm]

(g)　　　　　　　　(h)　　　　　　　　(i)

(i)

(B)
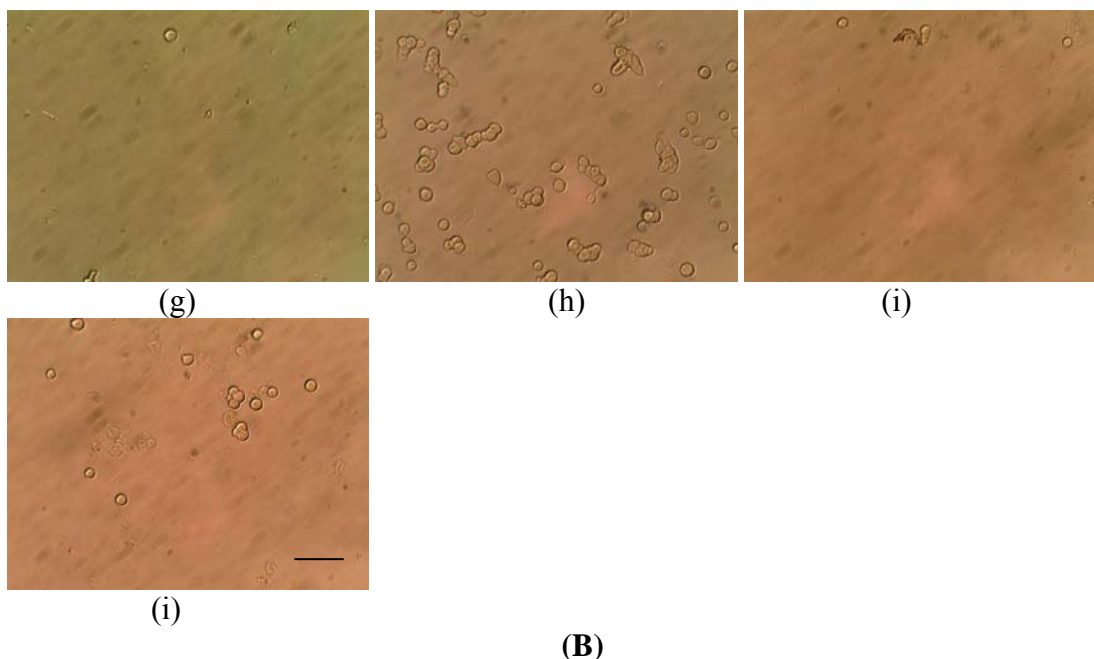
Fig. 5.20. (contd.) (B). Optical micrographs of bovine chromaffin cells attached to (g) Gold (h) Poly-d-lysine coated Gold (i) Teflon (j) Poly-d-lysine coated Teflon [Scale Bar represents 50 μm]

5.11. Summary for all Experiments: INS-1 vs Chromaffin Cells

Two sets of experiments have been consistently performed each on bovine chromaffin cells and INS-1 cells using the same set of substrates with and without surface modification of poly-d-lysine. In order to have a more substantial observation, it is pertinent to integrate the results of such duplicate experiments. The results of Experiment VII and IX are integrated for INS-1 cell attachment results as shown in Fig. 5.21. These results are the adhesion data presented as the mean ± SE from at least 40 images taken from 4 samples of each substrate in the two different cell preparations.
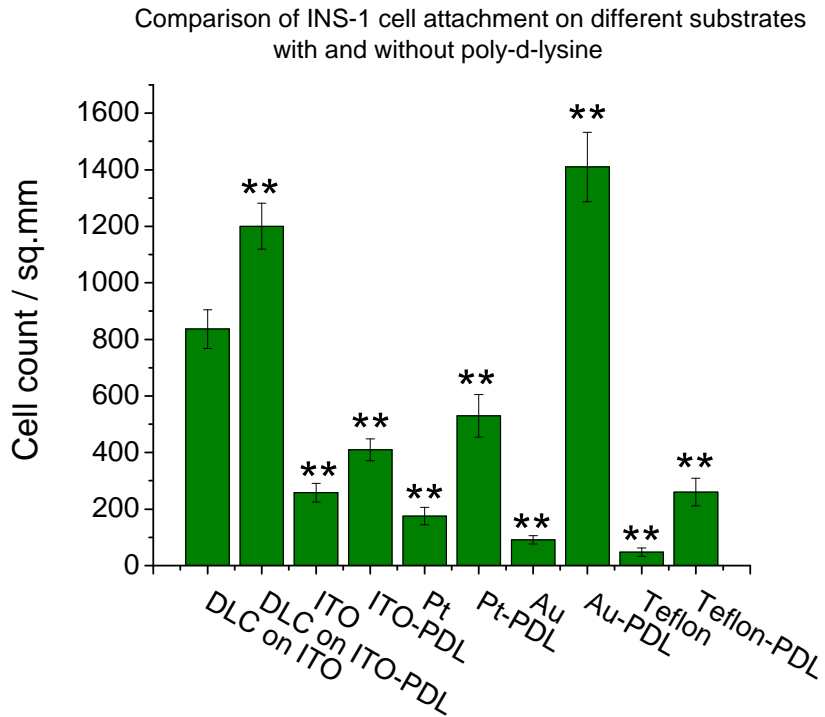
Fig. 5.21. Average number of INS-1 cells (cells/mm^2) that adhered to different substrates coated with and without polylysine. The adhesion data are presented as the mean ± SE from at least 40 images taken from 4 samples of each substrate in two different cell preparations. ** Represents statistically significant difference of the samples as compared to DLC on ITO (p < 0.01).

Similarly, the results of Experiments VIII and X are integrated for bovine chromaffin cell data (Fig. 5.22).
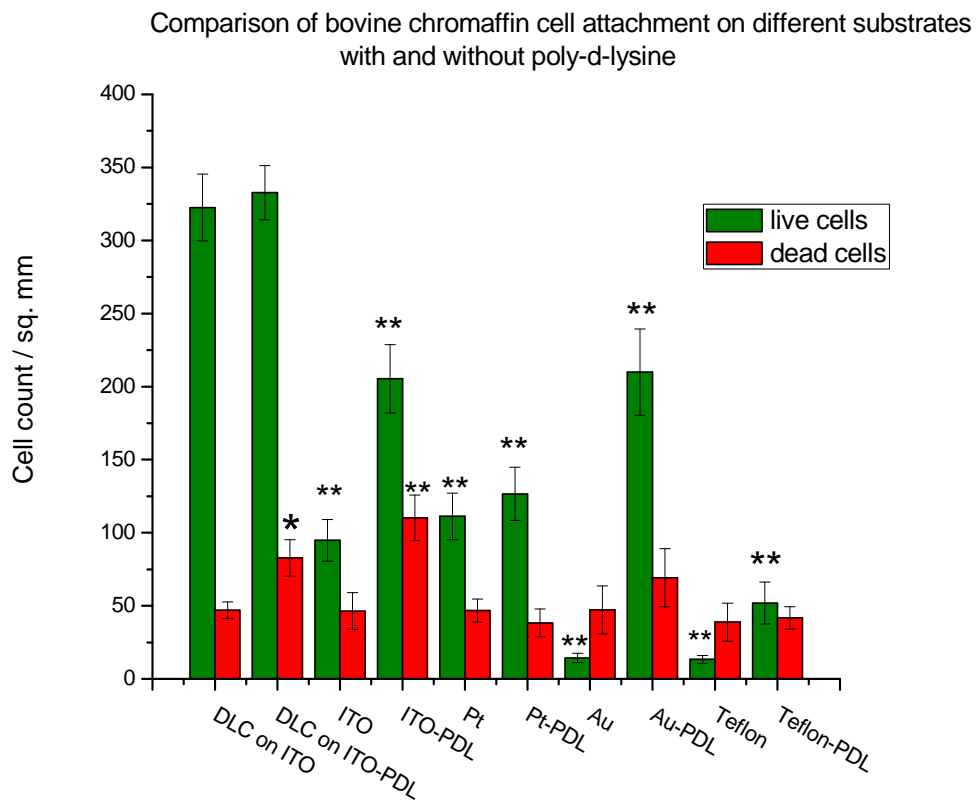
Fig. 5.22. Average number of bovine chromaffin cells (cells/mm^2) that adhered to different substrates with and without surface modification with poly-d-lysine. The adhesion data are presented as the mean ± SE from at least 40 samples completed on two separate occasions. *Represents a statistically significant difference of the surfaces as compared to DLC on ITO (p < 0.05)**Represents a statistically significant difference of the surfaces as compared to DLC on ITO (p < 0.01)

CHAPTER 6

CHARACTERIZATION-
Contact angle and SEM

6.1. Contact angle Measurements

Contact angle measurements have been carried out as described in Section 3.4. The measurements have been done on all the candidate electrodes with and without Poly-d-lysine to observe if there exists any relation between contact angle (or surface energy) and cell attachment as discussed earlier in Section 2.5.3.

| 59º | 56º | 45º | 47º |

(a)   (b)
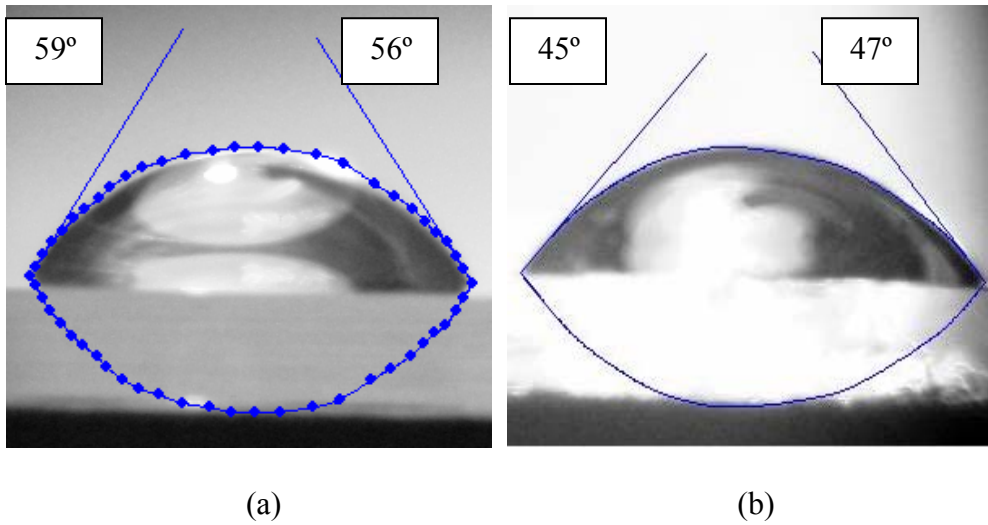
Fig. 6.1. Contact angle of DI water on (a) DLC on ITO (b) DLC on ITO coated with Poly-d-lysine
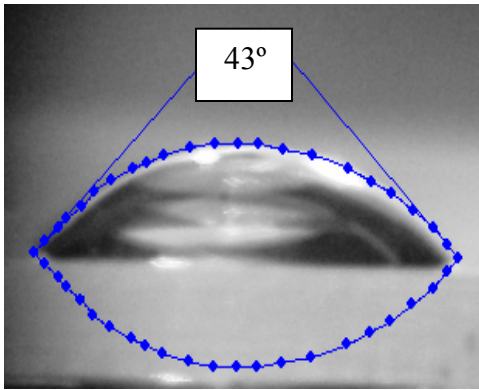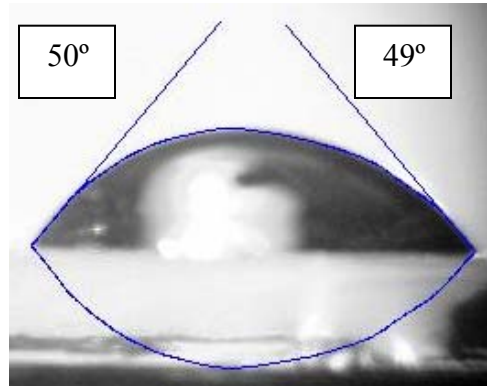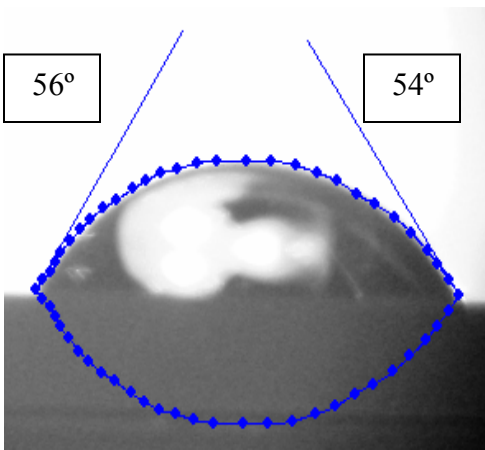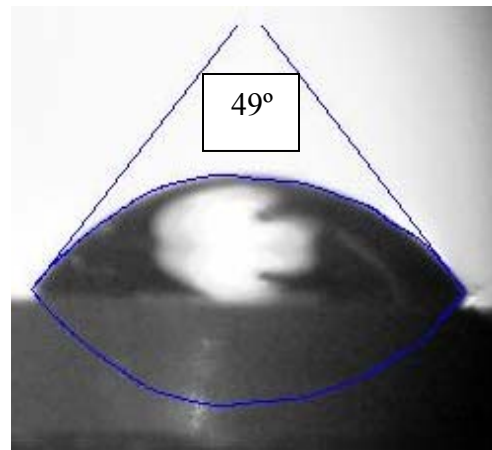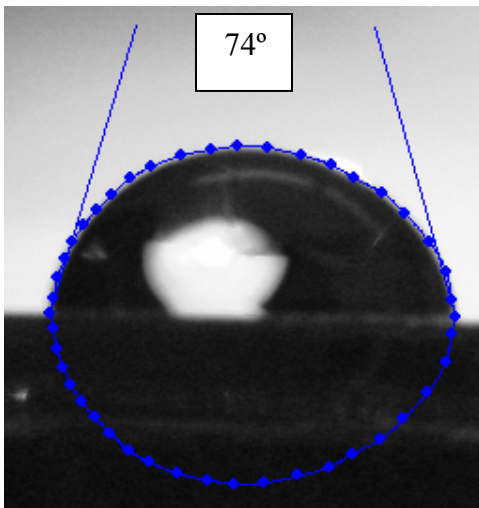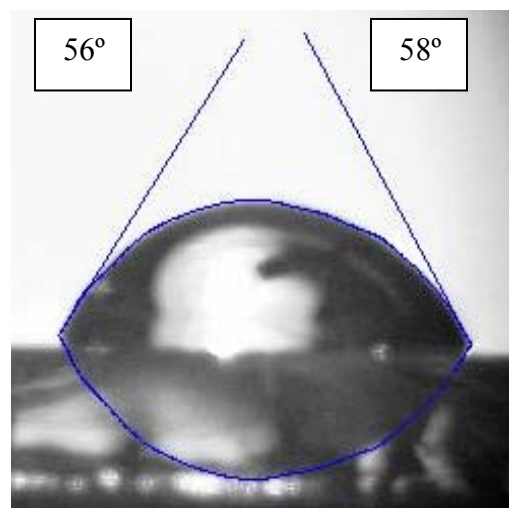
Fig. 6.1. Contact angle of DI water on (c) ITO (d) ITO coated with Poly-d-lysine (e) Platinum (f) Platinum coated with Poly-d-lysine (g) Gold (h) Gold coated with Poly-d-lysine
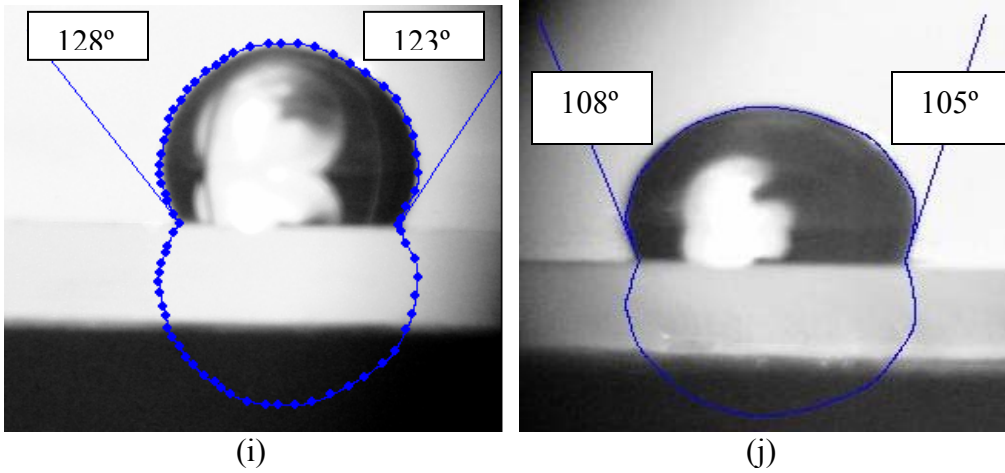
Fig. 6.1. Contact angle of DI water on (i) Teflon (j) Teflon coated with Poly-d-lysine
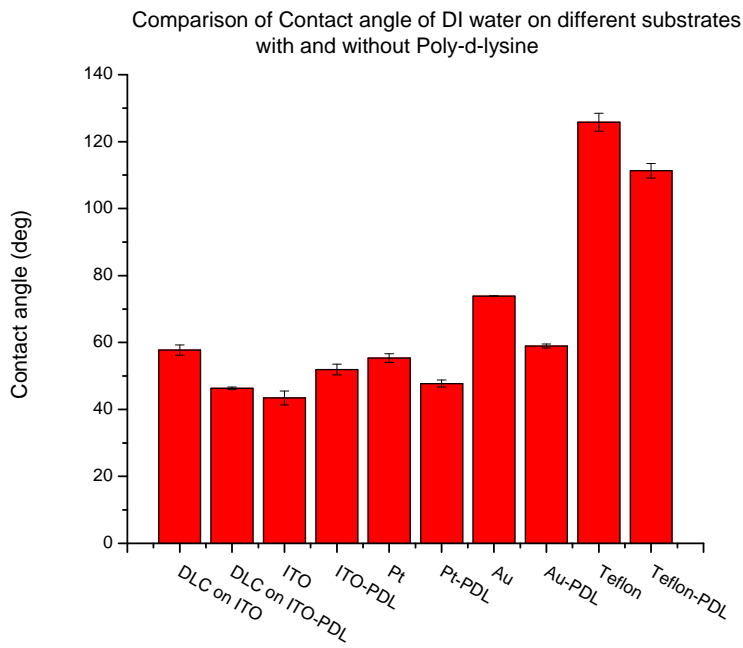
Fig. 6.2. Comparison of contact angle of DI (deionized) water on different substrates with and without poly-d-lysine coating

6.2. SEM Imaging of Bovine Chromaffin Cells

SEM imaging of bovine chromaffin cells on DLC on ITO and ITO only substrates was performed to observe cell spreading morphology on these substrates. No obvious differences were observed in these images probably due to inadequate time (overnight) given to the cells to express such changes ensuing from reactions in the cytoskeletal machinery.
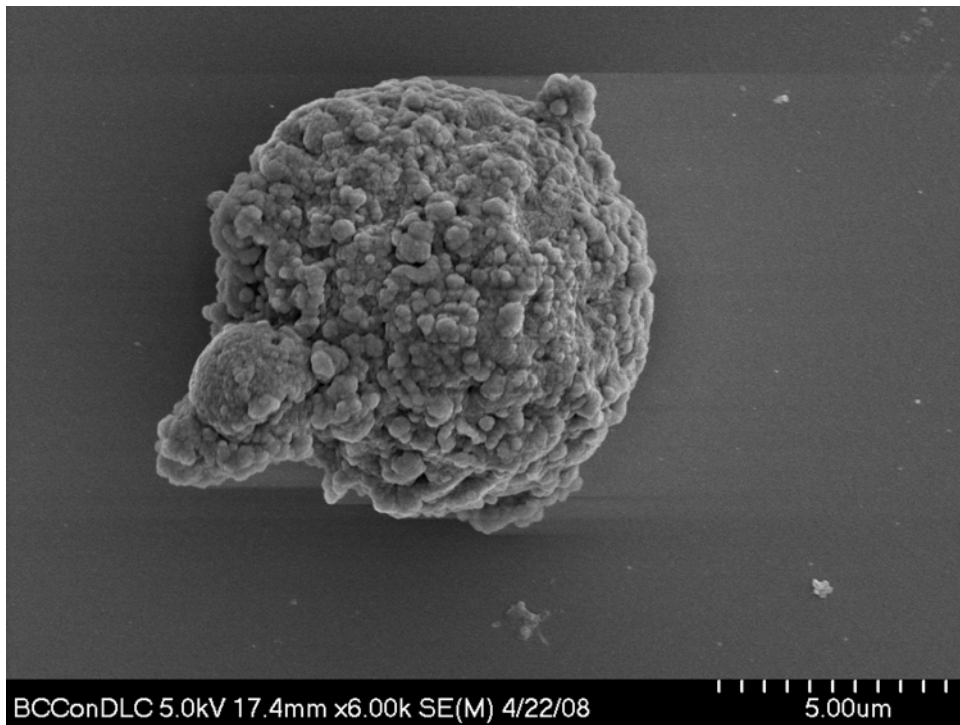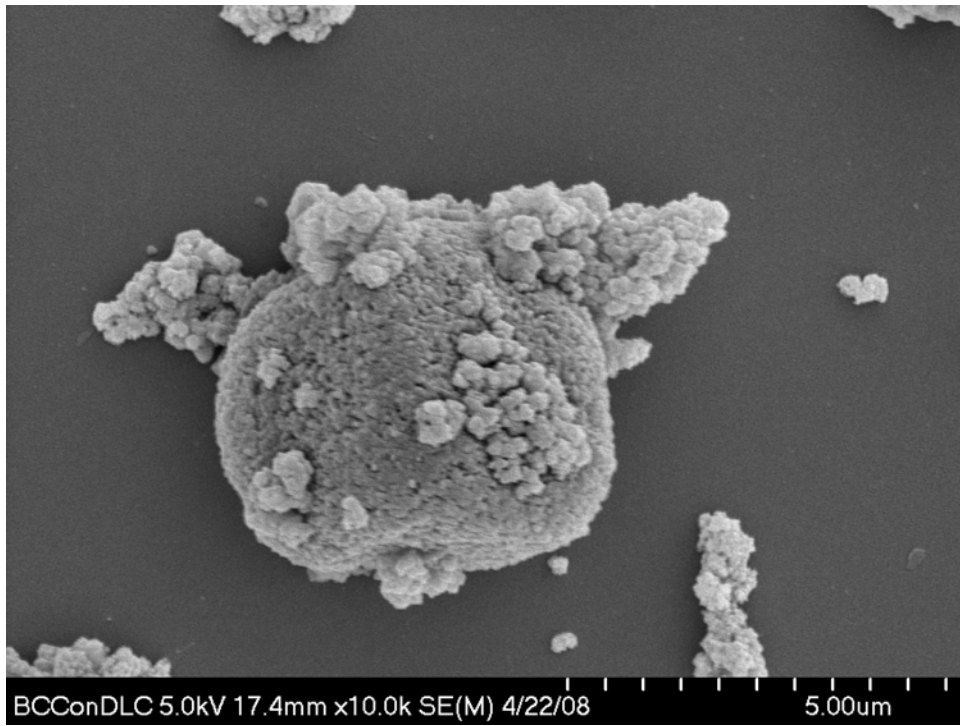
Fig. 6.3. SEM images of Bovine Chromaffin cells on DLC deposited on ITO substrate
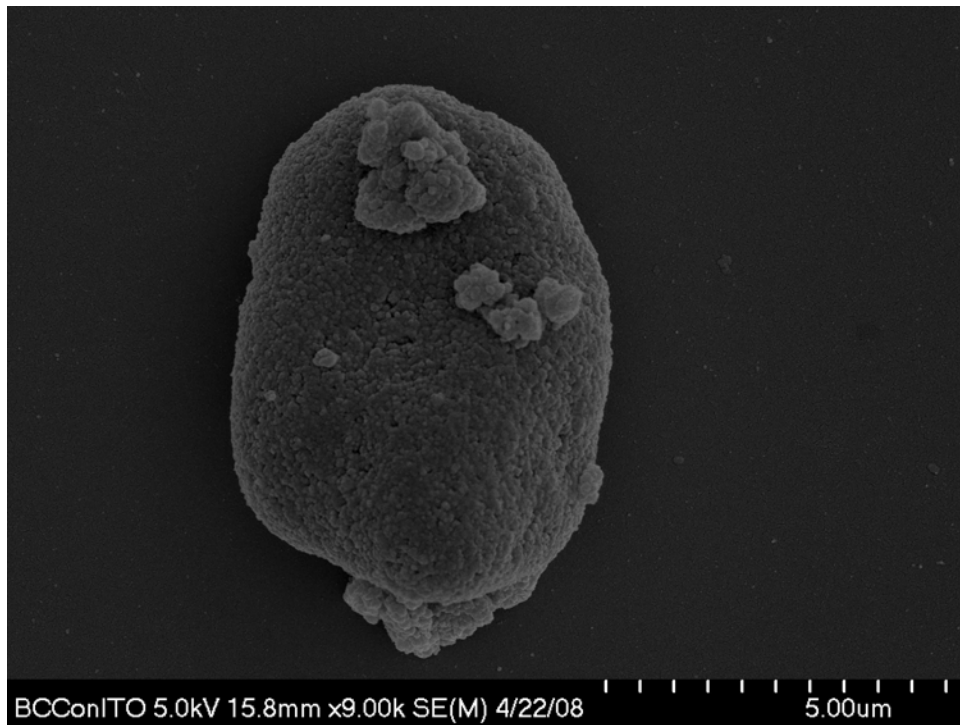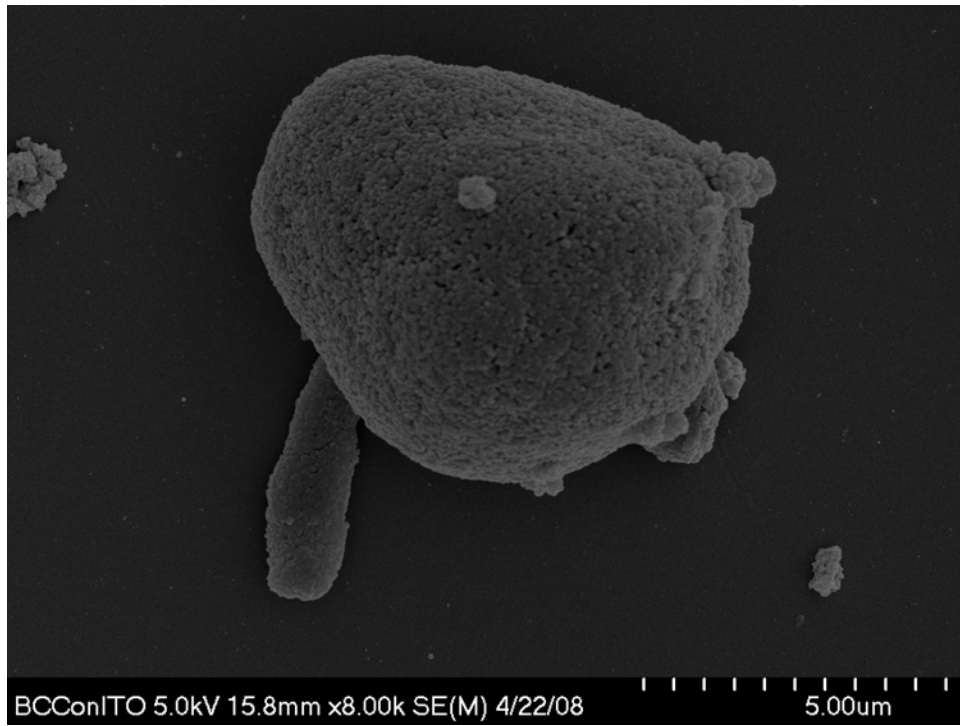
Fig. 6.4 SEM images of Bovine Chromaffin cells on ITO substrate

6.3. Viability of Bovine Chromaffin Cells

Bovine chromaffin cells are fairly sensitive cells and require utmost care to ensure their viability for best experimental results. It has been observed with Trypan Blue assay that these cells can remain healthy (or alive) when preserved in ice for a long time thereby allowing the user to go about preparing for cell attachment experiments without undue haste.

(a)

(b)
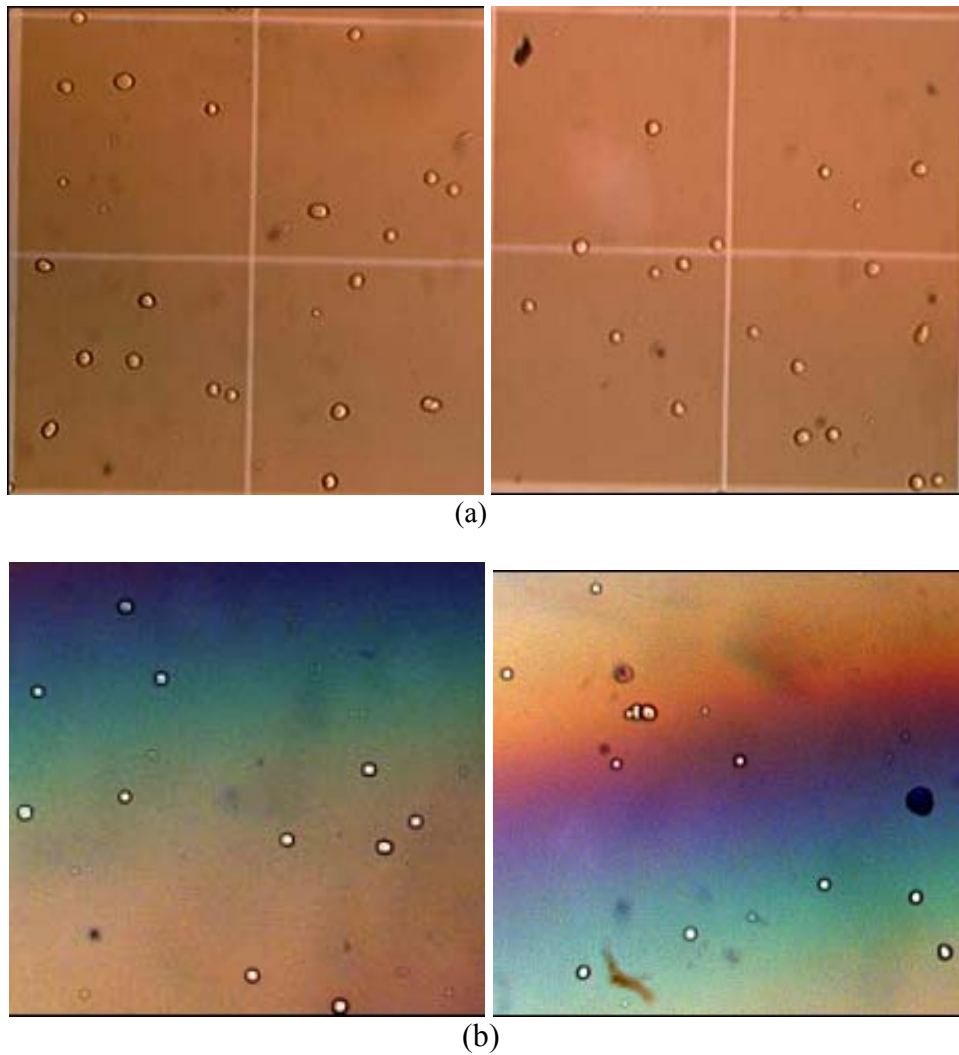
Fig. 6.5. (a) Bovine chromaffin cells preserved in ice (a) After 10 hours (b) After 24 hours

6.4. Cell Attachment on Thermanox

Cell attachment on Thermanox coverslips has been studied as described in Section 3.9.5 while trying different approaches to enhancing cell attachment. Although this may not be of any relevance to this project, but is considered worthwhile to document it for any future reference for cell attachment enthusiasts.
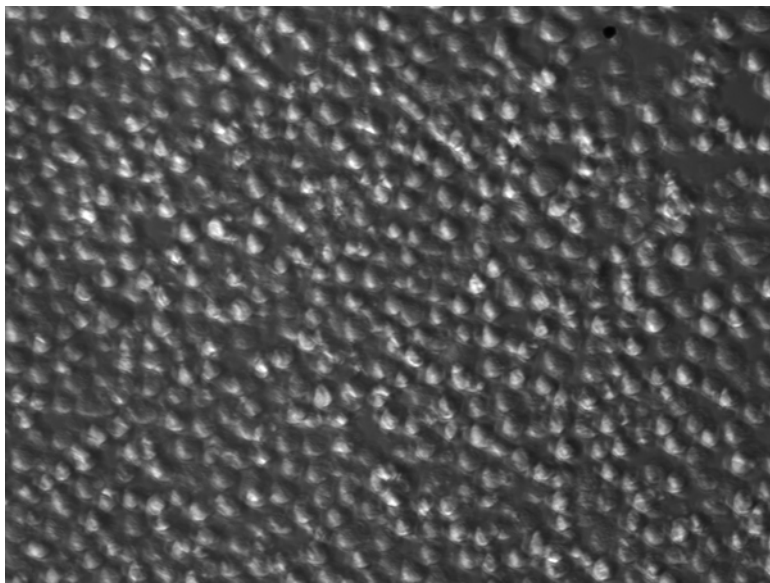
Fig. 6.6. Bovine Chromaffin cell attachment on Thermanox coverslip

Bovine chromaffin cells were incubated overnight on Thermanox coverslips, rinsed and imaged under the microscope. As seen in Fig. 6.6, cells attachment was high proving that Thermanox is conducive to the purpose. However, the viability test with Trypan Blue was not performed.

CHAPTER 7

DISCUSSION

Various experiments have been performed on a range of substrates and repeats done with two different types of cells to garner confidence to a specific trend, if any. It was being speculated that Diamond-like Carbon (DLC) would be a suitable electrode material for cell attachment and was therefore tested alongside others as Indium Tin Oxide (ITO), Platinum and Gold. DLC was also doped with Titanium in few experiments to study whether its 'cytophilic' properties are affected on incorporating Titanium in it. As seen in the experimental results, such doping would reduce cell attachment and therefore the deposition conditions for co-sputtering Ti with DLC needs to be optimized further. A consistent trend observed was that DLC would bind more cells than all other untreated surfaces and the same would be the case with surfaces modified with polylysine. An interesting observation was the drastic enhancement of cell binding on polylysine coated gold. Teflon was used as a negative control for cell attachment and was found to corroborate its 'cytophobic' nature although polylysine coated Teflon bound cells.

7.1. Comparison between Different Electrode Materials

Various materials have been compared for cell attachment namely DLC, DLC doped with Titanium, ITO, Platinum, Titanium (Ti) and Gold. Experiments described in Sections 5.3, 5.4 and 5.5 show higher attachment on DLC doped with Ti as compared to

176

just Titanium. This highlights the fact that DLC is indeed more biocompatible than Ti and has been proven in literature. Throughout all experiments it has been observed that DLC serves as a more "cytophilic" material as compared to ITO, Titanium, Platinum $(p<0.01)$.

The comparison of different substrates has been consolidated with DLC, ITO, Platinum and Gold with and without surface modifications with polylysine. Integrated results of duplicated experiments have set the trend in the sequence DLC > ITO, Pt > Gold. In case of polylysine modified surfaces, the sequence would be different with DLC-PDL> ITO-PDL, Pt-PDL. The cell attachment on Au-PDL would be equal to or less than that of DLC-PDL.

7.2. Comparison of Coatings of Surface Modifications on DLC

The experiment described in Section 5.1 had been performed exclusively on Diamond like Carbon (DLC) to explore possibilities of promoting cell attachment by various surface modifications. It was found that the attachment of bovine chromaffin cells was enhanced as compared to untreated DLC sample (control) when the surface of DLC was maleimide activated and the sulfhydryl groups were reduced on the cells as had been described in Section 3.9.6. The means were proven statistically significant with Student's t-test at $p<0.05$. Apart form this, attachments with other coatings as CellTak, Poly-l-lysine, Poly-d-lysine and Matrigel did not make much impact. However, antibody bound to maleimide activated DLC reduced cell attachment compared to the control

sample (p<0.01). This can be attributed to more than one reason. First, NCAM-13 was chosen as a trial antibody from scores of commercially available ones to target NCAM or L1 receptors known to exist on bovine chromaffin cell membrane. Such a choice requires more trial and error to get to the right pair of antibody-receptor. Secondly, the antibodies could be attached in a manner so as not to have the binding sites exposed for interaction with cell surface receptors as shown in Fig. 7.1.
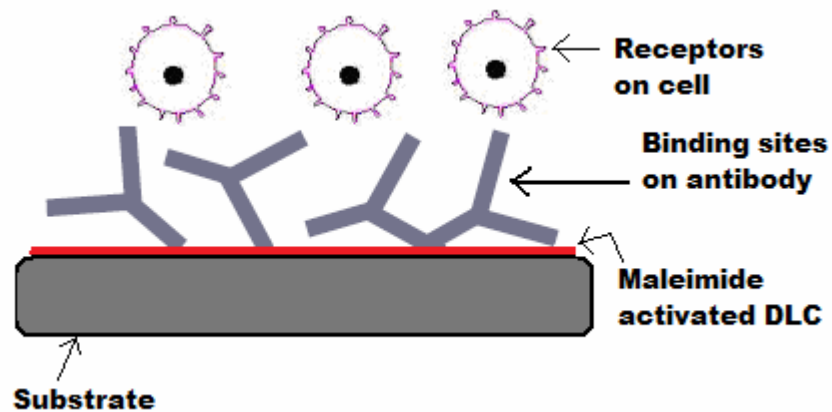
Fig. 7.1. Schematic of unoriented Antibodies on the surface not favoring cell attachment

This can be prevented by using Protein A on the surface which aligns the Antibodies as desired (Fig. 7.2).
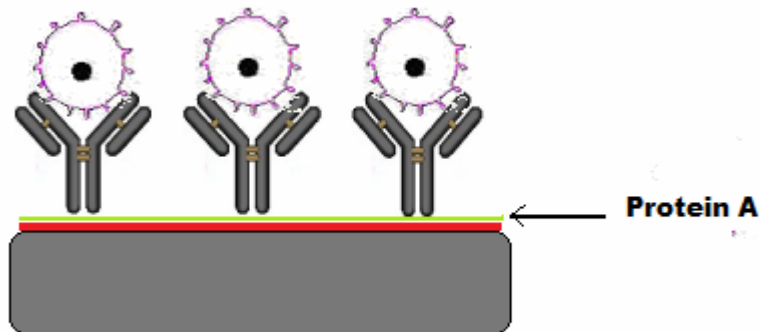
Fig. 7.2. Schematic of oriented Antibodies on the surface coated with Protein A

This set of experiment has not been repeated because sulfhydryl group reduction on the cell membrane surface was subject to speculations of probable effects on exocytosis activity.

Experiments described in Section 5.2 contradict the results described above. This is because the modified DLC samples had been treated with oxygen plasma prior to coating with polylysine of both forms and matrigel. This process has ensured that the surface modified layer bind to the surface electrostatically, inducing probable protein adsorption and hence higher cell attachment. In all latter experiments, the surface was simply immersed in polylysine without any plasma treatment because of an apparent adverse effect on the DLC surface.

Experiments described in Sections 5.4 and 5.5 showed decrease in cell attachment on oxygen plasma treated DLC as compared to the control sample ($p<0.01$). In these cases the samples would be immersed in deionized water after plasma treatment so as to allow the radical groups to react and form "cytophilic" groups. Apparently, such groups have not formed and plasma seems to be detrimental to the DLC surface. These results contradict those from Section 5.2 wherein there is no significant difference between the same samples being held in comparison because the approach involved herein was direct exposure of cell suspension to plasma treated surface without any immersion in deionized water.

7.3. Comparison of INS-1 with Chromaffin Cells

INS-1 and bovine chromaffin cells were incubated for 2 and 18-20 hours respectively. This is because INS-1 cells divide and also take lesser time to attach to a surface. Also, INS-1 cells were observed to spread out more on polylysine coated surfaces. Because of their robust nature, negligible dead INS-1 cells were observed while there was a considerable dead chromaffin cell population. On unmodified surfaces the trend for both INS-1 and chromaffin cells was established as DLC > ITO, Pt > Au. In case of surface modification with polylysine, the rank order for INS-1 cells was observed as DLC-PDL, Au-PDL > ITO-PDL, Pt-PDL while for the chromaffin counterpart it was DLC-PDL > Au-PDL, ITO-PDL > Pt-PDL.

7.4. Cell Viability

In case of bovine chromaffin cells, dead cells would be observed because of their sensitive nature. Quantification of such dead cells was performed to study whether different surfaces affect cell mortality. It was however found that there was no consistent difference in mortality on different substrates.

7.5. Mechanism Underlying Differences between Materials in Promoting Cell Attachment:

With ten sets of experiments and certain repeats yielding a net sequence as to the candidacy of electrodes, DLC deposited on ITO is established as the champion electrode material for measurement of exocytosis in this work. However, we do not fully understand the theory underlying this empirical trend.

A thorough literature review in Chapter 2 asserts that every biomaterial in contact with biofluids elicits an initial protein adsorption. The protein monolayer is the key to subsequent cell attachment. This attachment takes place by binding of integrin receptors on the cell membrane with active sites or motifs on the protein. Proteins tend to denature when in contact with a surface. The degree of denaturation may lead to more exposed active motifs for integrin binding or may lead to less-effective binding to integrin receptors. The chromaffin cell medium contains serum which is richer in vitronectin than fibronectin. It can be said that there could be receptors similar in behavior to $\alpha_v\beta_3$ on the bovine chromaffin cell membrane with affinity for RGD motifs of vitronectin. This is only one of the numerous receptor-motif pairs possible in this perspective since every receptor is known to behave 'promiscuously' while in search for an appropriate binding site on the protein.

There may be a relation between surface energy of the electrode material and protein adsorption in an active form. The contact angle measurements demonstrate that DLC is close enough (58º) to the value cited in most literature (60-65º) as being most conducive to fibronectin protein adsorption. ITO being hydrophilic with contact angle

around 43º presumably does not favor protein adsorption as much as DLC. Upon addition of polylysine to ITO, the contact angle increases to 52º and cell attachment is enhanced. Gold being more hydrophobic than DLC with a contact angle of 73º presumably does not support protein adsorption, yet upon treatment with polylysine the contact angle drops to 59º and cell attachment increases dramatically. Therefore it seems like a contact angle around 60º is the optimal value.
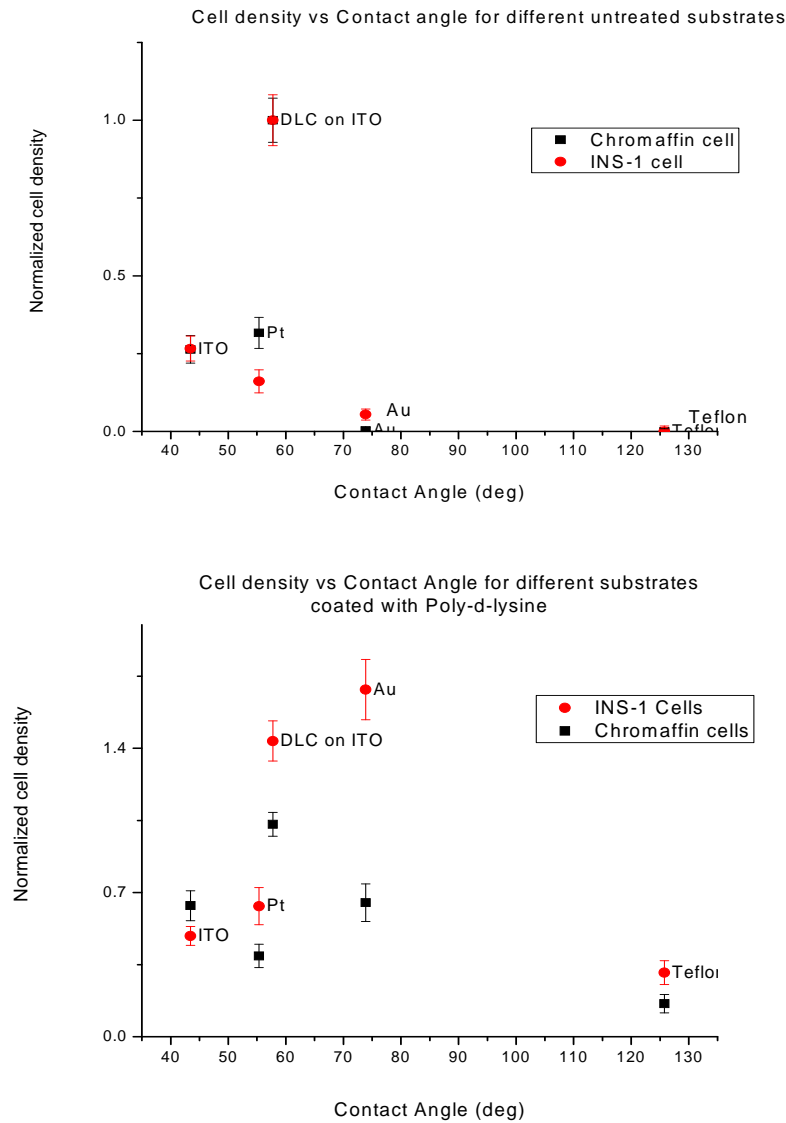
Fig. 7.3. Comparison of different substrates for Cell density vs Contact angle (a) Untreated samples (top) (b) Polylysine coated samples (below)

On the other hand, other data do not support tight correlation between contact angle and cell attachment. If contact angle is indeed a determining factor for cell attachment one would expect that polylysine coated DLC would have reduced cell binding owing to a contact angle of 46º which is hydrophilic. In addition Platinum has a contact angle (55º) close to that of DLC (58º), yet does not support cell adhesion as well as DLC (Fig. 7.3). Therefore, a definitive correlation between contact angle and cell attachment cannot be made from my data and this relationship is also controversial in the literature. With the data collected in this work, a definitive correlation cannot be established between contact angle and cell attachment properties of a surface. More experiments need to be done and surface energy measurements need to be performed using other solvents to explore the relationship between surface energy and cell attachment

One could speculate that one reason that cell attachment increases so dramatically upon addition of polylysine to gold is that it forms a uniform and continuous polylysine film on it which in turn brings about healthy protein adsorption and high cell attachment. This hypothesis could be tested by means of Atomic Force Microscopy (AFM) in future experiments.

CHAPTER 8

CONCLUSIONS AND FUTURE DIRECTIONS

8.1. Conclusion

The goal at the onset of this work was identifying potential electrode materials with good cell adhesion properties. With Teflon serving as a suitable insulating and cytophobic material around the wells, this electrode would need to incorporate properties of cell attachment, cell viability, transparency, conductivity and electrochemical activity. Metals seem to be the obvious choice for any electrode, but may not support cell attachment or viability without surface modification. Although Titanium and platinum have been used as biomaterials in the past, they have not been as successful as Diamond like Carbon (DLC) implants. Carbon fibers have been used for amperometric detection of quantal exocytosis because of their ability to measure signals with low noise. In general, carbon electrodes are widely used as electrochemical electrodes because they are stable, sensitive and exhibit small background currents. Clearly, it is not practical to integrate carbon fibers on a microchip. Deposition of graphite produces electrodes that may not be stable or adhere well to the substrate. Therefore, DLC is suitable as a "hard" carbon material. Indium Tin Oxide (ITO) deposited as a base layer beneath DLC serves to increase the conductivity of the electrode to acceptable levels, produce electrodes that are both transparent and conductive. The candidacy of various material electrodes for cell attachment has been established in the descending order of DLC (deposited on top of

ITO) > ITO (Indium tin oxide), platinum > gold. The attachment properties of the electrodes were enhanced with various surface modifications such as polylysine treatment. However, the results lead to the conclusion that a DLC electrode with a contact angle close to 60º by itself is the most preferable and any surface modifications on it may interfere with the cytophobic properties of the Teflon surrounding the wells. A robust protocol has been developed to quantify cell attachment to different electrode materials and exhaustive repeats have been performed to give confidence in the conclusions drawn.

8.2. Future Directions

The protocol developed for cell quantification is robust. The crucial step involved is the rinsing step to remove dead, floating or unbound cells which is followed by staining assay to observe viability and refrain from counting dead cells. Prior to Trypan blue assay, the cells could be fixed by adding methanol or ethanol to the wells. This will ensure that the bound cells are not lost in latter rinses to wash off Trypan blue and this data could be more statistically significant.

Although this work has not dealt with some aspects that will be faced with the microchip in latter stages, it is justified to define them. One aspect could be integrating microfluidics with the array. Since the arrays are made up of Teflon, there can be an issue with driving the cell suspension flow into he channels in order for the cells to be guided to the wells. Since Teflon is extremely hydrophobic, there has to be a relatively high pressure applied to the fluid. This flow rate also has to be optimum enough to support the

concept of cell docking in the wells since cells need time to tether and then bind to the electrode in the wells.

As discussed in the introduction, a similar biochip has been developed with MWCNTs serving as the electrodes insulated by surrounding SiO_2 (Li 2005). This insulating layer has been functionalized by PEG (polyethylene glycol) to serve as the cytophobic region and the CNT tips have been functionalized to attach relevant group to serve as DNA Microarray. This concept is appealing to our project and if the aim is to decrease the cost of the microchip, Teflon can be replaced with SiO_2 and functionalized. In that case our microchip will have DLC electrodes in place of CNTs. The whole surface can be silanized with Aminopropyltriethyoxysilane followed by applying 2-(2-Methoxyethoxy) acetic acid to form an amide bond with the – NH2 group facilitated by coupling reagents 1-ethyl-3(3-dimethyl aminopropyl) carbodiimide hydrochloride and N-hydroxysulfo-succinimide. This generates a surface terminated with ethylene glycol moieties, which repel proteins by steric repulsion and thereby prevent cell attachment (Lee and others 1997). Finally, molecules on the DLC surface can be removed by electrochemical etching in 1.0 M NaOH, which regenerates a well-defined DLC surface dominated by hydroxyl and hydroperoxide groups.

It can be concluded from this dissertation that cell attachment to a surface is a very complicated phenomenon. It has been found that there exists no direct relation between contact angle measurements and cell attachment to the surfaces. This finding can be consolidated by use of polar and non-polar liquids to measure surface energy of the surface. It is speculated that cell attachment is influenced by protein adsorption

186

phenomenon on the surface. The cells bind at the membrane receptor- ligand level, ligands being proteins as vitronectin and fibronectin present in serum. The roles of such proteins in cell attachment can be observed with protein specific experiments. For instance, serum containing a known protein say vitronectin or fibronectin can be used and its effect on cell attachment observed. This would lead to knowledge supporting the hypothesis of protein-ligand binding. Once this can be established, there are anticipations of RGD sequences in ligands playing a major role cell attachment. This can also be determined by using antibodies binding specifically to RGD to detect the presence of such sequences in the major proteins constituting the serum.

REFERENCES

Alanazi A, Nojiri C, Kido T, Noguchi T, Ohgoe Y, Matsuda T, Hirakuri K, Funakubo A, Sakai K, Fukui Y. 2000. Engineering Analysis of Diamond-Like Carbon Coated Polymeric Materials for Biomedical Applications. Artif Organs 24(8):624-7.

Allen M, Myer B, Rushton N. 2001. In vitro and in vivo investigations into the biocompatibility of diamond-like carbon (DLC) coatings for orthopedic applications. Journal of Biomedical Materials Research 58(3):319-28.

Asfari M. 1992. Establishment of 2-mercaptoethanol-dependent differentiated insulin-secreting cell lines. Endocrinology 130(1):167-78.

Ashery U, Betz A, Xu T, Brose N, Rettig J. 1999. An efficient method for infection of adrenal chromaffin cells using the Semliki Forest virus gene expression system. Eur J Cell Biol 78(8):525-32.

Augustine GJ, Neher E. 1992. Calcium requirements for secretion in bovine chromaffin cells. The Journal of Physiology 450(1):247-71.

Biesalski MA, Knaebel A, Tu R, Tirrell M. 2006. Cell adhesion on a polymerized peptide–amphiphile monolayer. Biomaterials 27(8):1259-69.

Bruns D. 2004. Detection of transmitter release with carbon fiber electrodes. Methods 33(4):312-21.

Cai K, Bossert J, Jandt KD. 2006. Does the nanometre scale topography of titanium influence protein adsorption and cell proliferation? Colloids and Surfaces B: Biointerfaces 49(2):136-44.

Campbell ID, Downing AK. 1998. NMR of modular proteins. Nature Structural Biology 5(7):496-9.

Carlo DD, Wu LY, Lee LP. 2006. Dynamic single cell culture array. Lab on a Chip 6(11):1445-9.

Castner DG, Ratner BD. 2002. Biomedical surface science: Foundations to frontiers. Surface Science 500(1):28-60.

Chai F, Mathis N, Blanchemain N, Meunier C, Hildebrand HF. 2008. Osteoblast interaction with DLC-coated Si substrates. Acta Biomaterialia.

Chang KC, Tees DFJ, Hammer DA. 2000. The state diagram for cell adhesion under flow: Leukocyte rolling and firm adhesion. Proceedings of the National Academy of Sciences:200240897: 11262-7.

Chen JY, Wang LP, Fu KY, Huang N, Leng Y, Leng YX, Yang P, Wang J, Wan GJ, Sun H. 2002. Blood compatibility and sp3/sp2 contents of diamond-like carbon (DLC) synthesized by plasma immersion ion implantation-deposition. Surface & Coatings Technology 156(1-3):289-94.

Cui FZ, Li DJ. A review of investigations on biocompatibility of diamond-like carbon and carbon nitride films. structure 3:481-7.

De Scheerder I, Szilard M, Yanming H, Ping XB, Verbeken E, Neerinck D. 2000. Evaluation of the biocompatibility of two new diamond-like stent coatings (Dylyn) in a porcine coronary stent model. Journal of Invasive Cardiology 12(8):389-94.

Dearnaley G, Arps JH. 2005. Biomedical applications of diamond-like carbon (DLC) coatings: A review. Surface & Coatings Technology 200(7):2518-24.

Du C. 1998. Morphological behaviour of osteoblasts on diamond-like carbon coating and amorphous C–N film in organ culture. Biomaterials 19(7-9):651.

Fulop T, Radabaugh S, Smith C. 2005. Activity-dependent differential transmitter release in mouse adrenal chromaffin cells. J Neurosci 25(32):7324-32.

Gao Y. 2006. Microfabricated devices for Single cell: University of Missouri.

Gupta S, Weiner BR, Morell G. 2002. Role of sp C cluster size on the field emission properties of sulfur-incorporated nanocomposite carbon thin films. Applied Physics Letters 80:1471.

Gutensohn K, Beythien C, Bau J, Fenner T, Grewe P, Koester R. 2000. In vitro analyses of diamond-like carbon coated stents. Reduction of metal ion release, platelet activation, and thrombogenicity. Thrombosis Research 99(6):577-85.

Hautanen A, Gailit J, Mann DM, Ruoslahti E. 1989. Effects of modifications of the RGD sequence and its context on recognition by the fibronectin receptor. Journal of Biological Chemistry 264(3):1437-42.

Hochstetler SE, Wightman RM. 1998. Detection of Secretion with Electrochemical Methods. Bloomfield, V. and De Felice, L., Editors.

Holmberg M, Stibius KB, Larsen NB, Hou X. 2008. Competitive protein adsorption to polymer surfaces from human serum. Journal of Materials Science: Materials in Medicine 19(5):2179-85.

Horbett TA. 1994. The role of adsorbed proteins in animal cell adhesion. Colloids and surfaces. B, Biointerfaces 2(1-3):225-40.

Horbett TA. 1996. Proteins: structure, properties, and adsorption to surfaces. Biomaterials Science: An Introduction to Materials in Medicine:133–41.

Huang N, Yang P, Leng YX, Wang J, Sun H, Chen JY, Wan GJ. 2004. Surface modification of biomaterials by plasma immersion ion implantation. Surface & Coatings Technology 186(1-2):218-26.

Hwang DS, Gim Y, Kang DG, Kim YK, Cha HJ. 2007a. Recombinant mussel adhesive protein Mgfp-5 as cell adhesion biomaterial. Journal of Biotechnology 127(4):727-35.

Hwang DS, Sim SB, Cha HJ. 2007b. Cell adhesion biomaterial based on mussel adhesive protein fused with RGD peptide. Biomaterials 28(28):4039-46.

Jäger M. 2007. Significance of Nano-and Microtopography for Cell-Surface Interactions in Orthopaedic Implants. Journal of Biomedicine and Biotechnology 2007:1-19.

Jones MI, McColl IR, Grant DM, Parker KG, Parker TL. 1999. Haemocompatibility of DLC and TiC-TiN interlayers on titanium. Diamond and Related Materials 8(2):457-62.

Jones MI, McColl IR, Grant DM, Parker KG, Parker TL. 2000. Protein adsorption and platelet attachment and activation, on TiN, TiC, and DLC coatings on titanium for cardiovascular applications. Journal of Biomedical Materials Research 52(2):413-21.

Joshi MS. 1991. Growth and differentiation of the cultured secretory cells of the cow oviduct on reconstituted basement membrane. J Exp Zool 260(2):229-38.

Kelly S, Regan EM, Uney JB, Dick AD, McGeehan JP, Mayer EJ, Claeyssens F. 2008. Patterned growth of neuronal cells on modified diamond-like carbon substrates. Biomaterials: 2573-80.

Klebe RJ, Bentley KL, Schoen RC. 1981. Adhesive substrates for fibronectin. Journal of Cellular Physiology 109(3):481-8.

Latour RA. 2004. Biomaterials: protein-surface interactions. Encyclopedia of biomaterials and biomedical engineering Marcel Dekker, New York.

Lau AY, Hung PJ, Wu AR, Lee LP. 2006. Open-access microfluidic patch-clamp array with raised lateral cell trapping sites. Lab on a Chip 6(12):1510-5.

Lawrence MB, Kansas GS, Kunkel EJ, Ley K. 1997. Threshold Levels of Fluid Shear Promote Leukocyte Adhesion through Selectins (CD62L, P, E). The Journal of Cell Biology 136(3):717-27.

Lawrence MB, Springer TA. 1991. Leukocytes roll on a selectin at physiologic flow rates: distinction from and prerequisite for adhesion through integrins. Cell 65(5):859-73.

Lee IS, Park JC, Lee YH. 2002. Plasma processing of materials for medical applications. Surface & Coatings Technology 171(1-3):252-6.

Lee JH, Jeong BJ, Lee HB. 1997. Plasma protein adsorption and platelet adhesion onto comb-like PEO gradient surfaces. Journal of Biomedical Materials Research 34(1):105-14.

Lehnert T, Gijs MAM. Patch-clamp microsystems. Lab-on-Chips for Cellomics: Micro and Nanotechnologies for Life Science.

Li DJ. 2002. Cell attachment on diamond-like carbon coating. Bulletin of Materials Science 25(1):7.

Li J. 2005. Inlaid Multi-Walled Carbon Nanotube Nanoelectrode Arrays for Electroanalysis. Electroanalysis 17(1):15.

Linder S, Pinkowski W, Aepfelbacher M. 2002. Adhesion, cytoskeletal architecture and activation status of primary human macrophages on a diamond-like carbon coated surface. Biomaterials 23(3):767-73.

Lord MS. 2006. Biomolecular and Cellular: The University of New South Wales: 234p.

MacDonald PE, Obermuller S, Vikman J, Galvanovskis J, Rorsman P, Eliasson L. 2005. Regulated Exocytosis and Kiss-and-Run of Synaptic-Like Microvesicles in INS-1 and Primary Rat {beta}-Cells. Diabetes 54(3):736.

Mazia D. 1975. Adhesion of cells to surfaces coated with polylysine. Applications to electron microscopy. The Journal of Cell Biology 66(1):198-200.

Michael KE, Vernekar VN, Keselowsky BG, Meredith JC, Latour RA, Garcia AJ. 2003. Adsorption-induced conformational changes in fibronectin due to interactions with well-defined surface chemistries. Langmuir 19(19):8033-40.

Miura M, Fujimoto K. 2006. Subcellular topological effect of particle monolayers on cell shapes and functions. Colloids and Surfaces B: Biointerfaces 53(2):245-53.

Ngankam AP, Mao G, Van Tassel PR. 2004. Fibronectin adsorption onto polyelectrolyte multilayer films. Langmuir 20(8):3362-70.

Nicosia RF, Ottinetti A. 1990. Modulation of microvascular growth and morphogenesis by reconstituted basement membrane gel in three-dimensional cultures of rat aorta: A comparative study of angiogenesis in Matrigel, collagen, fibrin, and plasma clot. In Vitro Cellular & Developmental Biology-Plant 26(2):119-28.

Nurdin N, Francois P, Mugnier Y, Krumeich J, Moret M, Aronsson BO, Descouts P. 2003. Haemocompatibility evaluation of DLC-and SiC-coated surfaces. European Cells and Materials 5:17-28.

Obara M, Kang MS, Yamada KM. 1988. Site-directed mutagenesis of the cell-binding domain of human fibronectin: separable, synergistic sites mediate adhesive function. Cell 53(4):649-57.

Okpalugo TIT, Murphy H, Ogwu AA, Abbas G, Ray SC, Maguire PD, McLaughlin J, McCullough RW. 2006. Human Microvascular Endothelial Cellular Interaction With Atomic N-Doped DLC Compared With Si-Doped DLC Thin Films. Power (W) 500:140.

Okpalugo TIT, Ogwu AA, Maguire PD, McLaughlin JAD. 2004a. Platelet adhesion on silicon modified hydrogenated amorphous carbon films. Biomaterials 25(2):239-45.

Okpalugo TIT, Ogwu AA, Maguire PD, McLaughlin JAD, Hirst DG. 2004b. In-vitro blood compatibility of aC: H: Si and aC: H thin films. Diamond & Related Materials 13(4-8):1088-92.

Potts JR, Campbell ID. 1996. Structure and function of fibronectin modules. Matrix Biology 15(5):313-20.

Qiu Q, Sayer M, Kawaja M, Shen X, Davies JE. 1998. Attachment, morphology, and protein expression of rat marrow stromal cells cultured on charged substrate surfaces. J Biomed Mater Res 42(1):117-27.

Ruoslahti E. 1996a. Integrin signaling and matrix assembly. Tumour Biol 17(2):117-24.

Ruoslahti E. 1996b. RGD and other recognition sequences for integrins. Annual Reviews in Cell and Developmental Biology 12(1):697-715.

Seo J, Ionescu-Zanetti C, Diamond J, Lal R, Lee LP. 2004. Integrated multiple patch-clamp array chip via lateral cell trapping junctions. Applied Physics Letters 84:1973.

Siebers MC, ter Brugge PJ, Walboomers XF, Jansen JA. 2005. Integrins as linker proteins between osteoblasts and bone replacing materials. A critical review. Biomaterials 26(2):137-46.

Singh A, Ehteshami G, Massia S, He J, Storer RG, Raupp G. 2003. Glial cell and fibroblast cytotoxicity study on plasma-deposited diamond-like carbon coatings. Biomaterials 24(28):5083-89.

Sorribas H, Braun D, Leder L, Sonderegger P, Tiefenauer L. 2001. Adhesion proteins for a tight neuron–electrode contact. Journal of Neuroscience Methods 104(2):133-41.

Sousa SR, Moradas-Ferreira P, Barbosa MA. 2005. TiO 2 type influences fibronectin adsorption. Journal of Materials Science: Materials in Medicine 16(12):1173-78.

Sugita S. 2008. Mechanisms of exocytosis. Acta Physiologica 192(2):185-93.

Toriello NM, Douglas ES, Mathies RA. 2003. Microfluidic Device for Electric Field-Driven Single-Cell Capture and Activation. Langmuir 19:1532-8.

Truskey GA, Yuan F, Katz DF. 2004. Transport phenomena in biological systems: Upper Saddle River, NJ: Pearson/Prentice Hall: 793p.

van den Beucken J, Vos MRJ, Thüne PC, Hayakawa T, Fukushima T, Okahata Y, Walboomers XF, Sommerdijk N, Nolte RJM, Jansen JA. 2006. Fabrication, characterization, and biological assessment of multilayered DNA-coatings for biomaterial purposes. Biomaterials 27(5):691-701.

Vroman L, Adams AL, Fischer GC, Munoz PC, Stanford M. 1982. Proteins, plasma and blood in narrow spaces of clot-promoting surfaces. Adv Chem 199:266-76.

Vroman LEO. 1987. Methods of Investigating Protein Interactions on Artificial and Natural Surfaces. Annals of the New York Academy of Sciences 516(1 Blood in Contact with Natural and Artificial Surfaces):300-5.

Wilson CJ, Clegg RE, Leavesley DI, Pearcy MJ. 2005. Mediation of Biomaterial-Cell Interactions by Adsorbed Proteins: A Review. Tissue Engineering 11(1-2):1-18.

Xu LC, Siedlecki CA. 2007. Effects of surface wettability and contact time on protein adhesion to biomaterial surfaces. Biomaterials 28(22):3273-83.

Yamada KM. 1991. Adhesive recognition sequences. ASBMB. p 12809-12.

Yang P, Huang N, Leng YX, Chen JY, Fu RKY, Kwok SCH, Leng Y, Chu PK. 2003. Activation of platelets adhered on amorphous hydrogenated carbon (aC: H) films synthesized by plasma immersion ion implantation-deposition (PIII-D). Biomaterials 24(17):2821-9.

Yang Y, Craig TJ, Chen X, Ciufo LF, Takahashi M, Morgan A, Gillis KD. 2007. Phosphomimetic Mutation of Ser-187 of SNAP-25 Increases both Syntaxin Binding and Highly Ca2+-sensitive Exocytosis. The Journal of General Physiology 129(3):233.

Yang Y, Gillis KD. 2004. A highly Ca-sensitive pool of granules is regulated by glucose, PKC, and cAMP in insulin-secreting INS-1 cells. J. Gen. Physiol 124:641-51.

Yokota T, Terai T, Kobayashi T, Iwaki M. 2006. Cell adhesion to nitrogen-doped DLCS fabricated by plasma-based ion implantation and deposition method. Nuclear Inst. and Methods in Physics Research, B 242(1-2):48-50.